

MOLECULAR BIOLOGY OF IRIDOVIRUSES

Yechezkel Becker, Series Editor
Julia Hadar, Managing Editor

DEVELOPMENTS IN MOLECULAR VIROLOGY

- Becker, Y. (ed.) *Herpesvirus DNA* (1981)
Becker, Y. (ed.) *Replication of Viral and Cellular Genomes* (1983)
Becker, Y. (ed.) *Antiviral Drugs and Interferon: The Molecular Basis of Their Activity* (1983)
Kohn, A. and Fuchs, P. (eds.) *Mechanisms of Viral Pathogenesis from Gene to Pathogen* (1983)
Becker, Y. (ed.) *Recombinant DNA Research and Viruses. Cloning and Expression of Viral Genes* (1985)
Feitelson, M. *Molecular Components of Hepatitis B Virus* (1985)
Becker, Y. (ed.) *Viral Messenger RNA: Transcription, Processing, Splicing and Molecular Structure* (1985)
Doerfler, W. (ed.) *Adenovirus DNA: The Viral Genome and Its Expression* (1986)
Aloni, Y. (ed.) *Molecular Aspects of Papovaviruses* (1987)
Darai, G. (ed.) *Molecular Biology of Iridoviruses* (1990)

DEVELOPMENTS IN VETERINARY VIROLOGY

- Payne, L.N. (ed.) *Marek's Disease* (1985)
Burny, A. and Mammerickx, M. (eds.) *Enzootic Bovine Leukosis and Bovine Leukemia Virus* (1987)
Becker, Y. (ed.) *African Swine Fever* (1987)
De Boer, G.F. (ed.) *Avian Leukosis* (1987)
Liess, B. (ed.) *Classical Swine Fever and Related Viral Infections* (1987)
Darai, G. (ed.) *Virus Diseases in Laboratory and Captive Animals* (1988)
Campbell, J.B. and Charlton, K.M. (eds.) *Rabies* (1988)
Alexander, D.J. (ed.) *Newcastle Disease* (1988)
Wittmann, G. (ed.) *Herpesvirus Diseases of Cattle, Horses, and Pigs* (1989)
Petursson, G. and Hoff-Jorgensen, R. (eds.) *Maedi-Visna and Related Diseases* (1990)

DEVELOPMENTS IN MEDICAL VIROLOGY

- Levine, P.H. (ed.) *Epstein-Barr Virus and Associated Diseases* (1985)
Becker, Y. (ed.) *Virus Infections and Diabetes Mellitus* (1987)
De Clercq, E. (ed.) *Clinical Use of Antiviral Drugs* (1988)
Revel, M. (ed.) *Clinical Aspects of Interferons* (1988)
Gilden, D.H. and Lipton, H.L. (eds.) *Clinical and Molecular Aspects of Neurotropic Virus Infection* (1989)

MOLECULAR BIOLOGY OF IRIDOVIRUSES

edited by

Gholamreza Darai
University of Heidelberg
Federal Republic of Germany



Kluwer Academic Publishers
Boston/Dordrecht/London

Distributors for North America:

Kluwer Academic Publishers
101 Philip Drive
Assinippi Park
Norwell, Massachusetts 02061 USA

Distributors for all other countries:

Kluwer Academic Publishers Group
Distribution Centre
Post Office Box 322
3300 AH Dordrecht, THE NETHERLANDS

Library of Congress Cataloging-in-Publication Data

Molecular biology of iridoviruses / edited by Gholamreza Darai.

p. cm. — (Developments in molecular virology)

Includes bibliographical references.

ISBN-13: 978-1-4612-8893-0 e-ISBN-13: 978-1-4613-1615-2

DOI: 10.1007/978-1-4613-1615-2

1. Iridoviruses. 2. Molecular microbiology. I. Darai,
Gholamreza. II. Series.

[DNLM: 1. Iridoviridae. 2. Molecular Biology. W1 DE998DG / QW
165.5.I6 M718j

QR401.M65 1990

576'.6484—dc20

DNLM/DLC

for Library of Congress

89-20096
CIP

Copyright © 1990 by Kluwer Academic Publishers

Softcover reprint of the hardcover 1st edition 1990

All rights reserved. No part of this publication may be reproduced, stored in a retrieval system or transmitted in any form or by any means, mechanical, photocopying, recording, or otherwise, without the prior written permission of the publisher, Kluwer Academic Publishers, 101 Philip Drive, Assinippi Park, Norwell, Massachusetts 02061.

CONTENTS

Contributing Authors	vii
Preface	xi
1	
Taxonomy of iridoviruses	
D.B. Willis	1
2	
Molecular biology of tipula iridescent virus	
S. Tajbakhsh and V.L. Seligy	13
3	
Molecular biology of insect iridescent virus type 6	
M. Fischer, P. Schnitzler, H. Delius, A. Rösen-Wolff, and G. Darai	47
4	
Protein composition of chilo iridescent virus	
M. Cerutti and G. Devauchelle	81
5	
Insect iridescent virus type 9 and type 16	
J. Kalmakoff, N. McMillan, and S. Davison	113
6	
Virus-cytoskeleton interaction during replication of frog virus 3	
K.G. Murti and R. Goorha	137
7	
The DNA-methylase of frog virus 3	
K. Essani	163
8	
Transcription of frog virus 3	
D.B. Willis, J.P. Thompson, and W. Beckman	173
9	
Regulation of protein synthesis in frog virus 3-infected cells	
A.M. Aubertin, T.N. Tham, and L. Tondre	187
10	
Molecular biology of fish lymphocystis disease virus	
P. Schnitzler, A. Rösen-Wolff, and G. Darai	203

11		
Hepatotoxicity of iridoviruses		
H. Lorbacher de Ruiz		235
12		
African swine fever virus		
J.V. Costa		247
13		
Diversity of the african swine fever virus genome		
L.K. Dixon, P.J. Wilkinson, K.J. Sumption, and F. Ekue		271
Index		297

CONTRIBUTING AUTHORS

ANNE MARIE AUBERTIN
Laboratoire de Virologie
3 Rue Koeberle
67000 Strasbourg, France

WILLIAM BECKMAN
University of Delaware
School of Life & Health Sciences
Newark, DE 19716, USA

MARTINE CERUTTI
Institut National de la
Recherche Agronomique
Station de Recherches de
Pathologie Comparée
30380-Saint-Christol-lez Alès, France

JOAO V. COSTA
Gulbenkian Institute of Science
Apartado 14
2781 Oeiras Codex, Lisboa, Portugal

GHOLAMREZA DARAI
Institut für Medizinische Virologie
der Universität Heidelberg
Im Neuenheimer Feld 324
6900 Heidelberg, Federal Republic of Germany

S. DAVISON
University of Otago
Department of Microbiology
P.O.Box 56
Dunedin, New Zealand

Hajo DELIUS
Institut für Angewandte Tumorstudiologie
am Deutschen Krebsforschungszentrum Heidelberg
Im Neuenheimer Feld 506
6900 Heidelberg, Federal Republic of Germany

GÉRARD DEVAUCHELLE
Institut National de la
Recherche Agronomique
Station de Recherches de
Pathologie Comparée
30380-Saint-Christol-lez Alès, France

LINDA K. DIXON
AFRC Institute for Animal Health
Pirbright Laboratory
Ash Road, Pirbright, Woking,
Surrey GU24 0NF, United Kingdom

F. EKUE
AFRC Institute for Animal Health
Pirbright Laboratory
Ash Road, Pirbright, Woking,
Surrey GU24 0NF, United Kingdom

KARIM ESSANI
St. Jude Children's Research Hospital
Department of Virology and Molecular Biology
332 North Lauderdale
Memphis, TN 38105, USA

MICHAELA FISCHER
Institut für Medizinische Virologie
der Universität Heidelberg
Im Neuenheimer Feld 324
6900 Heidelberg, Federal Republic of Germany

RAKESH GOORHA
St. Jude Children's Research Hospital
Department of Virology and Molecular Biology
Memphis, TN 38101, USA

JAMES KALMAKOFF
University of Otago
Department of Microbiology
P.O.Box 56
Dunedin, New Zealand

HILDEGARD LORBACHER DE RUIZ
Zentrale Versuchstieranlage
der Universität Heidelberg
Im Neuenheimer Feld 345
6900 Heidelberg, Federal Republic of Germany

N. McMILLAN
University of Otago
Department of Microbiology
P.O.Box 56
Dunedin, New Zealand

K. GOPALO MURTI
St. Jude Children's Research Hospital
Department of Virology and Molecular Biology
Memphis, TN 38101, USA

ix

ANGELA RÖSEN-WOLFF

Institut für Medizinische Virologie
der Universität Heidelberg
Im Neuenheimer Feld 324
6900 Heidelberg, Federal Republic of Germany

VERN L. SELIGY

Molecular Genetics Section
Division of Biological Sciences
National Research Council of Canada
100 Sussex Drive
Ottawa K1A 0R6, Ontario, Canada

K. J. SUMPTION

AFRC Institute for Animal Health
Pirbright Laboratory
Ash Road, Pirbright, Woking,
Surrey GU24 0NF, United Kingdom

PAUL SCHNITZLER

Institut für Medizinische Virologie
der Universität Heidelberg
Im Neuenheimer Feld 324
6900 Heidelberg, Federal Republic of Germany

SHARAGIM TAJBAKSH

Molecular Genetics Section
Division of Biological Sciences
National Research Council of Canada
100 Sussex Drive
Ottawa K1A 0R6, Ontario, Canada

T. N. THAM

Laboratoire de Virologie
3 Rue Koeberlé
67000 Strasbourg, France

JAMES P. THOMPSON

Veterans Administration Medical Center
Research Service, BE-106
1030 Jefferson Avenue
Memphis, TN 38104, USA

L. TONDRE

Laboratoire de Virologie
3 Rue Koeberlé
67000 Strasbourg, France

P. J. WILKINSON

AFRC Institute for Animal Health
Pirbright Laboratory
Ash Road, Pirbright, Woking,
Surrey GU24 0NF, United Kingdom

X

DAWN B. WILLIS
American Cancer Society
3340 Peachtree Road
Atlanta, GA 30026, USA

P R E F A C E

The importance of viruses as infectious biokybernetic elements is connected by their importance as model systems for the investigation of virus-cell interactions at the molecular level. Undoubtedly, the application of this powerful tool led to the discovery of certain cellular genes. So far as Iridoviruses are concerned, they are biologically and genetically fascinating and their investigation allows us unambiguously to learn so much more about the natural strategy of evolution, for example the architecture of viruses, genomic organization, and particularly viral replication.

Iridoviruses are icosahedral cytoplasmic DNA containing viruses belonging to the family Iridoviridae and are able to infect protozoa, algae, invertebrates, and vertebrates. The iridoviruses are ubiquitous in nature, have been found on all continents of the world and have been isolated from a variety of insect species. The discovery of the circular permutation and terminal redundancy as a genomic feature of several members of the Iridoviridae is of special importance, since such genomic arrangements and organization had been known only for prokaryotic viruses since the beginning of this decade. The other very intriguing genomic property common in two members of this virus family (Frog virus 3 and Fish lymphocystis disease virus) is the high degree of methylation at CpG residues. The toxic effect of the viral proteins on the liver Kupffer cells found for Frog virus 3 and Chilo iridescence virus is another interesting phenomenon of this virus family which deserves more attention. A chapter on this topic has therefore been included in the book.

It is now generally accepted that African swine fever virus as the fifth genus of the Iridoviridae family

should be separated from the other genera due to its genomic feature which contains a terminally cross-linked nonpermuted linear double-stranded DNA molecule. This genomic organization is characteristic for the members of the Poxviridae family. Two contributions on this subject will give the reader the basic information necessary for understanding this very sophisticated phenomenon.

Molecular biology and related disciplines have progressed to a remarkable degree in the last decade and are powerful and efficient instruments for the discovery of viral genes. The prime objective of this book is to summarize the recent data on the molecular biology of the iridoviruses which should demonstrate the state and the progress of iridovirus research which indeed merits more fundamental support. However, there are still too many authorities involved in managing and evaluating research grants who believe that their prime and overriding mission is to support only those investigations which seem to be of immediate benefit. I hope that reading this book will help to create new understanding within the inter-connected disciplines of basic science and inspire colleagues working in the field of virology. This book contains original studies and can be considered as a contribution to modern education in biology. Of course such way of thinking is not innovative for basic science. The book is addressed primarily to professional investigators, though I hope that junior and senior scientists who seek to know the actual progress in virology may also find it of interest. Each chapter endeavours to present concise data of those aspects of most interest to the scientist and key literature references are provided for those who wish to read further.

I am particularly indebted to Professors Rudolf Rott and Walter Doerfler, and the Deutsche Forschungsgemein-

schaft for supporting the molecular biological research on iridoviruses in Germany. Without their efforts the development and progress of this field in this country and consequently the editing of this book would not have been possible.

I wish to thank all the contributors of this volume. I have the privilege of particularly thanking my friend Professor Yechiel Becker who gave me the opportunity to edit this volume in his series "Developments in molecular virology". The editorial assistance of Julia Hadar and Karl Raab, and the excellent secretarial help by Barbara Holder, Dragica Lehmann, and Gudrun Pohle are much appreciated.

Gholamreza Darai

1

TAXONOMY OF IRIDOVIRUSES

DAWN B. WILLIS

Department of Virology and Molecular Biology, St. Jude
Children's Research Hospital, Memphis Tennessee 38101, USA

ABSTRACT

Originally grouped together on the basis of morphology, the iridoviruses are now beginning to reveal biochemical and genetic similarities--e.g. circularly permuted and terminally redundant genomic DNA--that set them apart from other eukaryotic virus groups and justify their inclusion in the same family.

BACKGROUND

The classification of viruses into taxonomic groups is a troublesome area of virology, even when there is a large background of information on the nucleic acid sequences, structure, and mode of replication. In the case of the iridoviruses, where very few comparative studies have been carried out, the problem is even more complex. The goal of any classification scheme is to place organisms that are closely related on morphological and biochemical grounds into groups that reveal evolutionary and phylogenetic relationships and, in addition, provide a convenient system of nomenclature. These concepts have served well for the classification of higher plants and animals, where there are fossil records stretching back millions of years, but are hardly adequate for establishing relationships among viruses, which probably do not have a common ancestry or evolutionary history (1). A relationship of viruses to cellular elements is as plausible as a relation of viruses to each other, and any classification of viruses is bound to be an artificial scheme set up with the main view of facilitating communication among virologists.

In the early days of virology, nomenclature consisted of giving the name of the disease produced in the host followed by the word "virus." But in the early 60's, as more information about viruses became available, the desirability of a nomenclature that grouped viruses with similar characteristics was apparent. Lwoff et al. (2) used the properties of the nucleic acid (RNA or DNA, single or double stranded) plus the presence or absence of an envelope to describe 7 major virus "groups." The International Committee on Nomenclature of Viruses, established in 1966 to bring some semblance of order to the haphazard naming of viruses by individual investigators, proposed a dual system of nomenclature consisting of generic names ending in -virus for individual virus groups and eight digit cryptograms that attempted to describe each virus according to a conventional key (3). Virologists were almost unanimous in their refusal to use this system, and by the time the committee (now called the International Committee on Taxonomy of Viruses, or ICTV) met in 1979, the cryptogram system was abandoned in favor of the classic Linnaean latinized binomial genus-species nomenclature (4). The new international nomenclature purportedly gave order and structure to virus research because it permitted scientists to use universally agreed upon names for the different virus groups, but in practice, most virologists continue to use the original vernacular names.

As mentioned earlier, the establishment of a satisfactory taxonomy for iridoviruses has been greatly complicated by the fact that there is, to date, no good evidence for any member of this group infecting humans or even mammals. The one possible related mammalian virus, African Swine Fever Virus (ASFV), has recently been shown to be more closely related to poxviruses than to iridoviruses (5). Thus, interest in securing the kind of nucleic acid sequence data that would advance the classification of iridoviruses has lagged considerably behind that in virus families whose members infect higher orders of animals. However, the biochemical evidence that is available suggests that

iridoviruses not only occupy a unique biological niche between nuclear and cytoplasmic DNA viruses, but have features similar to prokaryotic viruses as well.

IRIDESCENT INSECT VIRUSES

The first "iridovirus" to be described was the iridescent insect virus discovered by C.F. Rivers in 1954 in infected larvae of the crane fly Tipula paludosa in the fields of Shropshire, England (reviewed in 6). Because of the blue coloration conferred on systemically infected larvae, the term Tipula iridescent virus was applied to this early isolate. As a result of pioneering studies on this virus (7,8,9), Tipula iridescent virus became the prototype for similar iridescent viruses infecting insects. Several other insect viruses were subsequently isolated that shared common characteristics-- iridescence, large (120-200 nm) size, icosahedral morphology, and the production of DNA-containing cytoplasmic inclusions-- with the original Tipula isolate, which was thereafter called insect iridescent virus type 1. Iridescent virus type 2 was isolated in New South Wales from the coleopterous scabeb, Sericesthis paludosa (10); three other iridescent viruses, which produced a turquoise-green coloration rather than the blue to purple of the first two iridescent viruses, were discovered in three separate species of North American mosquitoes (11,12) and called insect iridescent virus type 3, 4, and 5. Iridescent virus type 6 was originally isolated from the lepidopterous rice stem borer Chilo suppressalis, found in the field in Kyushu, Japan (13). A non-iridescent insect virus with icosahedral morphology was observed by Stoltz et al. (14) in Chironomus plumosa; because it was not iridescent, the Chironomus virus was not classified as one of the insect iridescent viruses at that time. However, the icosahedral morphology, the large double-stranded DNA genome, and the cytoplasmic site of replication clearly marked this virus as a closely related member of the group, and it is now considered iridescent virus type 35 (15).

AMPHIBIAN AND PISCINE VIRUSES

In 1966, Granoff *et al.* (16) described 23 separate isolates of a polyhedral cytoplasmic deoxyribovirus from both normal and tumor tissue of the common leopard frog, Rana pipiens. Although bearing many similar morphological characteristics to the insect viruses, the amphibian viruses were not iridescent. Over the next few years, similar viruses were isolated from bullfrogs (17), toads (18), and newts (19). Also during this same decade, the virus causing lymphocystis disease in fish was identified as an icosahedral cytoplasmic deoxyribovirus (20), as was the causative agent of African swine fever, isolated in Kenya (21).

Based on common morphology (icosahedral), large (165-400 kbp) double-stranded DNA genomes, and an apparent cytoplasmic site of replication, all of these icosahedral cytoplasmic deoxyriboviruses were lumped together with the insect iridescent viruses into one group called "iridoviruses" (3), although not all of them were, in fact, iridescent. Many workers in the field objected to the use of the iridescent terminology, and promoted the use of either "polyhedral" or "icosahedral" cytoplasmic deoxyribovirus (ICDV) instead (22). But this term proved too unwieldy for general acceptance, and it did not conform to the international binomial nomenclature that the ICTV wished to adopt. (Possibly there was confusion between ICTV and ICDV as well!) In addition, the morphological description could also apply to a number of algae and plant viruses that would then have to be included in the same group with the animal viruses (22), and it seemed highly unlikely that there would be any relationship between viruses whose hosts were phylogenetically so far apart. The name "iridovirus", for both historical and esthetic reasons, had a lot of appeal to the executive committee of the ICTV, and in 1976 the family Iridoviridae was created to include both vertebrate and invertebrate viruses that could be described as icosahedral cytoplasmic deoxyriboviruses, whether they displayed iridescence or not (23).

CURRENT TAXONOMIC STATUS OF IRIDOVIRUSES

By 1982 (4), enough biochemical data had accumulated to warrant the establishment of the following 5 genera within the family Iridoviridae:

Table 1. Classification of the family Iridoviridae (4)

English vernacular name	International name	Type species
1. Small iridescent insect virus	<u>Iridovirus</u>	<u>Tipula</u> iridescent virus (Type 1)
2. Large iridescent insect virus	<u>Chloriridovirus</u>	Mosquito iridescent virus (Type 3)
3. Amphibian icosahedral deoxyribovirus	<u>Ranavirus</u>	Frog virus 3 (FV3)
4. Fish lymphocystis disease virus	<u>Lymphocystivirus</u>	Flounder lymphocystis disease virus (FLCDV)
5. African swine fever virus	(Removed from <u>Iridoviridae</u> by ICTV Edmonton, 1987)	

The insect viruses were subdivided into two genera, Iridovirus and Chloriridovirus. The Iridovirus genus consisted of the small (~120 nm) insect viruses with blue to purple iridescence, whereas the genus Chloriridovirus was made up of larger (~180 nm) viruses that possessed a yellow-green iridescence. Although Tipula iridescent virus (type 1) was taken as the original type species, it proved difficult to work with in tissue culture, and much more information is now available on Chilo iridescent virus (type 6), which was approved as the new type species at the ICTV meeting in Edmonton, August, 1987. Early serological comparisons and nucleic acid homologies (22) revealed that insect iridescent

viruses types 1 and 2 were strains of the same virus, as were types 9 and 18. Types 2 and 9 had 26-45% homologous sequences, and type 6 Chilo iridescent virus was unrelated to any of the above (22). Now that the techniques are available for intricate sequence and serological comparisons, it would be possible to determine exact relationships among all of the isolates, but lack of interest by both investigators and funding agencies in this type of research makes it unlikely that such studies will be carried out.

The members of the genus Chloriridovirus (iridescent insect viruses types 3-5, 7, 8, 11-15) appear to be serologically related to each other, but not to any members of the Iridovirus genus; no nucleic acid homology studies have been carried out (6). All of the isolates from mosquitoes can be transmitted transovarially, in contrast to the Iridovirus genus (6). The Chironomus plumosus virus has been tentatively classified as an Iridovirus, only on the basis of its relatively smaller size (4). It is not iridescent, and no serological or nucleic acid homology data is available (14).

Frog virus 3 (FV3) is undoubtedly the most widely studied member of the family Iridoviridae at the molecular level, yet its relationship to the other family members remains obscure. FV3 was selected from a panel of 22 similar viruses for further study because it had been isolated from the Lucké renal adenocarcinoma; however, it was later shown to be unrelated to the tumor except as a possible opportunistic virus infection (24). It has been classified as a genus according to international nomenclature under the name of Ranavirus; few investigators have adopted the new terminology. An interesting recent development comes from the work of Essani and Granoff (personal communication). FV3, the tadpole edema virus (TEV) isolated by Wolf (17), and an isolate from newts (19) have been shown by restriction enzyme patterns and nucleic acid homology to be strains of the same virus. All of the amphibian isolates are over 90% homologous with each other and share about 26% homology with a recent isolate from goldfish (25). The goldfish virus, like FV3,

does not cause overt disease in the host from which it was isolated. Coupled with the nucleic acid homologies, the goldfish virus is presumed to be more closely related to Ranavirus than to another fish virus, the lymphocystis disease virus (LCDV, genus Lymphocystivirus), which causes the formation of benign tumors in several species of flounder, dab and plaice (26). There is no nucleic acid homology between FV3 and LCDV (27). Other possible members of the Ranavirus genus are viruses that form DNA-containing inclusions in the cytoplasm of frog erythrocytes (28) or frog lymphocytes (29).

In the absence of any biochemical information, the Octopus vulgaris disease virus (30) is considered a probable member of the Lymphocystivirus genus because of the pathology observed in the host. In contrast to the systemic disease caused by the insect and amphibian viruses, both LCDV and the octopus virus are found in tumorous cells only (reviewed in 26).

Other iridovirus-like agents isolated from fish include carp gill necrosis virus (31), cod ulcer syndrome virus (32), and Nillahootie redbfin perch virus (33). Piscine erythrocytic necrosis virus (PENV), which has not yet been isolated, also appears to be an iridovirus (26). The host ranges in vivo and in vitro, in addition to the different cytopathic effects, indicate that PENV and LCDV are not the same virus-- but until serological or nucleic acid hybridization studies are performed, it is impossible to say whether any of these fish viruses belong to the Ranavirus or the Lymphocystivirus genera, or if some of them constitute a new genus.

RELATIONSHIPS AMONG IRIDOVIRUSES

Iridoviruses appear to be ubiquitous in nature, and it is only now that we are beginning to understand what parameters link them together. The original decision to place them all in the same group was based on their icosohedral morphology, their large, double-stranded DNA genomes, and the presence of a non-cellular membrane derived envelope

(3). The discovery that FV3 virions possess a wide variety of enzymatic activities, among them a highly active cyclic-AMP independent serine-threonine protein kinase (34), ATPase (35), and an assortment of nucleases (36), was eventually followed by descriptions of the same virion-associated enzymatic activities in LCDV (26) and Chilo iridescent viruses (37). Thus it appears that both invertebrate and vertebrate iridoviruses have these structural enzyme features in common, in addition to the cytoplasmic site of morphogenesis.

A puzzling aspect to the problem of iridovirus replication arose when Goorha et al. (38) reported that FV3 had a nuclear phase in which the initial round of DNA replication occurred, and that the virus required the host RNA polymerase II for the synthesis of early messenger RNA (39). Furthermore, a temperature-sensitive FV3 mutant was isolated in which viral DNA synthesis was confined to unit-sized pieces in the nucleus at the non-permissive temperature; when shifted down to the permissive temperature, the synthesis of long concatemeric DNA was observed in the cytoplasm (40). These data provided genetic support for the existence of a "two-stage" viral DNA replicative cycle, resembling in some respects that described for bacteriophages (41,42). The presence of a nuclear phase of viral replication made the classification of FV3 as a "cytoplasmic" virus dubious; however, such studies have not yet been reported with the other iridoviruses, and it may be that this unusual mode of replication will not only turn out to be a unifying mechanism for the Irididoviridae, but reveal a relationship between these unusual eukaryotic viruses and prokaryotic viruses as well.

One of the most interesting attributes of FV3 is the structure of its genomic DNA. Although it exists as a linear, double-stranded molecule in the virion, it is both circularly permuted and terminally redundant (43). A similar structure has been reported for LCDV (44), and more recently for two insect iridescent viruses--Chilo iridescent virus

(45) and iridescent virus type 9 from Wiseana species larvae (46). This structural feature has no counterpart in any other eukaryotic virus and is indeed more like that of bacteriophage P22 (42). Circular permutation and terminal redundancy of the genome may be another biochemical characteristic that unites the vertebrate and invertebrate Iridoviridae. This unusual DNA structure has important implications for the replication and packaging of the viral DNA, for it suggests that iridovirus DNA, like that of bacteriophage T4 (41) or P22 (42) forms concatemers that are then cleaved and packaged into preformed heads via a "headful" mechanism.

Although the invertebrate and vertebrate iridoviruses both appear to have circularly permuted and terminally redundant DNA genomes, they can be differentiated by the presence or absence of DNA methylation. FV3 genomic DNA is methylated at all cytosines in the dinucleotide sequence CpG by a virus-encoded DNA methyltransferase (47). Although the enzyme has only been purified from FV3-infected cells, TEV, a newt virus, the goldfish virus (Essani, personal communication), and LCDV (44) all possess similarly methylated DNA, as measured by resistance of the genomic DNA to cutting with C-methyl sensitive enzymes. On the other hand, the DNA of all insect viruses that have been tested is readily cut by C-methyl sensitive enzymes, implying that the insect virus genomes are not methylated (15). This is perhaps not surprising, since insect DNA itself contains no methylated cytosine, in contrast to the DNA of vertebrates. If viruses evolved from their host cells rather than from a primordial virus ancestor, one would expect the methylation status of the viral DNA to be similar to that of its host.

I might mention here that the only candidate mammalian cytoplasmic deoxyribovirus, AFSV, was removed from the family Iridoviridae because its DNA was not methylated, circularly permuted, or terminally redundant (48). Instead, the genomic DNA of ASFV is cross-linked and unmethylated, the virus carries its own virion-associated RNA polymerase, and its

promoters can be recognized by the vaccinia virus RNA polymerase (5). Despite the obvious biochemical similarity between ASFV and vaccinia virus, the Poxvirus Study Group has been reluctant to adopt ASFV into the poxvirus family, so it remains today an orphan virus in a class of its own.

The final association among the members of the family Iridoviridae is an epidemiological one. They all appear to be confined to poikilothermic animals who are associated with an aquatic environment at some stage of their life cycle. Kelly (6) has postulated that it is this aquatic association that accounts for the internal membrane structure that permits the high degree of stability these viruses display in aqueous solutions. One could hypothesize that the insect viruses arose first, and were later adapted to life in a vertebrate host as a result of being eaten by fish and frogs! If the insect viruses prove to have a nuclear replicative phase, as well they might since Devauchelle et al. (37) have been unable to demonstrate the existence of a virion-associated RNA polymerase in the Chilo virus system, the relationship between the insect viruses and the piscine and amphibian viruses will be more apparent. One might even speculate that ASFV, which does after all morphologically resemble an iridovirus, is the "missing link" between the Iridoviridae, with their nuclear and cytoplasmic phases, and the truly cytoplasmic Poxviridae, the only other double-stranded DNA virus family infecting both vertebrates and invertebrates. Or it may be that there is no connection between nuclear and cytoplasmic viruses, but that each virus family arose independently to fill a particular ecological niche.

ACKNOWLEDGMENTS

This work was supported by research grant CA 07055 and Cancer Center Support (CORE) grant CA 21765 from the National Cancer Institute, and by the American Lebanese-Syrian Associated Charities (ALSAC).

REFERENCES

1. Luria, S.E., Darnell, J.E., and Baltimore, D. General Virology. John Wiley and Sons, New York, 1978.
2. Lwoff, A., Horne, R., and Tournier, P. Cold Spring Harbor Symposium Quant. Biol. 27:51-55, 1962.
3. Wildy, P. In: Monographs in Virology, vol. 5, Karger, Basel, 1971, 82 pp.
4. Matthews, R.E.F. Intervirology 17:55-58, 1982.
5. Talavera, A., Beloso, A., Granoff, A., Willis, D.B., Moss, B., and Viñuela, E. Abstracts of 6th Poxvirus/Iridovirus Workshop, Cold Spring Harbor Laboratory, New York, 1986, p.36.
6. Kelly, D. Cur. Top. Micro. Immunol. 116:23-35, 1985.
7. Smith, K.M. Virology 5:168-175, 1958.
8. Xeros, N. Nature 174:562-565, 1954.
9. Glitz, D.G., Hills, G.J., and Rivers, C.F. J. Gen. Virol. 3:209-220, 1968.
10. Steinhaus, E.A., and Leutenegger, R. J. Invertebr. Pathol. 5:246-248, 1963.
11. Weiser, J. Bull WHO 33:586-588, 1963.
12. Clark, T.B., Kellen, W.R., and Lum, P.T.M. J. Invertebr. Pathol. 7:519-524, 1965.
13. Fukaya, T., and Nasu, S. Appl. Ent. Zool 1:69-72, 1966.
14. Stoltz, D.B., Hilsenhoff, W.L., and Stich, H.F. J. Invertebr. Pathol. 12:118-126, 1968.
15. Devauchelle, G. Stoltz, D.B., and Darcy-Tripier, F. Cur. Top. Micro. Immunol 116:1-21, 1985.
16. Granoff, A., Came, P.E., and Breeze, D.C. Virology 29:133-148, 1966.
17. Wolf, K., Bullock, G.L., Dunbar, C.E., and Quimby, M. C. J. Infec. Dis. 118:253-262, 1968.
18. Balls, M., and Ruben, L.N. Prog. Exp. Tumor Res. 10:238-260, 1968.
19. Clark, H.F., Gray, G., Fabian, F., Zeigel, R., and Karzon, D.T. J. Virol. 2:629-640, 1968.
20. Christmas, J.Y., and Howse, H.D. Gulf Res. Rep. 3:131-154, 1970.
21. Greig, A.S., Boulanger, P., and Bannister, G.L. Can. J. Comp. Med. 31:24-31, 1967.
22. Kelly, D. and Robertson, J.S. J. Gen. Virol. 20:17-41, 1973.
23. Fenner, F. Intervirology 7: Karger, Basel, 1976, 115 pp.
24. Granoff, A. Curr. Top. Micro. Immunol. 50:107-137, 1969.
25. Berry, E.S., Shea, T.B., and Gabliks, J. J. Fish Dis. 6:501-510, 1983.
26. Flügel, R.M. Curr. Top. Micro. Immunol. 116:133-150, 1985.
27. Darai, G., Anders, K., Koch, H.G., Delius, H., Gelderblom, H., Samalecos, C., and Flugel, R.M. Virology, 126:466-479, 1983.
28. Briggs, R.T., and Burton, P.R. J. Submicro. Cytol. 5:71-78, 1973.

29. Desser, S.S., and Barta, J.R. *Can. J. Zool.* 62:1521-1524, 1984.
30. Rungger, D., Rastelli, M., Braendle, E., and Malsberger, R.G. *J. Invertebr. Pathol.* 17:72-80, 1971.
31. McAllister, P.E. *Comp. Virol.* 14:401-470, 1979.
32. Wolf, K. *In: Microbial Diseases of Fish* (Ed. R.J. Roberts), Academic Press, London, 1982, pp. 59-90.
33. Langdon, J.S., Humphrey, J.D., Williams, L.M., Hyatt, A.D. and Westbury, H.A. *J. Fish Dis.* 9:263-268, 1986.
34. Silberstein, H., and August, J.T. *J. Virol.* 12:511-522, 1973.
35. Vilagines, R. and McAuslan, B.R. *J. Virol.* 7:619-624, 1971.
36. Willis, D.B., Goorha, R., and Chinchar, V.G. *Cur. Top. Micro. Immunol.* 116:77-106, 1985.
37. Devauchelle, G., Attias, J., Monnier, C., Barray, S., Cerutti, Guerillon, G., and Orange-Balange, N. *Cur. Top. Micro. Immunol.* 116:37-48, 1985.
38. Goorha, R., Murti, K.G., Granoff, A., and Tirey, R. *Virology* 84:32-50, 1978.
39. Goorha, R. *J. Virol.* 37:496-499, 1981.
40. Goorha, R. *J. Virol.* 43:519-528, 1982.
41. Streisinger, G., Emrich, J., and Stahl, M.M. *Proc. Nat. Acad. Sci. USA* 57:292-295, 1967.
42. Tye, B., Huberman, J.A., and Botstein, D., *J. Mol. Biol.* 85:501-532, 1974.
43. Goorha, R., and Murti, K.G. *Proc. Natl. Acad. Sci. USA* 79:248-252, 1982.
44. Darai, G., Anders, K., Koch, H., Delius, H., Gelderblom, H., Samalecos, C. and Flügel, R.M. *Virology* 126:466-479, 1983.
45. Delius, H., Darai, G. and Flügel, R.M. *J. Virol.* 49:609-614, 1984.
46. Ward, V.K., and Kalmakoff, J. *J. Virol.* 160:507-510, 1987.
47. Willis, D., Goorha, R., and Granoff, A. *J. Virol.* 49:86-91, 1984.
48. Viñuela, E. *Cur. Top. Micro. Immunol.* 116:151-170, 1985.

2

MOLECULAR BIOLOGY OF *TIPULA* IRIDESCENT VIRUS

S. TAJBAKSH and V. L. SELIGY

Molecular Genetics Section, Division of Biological Sciences, National Research Council of Canada, Ottawa K1A 0R6, Ontario, Canada

ABSTRACT

Tipula iridescent virus (TIV) is an icosahedral insect virus that replicates cytoplasmically in infected cells. The TIV virion has a diameter of 130 nm containing between 25 and 30 polypeptides. Within the core resides the double-stranded genome which is comprised predominantly of two DNA components, L (176-247 kbp) and S1 (10.8 kbp), both of which are seen consistently in agarose gels of total TIV DNA. We present here a review of available literature on TIV and other iridoviruses, and discuss in particular the molecular approaches that we have introduced to study this virus. We also extend our observations on the multiple DNA components of TIV by comparing our isolate with one obtained from Ireland. These studies indicated that the latter isolate lacked the S1 DNA component suggesting a separate evolutionary origin for this DNA component. A strategy for isolating transcripts on the basis of abundance is also described along with a discussion on the relative abundance of the TIV capsid protein in purified virions.

INTRODUCTION

Background and Classification

In 1954, Xeros reported an insect pathogen isolated from the European crane fly *Tipula paludosa* (Diptera) (1). The fat body of the diseased larvae appeared iridescent blue through the integument. The purified, pelleted virus particles also displayed the same iridescence as the infected tissue and this virus was later named *Tipula* iridescent virus (2). These early studies established a cytoplasmic site of replication for TIV and DNA as its genetic material.

Several characteristics of TIV have made this virus very suitable for fundamental studies on iridoviruses. These include the stability of TIV (3, 4), and the ability to purify large quantities of virus from infected larvae (5). As a result, some of our basic understanding of the structure of icosahedral viruses came from the pioneering studies carried out with TIV (6). Some of the biophysical properties of TIV are listed in Table 1.

Table 1. Biological and biophysical properties of *Tipula iridescent virus**.

Property	Details	References
Host range	Diptera Lepidoptera Coleoptera	14
Replication site	cytoplasm- all tissues of insect	1 14
Chemical composition	80% protein 12.4-19% dsDNA 5.2% lipid	15 16 17
Size (diameter)	130nm (dehydrated) 250nm (hydrated)	18 19
Shape	skewed icosahedron	20 21
Genome	ds-DNA 176-247 kbp estimated from restriction enzyme analysis; Identification of L (large) (176-247 kbp) and small DNA components (S1: 10.8 kbp)	22 22
	190-235 kbp estimated from reassociation kinetics	23

*Updated from (24).

Since the discovery of TIV, a number of other vertebrate and invertebrate viruses with similar properties have been isolated. These viruses were called icosahedral cytoplasmic deoxyriboviruses (ICDVs) and were grouped in the family *Iridoviridae* (7). The best studied members of this family are frog virus 3 (FV3; 8) and African swine fever virus (ASFV; 9), the latter causing an important disease of domestic pigs. Other prominent members include fish lymphocystis disease virus (FLDV) which is the causative agent in a chronic disease of several higher order salt and freshwater fish (10), and *Chilo* iridescent virus (CIV; 11). There have also been recent reports of a large (about 190 nm) ICDV that infects certain eukaryotic *Chlorella*-like green algae and has cytopathic properties similar to the other ICDVs (12, 13). Comparative molecular studies between this and other *Iridoviridae* should be useful in determining how these viruses are related.

Insect viruses form the largest group within the *Iridoviridae* spanning the *Iridovirus* (small iridescent virus) and *Chloriridovirus* (large iridescent virus) genera. To date, over 30

insect iridescent viruses have been isolated of which TIV is Type 1 (25). These viruses are referred to by their common name such as "TIV" (type 1) and "SIV" (*Sericesthis* iridescent virus, type 2) or by the proposed number IV1 (iridescent virus 1) and IV2, respectively. The insect iridescent viruses will be referred to here by their numerical assignment. Those that have appeared more commonly in the literature such as TIV, SIV, and CIV (*Chilo* iridescent virus, IV6) will be referred to by their more historical designation.

The term "iridescent" was first used to describe the turquoise coloration of systemically infected larvae and pellets of purified TIV (5). This property was investigated in detail by Klug and coworkers (19) who showed that crystals of TIV can diffract light in a manner similar to the diffraction of X-rays by ordinary crystals. By selecting conditions of growth of TIV crystals, they established that the iridescence is due to Bragg reflections (constructive interference) where the wavelength reflected is a function of the distance between successive reflecting planes (interparticle distance) in the crystals. These investigators also concluded that the virus particles were packed in a face-centered array with an interparticle spacing of 250 nm, approximately twice the distance of dehydrated virions.

Host range

The small insect iridescent viruses have been demonstrated to have broader host ranges when artificially injected, compared to entry occurring naturally by injection. This suggests that host range is mediated either by breakdown of the virus by gut enzymes or the susceptibility of gut epithelial cells to infection (see 26 for discussions). TIV infects a wide range of species in at least 3 different orders: Lepidoptera, Diptera, and Coleoptera (14).

Enzymes associated with TIV

Enzyme activities that have been shown to be associated with the insect iridescent virions include protein kinase, nucleotide phosphohydrolase, and DNA-dependent RNA polymerase (27-30). Recent studies by Franke and Hruby (31) have shown that vaccinia virus will fortuitously package chloramphenicol acetyl transferase, a bacterial enzyme produced in the eukaryotic cell by recombinant means, into virions by way of "hitchhiking". Therefore the significance of enzymes and proteins reported to be associated with virus particles is questionable as they may not be virally encoded.

Serological relationships

In early studies on ICDVs, a popular method of comparing viruses within the *Iridoviridae* involved protein analysis by serological and acrylamide gel electrophoresis techniques (32). Unfortunately, these studies have not proven to be very conclusive. Comparisons using DNA hybridization techniques should prove to be a better approach, particularly in the classification of the numerous insect iridescent virus isolates.

Physical and structural properties

Iridoviridae form the largest known isometric viruses with sizes ranging from 120 nm for some of the insect viruses (11) to the recently discovered frog erythrocytic virus which measures 370-450 nm in size (33, 34). Many of the reported values of particle diameter vary due to particle orientation, degree of hydration, and the presence or absence of an outer envelope. The latter is acquired by some of the viruses through budding at the cell membrane. These viruses are not occluded in a proteinaceous matrix like other viruses such as the nuclear polyhedrosis viruses (35).

Members of the *Iridoviridae* family share some common structural features. By using biophysical techniques such as negative staining and thin sectioning, freeze-etching, and neutron scattering, a number of investigators have determined that the *Iridoviridae* shell is composed of three concentric domains: a proteinaceous icosahedral capsid, an intermediate unit membrane composed of lipids and proteins, and a central core containing the viral DNA and its associated proteins (21, 36, 37). Viral cores represent the internal structure comprising the DNA and its associated proteins. Cores can be released from the shell by treatment of viral suspensions with the non-ionic detergent NP40 or chymotrypsin (38, 39). Klump and coworkers (40) have demonstrated that the viral DNA within the core is attached to the coat protein to form a chromatin-like structure.

Iridescent virus particles are not sensitive to ether (41), suggesting that the external lipid membrane is not essential for infectivity. With FV3, the outer envelope is not required for infectivity since nonenveloped particles are also infectious (38) albeit 150 fold less than enveloped virions (42).

Electron microscope observations have revealed an interesting structural feature of purified *Iridoviridae* virions. Several investigators have shown the presence of a microfibrillar fringe located at the surface of a certain number of these viruses such as FLDV, mosquito iridescent virus (MIV), and CIV. This fringe seems to be absent from others such as ASFV and FV3 (11). These microfibrillar structures can be 3-5 nm in diameter and up to 150 nm in length (45). Their presence was also demonstrated with iridescent virus type 29 (IV29) as the particles became ordered in the host cell. Kelly and Robertson (32) have suggested that these fibers might cause the interplanar spacings in crystals of these viruses.

Virion shell. When a crude preparation of TIV virions is centrifuged on a linear sucrose gradient, several bands are often evident (46). The main viral band of highest density represents intact virions corresponding to infectious virus. A less dense band called "top component" (TC; 46) is located immediately above the main band. A band consisting of empty capsids is found near the meniscus of the gradient. The three bands of virus indicated here correspond to "full", "partially filled", and "empty" virions, respectively,

referring to the state of the viral core (permeability to negative stains) as visualized under the electron microscope (47). Recently, we showed that the TC fraction corresponding to partially filled virions contained less DNA than full virions and that the DNA of TIV virions consisted of two main components L and S1 (22). This TC fraction contained the highest molar ratio of S1 DNA to the L DNA component.

In other studies on the virion structure, investigators have shown that a major polypeptide, approximately 50 kDa in size, is present in the iridescent viruses. This protein constitutes up to 45% of the total proteins in the virion (48-50; also present study). Two obvious locations for such an abundant protein are the capsid of the virus or the core in association with the DNA. Tripier-Darcy and coworkers (51) using biochemical fractionation of FV3 particles localized the major 48 kDa FV3 protein in the capsid of the virion. Moore and Kelly (52) isolated the major structural polypeptide from three types of iridescent viruses (2, 6 and 9) by preparative polyacrylamide gel electrophoresis. By using amino acid analysis, these authors revealed that these proteins showed a close similarity, although their mobilities on SDS-PAGE were slightly different from each other but about 50 kDa in size. Surface labelling of IV9 with ^{125}I revealed that the capsid protein was at least partly exposed at the surface (52). Structurally, TIV has been found to be remarkably stable since it can be stored at 4°C for 2 months (4) or greater (present study) with breakdown of only some of the virions.

Post-translational modifications

Studies on TIV by Krell and Lee (46) have indicated that none of the virion proteins are glycosylated. Glycosylation was also not detectable with mosquito iridescent virus and FV3 proteins (53, 54). However, Aubertin and coworkers (55) have reported that some FV3 core proteins are phosphorylated, while the capsid (48 kDa) protein was never found to be phosphorylated *in vivo* or *in vitro*.

Icosahedral virus assembly

In constructing a virion, there are a limited number of efficient designs that can be formed from a large number of identical protein molecules. Two basic designs are icosahedral heads and helical tubes (6). Most closed-shelled virus particles have been shown to have icosahedral symmetry (56). The icosahedron consists of 20 equilateral triangular faces consisting of smaller morphological subunits called capsomeres. Icosadeltahedra have 20T facets, where T is the triangulation number (6). The advantages of an icosahedral structure over that of other types of cubic structures (tetra and octahedral) in the formation of virions is that it allows for the smallest subunit repeat for shell formation as economically as possible (57).

With improvements in electron microscope technology by the late 1960s, more accurate determinations of the structural features of viruses were made. Wrigley (20),

using the nasal decongestant Afrin on SIV, showed an icosahedral structure of skewed orientation that probably contained 1562 capsomeres. Subsequently, a study using TIV showed a similar structure with a revised estimate of 1472 capsomeres (58). This finding was confirmed by Manyakov (4) who used long term storage of TIV at 4°C or treatment with chloroform to break up the virus into its structural elements. He predicted that TIV was formed by 12 pentagons and 20 equilateral triangles composed of 1472 capsomeres per virion.

Several models have been proposed for the assembly of iridescent viruses. These include: **a)** the formation of viral membranes or shells before development of the core (59); **b)** development of the core first followed by encapsidation with protein (60); and **c)** a parallel formation of the viral shell and DNA fibrils (61). In a study by Yule and Lee (62), an hypothesis was proposed which combined features of particle assembly suggested by Smith (59) and Xeros (61). By using cytological and immunological techniques, Yule and Lee (62) demonstrated that ferritin labelled antibody was closely aligned to the inner faces of empty capsids in various stages of assembly. These data provided evidence that the viral shell is assembled prior to entry of the DNA. Similar models have been suggested for adenovirus and herpes virus assembly (63, 64).

It is evident that a large amount of information has accumulated on the gross structural properties of TIV in the last three decades. These studies have increased our understanding of viral architecture and have helped in the creation of models to explain the icosahedral design (6). However, aside from these pioneering studies, little or no molecular information has been produced to explain the mode of replication, pathogenesis, and the regulation of gene expression of this and other iridescent insect viruses. Recent investigations of the TIV genome (22) have indicated that this virus has some novel features that have not been described for other *Iridoviridae* members or other large double-stranded DNA viruses. In addition to these features, the ability to purify large quantities of this virus from infected larvae make TIV a good candidate for experimentation to answer some of the questions raised in this section.

In our lab, we have been interested in obtaining more molecular information on TIV genes. For this purpose, the TIV capsid gene was chosen as the main candidate for detailed analysis. This gene was selected for a number of reasons. First, this gene is interesting since a significant biological function can be ascribed to its protein product. Studies with some of the other *Iridoviridae* have indicated that this protein is expressed at very high levels and is the major component in the morphological subunits that constitute the virion. Second, the isolation of this gene and the study of its protein product with respect to self-assembly properties should complement and advance some of the earlier structural studies that were carried out with TIV. Third, the purification of the capsid

protein, by virtue of its abundance in virions, should facilitate the production of capsid-specific antisera for the identification of this gene and the study of its biosynthetic properties. Fourth, very little is known about late genes of large cytoplasmically replicating viruses such as vaccinia virus or FV3. The strategy that was chosen to isolate the TIV capsid gene involved using amino acid sequence information derived from the purified protein (65).

Pathway of TIV infection

Gross pathology. Information on the pathogenesis of iridescent viruses is incomplete largely because little is known about how the virus gains access to the initial replication site. These viruses have a low infectivity when administered orally and are probably transmitted in the field through wounds, cannibalism, or by parasites (66-68).

Carter (69) found TIV to be infective to all four larval instars, to pupae, and to adults of both sexes of *Tipula oleracea*. The most effective method of transmission of TIV appeared to be by injection and the infection was characterized by a blue iridescence of the affected organ.

The initial site of TIV multiplication is not known, however, the fat body and hemocytes have been implicated (14, 25). The virus then produces a systemic infection by rapidly multiplying in skin, muscles, wingbuds, legs and head (14). Interestingly, an anomaly of TIV infection of the silkworm *Bombyx mori* is the production of epidermal "tumors" which result from the proliferation of epidermal cells to form a multilayered epidermis (70). However, these tumors were not demonstrated to contain virus. Tumor formation has not been reported from other insect species, although some iridescent viruses of vertebrates and of the octopus are associated with tumors (26, 71).

Massive amounts of virus can result from a productive infection of larvae. TIV was reported to constitute at least 25% of the body weight of dead larvae (5), the highest concentration often being found in the epidermis and fat body. The fat organ in insects is similar to the vertebrate liver in function. This organ, which is most extensively developed in larvae, serves as a storage organ for lipids, protein, and glycogen as well as playing a crucial role in metamorphosis (72). The resulting infection renders larvae flaccid within 7-10 days of infection, although death may take longer (25).

Cytopathology. Much of our understanding of insect iridescent virus cell pathology comes from infection studies carried out on cells *in vitro*. The major features of replication are common among the iridescent viruses with some variations in the timing of events (26). The focal point of viral replication and assembly is the cytoplasm (3, 25), although it is not clear if nuclear involvement occurs, as happens with FV3 (73, 74). Following inhibition of host DNA synthesis with heat-inactivated FV3, Goorha and coworkers (74) observed by electron microscope autoradiography that 30% of the viral DNA was synthesized in the

nucleus. These authors showed by DNA-DNA hybridizations that this labelled viral DNA was associated with extensively purified nuclei. Nuclear involvement during TIV replication has not been determined.

The pathway of TIV infection in *Estigmene acrea* hemocytes in suspension culture has been extensively studied by light and electron microscopy (47, 75-77). Electron microscope studies by Mathieson and Lee (75) determined that the virus inoculum adsorbed to the plasma membrane of the cultured cells is internalized by phagocytic engulfment into membrane bound vesicles within 1.5 hours post-inoculation (p.i.). A general breakdown of the virus occurs within the vesicles, and as early as 4 hours p.i., cytoplasmic lesions called viroplasmic centers (VCs) appear in the cytoplasm. The VCs increase in size and number over the course of infection.

Viroplasmic centers appear as membrane-free isolated pockets of cell cytoplasm containing ribosomes, engulfed by a homogeneous "dense matrix" resembling chromatin in appearance and devoid of ribosomes. Electron microscope autoradiography has localized viral DNA exclusively in the dense matrix zones whereas progeny virions are assembled within the cytoplasmic component of the VC (75). These studies also revealed that viral DNA synthesis occurs as early as 6 hours p.i. and progeny virions can be seen at 16 hours p.i. Viral release occurs by exocytosis or lysis, giving enveloped and non-enveloped virions, respectively, although the majority of virus particles remains cell associated and therefore non-enveloped (32).

Studies on the formation and composition of TIV VCs have revealed that there may be differences in the assembly sites of some members of the *Iridoviridae*. For example, investigations of FV3 assembly sites by electron microscopy and the use of cytoskeletal disruptive agents, implicated a functional role for intermediate filaments in the formation of FV3 assembly sites (78-80). In contrast, similar studies carried out on TIV VCs in *E. acrea* and *Aedes albopictus* cells revealed that microtubules and microfilaments are not involved in VC formation or maintenance (81, 82). More recently, immunofluorescent studies by Bladon and coworkers (83) showed that *in situ* VCs and fractionated VCs reacted with monoclonal antibodies raised against lymphocyte nuclear matrix proteins. The possibility that highly conserved mammalian nuclear scaffolding proteins are involved in TIV VC formation warrants further study.

Some of the cytopathic effects caused by TIV infection include a profound decline in cellular DNA, RNA, and protein synthesis and the formation of multinucleate cells due to cell fusion (75). The inhibition of host macromolecular synthesis is a common feature of invertebrate and vertebrate viruses and with a few exceptions, is poorly understood (84).

Recent studies by Chinchar and Caughman (85) suggest that heat inactivated FV3 selectively inhibited equine herpesvirus type 1 protein synthesis at the level of translation

initiation. Although no such detail is available on the other iridescent viruses, Lee and Brownrigg (47) showed that nuclei of cells inoculated with UV-inactivated virus and empty viral capsids failed to incorporate [^3H]-thymidine whereas virus treated with the protein inactivator β -propiolactone had no effect. These findings suggest that a protein component of the invading virus subverts nuclear nucleic acid metabolism. Similar observations have been made with FV3 and poxvirus inhibition of host DNA synthesis (86, 87).

Semipermissive replication of TIV

During our studies on TIV we discovered that an *A. albopictus* cell line was semipermissive for TIV replication. We carried out comparative studies between *E. acraea* (permissive) and the *A. albopictus* (semipermissive) cells, for TIV propagation (88). Light microscope autoradiography showed viral DNA present in viroplasmic centers (VCs) and these VCs appeared morphologically similar in both cell lines when examined by light and electron microscopy. Radiolabelled cDNA was then synthesized from RNA samples obtained from infected cells, at different times after infection and hybridized to TIV DNA restriction endonuclease digests. These experiments indicated that transcription levels and the kinetics of TIV infection were similar in both cell lines. The cDNA hybridization studies also revealed that the S1 DNA component of TIV carries sequences that are transcribed and are TIV specific. In spite of the similarities between these two cell lines, electron microscope studies revealed that *A. albopictus* VCs were devoid of progeny virions. However, the TIV capsid protein was synthesized in both cell lines. These data suggested a block in TIV replication in the *A. albopictus* cell line occurring late in infection, likely just prior to the assembly of progeny virions.

The use of viral mutants to study the effects of specific lesions in the viral replication cycle has been well documented in the literature (63, 64, 89). Probably the best studied semipermissive cell system is the infection of African green monkey kidney cells with human adenovirus type 2 (Ad2; 90). Replication of human adenoviruses is often incomplete in most cultured cells of nonhuman origin. For example, the infection of rodent or monkey cells by Ad2 is semipermissive, resulting in limited viral replication (90-92). The lesion in viral replication in these cells involves aberrant late gene expression at the level of transcript processing and translation (93-95). Such detailed studies are lacking for the insect iridescent viruses. The semipermissive *A. albopictus* cell line described above should allow us the opportunity to carry out similar studies with TIV.

The establishment of cell lines from primary cells of a host organism has been a routine practise in the study of viral replication *in vitro*. However, cells that have undergone continual passage often have chromosome numbers, growth rates, cell morphologies, and nutrient requirements that are very different from their counterparts *in vivo* (96). Although the *in vitro* studies provide a convenient framework for studying viral

pathogenesis, it is necessary to exercise extreme caution when extrapolating back to the original host organism, particularly when considering host range (see 88 for discussions).

Molecular information available on *Iridoviridae*

Genome organization. In a recent study of the CIV genome, Delius and coworkers (97) concluded that the DNA is linear and about 158 million daltons in size, is circularly permuted and has a terminal redundancy of about 12%. Two other *Iridoviridae* genomes, FV3 and FLDV, have also been shown to be circularly permuted and terminally redundant (98, 99). These physical features are common to some prokaryotic viruses like bacteriophages T4 and lambda (100, 101) and have not been demonstrated for any other eukaryotic viruses.

As mentioned earlier, Goorha and coworkers (74) showed that the FV3 genome enters the nucleus where it is transcribed during the early stages of replication, probably by a modified host RNA polymerase II (102). Goorha (103) later showed that FV3 DNA replicated in two stages which were distinguishable by the genome size and the site of replication. The first stage was confined to the nucleus where the DNA ranged from genome to twice genome size. The second stage took place exclusively in the cytoplasm, and the replicating DNA was concatemeric. Results of pulse-chase experiments showed that this concatemeric DNA served as the precursor for the production of mature FV3 DNA. This concatemeric arrangement is consistent with the finding that FV3 DNA is circularly permuted and terminally redundant and provides additional evidence for a specific pathway of virus assembly, namely packaging of DNA into preformed heads (98). We are currently investigating the termini of TIV DNA to determine if TIV is also circularly permuted and terminally redundant.

The study of FV3 genes has revealed that, like vaccinia virus, there is a lack of consensus with prokaryotic or eukaryotic transcription regulatory sequences. DNA sequencing of two immediate-early FV3 genes revealed the lack of a classical TATA box and no significant identity in DNA sequence between their promoters (104, 105). Further, these regulatory sequences did not resemble those of known vaccinia viral gene sequences (105).

Polyadenylation. Unlike other animal DNA viruses, the majority of FV3 transcripts do not appear to undergo processing and polyadenylation at their 3' ends (106). This feature is common to prokaryotes and their viruses, which provides further evidence for evolutionary links between prokaryotic and eukaryotic viruses. Studies on the invertebrate TIV should reveal whether this virus produces polyadenylated transcripts (see Results and Discussion).

TIV genome. The TIV genome is complex consisting of four DNA components. Two of these, L (176-247 kbp) and S1 (10.8 kbp) are seen consistently in ethidium bromide

stained agarose gels of total TIV DNA. TIV L DNA is a linear, double-stranded molecule, and its size was estimated from summations of DNA fragment sizes produced by 7 restriction endonucleases (22; and present study). Size estimates for the other *Iridoviridae* genomes range from 100-250 X 10⁶ Da or 150-280 kbp (7). Other components measuring ~6 (S2) and ~3.5 (S3) in size have also been observed in association with total TIV DNA. We have speculated that these components (S2 and S3) may be deletion products of L and/or S1 DNA (22, 107). To date, no other *Iridoviridae* or large DNA containing viruses have been reported to contain multiple DNA components, although an earlier study with an iridescent virus from mosquitoes (RMIV) suggested that this virus may contain two identical DNA molecules (108).

There are several examples of viruses with more than one component. The genome of herpesvirus consists of two covalently linked DNA components in a linear arrangement (L: long-82%; S: short-18%), each containing unique sequence (64). Other studies by Krell and coworkers (109) have revealed that the *Campoletis sonorensis* virus, which belongs to the recently discovered polydnavirus family, contains a multipartite genome. This viral genome is believed to consist of at least 28 molecules of covalently closed, superhelical, double-stranded DNA. The size of these molecules ranges from 6 to 21 kbp and they are non-equimolar in distribution (109, 110).

As previously mentioned, the presence of a small DNA component (S1) existing separately from the main genomic DNA is a novel finding among the large double-stranded DNA containing viruses. To fulfill any long term goal of solving TIV genomic organization, it was necessary to determine if S1 DNA is packaged within virions and is TIV specific. By treating TIV particles with nucleases and subsequently purifying total DNA, it was demonstrated that S1 DNA is indeed of viral origin and is packaged within virions (107). Furthermore, CsCl fractionation of TIV particles and extraction of total viral DNA from the "empty", "partially filled" and "full" particles showed that partially filled virions contain a higher S1 to L ratio than does the main viral fraction (22, 107). To ensure that these and other TIV preparations used in these studies were free of other contaminating particles, TIV suspensions were regularly monitored by electron microscope examination (111). These studies were then extended to determine if the S1 DNA component is made by infected cells. Recently, we showed that that S1 DNA was indeed synthesized in both *E. acrea* and *A. albopictus* cells (88). Additionally, the intracellular ratio of S1 to L DNA was at least 10 fold greater than in mature virions where the ratio for these DNA components is approximately 1:1 (22, 88, 107). The presence of more S1 than L DNA in partially filled capsids (22) implies that the S1 DNA component, by virtue of its smaller size, is preferentially packaged into empty viral capsids first followed by the L component.

In order to study the production of TIV transcripts in infected insect cells, we used

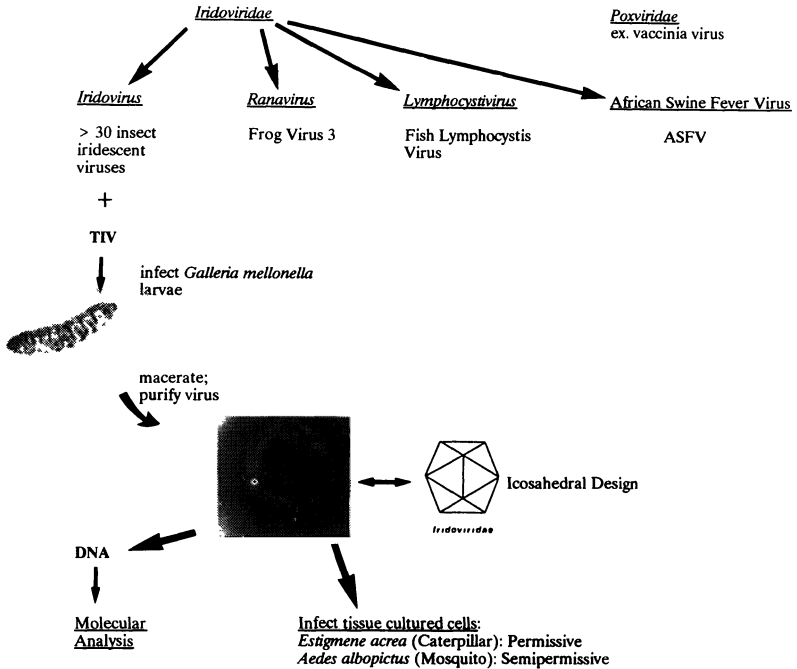


Figure 1. Schematic representation of some of the experimental approaches used in our laboratory to study TIV.

radiolabelled cDNA made from infected cell RNA to monitor TIV transcription (see present study). These studies revealed that both L and S1 DNA hybridized to the cDNA (88). Although these results suggest that transcribed sequences are present on S1 DNA, we do not know in fact, whether S1 DNA serves as the transcriptional template. Of five genes that have been isolated recently in our lab, none were found to hybridize to S1 DNA (65; S. Tajbakhsh and V. L. Seligy, unpublished results).

The high levels of S1 DNA in infected cells argues that S1 DNA may replicate autonomously in insect cells. Alternatively, S1 DNA may be generated from L DNA during infection in a way that is analogous to the "onionskin" model proposed by Sambrook and coworkers (112). This model assumes that repeated activation of an origin of replication would ultimately result in production of extrachromosomal copies and of intrachromosomal duplications and deletions. These events could account for the release of free cyclic molecules (113). Although S1 DNA has sequences common to L (22), it is not certain if all of the S1 DNA sequences are exclusive to L DNA. It would be of interest to determine if

purified S1 DNA can replicate autonomously in insect cells, or if this DNA component requires coinfection with TIV. If the former is true, then S1 will be a good candidate for the development of an expression vector for insect cells.

Although the small DNA components are present in virions, we demonstrate in this study that a TIV isolate from Ireland (Ir-TIV) that was also propagated in *Galleria mellonella*, lacked the S1 DNA component as determined by ethidium bromide staining of total viral DNA in agarose gels. Further, hybridization with a 0.75 kbp EcoRI fragment of S1 DNA indicated that this sequence was lacking in the Ir-TIV. Therefore, we believe that the smaller DNA components that are associated with TIV are not essential for a productive TIV infection (see Results and Discussion). The possibility that S1 and L are both essential for TIV replication has not been tested yet in infected cells.

As discussed above, information on the gross structural properties of TIV has accumulated in the last three decades. These studies have increased our understanding of viral architecture and have helped in the creation of models to explain the icosahedral design (6). However, aside from these pioneering studies, little or no molecular information has been produced to explain the mode of replication, pathogenesis, and the regulation of gene expression of this and other iridescent insect viruses. The main objective of our studies is to provide molecular genetic information on gene regulation, host-cell interactions, and related events that lead to TIV pathogenesis. A schematic representation of some of the approaches we have used in studying TIV is illustrated in Figure 1.

MATERIALS AND METHODS

Virus and Cells

TIV was propagated and purified from *Galleria mellonella* larvae essentially as described by Yule and Lee (62) with some modifications. Larvae were macerated in liquid nitrogen with pestal and mortar, resuspended in 10 mM sodium phosphate buffer pH 7.2 and subjected to two cycles of low speed (2000 g for 5 min) and high speed (55,000 g for 1 h, SW 25.1) differential centrifugation. Viral pellets were resuspended in buffer, layered on to 10-40% linear sucrose gradients, and centrifuged at 25,000 g for 30 min. The main viral band was removed, diluted with buffer, pelleted, and layered on to a second sucrose gradient. The final viral pellet was resuspended in buffer containing 50 µg/ml garamycin. Viral concentration was determined as described by Younghusband (114) by measuring absorbance at 260 nm.

Cell lines were grown at 28°C with 2.5% CO₂. *Estigmene acrea* (BTI-EAA) cells were obtained from Dr. R. Granados (Boyce Thompson Research Institute, Ithaca, N.Y., USA) and propagated in GTC-100 medium containing Grace's insect medium, 10% Fetal Bovine

Serum (FBS), 0.26% bactotryptose broth and 50 µg/ml garamycin at pH 6.25. *Aedes albopictus* C6/36 cells were obtained from Bonnie M. King (US Department of Agriculture, Denver, CO., USA) in 1984 and grown in minimal essential medium (MEM) pH 7.2, supplemented with 10% FBS, non-essential amino acids and penicillin (5000 units/ml)/streptomycin (5000 µg/ml).

Cells were infected with TIV at a viral concentration of 80 µg/ml for 1-2 h at 28°C. After this period, cells were centrifuged for 5 min at 200 g, washed twice with medium, resuspended in fresh medium, and incubated at 28°C until harvesting. TIV-infected cells were assayed for infection as already described (88).

The Irish TIV (Ir-TIV) was kindly provided by Maeve S. Kelly (Queen's University of Belfast, Northern Ireland). This isolate was obtained from a Tipulid larvae (leatherjacket) from Fermanagh county, Northern Ireland in 1987, and propagated in *G. mellonella* larvae. The small icosahedral particles (sv) were obtained from the top of the initial sucrose gradient in the TIV purification scheme. They were repurified on a second sucrose gradient and were subsequently layered onto CsCl step gradients (1 ml each of 1.3, 1.4, 1.5, and 1.6 g/cm³) and centrifuged using a SW 50.1 rotor, at 30 Krpm for 1 h. Viral bands were then removed and viewed by electron microscopy as described previously (75).

Bacterial transformations and molecular manipulations

Competent cells for plasmid and M13 transformations were prepared as described by Hanahan (115). The protocol for M13 transformation and media used are outlined in Messing (116). Throughout our studies, several *Escherichia coli* bacterial strains were used for different purposes. The JM101 strain was used for M13 transfections and pUC transformations, however other strains were also used: JM103, JM109, HB101, DH5α, and DH5αF'.

DNA from different sources was digested with restriction endonucleases using low, medium, or high salt buffers, and fractionated on horizontal agarose (Seakem) as described by Maniatis and coworkers (117). Digests were terminated by addition of 1/10th volume of stop buffer (100 mM EDTA, 0.5% SDS, 25% glycerol, and 0.1% bromophenol blue) and heated at 65°C for 3-5 min before loading, or stored at 4°C. DNA ligations and recombinant DNA manipulations such as preparation of labelled markers were also carried out as described by Maniatis and coworkers (117).

DNA purifications

DNA from TIV. TIV DNA was isolated as previously described (22) from virus obtained from experimentally infected *G. mellonella* larvae.

S1 DNA component. In initial studies with the S1 DNA component, the source of this DNA was from virions (22). This DNA component is now obtained from infected *E. acrea* cells as described recently (88).

Plasmid, M13 RE. Both miniprep and bulk preparations of plasmid and M13 RF DNA were isolated by the alkaline lysis procedures outlined by Maniatis and coworkers (117). Plasmids were isolated from *E. coli* grown in 2YT or LB media whereas M13 RF was isolated from *E. coli* grown in 2YT medium.

ssDNA template. To prepare M13 template DNA, a 1/50 dilution of an overnight culture of *E. coli* JM101 cells was used to inoculate 2YT media. After 30 min of growth at 37°C the cultures (1.5 ml or 10 ml) were inoculated with a plaque or 50 µl of phage supernatant and grown for 7-12 h. The cultures were centrifuged at 10,000 rpm for 15 min and phage was precipitated from the supernatant by addition of 1/5 volume of 20% polyethylene glycol (PEG)/2.5 M NaOAc pH 7.0 at room temperature (RT) or 4°C for 20-30 min. After centrifugation at 10,000 rpm for 20 min (or 13,000 rpm for 15 min in a micro-centrifuge), the tubes were inverted for 1-3 h and excess PEG was wiped from the sides of the tube with a sterile cotton swab. The phage pellets were resuspended in 600 µl STE and extracted once with an equal volume of phenol, twice with phenol: chloroform: isoamyl alcohol (25:24:1) and once with chloroform: isoamyl alcohol (24:1) before ethanol precipitation. DNA pellets were washed once with 70% ethanol and resuspended in TE* (10 mM Tris-HCl pH 7.5/0.1 mM EDTA).

Immobilization of nucleic acids, probe preparation and hybridization

DNA fractionated on agarose gels was transferred to nylon membranes (Biotrans, ICN; Hybond, Amersham) by alkaline blotting according to Reed and Mann (118). The DNA was depurinated in 0.25 N HCl for 7-10 min (119), denatured in 0.3 M NaOH/1.5 M NaCl for 30 min and transferred to nylon in the same buffer for 2 h. After the transfer was completed, the filter was briefly rinsed in 2X SSC (1X saline sodium citrate: 150 mM NaCl, 15 mM sodium citrate pH 7.0), baked for 1 h at 80°C and stored dry until use.

Double stranded DNA was radiolabelled with [α -³²P]dATP by nick translation (117, 120) or by the method of "random primed" DNA labelling developed by Feinberg and Vogelstein (121). For nick translation, DNA (100-500 ng) was combined with 60 µM each of dGTP, dCTP and dTTP, 50-100 µCi [α -³²P]dATP (800 Ci/mmol, 10 µCi/µl) in 50 mM Tris-HCl pH 7.2, 10 mM MgSO₄, 100 µM DTT, 50 µg/ml BSA. One µl DNaseI (0.1 µg/ml) and 7-10 units of *E. coli* DNA polymerase I were added and the reaction incubated at 16°C for 1 h. The reaction was terminated by heating at 65°C for 10 min and addition of 2 µl 250 mM EDTA. Fifty µl STE (10 mM Tris-HCl pH 8.0, 1 mM EDTA, 100 mM NaCl) was added and the unincorporated nucleotides removed by spin-column chromatography in Sephadex G-50 (117). To calculate the percent incorporation of label into DNA, 1 µl of pre- and post-spin column solutions were spotted on Whatman glass microfiber filters and total cpm were calculated by scintillation counting (122) using a Beckman LS 7000 liquid scintillation counter. Typically, probes were obtained with specific

activities up to 2×10^8 dpm/ μ g with approximately 20-30% of the label being incorporated.

Random priming was performed using a random hexaoligomer obtained from a DNA labelling kit (Boehringer Mannheim). DNA was denatured by boiling for 10 min in the presence of 2 μ l of the hexanucleotide mixture in 10X reaction buffer, and subsequently cooled on ice. To the primer-annealed DNA, 1 μ l each of dGTP, dCTP, and dTTP (0.5 mmol/l), 50 μ Ci [α - 32 P]dATP (800 Ci/mmol), 2 units pol I Klenow were added and the reaction made to 20 μ l with H₂O. After incubation for 30 min at 37°C, the reaction was terminated and unincorporated nucleotides removed by use of a spin column. Typical specific activities were up to 8×10^8 dpm/ μ g with approximately 30% of the label being incorporated. Radiolabelled single stranded cDNA was made as described recently (88).

Filters containing DNA were hybridized in plastic bags (Seal-a-Meal) at different stringency conditions. Generally, DNA-filters were prehybridized in hybridization solution (1 M NaCl, 1% SDS, 100 μ g/ml denatured salmon sperm DNA; Gene Screen Plus Manual) for at least 1 h before addition of boiled (10 min) probe to the bag containing fresh buffer. Probe concentration ranged from 10^5 to 2×10^6 cpm/ml. After hybridization (18-24 h), the filters were washed at high stringency in 2X SSC/0.1% SDS, 3 times 5 min at RT, followed by 2 times at 65°C for 30 min each, and finally in 0.1X SSC for 15 min at RT. The filters were kept damp by placing in between Saran wrap and exposed to X-ray film with or without the use of intensifying screens.

Electrophoresis and detection of proteins

Procedures for SDS-PAGE of proteins, western blotting and capsid protein detection using the anti-capsid antibody and alkaline phosphatase conjugated anti-rabbit antibody were carried out as recently described (88). Silver staining was carried out as outlined by Morrissey and coworkers (123). Coomassie blue staining was done by soaking the gel in 0.1% Coomassie Blue R-250 (Sigma) in 40% methanol/10% acetic acid for 1 h and destaining in 40% methanol/10% acetic acid. Procedures for isolation of 35 S-labelled TIV and fluorography are described in (65).

Immunodetection was also carried out with 125 I-protein A using a modification of the procedure described by Towbin and coworkers (124). All reactions were performed at RT. Filters were washed for 10 min in TBS buffer (20 mM Tris-HCl pH 7.5, 500 mM NaCl, 0.05% v/v Tween 20) containing 20% Fetal Calf Serum (Flow Laboratories) or 1% gelatin as the blocking agent. The filters were then rinsed briefly with TBS prior to the addition of anticapsid antiserum (100 μ l/10 ml) and gently rocked for 2 h. The filters were washed with 25 ml TBS/blocking agent for 5 min followed by 3 X 5 min washes in 20 ml TBS. Filters were then placed in a solution containing 125 I-protein A (ICN; 125) in TBS/blocking agent at 1×10^6 cpm/filter for 20-30 min with gentle rocking, followed by a 5 min wash in TBS/blocking agent and 3 X 5 min washes in TBS. Filters were air dried and exposed to

Kodak X-Omat AR film with intensifying screens overnight at -70°C.

RESULTS AND DISCUSSION

TIV genome

Evaluation of genome size. The estimated genome size of TIV from our studies was obtained by averaging totals from restriction digests and eliminating the submolar fragments (22; Table 2). This analysis revealed the presence of numerous submolar fragments and a genome that is heterogeneous in size. Our estimate of 176-247 kbp is within the range of earlier studies (23) which indicated that the molecular mass of this genome is 1.26×10^8 to 1.55×10^8 Da (~190-235 kbp). This value is also in close agreement with the size of IV22 DNA, isolated from a *Simulium* species, aquatic Blackfly larvae (Diptera), which was found to be 173-220 kbp by restriction endonuclease analysis (126). Further, genomic size heterogeneity in the uncloned viral preparation of IV22 was suggested by these authors as one of the reasons for the presence of submolar fragments. More recently, Ward and Kalmakoff (127) reported a genome size of 192.5 kbp for IV9 isolated from *Wiseana cervinata*, and the presence of submolar fragments in restriction digests of total IV9 DNA. Serial passage of this virus in *G. mellonella* larvae resulted in a complete loss of one of these submolar fragments. These authors also attributed the presence of submolar fragments to a mixed population of virus in their preparations. The genomic size variation observed with TIV was only partly resolved by the finding of the smaller "S" DNA components associated with this virus. It is likely that measurement error of large molecular weight fragments accounts for some differences. As mentioned previously (see Introduction), it has been demonstrated that several members of the *Iridoviridae* family have genomes that are circularly permuted and terminally redundant. The observed heterogeneity in the termini of these viral genomes could also account for some of the variability in genome size seen with TIV. However, preliminary electron microscope studies carried out in collaboration with Dr. K. G. Murti (St. Jude Children's Research Hospital, Memphis, Tennessee) have so far failed to demonstrate that the TIV genome is circularly permuted. Further EM studies and analysis of the genomic termini with 5' lambda exonuclease and T4 DNA polymerase are planned for the immediate future to determine if this is in fact the case.

Methylation of DNA. Another potential source of heterogeneity in genomic size measurement involves the methylation of cytosine to 5-methylcytosine in DNA which would affect cutting by various restriction endonucleases. Methylation has been suggested to be involved in the regulation of eukaryotic and, in some cases, viral gene expression (128, 129). Willis and Granoff (130) have reported that FV3 DNA is methylated by analyzing this DNA using various isoschizomeric restriction enzymes which differentiate

Table 2. Size estimates of TIV DNA restriction fragments¹.

Band No.	Fragment Size (kbp)						
	BamHI	EcoRI	HindIII	PstI	SalI	XbaI	XhoI
1	19.0	>25	(14.0)	32.0	(23.0)	21.5	26.0
2	18.0	(22.0)	(12.2)	26.0	19.5	(20.0)	22.0
3	17.0	14.0	(10.2)	23.0	18.0	17.0	19.0
4	15.2	(13.5)	8.5	(21.0)	(17.0)	(15.3)	(18.0)
5	14.9	(13.0)	8.0	(19.0)	16.0	(13.7)	13.5
6	14.3	12.5	(7.3)	18.0	15.0	12.8	(13.0)
7	13.5	11.8	(7.1)	(14.0)	14.5a,b	12.2	12.5
8	(12.5)	9.0	6.7	13.0	13.4	9.8a,b	11.9
9	(11.8)	8.7	6.0	11.0	(13.0)	(9.5)	10.2
10	10.8a,b	8.5	5.9	10.2	(11.0)	9.0	9.7
11	(10.2)	(8.0)	5.5a,b	(10.0)	10.2	8.7	9.4
12	(10.0)	(7.4)	5.4	8.7	8.6	8.4a,b	8.5
13	(9.8)	(7.1)	5.2	(8.6)	(8.3)	(8.2)	7.9
14	(9.5)	(6.9)	4.6	(8.4)	8.1	7.5	(7.4)
15	(8.7)	5.8	4.4	8.0	7.6a,b	7.4	6.6
16	6.7a,b	4.9	4.1a,b	5.5	(7.0)	7.1	6.2
17	5.2	4.5a,b	3.8a,b	(5.4)	6.6	6.3a,b	5.1
18	4.4	4.4	3.7	4.8	(6.2)	5.7	3.7a,b
19	3.3	4.3	3.5	4.4	5.9	5.4a,b	2.95
20	0.75	4.0	3.3	2.10	5.6a,b	4.4	(2.35)
21	0.65	3.9	3.2a,b	1.50	5.2	3.7	(1.82)
22	0.60	3.6a,b	3.0	1.40	(5.0)	3.0	(1.65)
23		3.5a,b	2.9		4.8	2.80	
24		3.4	2.75		4.4a,b	2.65	
25		3.3	2.60a,b		(4.0)	2.50	
26		3.0	2.47a,b		3.7	2.3	
27		2.70	2.25		3.4	1.9	
28		2.50	2.15		(3.1)	1.8	
29		2.35	1.87		2.55	1.45	
30		2.1	1.82a,b		2.3	1.3	
31		1.74	1.70a,b		2.2	0.85	
32		1.40	1.6		2.0	0.75	
33		1.36	1.25		1.95a,b		
34		1.30	1.15		1.94		
35		1.20	1.05		1.45		
36		0.95	0.87a,b		1.1		
37		0.70	0.80a,b		0.3		
38		0.40	0.60				
39			0.3a,b				
Total	234.3	242.8	190.9	256.0	317.9	264.8	223.1
Total of submolar fragments	161.8	164.9	140.1	169.6	220.3	198.1	178.9

Average size of genome = 176 ± 10^6 to 247 ± 17 kbp¹Revised from (22). Values in parentheses represent submolar fragments.

*Value determined by elimination of submolar fragments.

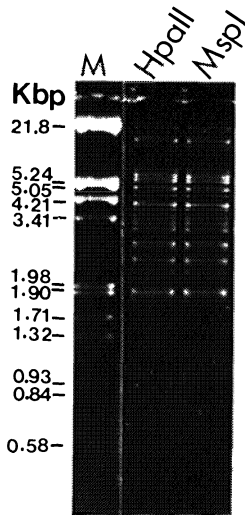


Figure 2. Analysis of possible TIV DNA methylation. TIV DNA was digested with restriction endonucleases HpaII and MspI and electrophoresed in 1% agarose. Markers (M, kbp) represent lambda phage DNA digested with HindIII and EcoRI.

between methylated and non-methylated sequences. For example, DNA cleavage by HpaII (C/CGG) does not occur in the presence of a 5-methyl group at the internal cytosine residue, while MspI (C/CGG; C/^{Me}CGG) cleaves at the same residue of the recognition sequence irrespective of the presence of a methyl group at this position (131).

Since methylation of FV3 DNA is extensive (130), similar modifications of TIV DNA could potentially obscure interpretation of TIV restriction fragment analysis. To determine if TIV DNA is modified by methylation, total TIV DNA was digested with the isochizomeric nucleases HpaII and MspI. This data shown in Figure 2 shows similar restriction profiles for TIV DNA using these restriction endonucleases. This preliminary analysis revealed that unlike FV3 (130) and FLDV (132) DNAs, TIV DNA does not contain methylated CpG sequences. These results agree favorably with those of Thomas (133) which indicated that no methycytosine or 5'-hydroxymethylcytosine residues were present in TIV DNA. Therefore, methylation may not contribute much to TIV genomic size variation. It would be of immediate interest to obtain genomic size estimates of a plaque pure TIV from a homogeneous tissue culture system when it is available.

TIV DNA S1 Component

In order to localize the S1 DNA component in L DNA, we hybridized a cloned 0.75 kbp EcoRI fragment of S1 DNA (88) to restriction digests of total TIV DNA. These results shown in Figure 3 revealed that, in addition to the S1 DNA fragment, this sequence can be located on specific restriction fragments of L DNA. This finding provides further evidence that S1 DNA is in fact present in the L DNA component.

Although we have sufficient evidence that the S1 DNA component is indeed a part of L DNA, we do not know if it is necessary for a productive TIV infection. In an attempt to answer this question, we chose to examine another TIV isolate for the presence of S1 DNA. A preliminary comparative analysis was carried out between our TIV isolate and a TIV isolate that was propagated in *G. mellonella* originally obtained from Ireland. When total DNA was isolated from this Ir-TIV sample and fractionated in agarose gels, we discovered that only the L DNA component was present. This result is shown in Figure 4. Further, hybridization of the radiolabelled 0.75 kbp sequence of S1 DNA to both genomes revealed that this sequence was absent in the Ir-TIV isolate (Figure 4B). These results strongly suggest that S1 DNA is not essential for a productive TIV infection. If this is indeed the case, our TIV isolate must have acquired this sequence independently of at least the Ir-TIV isolate. We have observed that the 0.75 kbp EcoRI fragment of S1 DNA did not hybridize with either *A. albopictus*, *E. acraea*, or *G. mellonella* insect DNAs (S. Tajbakhsh and V. L. Seligy, unpublished observations). We have not checked if all of S1 is missing or S2 and S3. These small DNA components could have originated from a number of sources including the integration of another viral genome in TIV, or a mobile genetic element.

In addition to lacking the S1 DNA component, the Ir-TIV showed some differences in restriction fragment sizes when compared to endonuclease digests of TIV DNA (Figure 4A). Hybridization of the TIV capsid gene to both genomes revealed some differences in the hybridization pattern between the two isolates (Figure 5). Clearly, more extensive analyses must be carried out between these two isolates and other iridescent viruses in order to determine their evolutionary relationships, and the origin of S1 DNA.

TIV Transcription

As mentioned in the introduction, our long term goals are to obtain detailed molecular information on TIV. To do this, we chose to isolate and characterize the TIV capsid gene. One of our approaches was to identify the most abundantly produced transcripts during viral replication. Based on other examples (134-137) one might expect that the TIV capsid gene will also be expressed in relatively abundant amounts late in infection. To identify the most abundant transcripts, a method that does not require direct labelling of the RNA was employed. Total RNA was extracted from TIV-infected cells and radiolabelled first strand cDNA was made from this RNA using oligo dT as a primer and

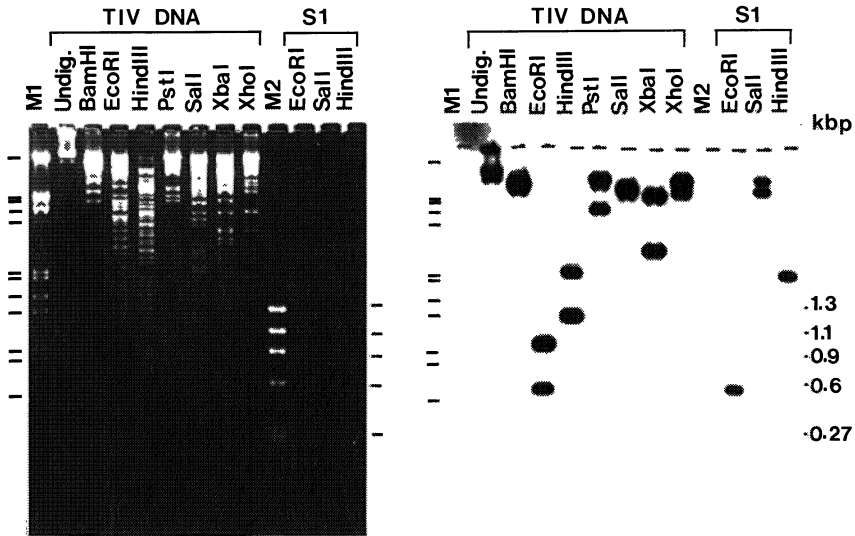


Figure 3. Hybridization of S1 DNA to total TIV DNA. A) Total TIV DNA and purified S1 DNA were restriction endonuclease digested and electrophoresed in 0.7% agarose. B) The DNA in A was denatured, transferred to nylon membrane (Hybond) and hybridized with nick translated insert of pSE3 containing a 0.75 kbp EcoRI fragment of S1 DNA. The upper band in Sall digest of S1 DNA represents undigested S1 DNA. Markers are lambda DNA digested with HindIII/EcoRI (M1; see Figure 2) and phi X174 DNA digested with HaeIII (M2).

AMV reverse transcriptase. The single stranded cDNA probes were then hybridized to a blot of TIV DNA digests (Figure 6; 88). A method similar to this was used successfully to isolate the abundant transcript of the polyhedrin gene of *Bombyx mori* nuclear polyhedrosis virus (138). Using this approach, we isolated two TIV DNA restriction endonuclease fragments, Sall fragments #24a (4.4 kbp) and #36 (1.1 kbp), for analysis (see Figure 7B). The transcripts located on these fragments were called AB1 (1.1 kb) and AB2 (0.75 kb) respectively. The transcripts coded by these genes were too small to be considered as candidates for the capsid gene and are being studied independently.

An insert containing sequences for the putative AB1 gene was isolated from a pBR322 plasmid, L13, shown in Figure 7C. This plasmid was selected from several such recombinant clones by hybridization of radiolabelled cDNA (data not shown) to a partial TIV DNA bank in pBR322 (22). More detailed mapping revealed that this plasmid contains BamHI fragment #4 (15.2 kbp) which harbors a 2.2 kbp Sall/BamHI fragment of

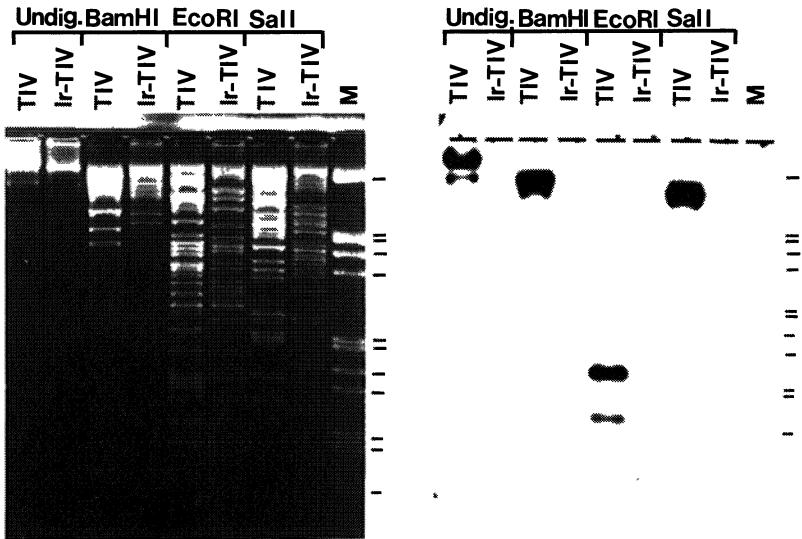


Figure 4. Comparison of two TIV isolates for the presence of S1 DNA. A) A 0.7% agarose gel of undigested and digested TIV DNA and TIV DNA from an Irish isolate. Note the presence of S1 DNA in the TIV but not the Ir-TIV sample. B) To determine if S1 DNA is present in the Ir-TIV sample, the gel in A was blotted and hybridized as described in Figure 3. See Figure 2 for markers (M).

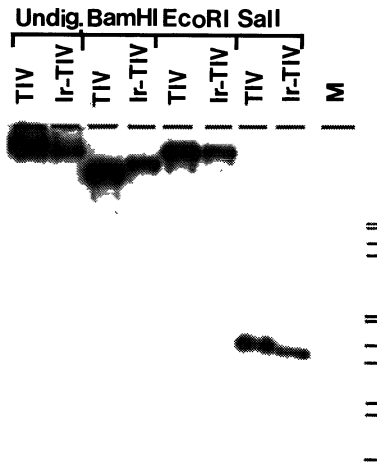


Figure 5. Hybridization of TIV and Ir-TIV DNA with the TIV capsid gene. The blot from Figure 4 was reused to hybridize with HindIII fragment #26b containing the TIV capsid gene (65). See Figure 2 for markers (M).

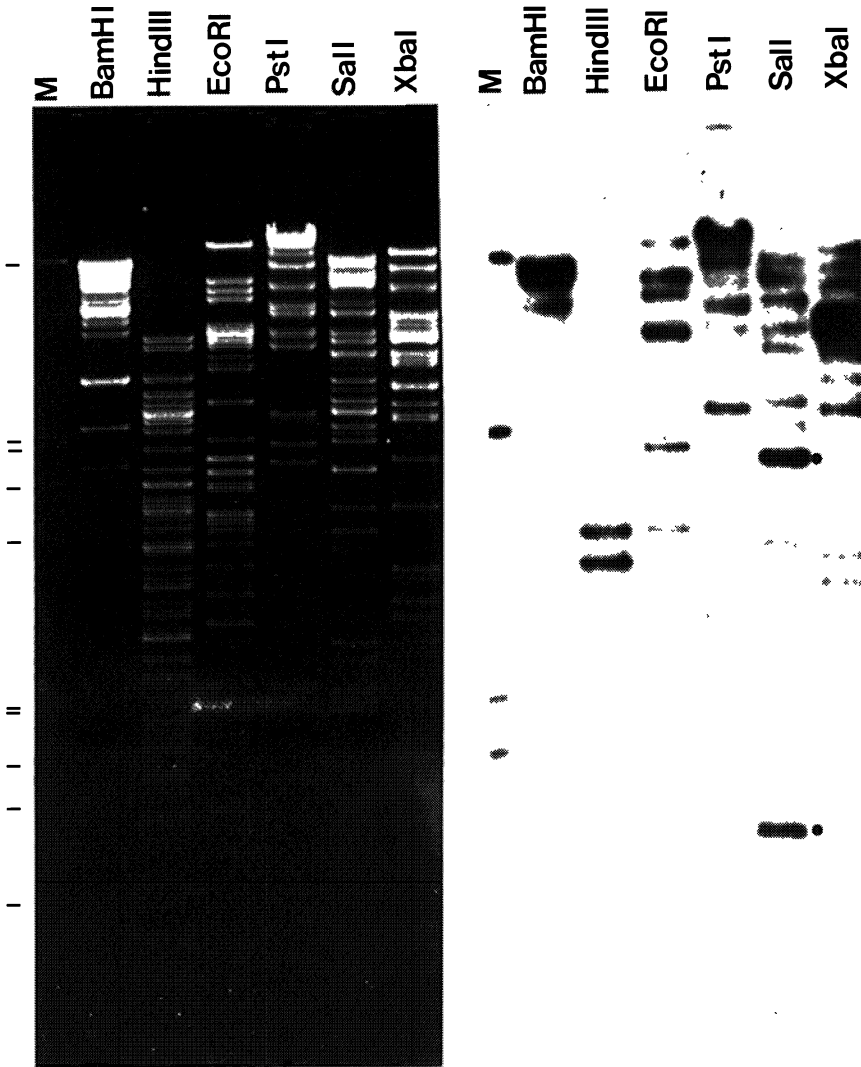


Figure 6. Hybridization analysis of the major TIV transcripts. A) A 0.7% agarose gel of undigested and endonuclease digested TIV DNA. B) Total RNA was extracted from TIV-infected *A. albopictus* cells at 13 h p.i. and radiolabelled single-stranded cDNA was made using AMV reverse transcriptase and oligo dT as primer. This cDNA was then used as probe to hybridize against an alkaline transfer of the DNA in A. Radiolabelled marker (M) is lambda DNA digested with HindIII and EcoRI (see legend to Figure 2 for sizes). Dots indicate Sall # 24a and #36 (88).

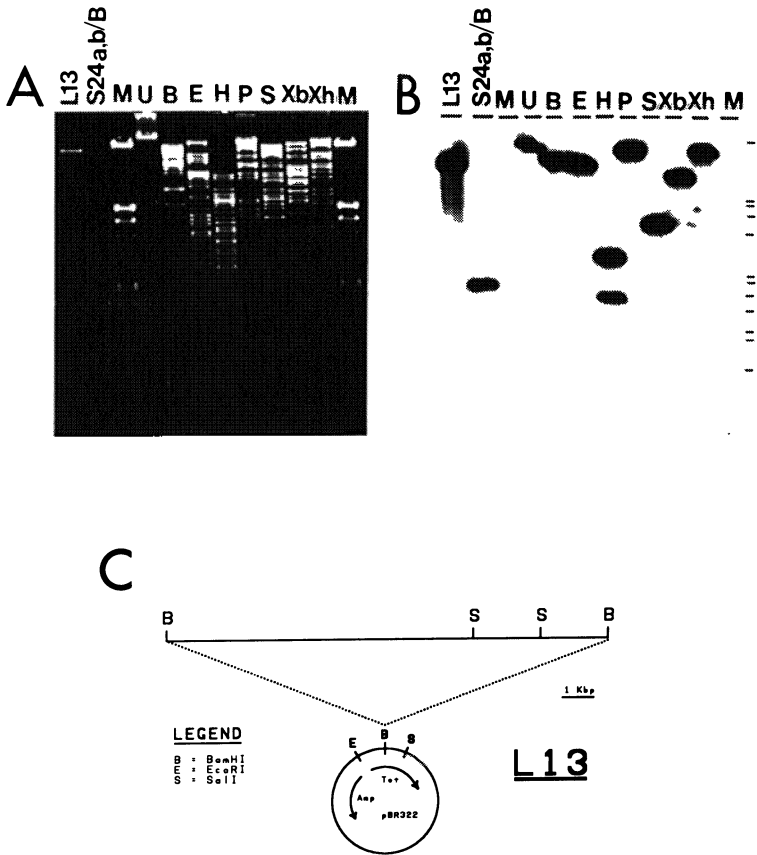


Figure 7. Hybridization of the AB1 gene to TIV DNA digests. TIV DNA was digested with various restriction endonucleases, electrophoresed in 0.7% agarose (A) and alkaline transferred to nylon (Hybond) membrane. (B) X-ray film of a hybridization using insert DNA from SL13-1A radiolabelled with ^{32}P by nucleotide chain extension using random primers. The first lane contains L13 insert DNA. The adjacent lane contains a mixture of SalI fragments 24a,b digested with BamHI. (C) Restriction endonuclease map of plasmid L13 from which clone SL13-1A was obtained. M = markers; lambda digested with HindIII/EcoRI (see legend to Figure 2); U = Undigested TIV DNA; B = BamHI; E = EcoRI; H = HindIII; P = PstI; S = SalI; Xb = XbaI; Xh = XhoI.

SalI fragment #24a. This 2.2 kbp SalI/BamHI fragment was subsequently cloned into M13 mp19 and called SL13-1A. Hybridization of insert DNA from SL13-1A back to digests of TIV DNA (results shown in Figure 7A, B) confirmed that this fragment is a subset of SalI

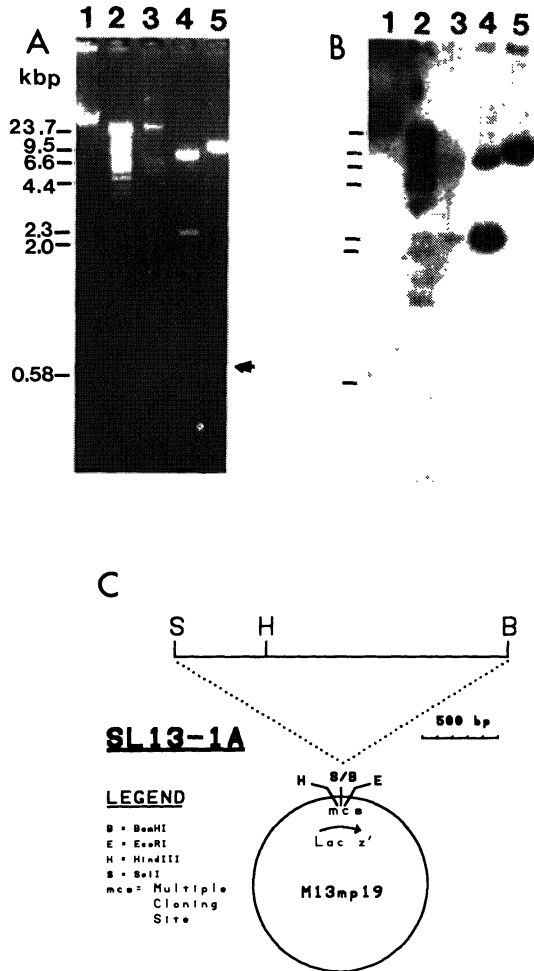


Figure 8. Mapping of the AB1 gene on SL13-1A. SL13-1A RF DNA was restriction endonuclease digested, electrophoresed in 1% agarose (A) and alkaline transferred to nylon (Biotrans) membrane. Radiolabelled cDNA, made by oligo dT priming of *E. acra* RNA isolated 16 h after TIV infection, was hybridized to this blot (B). Marker sizes for lambda DNA digested with HindIII are indicated. (C) Restriction map of SL13-1A. Lane 1 = total TIV DNA; Lane 2 = Sall digested TIV DNA; Lane 3 = single stranded DNA from SL13-1A; Lane 4 = SL13-1A digested with Sall/BamHI; Lane 5 = SL13-1A digested with HindIII; Arrow = 600 bp HindIII fragment.

fragment #24a and is present as a single copy in the genome. Hybridization of ^{32}P -labelled cDNA made from 16 h total TIV-infected *E. acraea* RNA revealed that the 1600 bp HindIII/BamHI of SL13-1A contains the AB1 gene (Figure 8A, B). In addition, single stranded template prepared from SL13-1A failed to hybridize with the radiolabelled cDNA (Figure 8A, B; lane 3) suggesting that this template (plus strand) contains the DNA coding strand for the AB1 gene. The SL13-1A clone was used to screen a cDNA band and several cDNA clones were subsequently isolated. The genomic and cDNA clones are currently being analysed by sequencing to determine if TIV transcripts are polyadenylated. The AB2 gene is also being studied by DNA sequencing.

Analysis of TIV proteins

Although the cDNA hybridization approach was not successful in determining the relative abundance of the TIV capsid transcript, we investigated the relative abundance of the capsid protein in virions using several protein detection methods. These methods involved the use of protein binding reagents such as silver and Coomassie Blue, and radioactive labelling with ^{35}S -methionine. A preliminary comparison of these techniques was conducted in order to evaluate the relative abundance of the capsid protein compared to the other virion proteins. Such a comparison, shown in Figure 9, revealed the presence of 25-30 polypeptides. These results are in good agreement with an earlier study on TIV, using a different electrophoretic system, that TIV virions contained 28 polypeptides with a total estimated molecular weight of 1.72×10^6 Da (46). Assuming that all these polypeptides are encoded by TIV, this value corresponds to 30-40% of the coding capacity of the TIV genome. Our analysis in Figure 9 indicated, as expected, that the 50 kDa capsid protein (size determined from gene sequence, 65) is the most abundant protein in the virion. However, some striking differences were evident when some of the other minor proteins were examined. For example, silver staining of virion proteins revealed the presence of an intensely staining 33 kDa protein, and a 29 kDa that was barely detectable. In contrast, Coomassie Blue staining of an identical viral preparation revealed these bands to be of equivalent staining intensity. These dramatic differences can be attributed to the specific properties of the protein that is being detected. Tal and coworkers (139) reported a strong correlation between the intensity of response to Coomassie dyes and the basicity of a protein, which depends on the number of lysine, histidine, and arginine residues, and the nature of the N-terminal amino acid. These authors also reported that hydrophobic interactions of the dye molecule with the polypeptide backbone adjacent to positively charged amino acids, enhances the binding. The Coomassie R molecule contains two sulfonic groups and three nitrogens, two of which are likely positively charged under the staining conditions (139). According to these studies, the binding of Coomassie R to proteins is a consequence of electrostatic forces between the sulfonic groups and the basic

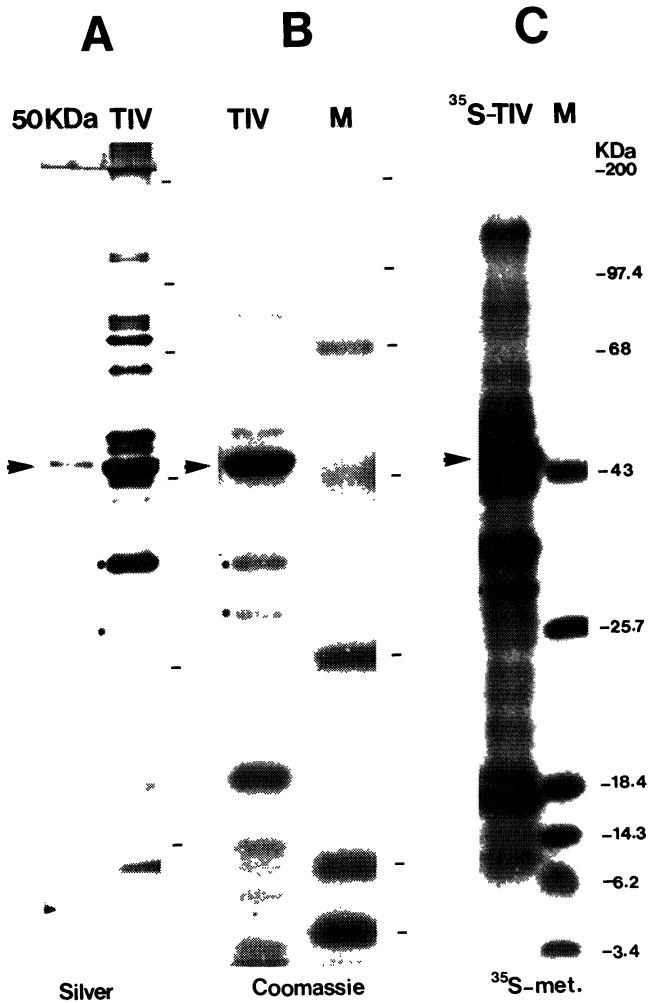


Figure 9. A comparison of TIV proteins using various protein detection methods. Purified TIV was analyzed by SDS-PAGE (4% stack/10% base) and either silver (A) or Coomassie blue (B) stained. (C) Fluorograph of ³⁵S-methionine labelled virions from *E. acrea* cells (65). The capsid protein (arrow) and minor proteins are indicated (dots; see text).

amino acids as well as hydrophobic interactions with the peptide backbone. The number of dye molecules bound was found to be approximately proportional to the number of

positively charged amino acids in the protein, therefore, estimation of the relative molar ratios of proteins in a sample is possible if the sequence is known. Our studies have indicated that the capsid protein contains 35 basic amino acid residues, the predominant one being arginine (20 residues) (65).

Although silver staining of proteins in gels is reported to be up to 100 times more sensitive than Coomassie Blue staining, the basis of the silver stain is not as well defined and extreme caution has been suggested for quantitation of proteins following silver staining (140, 141). Additionally, lipopolysaccharides have been shown to stain with silver (142). Nielsen and Brown (140) suggested that the different shades of blue, yellow, red, and gray that characterize different proteins stained with silver, can be predicted if the amino acid sequence is known. Further, they suggested that the color of protein/silver complexes is related to the binding of silver to the side chains of charged amino acids. In contrast, Chuba and Palchaudhuri (141) showed a strong correlation existed between increased staining with silver and the cysteine content of the protein. Regarding the mechanism of action, Dion and Pomenti (143) reported that protein-aldehyde adducts that result from glutaraldehyde pretreatment, directly participate in metallic silver deposition in a manner that resembles latent image formation in the photographic process. Although the precise mechanisms for these protein stains remains obscure, it is evident that quantitation of proteins using Coomassie Blue staining gives a more reliable indication of the relative quantities of proteins than does staining with silver.

Lastly, quantitation using ^{35}S -methionine labelling is dependent on the methionine content of the protein. We know from translation of the capsid DNA sequence that the capsid protein contains 9 methionine residues (65). Cell associated capsid protein was found to be the third most abundant *de novo* synthesized protein in infected cells as determined by ^{35}S -methionine labelling, however, our analysis of ^{35}S -labelled TIV indicated that the capsid protein was the most abundant protein in virions (Figure 9; 65). For a more accurate evaluation of the relative abundance of proteins, it would be suitable to label proteins with a mixture of labelled amino acids such that none of these precursor molecules are limiting during the synthesis of the protein(s). This approach should help minimize some of the obvious biases inherent in the techniques discussed above.

TIV capsid protein stability. On one occasion over the course of our studies, during conventional purification of TIV from *G. mellonella*, it was found that the sucrose gradient fractionation yielded a much wider top component band. After further purification of this band by sucrose and CsCl gradients, EM observations revealed that this band contained numerous small icosahedral particles ~26 nm in diameter that were not as intensely stained as "full" or "empty" TIV virions which measured about 130 nm (see Figure 10A, B). These small particles were non-occluded but were sometimes associated loosely with

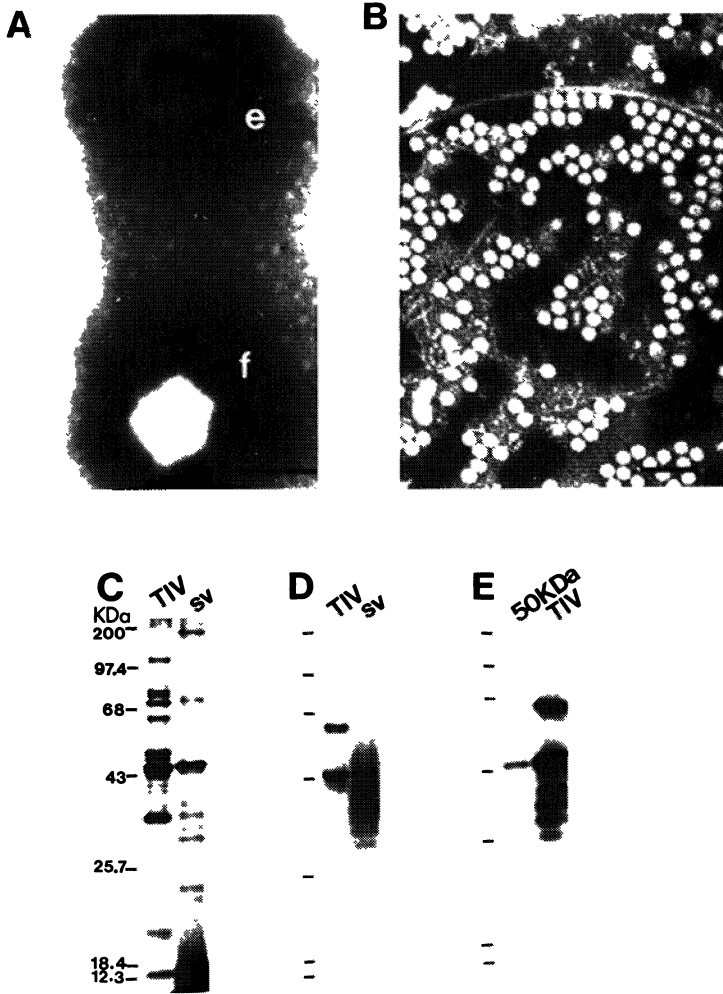


Figure 10. Comparison of TIV and small icosahedral virus (sv) particles from *G. mellonella*. (A) and (B) Negatively stained electron micrographs of TIV and small icosahedral particles, respectively. Silver stain (C) and western analysis (D) of TIV (lane 1) and sv (lane 2) particles. (E) Western analysis using ^{125}I protein A of TIV frozen and thawed ~ 10 times (lane 2). Lane 1 contains purified capsid protein. Western analysis was done as described in Materials and Methods. Bar represents 80 nm.

membranous material or engulfed within a membrane. However, most often these particles appeared free, or arranged in arrays. Small particles have been previously reported by Yule (144), in *G. mellonella* larvae; these particles were estimated to be about 50 nm in size. In this study, it was initially thought that these particles may be due to a contaminating latent virus induced from the larvae. However, SDS-PAGE analysis, Coomassie Blue (not shown) and silver staining (Figure 10C) revealed the presence of a major band co-migrating with the major TIV capsid protein, and some other minor bands. Further, no nucleic acid other than the TIV DNA regular components (L and S1) were isolated from this sucrose gradient fraction. Repeated attempts were made in this study to obtain a homogeneous sample from this fraction that was devoid of the larger TIV particles, but such a homogeneous sample was difficult to obtain because of the tendency of these particles to aggregate. Whether the 26 nm particles are comprised of aggregated capsid protein and/or breakdown products of TIV virions has not yet been determined.

The capsid protein was found to be quite stable since long term storage at 4°C (over 3 years) resulted in at least 30% of the protein remaining intact and of the expected size (46 kDa) as seen by SDS-PAGE followed by silver staining and western analysis (Figure 10C, D). The degraded capsid protein formed discrete bands as a consequence of long term storage at 4°C (Figure 10D). This phenomenon was also observed by western analysis of virus that had been extensively frozen and thawed (Figure 10E).

CONCLUSIONS

The TIV which we are studying has a fairly complex genome consisting of two major DNA components, L (176-247 kbp) and S1 (10.8 kbp). The S1 DNA component that exists both as a free molecule and integrated, at least in part, in the major genomic component of TIV is of particular interest (22, 65, 88, 107, 111; present study). The studies presented here further show that a TIV isolated from Ireland lacked this sequence, implying that this DNA component is not essential for a productive TIV infection. We are currently investigating this DNA component in detail by transcript analysis and DNA sequencing to determine its exact location in L, its possible origin and whether it can replicate autonomously in insect cells. Additionally, the nature of the TIV DNA termini is being investigated since circular permutation and terminal redundancy has been shown for FV3, FLDV, and CIV. The finding that TIV DNA is not methylated suggests that this virus differs from some of the other *Iridoviridae* members. DNA sequence comparisons are also being made between genomic and cDNA clones to help determine if, unlike FV3, TIV transcripts are polyadenylated. DNA sequence analysis of TIV genes should also allow sequence comparisons to be made with the consensus regulatory sequences from other systems. Finally, our investigations of the TIV proteins and expression of these proteins,

particularly the capsid protein, could give us insights into the complexities of virion assembly.

ACKNOWLEDGEMENTS

We would like to thank M. Kelly for kindly providing us with the Irish TIV strain. This work was partially supported by an NSERC fellowship to S. Tajbakhsh and NSERC and NRCC intramural funds to V. L. Seligy. This is NRCC publication no. 29933.

REFERENCES

1. Xeros, N. *Nature* **174**: 562-563, 1954.
2. Smith, K. M. and Williams, R. C. *Endeavour* **17**: 12-21, 1958.
3. Youngusband, H. B. and Lee, P. E. *Virology* **38**: 247-254, 1969.
4. Manyakov, V. F. *J. gen. Virol.* **36**: 73-79, 1977.
5. Williams, R. C. and Smith, K. M. *Nature* **179**: 119-120, 1957.
6. Caspar, D. L. D. and Klug, A. *Cold Spring Harbor Symp. Quant. Biol.* **27**: 1-24, 1957.
7. Matthews, R. E. F. *Intervirology* **17**: 56-58, 1982.
8. Willis, D. B., Goorha, R. and Chinchar, V. G. *Curr. Top. Microbiol. Immunol.* **116**: 77-106, 1985.
9. Viñuela, E. (1985). *Curr. Top. Microbiol. Immunol.* **116**: 151-170, 1985.
10. Flügel, R. M. *Curr. Top. Microbiol. Immunol.* **116**: 133-150, 1985.
11. Devauchelle, G., Stoltz, D. B. and Darcy-Tripier, F. *Curr. Top. Microbiol. Immunol.* **116**: 1-21, 1985.
12. Van Etten, J. L., Burbank, D. E., Kuczarski, D. and Meints, R. H. *Science* **219**: 994-996, 1983.
13. Meints, R. H., Lee, K. and Van Etten, J. L. *Virology* **154**: 240-245, 1986.
14. Smith, K. M., Hills, G. J. and Rivers, C. F. *Virology* **13**: 233-241, 1961.
15. Thomas, R. S. *Virology* **14**: 240-252, 1961.
16. Glitz, D. G., Hills, G. J. and Rivers, C. F. *J. gen. Virol.* **3**: 209-220, 1968.
17. Kalmakoff, J. and Tremaine, J. H. *J. Virol.* **2**: 738-744, 1968.
18. Williams, R. C. and Smith, K. M. *Biochem. Biophys. Acta.* **28**: 464-469, 1958.
19. Klug, A., Franklin, R. E. and Humphreys-Owen, S. P. F. *Biochem. Biophys. Acta.* **32**: 203-219, 1959.
20. Wrigley, N. G. *J. gen. Virol.* **5**: 123-134, 1969.
21. Stoltz, D. B. *J. Ultrastruct. Res.* **43**: 58-74, 1973.
22. Tajbakhsh, S., Dove, M. J., Lee, P. E., and Seligy, V. L. *Biochem. Cell Biol.* **64**: 495-503, 1986.
23. Bellet, A. J. D. and Inman, R. B. *J. Mol. Biol.* **25**: 425-432, 1967.
24. Mathieson, W.B. A cytological and biochemical study of *Estigmene acrea* continuous cell cultures infected with *Tipula* iridescent virus. M.Sc. Thesis, Carleton University, Ottawa, Canada, 1978.
25. Kelly, D. C. *Curr. Top. Microbiol. Immunol.* **116**: 23-35, 1985.
26. Hall, D. W. *Viral insecticides for biological control* (Eds. K. Maramorosch and K. E. Sherman). Academic Press, Inc. USA. p. 163-196, 1985.
27. Kelly, D. C. and Tinsley, T. W. *J. Invertebr. Pathol.* **22**: 199-202, 1973.
28. Kelly, D. C., Elliot, R. M., and Blair, G. E. *J. gen. Virol.* **48**: 205-212, 1980.
29. Monnier, C. and Devauchelle, G. *J. Virol.* **19**: 180-186, 1976.
30. Monnier, C. and Devauchelle, G. *J. Virol.* **35**: 444-450, 1980.
31. Franke, C. A. and Hruby, D. E. *Vith Poxvirus/Iridovirus workshop*; Sept. 24-28; Cold Spring Harbor Laboratory, 1986.

32. Kelly, D. C. and Robertson, J. S. *J. gen. Virol.* 20: 17-41, 1973.
33. Desser, S. S. and Barta, J. R. *Can. J. Zool.* 62: 1521-1524, 1984.
34. Gruia-Gray, J., Petric, M., and Desser, S. S. VII International Congress of Virology, Aug. 9-14. Edmonton, Alberta, Canada, 1987.
35. Kelly, D. C. *J. gen. Virol.* 63: 1-13, 1982.
36. Cuillel, M., Tripier, F., Braunwald, J. and Jacrot, B. *Virology* 99: 277-285, 1979.
37. Darcy-Tripier, F., Nermut, M. V., Braunwald, J. and Williams, L. D. *Virology* 138: 287-299, 1984.
38. Willis, D. B. and Granoff, A. *Virology* 61: 256-269, 1974.
39. Wagner, G. W., Webb, S. R., Paschke, J. D., Campbell, W. R. *Virology* 64: 430-437, 1975.
40. Klump, H., Beaumais, J. and Devauchelle, G. *Arch. Virol.* 75: 269-276, 1983.
41. Day, M. F. and Mercer, E. H. *Aust. J. Biol. Sci.* 17: 892-902, 1964.
42. Braunwald, J., Tripier, F. and Kirn, A. *J. gen. Virol.* 45: 673-682, 1979.
43. Stoltz, D. B. *J. Ultrastruct. Res.* 37: 219-239, 1971.
44. Yamamoto, T., McDonald, R. D., Gillespie, D. C., and Kelly, R. K. *J. Fish Res. Board Can.* 33: 2408-2419, 1976.
45. Willison, J. H. M. and Cocking, E. C. *J. Micros.* 95: 397-411, 1972.
46. Krell, P. and Lee, P. E. *Virology* 60: 315-326, 1974.
47. Lee, P. E. and Brownrigg, S. *J. Ultrastruct. Res.* 79: 189-197, 1982.
48. Kelly, D. C. and Tinsely, T. W. *J. Invertebr. Pathol.* 19: 273-275, 1972.
49. Willis, D. B., Goorha, R., Miles, M. and Granoff, A. *J. Virol.* 24: 326-342, 1977.
50. Black, P. N., Blair, C. D., Butcher, A., Capinera, J. L. and Happ, G. M. *J. Invertebr. Pathol.* 38: 12-21, 1981.
51. Tripier-Darcy, F., Braunwald, J. and Kirn, A. *Virology* 116: 635-640, 1982.
52. Moore, N. F. and Kelly, D. C. *J. Invertebr. Pathol.* 36: 415-422, 1980.
53. Wagner, G. W., Paschke, J. D., Campbell, W. R. and Webb, S. R. *Intervirology* 3: 97-105, 1974.
54. Goorha, R. and Granoff, A. *Comprehensive Virology* (Eds. R. R. Wagner and H. Fraenkel-Conrat). Plenum, New York. Vol. 14: 347-399, 1979.
55. Aubertin, A. M., Tondre, L., Martin, J. P. and Kirn, A. *FEBS Letters* 112: 233-238, 1980.
56. Harrison, S. *Virology* (Ed. B. N. Fields). Raven Press, New York. p. 27-44, 1985.
57. Finch, J. T. and Klug, A. *Nature* 183: 1709-1714, 1959.
58. Wrigley, N. G. *J. gen. Virol.* 6: 169-173, 1970.
59. Smith, K. M. *J. Biophys. Biochem. Cytol.* 2: 301-306, 1956.
60. Bird, F. T. *Can. J. Microbiol.* 7: 827-830, 1961.
61. Xeros, N. *J. Insect Pathol.* 6: 261-283, 1964.
62. Yule, B. G. and Lee, P. E. *Virology* 51: 409-423, 1973.
63. Horwitz, M. S. *Virology* (Ed. B. N. Fields). Raven Press, New York. p. 433-476, 1985.
64. Roizman, B. and Batterson, W. *Virology* (Ed. B. N. Fields). Raven Press, New York. p. 497-526, 1985.
65. Tajbakhsh, S., Lee, P. E. and Seligy, V. L. Isolation and characterization of the *Tipula* iridescent virus capsid gene. In preparation.
66. Fowler, M. and Robertson, J. S. *J. Invertebr. Pathol.* 19: 154-155, 1972.
67. Carter, J. B. *J. Invertebr. Pathol.* 21: 123-130, 1973.
68. Carter, J. B. *J. Invertebr. Pathol.* 21: 136-143, 1973.
69. Carter, J. B. *J. Invertebr. Pathol.* 24: 271-281, 1974.
70. Hukuhara, T. *J. Insect Pathol.* 6: 246-249, 1966.
71. Runnger, D., Rastelli, M., Braendle, E. and Malsberger, R. G. *J. Invertebr. Pathol.* 17: 72-80, 1971.
72. Wigglesworth, V. B. *Insect Physiology* (8th ed.). Chapman and Hall. Oxford. p. 1-191, 1984.
73. Goorha, R., Willis, D. B., and Granoff, A. *J. Virol.* 21: 802-805, 1977.

74. Goorha, R., Murti, G., Granoff, A. and Tirey, R. *Virology* **84**: 32-50, 1978.
75. Mathieson, W. B. and Lee, P. E. *J. Ultrastruct. Res.* **74**: 59-68, 1981.
76. Kloc, M., Lee, P. E., Tajbakhsh, S. and Matthie, B. D. *J. Invertebr. Pathol.* **42**: 113-123, 1983.
77. Kloc, M., Lee, P. E. and Tajbakhsh, S. *J. Invertebr. Pathol.* **43**: 114-123, 1984.
78. Murti, K. G. and Goorha, R. *J. Cell Biol.* **96**: 1248-1257, 1983.
79. Murti, K. G., Porter, K. R., Goorha, R., Ulrich, M. and Wray, G. *Exp. Cell Res.* **154**: 270-282, 1984.
80. Murti, K. G., Goorha, R. and Klymkowsky, M. W. *Virology* **162**: 264-269, 1988.
81. Seagull, R., Lee, P. E. and Frosch, M. *Can. J. Biochem. Cell Biol.* **63**: 543-552, 1985.
82. Bertin, J., Frosch, M. and Lee, P. E. *Eur. J. Cell Biol.* **43**: 215-222, 1987.
83. Bladon, T., Frosch, M., Sabour, P. M. and Lee, P. E. *Virology* **155**: 524-533, 1986.
84. Wagner, R. R. *Comprehensive Virology* (Eds. H. Fraenke-Conrat and R. Wagner). Plenum Press, New York. **19**: 1-63, 1984.
85. Chinchar, V. G. and Caughman, G. B. *Virology* **152**: 466-471, 1986.
86. Willis, D. B. and Granoff, A. *Virology* **70**: 397-410, 1976.
87. Pogo, B. G. and Dales, S. *Proc. Natl. Acad. Sci. USA* **70**: 1726-1729, 1973.
88. Tajbakhsh, S., Kiss, G., Lee, P. E. and Seligy, V. L. Semipermissive replication of *Galleria mellonella*-*Tipula* iridescent virus in *Aedes albopictus* C6/36 cells. Submitted.
89. Moss, B. *Virology* (Ed. B. N. Fields). Raven Press, New York. p. 685-703, 1985.
90. Eggerding, F. A. and Pierce, W. C. *Virology* **148**: 97-113, 1986.
91. Gallimore, P. H. *J. gen. Virol.* **25**: 263-273, 1974.
92. Baum, S. G. *J. Virol* **23**: 412-420, 1977.
93. Hashimoto, K., Nakajima, K., Oda, K. and Shimojo, H. *J. Mol. Biol.* **81**: 207-223, 1973.
94. Nakajima, K. and Oda, K. *Virology* **67**: 85-93, 1975.
95. Klessig, D. F. and Chow, L. T. *J. Mol. Biol.* **139**: 221-242, 1980.
96. Mitsuhashi, J. *Biomed. Res.* **2**: 599-606, 1981.
97. Delius, H., Darai, G., Flügel, R. M. *J. Virol.* **49**: 609-614, 1984.
98. Goorha, R. and Murti, K. G. *Proc. Natl. Acad. Sci. USA* **79**: 248-252, 1982.
99. Darai, G., Anders, K., Koch, H.-G., Delius, H., Gelderblom, H., Samalecos, C. and Flügel, R. M. *Virology* **126**: 466-479, 1983.
100. Miller, R. C. *Ann. Rev. Microbiol.* **29**: 355-376, 1975.
101. Skalka, A. M. *Curr. Top. Microbiol. Immunol.* **78**: 201-237, 1977.
102. Goorha, R. *J. Virol.* **37**: 496-499, 1981.
103. Goorha, R. *J. Virol.* **43**: 519-528, 1982.
104. Willis, D. B., Foglesong, D. and Granoff, A. *J. Virol.* **53**: 905-912, 1984.
105. Beckman, W., Tham, T. N., Aubertin, A. M. and Willis, D. B. *J. Virol.* **62**: 1271-1277, 1988.
106. Willis, D. B. and Granoff, A. *Virology* **73**: 543-547, 1976.
107. Tajbakhsh, S., Lee, P. E. and Seligy, V. L. *Invertebrate Cell Systems Applications* (Ed. J. Mitsuhashi). Chapter 6. CRC press, Inc., 1989.
108. Wagner, G. W. and Paschke, J. D. *Virology* **81**: 298-308, 1977.
109. Krell, P. J., Summers, M. D. and Vinson, S. B. *J. Virol.* **43**: 859-870, 1982.
110. Blissard, G. W., Fleming, J. G. W., Vinson, S. B. and Summers, M. D. *J. Insect Physiol.* **32**: 351-359, 1986.
111. Tajbakhsh, S. Isolation and characterization of the *Tipula* iridescent virus capsid gene. Ph. D. Thesis, Carleton University, Ottawa, Canada, 1988.
112. Sambrook, J., Botchan, M., Gallimore, P., Ozanne, B., Pettersson, U., Williams, J. and Sharp, P. A. *Cold Spring Harbor Symp. Quant. Biol.* **39**: 615-632, 1974.
113. Borgaux, P., Sylla, B. S. and Chartrand, P. *Virology* **122**: 84-97, 1982.
114. Younghusband, H. B. Some aspects of the replication of *Tipula* iridescent virus in hemocytes of *Galleria mellonella* (L.). M.Sc. Thesis, Carleton University, Ottawa, Canada, 1969.

115. Hanahan, D. DNA cloning (Ed. D. M. Glover). IRL press, Oxford. Vol I. p. 109-135, 1985.
116. Messing, J. Meth. Enzymol. 101: 20-78, 1983.
117. Maniatis, T., Fritsch, E. F. and Sambrook, J. Cold Spring Harbor Laboratory, Cold Spring Harbor, N.Y., 1982.
118. Reed, K. C. and Mann, D. A. Nucl. Acid Res. 13: 7207-7221, 1985.
119. Wahl, G. M., Stern, M. and Stark, G. R. Proc. Natl. Acad. Sci. USA 76: 3683-3687, 1979.
120. Rigby, P. W. J., Diekmann, M., Rhodes, C. and Berg, P. J. Mol. Biol. 113: 237-251, 1977.
121. Feinberg, A. P. and Vogelstein, B. Anal. Biochem. 132: 6-13, 1983.
122. Berger, S. L. Anal. Biochem. 136: 515-519, 1984.
123. Morrissey, J. H. Anal. Biochem. 117: 307-310, 1981.
124. Towbin, H., Staehelin, T. and Gordon, J. Proc. Natl. Acad. Sci. USA 76: 4350-4354, 1979.
125. McConahey, P. J. and Dixon, F. J. Meth. Enzymol. 70: 210-213, 1980.
126. Hibbin, J. A. and Kelly, D. C. Arch. Virol. 68: 9-18, 1981.
127. Ward, V. K. and Kalmakoff, J. Virology 160: 507-510, 1987.
128. Razin, A. and Riggs, A. D. Science 210: 604-610, 1980.
129. Youssoufian, H., Hammer, S. M., Hirsch, M. S. and Mulder, C. Proc. Natl. Acad. Sci. USA 79: 2207-2210, 1982.
130. Willis, D. B. and Granoff, A. Virology 107: 250-257, 1980.
131. Waalwijk, C. and Flavell, R. A. Nucl. Acids Res. 5: 3231-3236, 1978.
132. Wagner, H., Simon, D., Werner, E., Gelderblom, H., Darai, G. and Flügel, R. M. J. Virol. 53: 1005-1007, 1985.
133. Thomas, R. S. Virology 14: 240-252, 1961.
134. Wittek, R., Hanggi, M. and Hiller, G. J. Virol. 49: 371-378, 1984.
135. Tham, T. N., Mesnard, J. M., Tondre, L. and Aubertin, A. M. J. gen. Virol. 67: 301-308, 1986.
136. Heine, J. W., Honess, R. W., Cassai, E. and Roizman, B. J. Virol. 14: 640-651, 1974.
137. Horwitz, M. S., Scharff, M. D. and Maizel Jr., J. V. Virology 39: 682-694, 1969.
138. Maeda, S., Kawai, T., Obinata, M., Fujiwara, H., Horiuchi, T., Saeki, Y., Sato, Y. and Furusawa, M. Nature 315: 592-594, 1985.
139. Tal, M., Silberstein, A. and Nusser, E. J. Biol. Chem. 260: 9976-9980, 1985.
140. Nielsen, B. L. and Brown, L. R. Anal. Biochem. 141: 311-315, 1984.
141. Chuba, P. J. and Palchaudhuri, S. Anal. Biochem. 156: 136-139, 1986.
142. Tsai, C.-M. and Frasch, C. E. Anal. Biochem. 119: 115-119, 1982.
143. Dion, A. S. and Pomenti, A. A. Anal. Biochem. 129: 490-496, 1983.
144. Yule, B. G. An immunological and cytological study of *Tipula* iridescent virus in hemocytes of *Galleria mellonella* (L.). M.Sc. Thesis, Carleton University, Ottawa, Canada, 1971.

3

MOLECULAR BIOLOGY OF INSECT IRIDESCENT VIRUS TYPE 6

Michaela Fischer, Paul Schnitzler, Hajo Delius*, Angela Rösen-Wolff, and Gholamreza Darai

Institut für Medizinische Virologie an der Universität Heidelberg, Im Neuenheimer Feld 324, 6900 Heidelberg and *Institut für Angewandte Tumorstudiologie am Deutschen Krebsforschungszentrum Heidelberg, Im Neuenheimer Feld 506, 6900 Heidelberg, Federal Republic of Germany

ABSTRACT

The genome of the insect iridescent virus type 6 -Chilo iridescent virus (CIV)- contains a double-stranded linear DNA molecule of 209 kbp which is circularly permuted and terminally redundant. A defined and complete gene library of the viral genome was established which represents 100% of the CIV DNA sequences. The physical maps of the viral genome were constructed for the restriction enzymes ApaI, Asp718, BamHI, EcoRI, NcoI, PvuII, SalI, SphI, and SmaI. Although the CIV genome is linear the restriction maps of the viral genome are circular due to circular permutation of the CIV DNA molecule. The CIV genome contains repetitive DNA sequences located in the EcoRI DNA fragments H and PvuII CIV DNA fragment L (5064 bp) at the coordinates 0.535 to 0.548 and 0.920 to 0.944, respectively. A DNA element (91 bp) at the nucleotide position 1981 to 2072 of the EcoRI CIV DNA fragment H had been found to be complementary (>90%) to nine regions of the PvuII DNA fragment L. A stem-loop structure has been identified by heteroduplex mapping at the genome coordinates 0.571 to 0.582 (HindIII/EcoRI subfragment (2555 bp) of the EcoRI

CIV DNA fragment H). The DNA nucleotide sequence of the PvuII DNA fragment L contains many perfect direct repeats of sizes up to 145 bp. In addition to these repetitions a cluster of four imperfect repetitive DNA elements (R1 to R4) with a complex structural arrangement was detected. R1, R2 and R3 exist in duplicate (two boxes (B)) between nucleotide positions 271 to 3466). The R4 repetitive element was found in 12 boxes (between bases 1301 and 4417). Five open reading frames (ORFs of 118 to 333 amino acid (AA) residues) were detected. The analysis of the amino acid sequences of the largest ORF revealed that the deduced amino acid sequence of the putative gene product contains two repetitions. Sequences of 43 amino acid residues of ORF 5 (160 to 202 AA) were found to be homologous within the majority of ORFs. A consensus sequence -MANL(X)₆ IGSSST(X)₆ L(X)₁ LGS(X)₁ LQISG(X)₂ L(X)₁ VN- was found in all five ORFs. The origins of DNA replication of the CIV genome were identified within the DNA sequences of the EcoRI DNA fragments C (13.5 kbp, 0.909 to 0.974 map units (m.u.)), H (9.8 kbp, 0.535 to 0.582 m.u.), M (7.3 kbp, 0.310 to 0.345 m.u.), O (6.6 kbp, 0.196 to 0.228 m.u.), Q (5.9 kbp, 0.603 to 0.631 m.u.), and Y (2.0 kbp, 0.381 to 0.391 m.u.).

INTRODUCTION

Iridoviruses are icosahedral cytoplasmic DNA viruses which have been isolated from a variety of invertebrate and vertebrate host species, principally from insects. Tinsley and Kelly (1) have suggested a provisional classification scheme whereby isolates are listed in numerical sequence according to their date of isolation.

Iridovirus type 6 or Chilo iridescent virus (CIV) was isolated by Fukaya and Nasu (2) from the rice stem borer, Chilo suppressalis (Lepidoptera); this virus occurs in Japan and the United States (3). CIV might be of agricultural importance, since it has been shown to

infect the green rice leafhopper Nephtotettix cincticeps and to be lethal for 99% of the leafhopper Colladonus montanus (Homoptera: Cicadellidae), the vector of a mycoplasma agent of stone fruits (4). Serological studies by Kelly et al. (5) have shown that CIV is not closely related to any of the 29 iridoviruses isolated so far (6). The first analysis of the DNA properties of CIV such as G+C content and molecular weight were performed in 1967 by Bellet and Inman (7). However, the discovery of the circular permutation and terminal redundancy in frog virus 3 (FV3) (8) and fish lymphocystis disease virus (FLDV) (9, 10) both members of the Iridoviridae family (11), made it necessary to analyse the structural properties of the genomes of the members of the other genera of this interesting virus family. From this point of view and with respect to the fact that CIV can be utilized in agriculture and be considered as a biological insecticide, e.g. to eliminate plant diseases transmitted by insects in which CIV induces a lethal infection, we chose the CIV as a suitable candidate for genetic analyses.

MATERIALS AND METHODS

The experimental approach for this study (e.g. isolation and purification of virions, DNA extraction, electron microscopy, restriction enzyme analysis, nick translation, DNA hybridization, molecular cloning, physical mapping, DNA nucleotide sequence determination, and computer-assisted analysis) was carried out as described previously (12-17).

RESULTS

STRUCTURE OF THE VIRAL GENOME

Circular permutation of the viral genome

The analysis of the CIV genome by electron microscopy revealed that the majority of the DNA molecules were linear double-stranded DNA with a size of

above $84.9 \pm 1.1 \mu\text{m}$ corresponding to 238 kilobase pairs (kbp) (12). However, the self-annealed single-stranded viral DNA led to the formation of double-stranded circular DNA molecules with single-stranded protruding tails (12). The average size of the reannealed circles was found to be $76.9 \pm 2.6 \mu\text{m}$, corresponding to 209 kbp. An example of this study which had been described previously (12) is shown in Fig. 1. This analysis indicate that the circles were obtained by the reannealing of two single strands which were terminally redundant and circularly permuted.

To test for a circularly permuted DNA structure, a combined 3' Escherichia coli exonuclease III digestion of the CIV DNA was performed. This study revealed that all resulting DNA fragments were degraded without preference for any DNA fragment (12). These results are consistent with a circularly permuted DNA structure as found by electron microscopy described above, indicating that the genome of CIV is circularly permuted and terminally redundant (about 12%), a property which it has in common with FV3 (8) and FLDV (9, 10) both eukaryotic viruses and members of the iridovirus family. Therefore it was of importance to prove whether direct molecular cloning of the complete genome of CIV is possible and whether the physical maps of the viral genome are circular as shown for FV3 (18) and FLDV (10).

Molecular cloning and physical mapping of the viral genome

To clone the CIV genome, viral DNA was analysed by digestion with different restriction endonucleases and by electrophoretic separation of the resulting DNA fragments in agarose slab gels. The results of this study for the restriction endonucleases ApaI, Asp718, BamHI, EcoRI, NcoI, PvuII, SalI, SphI, and SmaI as described previously (12-14) are summarized in Table 1. When the CIV genome was cleaved with the restriction enzyme EcoRI, 32 DNA

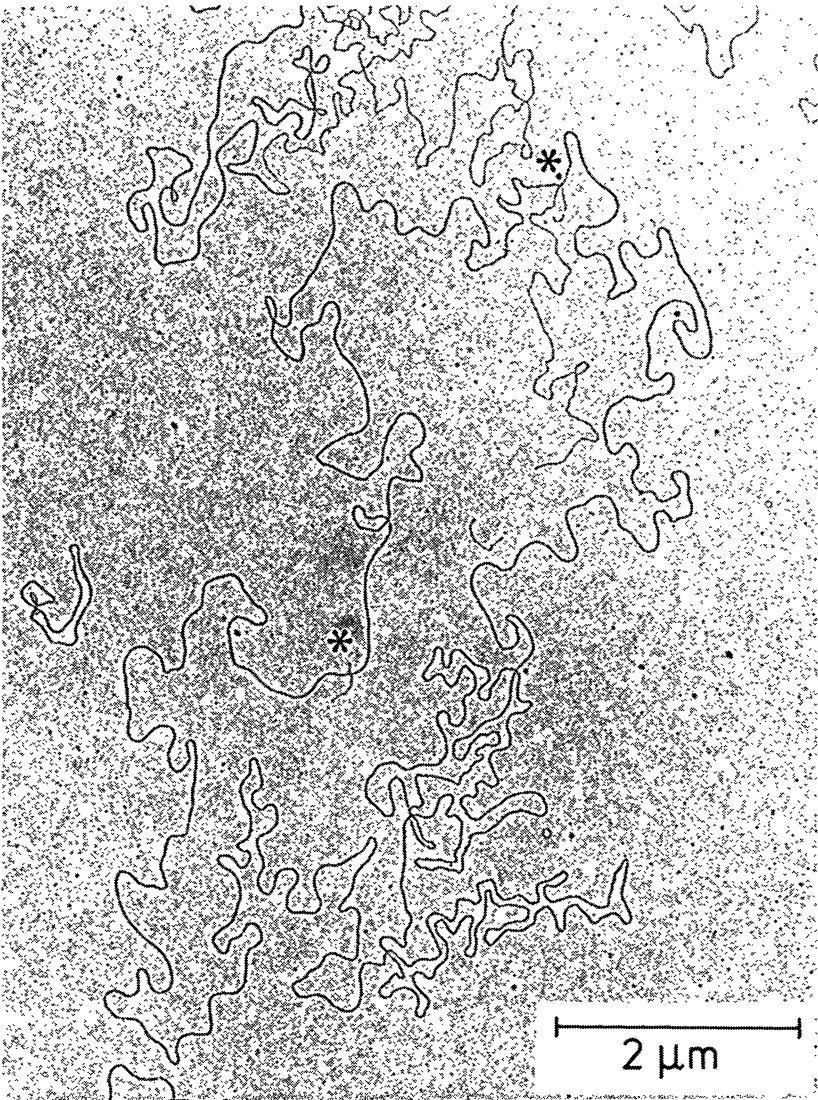


Fig. 1. A circular double-stranded molecule formed by self-annealing of denatured CIV DNA. The stars indicate positions of single-stranded tails on the circle. The photograph was taken from (12).

fragments (A to Z and A' to F') were generated. The individual DNA fragments were isolated after electrophoresis and directly inserted into the EcoRI site of the plasmid vector pACYC184 (13). In parallel experiments BamHI, BamHI/SalI, SphI, and NcoI DNA fragments of the viral genome were inserted into the corresponding sites of the plasmid vectors pAT153 or pKm2, respectively. The identity of the viral insert of each recombinant plasmid to CIV DNA was confirmed by Southern blot hybridization as described elsewhere (13). This analysis revealed that all of the 32 EcoRI DNA fragments A to Z and A' to E' representing the complete CIV genome, have been molecularly cloned directly into the corresponding site of the plasmid vector pACYC184 without any linker or adapter (13).

As a first step towards the understanding of the underlying mechanisms which determine this unique genomic feature among eukaryotic viruses, the arrangement of the DNA sequences of the viral genome must be elucidated. The established and defined gene library of the CIV genome was used for construction of restriction maps of the viral genome for the restriction endonucleases ApaI, Asp718, BamHI, EcoRI, NcoI, PvuII, SalI, SphI, and SmaI (13, 14). Physical mapping of the CIV genome was carried out by Southern blot hybridization tests as described previously (13, 14).

Although the CIV genome is a linear DNA, according to the results obtained by molecular cloning and physical mapping the restriction maps of the viral genome must be constructed as circles as shown in Fig. 2 (13, 14). The ApaI recognition site located within the EcoRI DNA fragment J was fixed as the start and end point of the genome coordinates (0/1). This finding supports the results of earlier analyses and is strong evidence that the genome of CIV is indeed circularly permuted.

Table 1: Size of DNA fragments of insect iridovirus type 6 obtained by cleavage with restriction endonucleases

F*	Size of DNA fragment (kbp)								
	ApaI	Asp 718	BamHI	EcoRI	NcoI	PvuII	SalI	SphI	SmaI
A	158	50	72.76	17.0	57.77	46	85	39	102
B	51	39	40.56	14.8	31.55	36	57	30	55
C		25	29.59	13.5	16.5	25	26	30	52
D		17	21.2	12.7	13.4	18	20.6	26	
E		17	19.7	11.1	13.1	15	19.9	24	
F		16	15.6	10.8	12.5	13.6	0.58	19	
G		13	8.1	10.0	10.8	11.2		12.2	
H		9.5	1.0	9.8	9.0	11.0		10.7	
I		8.7	0.4	9.2	8.1	9.4		6.4	
J		7.8		7.9	7.2	8.5		5.5	
K		4.6		7.6	5.7	6.2		2.6	
L		2.0		7.3	5.1	5.1		2.6	
M				7.25	4.6	3.2		1.4	
N				7.1	4.2	1.15			
O				6.5	3.3				
P				6.4	3.1				
Q				5.9	0.9				
R				5.5	0.56				
S				5.25					
T				5.2					
U				4.5					
V				3.5					
W				3.1					
X				2.85					
Y				2.2					
Z				1.8					
A'				1.78					
B'				1.65					
C'				1.5					
D'				1.35					
E'				1.1					
F'				0.38					
Sum:	209	209.6	208.91	206.51	207.38	209.35	209.4	209	

* DNA fragment

Note. The corresponding map coordinates for the individual DNA fragments had been described periviously (13, 14).

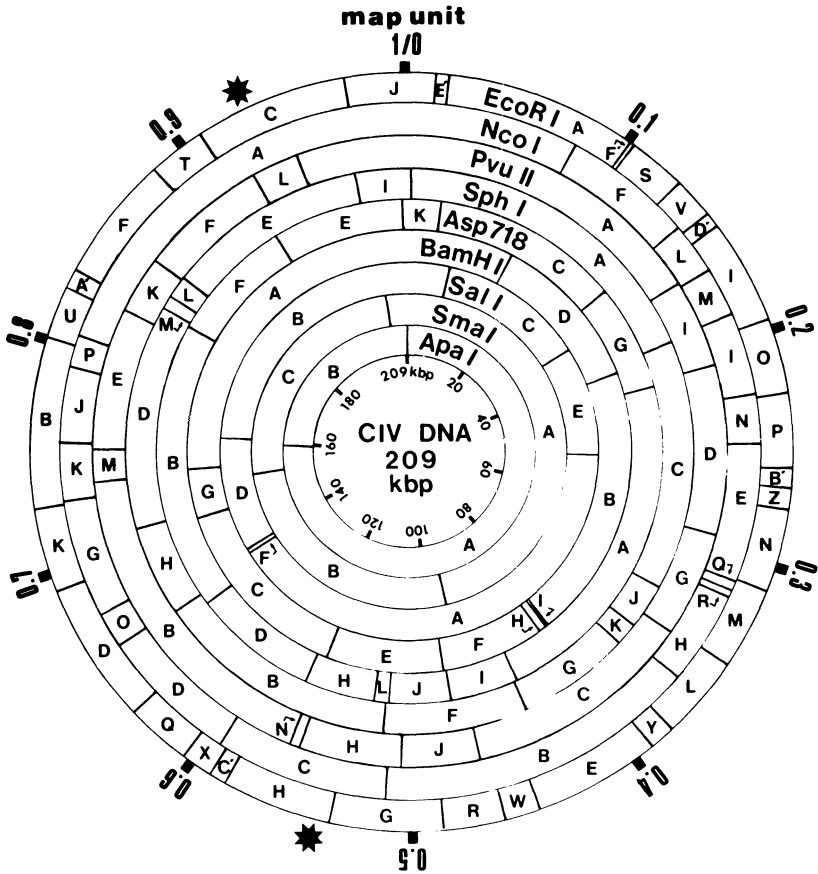


Fig. 2. Physical maps of the CIV genome for restriction endonucleases ApaI, Asp718, BamHI, EcoRI, NcoI, PvuII, SalI, SmaI, and SphI. The restriction maps are circular and start at the boundary of the ApaI DNA fragment B to A. For detail see (13, 14).

Detection and characterization of repetitive DNA sequences in the CIV genome

To detect possible repeat DNA sequences within the genome of CIV the defined gene library of the viral genome was tested in hybridization assays. A significant homology was detected between the EcoRI DNA fragments C (13.5 kbp, 0.909 to 0.974 map units (mu)) and H (9.8 kbp, 0.535 to 0.582 mu) of the CIV genome as described

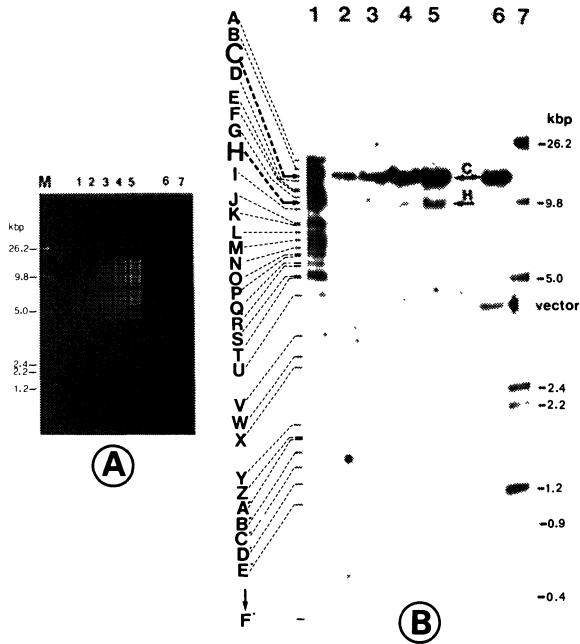


Fig. 3. Determination of the DNA sequence homology between the EcoRI CIV DNA fragments C and H by Southern blot hybridization experiment. The labeled recombinant plasmid pyIV6-E-C harboring the EcoRI DNA fragment C of the viral genome was hybridized to the EcoRI digest of CIV DNA at various concentrations (lane 2 = 0.9 fM, lane 3 = 0.4 fM, lane 4 = 7 fM, and lane 5 = 0.01 pM). The labeled CIV DNA (lane 1) and unlabeled DNA of recombinant plasmid pyIV6-E-C (lane 6) cleaved with EcoRI served as internal marker. The DNA fragments were separated electrophoretically on a 0.8% agarose slab gel. (A) Ethidium bromide staining and (B) autoradiogram of the blot hybridization experiment. Labeled phage lambda DNA digested with MluI (lane 7) served as molecular weight marker. The big arrow marks the position of the vector and the small arrows indicate the positions of EcoRI CIV DNA fragments C and H.

previously (15). As shown in Fig. 3 it was found that the EcoRI DNA fragment C hybridized not only to itself but also to the EcoRI DNA fragment H of the viral genome. Similar results were found when the DNA of recombinant plasmid pyIV6-E-H which harbors the EcoRI DNA fragment H of the viral genome was used as hybridiza-

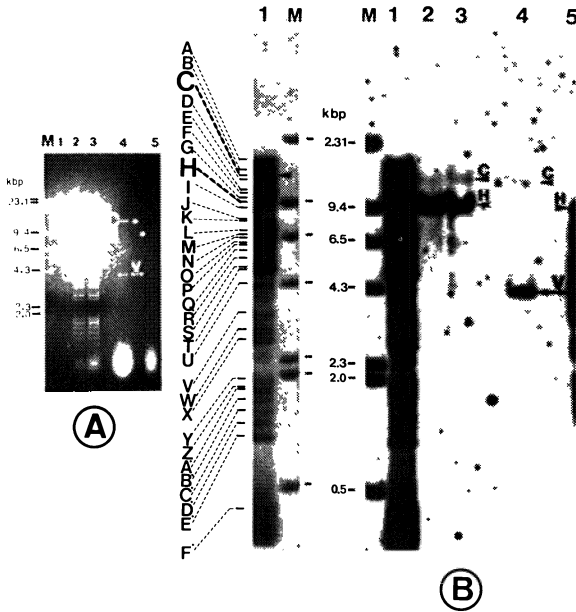


Fig. 4. Determination of the DNA sequence homology between the EcoRI CIV DNA fragment C and H by Southern blot hybridization experiment. The labeled recombinant plasmid pyIV6-E-H harboring the EcoRI CIV DNA fragment H of the viral genome was hybridized to the EcoRI digest of the viral DNA at the concentration of 7 fM (lane 2), 0.014 pM (lane 3), and to the DNA of recombinant plasmids pyIV6-E-C (lane 4) and pyIV6-E-H (lane 5) cleaved with EcoRI. The labeled CIV DNA digested with EcoRI (lane 1) served as internal marker. The DNA fragments were separated electrophoretically on a 0.8% agarose slab gel. (A) Ethidium bromide staining and (B) autoradiogram of the blot hybridization experiment. Labeled phage lambda DNA digested with HindIII (M) served as molecular weight marker. The arrowheads mark the position of the EcoRI CIV DNA fragments C and H and the arrows indicate the position of the vector.

tion probe (Fig. 4). The position of the repetitive DNA sequences were localized at the map coordinates 0.535 to 0.548 and 0.920 and 0.944 of the viral genome using fine mapping by DNA-DNA hybridization assays (15) as shown in Fig. 5.

For further characterization of the DNA sequence homology between the EcoRI CIV DNA fragments C and H

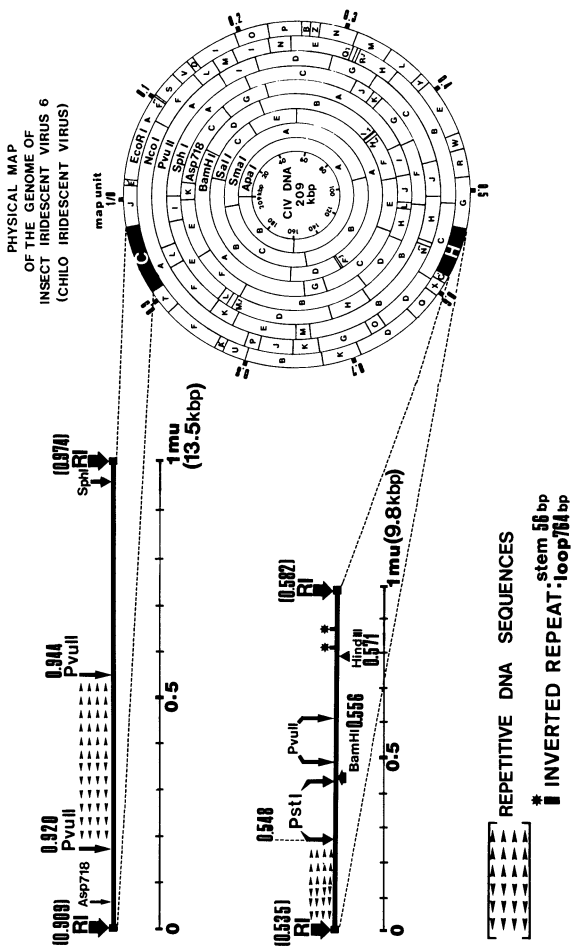


Fig. 5. Fine mapping of two repetitive DNA elements in the CIV genome corresponding to the EcoRI DNA fragment C and H (black boxes). The photograph was taken from (15).

electron microscopical heteroduplex analysis was carried out as described elsewhere and the results are given in Fig. 6. In this study the recombinant plasmids (pyIV6-E-C-C1, pyIV6-E-H-C100, and pyIV6-E-H-C217 (15)) harboring the EcoRI CIV DNA fragments C and H (in two different orientations) were linearized by the restriction endonuclease SalI within the vector sequence, denatured and reannealed to form heteroduplexes. Only heteroduplexes with fragment H in one orientation (pyIV6-E-H-C217) displayed an interaction between the two strands. Examples are shown in Fig. 6A to C. The results of the measurements on the heteroduplexes (15) revealed that the region of homology between the two EcoRI fragments maps at a distinct position on fragment H (2.12 ± 0.16 kbp from the EcoRI site; 0.545 mu). But the maps obtained for the position of the duplex on EcoRI fragment C (15) indicate that it is found at variable locations on fragment C. As deduced from a histogram (15) the region is extended between 4.14 to 7.86 kbp from the EcoRI site (0.924 to 0.938 mu). This indicates the presence of tandem repeats distributed through a wide region on EcoRI fragment C, corresponding to the PvuII CIV DNA fragment L (0.920 to 0.944 mu).

In addition it was found that the strand of the EcoRI H fragment can be recognized by an inverted repeat causing a stem-loop structure (Fig. 6A to C). Its position was determined using a HindIII/EcoRI subclone (0.571 to 0.582 mu) of the EcoRI DNA fragment H (15). The distance of the inverted repeat from the HindIII site (0.571 mu) was determined to be 260 ± 40 bp (Fig. 6D). The length of the stem is about 65 ± 10 bp, and the size of the loop approximately 650 ± 80 bp. The length of the stem is quite variable and indicates that the inverted repeat does not have a very good homology. To ascertain these results and to clarify the structural arrangement of these repeat regions it was necessary to perform the DNA nucleotide sequence analysis.

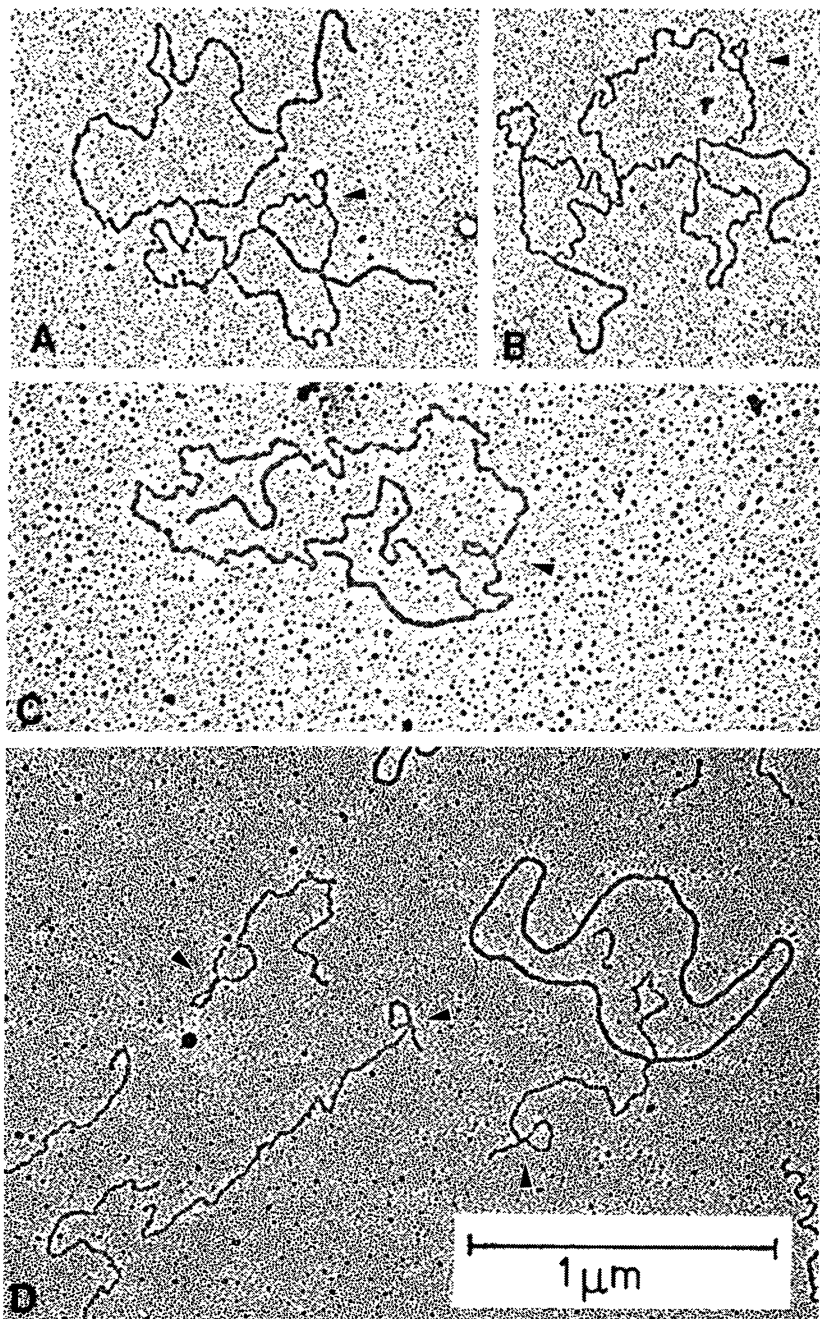


Figure 6

Fig. 6. Electron micrographs of recombinant DNAs carrying inserts of the CIV DNA EcoRI fragments C and H. (A) and (B) Electron micrographs of heteroduplexes between the recombinant plasmids pyIV6-E-C and pyIV6-E-H which harbor the EcoRI DNA fragments C and H of the viral genome, respectively. The recombinant plasmids were linearized with the restriction endonuclease Sall approximately in the center of the cloning vector pACYC184. While the distance of the site of interaction between the two strands is always at the same position on the strand from the shorter fragment H carrying the stem-loop structure, the position on the strand from fragment C varies between extremes represented in the two pictures (A) and (B). (C) Electron micrograph of heteroduplexes between the recombinant plasmid pyIV6-E-C and pyIV6-E-H100, harbouring the CIV EcoRI DNA fragment H in the opposite cloning orientation. (D) Electron micrograph of the single stranded DNA of the plasmid pUC18-IV6-E-H-C1, an EcoRI/HindIII subclone of pyIV6-E-H linearized with HindIII. This insert contains the region of the stem loop structure in the EcoRI DNA fragment H. The double stranded circular DNA is PM2 DNA added as length reference. The samples were prepared as described previously (15). The arrowheads point to the stem-loop structure contained in the EcoRI restriction fragment H.

The characterization of the repetitive DNA sequences in the CIV genome by DNA nucleotide sequence analysis.

The complete nucleotide sequence of the EcoRI/PstI subfragment (0.535 to 0.548 μ) of the EcoRI CIV DNA fragment H was determined as described previously (15). The obtained nucleotide sequence is shown in Fig. 7. This DNA fragment has a size of 2708 bp and a base composition of 33.9% G+C and 66.1% A+T and contains many perfect short direct and inverted repeats (15). Only short open reading frames were identified. The largest one (294 bp; 98 amino acid residues) is located between nucleotide positions 1057 and 1351 of the complementary strand. The determination of the nucleotide sequence of the PvuII CIV DNA fragment L (0.920 to 0.944 μ) (Fig. 8) revealed that this DNA fragment has a size of 5064 bp and a base composition of 39.79% G+C and 60.21% A+T (16).

The search for DNA sequence homologies between the obtained DNA sequences and the DNA sequences was performed by dot matrix analysis (Fig. 9). These studies

EcoRI (0.535 mu)

1 GAATTCAAACCAATCCATTTGSAATTTTAAAGAAGAAAACCTAAACCTGTTTACAAT TTTATAAACTTTTCCCTGGATTAAGAGTCAAGTTTATAGATGATTCGTGCTCTTAAIT

124 CATCTAAATTTTGATGCAGCTTTTTTATTCGTTCTGACTTTTATGAATATATTTCTCTC CAGTAGGAATTCCTATAACGGATGATGAAGAAGTTGAAAAATTTTATCGTCCAAAAGAAA

241 AATATTTATAAACTTCAGTGTTACGGAATAAACAATAATTATAATGAAAACGAACCGGAAA TTATTCATGTTAAATGGAATAACCGAGAAATTTATTCAAAATTCGCTTTTGACTGAAA

361 ATAGAGGATTTCTTATACAAGAAGCAGATATTTTACCTAGCAGAAAGGATTTTATAGAA AATTGGTTAGGAAAATCTGATAAAGACGTGAAGAATTTATAATTCCTGTTAATATTC

481 TCAGATGCAAAAGCAGTGGCCAGAAATGAATTTTGAGATCGCTTTTAAATGTTATTCCA AATGCAGATCTTTTATAACAACAATAAGAATTTTGACAAATATAGTTGAAAAAATAGTAG

601 ATTTGAGTTAAATACGTGATTTTTTAAAGATTCAGATTTAATAGTTTCATCAACCCAAA AATTAATTTGTTCTCTGTATTTCCAAAAGACCTGCTAAAATGCAATATAACCGAAA

721 ATTTACCCTCTTTAACTCAAGAGAGAATTCCTGAATTTTGATGATAATCGTATACCGAA GCAACAATTTGAATATGTAATCGCAATTCAC??CAAAATAGAAAATATACGAGGAT

841 TAGTTAATATACTGTCATGATAATGTTATTCACACTGAAAAGCAACTCGACCATTTT CAAATGGGAGGCAAGTTAAACCAACAGGTCGTGATGACAAAATAATATAGGTTCTCCAG

961 AATGGAAAAATGCATGTGGAATGTTAAGATGTTATAAATATCCCGATGAAGATTTAA TTTTACTCTGATATCGAAGATCTTATCCGAAATTCGAACCATCAAGCGGAAAAGAGG

1081 TGTAGAAGGTTAAGAAGAGTGAGATTAATATCCAGAGGTCGGTTAATAAAATTAATTA AAGCAGTCTTTAAGTTAGAAAATAATCTTATGAAACAGAACTCTCCAAAGAAAGA

1201 AATTAATGTTTGAATGTAAGAAAGCTGTTCTGCTGGGAAGGAATGTGAGATTTTC AAAGGTAAGAAAGTTGCTTTTGTAAATGGAAGTTTGAAAAATAAAAATGTTAAAT

1321 TTAATGTTAATAACCAATAAAATTTAAAAAATAAATTAACAGAGATAAGACAGATACA AAAAAATGAATTCAGCAATTCGAGAAATCTATATATCCATGTTTACAAAATGTTGA

1441 TCTATAAGGACATATGTTGCATACCTCCAACCTGACTTAAAAATCTCCACCCCACTACT TTTGCAATCCACAAAAGTACCAGAAATAGGTTGGTACATATTTCCAATATTTGAGC

1561 ACTCCCATATAGCAGCATATGCTGTAATAGCTGGCAGTACATTTGATGTTTGGAGATC ATTAACATAACAATAATGAAACAATTTGCATTTATAACAATGCCTCCAACCTGTACAAC

1681 CAATATCCAAATGTTATATAGTTAACTGCAACTATACTCCCGTTGATGTTAAACC AGAGTTTATTTTTTACATAATTAGTACCATTATATAACCAAAATAGATCCATGTTCCA

1801 GAATATAAGTATTTTGTGTCAGGCTATCTGAGGAGCGGTTGTTGGGATATTTCCGCT TGTAAAAACGAAATAGGCGCATTTAATGGAGAAATGTCATCGACATGCTAGGT

1921 CCAAGAGTAAATAGTGGGAGTAGTACTGTTTTCCTAGATCATAGTTGGAGTTGCAAG GTTAGCCATCTGCAAGTGAATGGCACCCTGGGCAACGTTGGGGCTGTGCAACACTGC

2041 CTGTAAGCTCCCCAGCATTTGAAATACCTCCAGAGATGAGAGTAGCGTGGATAGAACCC CTGTTAAGTTAACGCTCAATGACTCCGCACTCATACAGACGGAAACCGAGAGTAAATAGCA

2161 GAGTCGATGTTGATCCACTGAAGAACCAATTAATTCAGATGTCGGGTAAAGCAAGTTG ACTAAACCTACTGCTCCATAGCAAGTTGTCAGTTTCTACAGCGTTGTTGCAAGTTG

2281 TGCAGTGCCCTATGCAATTAATGCAATAGTAGGAGCAGTTGCTGTACCCGATAATAACCG GCTAGCTGAATTTGACCAATGAAGTAGAAGTAGAAGTTGCTGGGGCAGCTATGCGCGTT

2401 GCGGAAAGAACTCTCCAGAAGCTATTGACAACCAAGTCGCTAGAGTGATATTTGTTGCT GCACCTGAAGAGCTATTCGAACCAATTAATGTTGAAGTTGCGAAAGTCTGCCAATG

2521 CCAGTGCCCACTGAGTTGGCAGCTATTTGTGTAGCTCAACAGCACCATTAGCAATTTTA GATGCTCTACAGCACCATCGGCAATTTGTTGATAGTCAACAGACGCTCGGGATAAGTTG

2641 AGATGTAGCAGAACCAGCAATGCTCCTGAAGTTGAATAGTTCCTAACTAGATGATGT TGCTGCA 2708

PstI (0.548 mu)

Fig. 7. DNA nucleotide sequence of the EcoRI/PstI subfragment (0.535 to 0.548 m.u., 2708 bp) of the EcoRI CIV DNA fragment H. The positions of the DNA sequences which are complementary to DNA sequences of the PvuII CIV DNA fragment L are indicated in box A (nucleotide positions 1981 to 2072) and in box B (nucleotide positions 1817 to 1863). The figure was taken from (15).

revealed that the DNA sequence of the EcoRI CIV DNA fragment H at the coordinate 0.535 to 0.548 mu contains two regions which are complementary (>90%) DNA sequences of the PvuII CIV DNA fragment L. These regions were termed box A (91 bp at the nucleotide positions 1981 to 2072) and box B (46 bp at the nucleotide positions 1817 to 1863) (Fig. 7). As shown in Fig. 10 the DNA sequences of the repeat box A are complementary to nine regions within the PvuII DNA fragment L of the viral genome (Fig. 11). This indicates that the PvuII DNA fragment L should possess a cluster of direct repeat DNA elements. In contrast the DNA sequences of the box B are only

(0.920 mu)
PvuII SpeI
1 CAGCTGTAAGTAGTATACCTGTTCAAATGTAATGGTCTGTTCAATCTGTTAATGGGTTTTCCAGACTGTCTGGAAATGTAACGTAACTCTGGAACAGTACTACAGGTACTT
121 TAGCTGCACCTACCCTCGTGGGTCTCCATTAGTAAACGGAGATATATAGTAGTTCTCGGAACTCCACACCATCAATAATGGGTAACACTTATATATAGTACAACCTCCAAATC
241 AATGGTTAGAAATTTCTCCAAAGTTTGGTCTTTAGATGACGCAATATTACAGCTATCAGGTGGAAACAATGTCTGGGAATATAGTTATCTTAGCGGTAATTTTACACATTAAGT
361 GCCTGCAATCCAACAGATGCAGCTAATAAATCATATGAAGATGCATATATACACCAT TGCACACAATCTTTACAGGGAAGAGTTCAACTATCTGGTGAATTTACAGGGGTGGCGTC
481 AGCTCCAGTTATAACTACCGGACCAATCTTTAACTAAAATGGCAAAATTTAACTACAACAGGTTCTTCTAGTAAGTCTCAACAGCAGTACAGTACGACCTCACTCAATTAAGTTAGGTT
601 TAATTTACAAAATTTCTGGAAAGTTTATAGTGGAAACAAGTTCACTTTCCAGGAACATTTTACACCTACCAGGAGG14:4#GTGCAGGAATAATTTGATACCAACAGGAGATTAAT
721 TTGAAATAACAGATGCACCAAAATGGAAACAGTCTGCAAAATAGCTTTATGTTGATGC AAATAAATCCAAATGCAACTCAACTGTTTGAAGAAATTTAGAAATTCAGTGGAGATTTAT
841 TAGGAACCTCTGCAAGACTTCCAATTTTCTGAGAGAGCTGTACCTTATCAAAAATGGCTAAATTTATCAACTACAATGCTTTAATAGGTTTCATCTCTACAGATAATTTAGTATCTC
961 AATTAAGTTTAGGTTCTAAATTTACAATAATCTTGGAAACAATTTTATAGTGGAAACAAGTTCACTTTCCGGAACTTTTACCACTGGGATGGGGTACAATGCTGGAAATATTGTTATA
1081 CCATCGGAGATTAATTTCAATAGCAGACGCTCCAATCTGGAACTAGTCTGCTGCAAAATAGGCTTATGATAGCAAAATAAATCTCCAATTCACAAATGCAACAACAGCGTCTTGGCAACCCCA
1201 ATATCTGGGTGATTTTGACTCTAGCTCAACCGCAACAGTTCCGTTAAATAAAGTGCACA TCGTCAATAACAGGTAATAATCAACCTTTCCGGAGATCTAACAGCTATCGCCATCTCAA
1321 CAATTTGCTGGCGGTGCCATTAAGTGAAGATGGGAATCTTTCCAGGAACTCTCAAATTTTGGGTTCTAGCAGTACTGCATCAACGGTCAAAATCTCACATTAGGTTCTGGACTACA
1441 ATTTCTGGAAACCGGTGGAGGCTTAATTCAGCAACGTAACCTGGCTCCAGCAACTGCTACA ACTATTGGAGTATGAAATTTAGGAGACTAACAGGCAAGTCTTGCACAGCCCA
1561 CGTTCGCCACTGGTGCATTAACATAGCAAGATGGCCAACTTTACCACTTTCTGGAGG TACAATGTCGGGAATATTTACCACTGGAGATTAATTTCAATAGCAGACGCTCCCA
1681 TGAACCGGGTGGAGGCTTAATTCAGCAACGCTACTGTTCCCGGCTACATCAACTCTCTCTGGAGGTTGAAAGTTAGGAGACTAACAGGCAAGGTTGCACAGCCCA#26TGGG
1801 TGGTGTATAACACTAGCAAAAATGGCAATCTTTCCAGGAACTCTCAAATTTGGTCT TAGTAGTACTGCATCACTCTGAAATTTAAGCTTGGAAATTTTTGGCAATGACAGG
1921 AACAGTTTTAAATGTAACCTCAAGTCTCACTTTCCGGAACATTTTACCACTTTCTGGAGG TACAATGTCGGGAATATTTACCACTGGAGATTAATTTCAATAGCAGACGCTCCCA
2041 ACTGTTGGAACTAGTCTGCAAAATAGGCTTTATGATAGTCTCAAAATATACAGCAACT CCAATGCAACCCCAACAACACTTGGAAAAATTCAAATTTCTGGGATTTGATCTGACA
2161 TCAACAGCAACAGTCTCTAATTAATAAAGTCAACTCATCAATAACAGGTAATAATCAAACTTTCTGGAGATCTAACAGGATCTGCTTATTTCTCCAAGGTTGCTGAGGCTCAAT
2281 CTCTCAAGATGGCCAACTCTCTGGAAATTTCTACCTTCTGAGGATTTGAAATTTAGGACTTCACTTGGGTTCCGAGACTGCAAAATTTCTGGAAACCGTATGAGGCTTAAGC
2401 GTTAATTCAGCAACCGCTAACGTTTCCCCGGCTACTGCTACAATTTGGAGGATTTGA AATGTTAGGAGACTTAAACAGGAGTGTGCAACAGCCCAAGGTTGGCTGGTGGCCAT
2521 TACATTAGCAAGATGGCAAACTTTCTACCGTCTCTCAAATTTAGGTTCAAGGAGCA CAACATCAGCAGCTACAATCTCACATAGGTTCCGCTTCAACAATTAACAGTCTGCTG
2641 TAAGATTTTCTGAGCTACTTCTCTACCGTCTCTCAAAATTTGGTCTTAGTAGCAGCAACTTAA CAGGCAAGTGTGCAACAGCCCTGAGGCTGGTGGCCATTACACTTGCAAAGATGG
2761 CCAATCTTTCCAGGAACTCTCAAATTTAGGTTCTAGTAGCAGTCACTCAACGGCTACA AATCTCACATGGGTTCTGGACTACAATTTCTGGAAACCGTGTGAGGCTTAATCAGCAA
2881 CTTAACCGTCCCCGGCTACTGCTACAATTTAGGAGTATGAAATTTAGGAGACTTAA CAGGCAAGGTTGCAACAGCCCAAGGTTCCGCTGGCCACTTACACTGCAAA
3001 ATGGCCAACTCTTCCAGGAACTCTCAAATTTAGGTTCTAGTAGCAGTCACTCAACGGCT CAAAAATCTCAATTTGGTCTGGACTACAATTTCTGGAAACCGTGTGAGGCTTAATCA
3121 GCAACGCTAACGTTCCCCGGCTACTGCTACAATTTAGGATTTGAAATTTAGGA GACTTAAACAGGCAAGTGTGCAACAGCCCAAGGTTCCGCTGGGCTATAACAGTGC
3241 AGATGGCAACTTTCCAGGAACTCTCAAATTTAGGTTCTAGTAGCAGTCACTCAACGG CTAACAATCTCACATGGGTTCTGGACTACAATTTCTGCAACTTTTGAATGTTAATCA
3361 ACACTCTATTACAAGTAACTTTTACCAATAGCAGGTTGCAAAATCTGAAATATTATT ATTTCCAACAGGAGATTAATTAATAAGTAGCAGTCTCCACTTGAAGTACAAGCGGAGCC
3481 TAATAAATCTTATAGACTCACAATAATGCTAATGCAACACTCTTCCCAACACTGG TATTCAAGGCCAAATTCAAATTTGGTGGAGATTTGGTGGCTGGCAACTGCAAGTCTC
3601 ACCTGTCTTTCTCGGGTGCATTAACATAAACAATAAGGCTAATCTTCTGGAATCTC ACAAAATCTGGTAGTGGAGTACTAGTTCTGAGTCAGTAACTTAACAATAGGTTCTGG
3721 ACTCAAATTTCTGGAAACCGTGTGAGGCTTAATTCAGCAACACTCAACCGTCTCCCGGGC TACTGCTACAACTATTGGAGGATTTGAAATGTTAGGAGACTAACAGGCAATTTGCAAC
3841 AGCCCCAACGATTCGGCTGGCCATAAACAATTTGCAAAAATGGCCAACTTTCCAGGGA CTCTCAAATTTGGTCTTAGTAGTACAACACTTACGCTCAACAATCTCACAATGGGTT
3961 TGGACTACAATTTCTGGAAACCGTGTGAGGCTTAATTCAGCAACGCTAAGTCTCTCC AAGAACTGCTACAACACTTTGGAGGATTTGAAATGTTAGGAGACTTAAACAGGCAAGTCTG
4081 AACAGCCCAACGCTTCCCACTGGTGCATTAACCTTTCAAGATGGCCAACTTTCCAGG GAACCTCAAATTTAGGTTCTAGTAGCAACAACACTTACGCTCAACAATCTCAAT#4#5
4201 TTTCTGGACTACAATTTCTGGAAACCGTGTGAGGCTTAATTCAGCAACGCTAAGTCTCC CCGGCTACTGCTACAACACTTGGAGGATTTGAAATGTTAGGAGACTTAAACAGGCAAGCT
4321 TGCACAGCCCCAACGCTTCCGCTGGTGCATTAACCTTTCAAGATGGCCAACTTTGCA GAACCTTCCCAACTTTAGGTTCTAGCAGCAGCACTACTGCTGCTGTAATATCTTTAG
4441 GAAGTACATTAACAATCTCAGAACCAACTAAGTAAACACACTCAACATAAGTATTAGG TTCCATCATCAGTAATAATGAGATTTGGCAACAATAAGTGCATCTGGCAAGTATAGACAG
4561 CGGTGTTCTAATAATTCGTTAARCAAGTCCAAGTTTATGGAATGCTGCAAAAATAG CTATTACAACAATAATCTGTTGCTGGACAAATCCAATACAAGTCTCCCAACAGATA
4681 GACCAAGCACTCTAGGTTTGTATGTTGGCAAGATGACTCATATAGGATTTGGAATGG TCTGTGTATATAAGTTAATAGCAGTAAATGACCTACATCAGTAAAGAACCTTTTA
4801 CACAAGCACTGGTCTCAGGATTTCAAATCTCAACAGATAAATGGAGCAATTTGTCTAAT AITCTGTATCAATATTCTACTACAATGGAGTGGAGGACTACTCTACAGGCACTGTTAAT
4921 TAGAAGTTTCTCTACAATTCAGCAACTCCAGCACTGGTGGATTTGAACGGAGTTATAT CTAATCTCAATCATTTGGTGGATTAATAACACTACTAAGTGTCAAGTCAAGGAGGAC
5041 AACTATGACATATGTTCCAGCTG
PvuII SpeI
(0.944 mu)

Fig. 8. Nucleotide sequence of the PvuII CIV DNA fragment L. The figure was taken from (16).

complementary to the other one region of this DNA fragment (Fig. 10). With exception of these repetitions which show a high degree of DNA sequence homology to the DNA sequences of the PvuII CIV DNA fragment L the DNA sequences of this particular region contain a number of other repetitions with a very weak homology to a variety of the DNA sequences of the PvuII DNA fragment L (9).

The analysis of the DNA sequence of the PvuII CIV

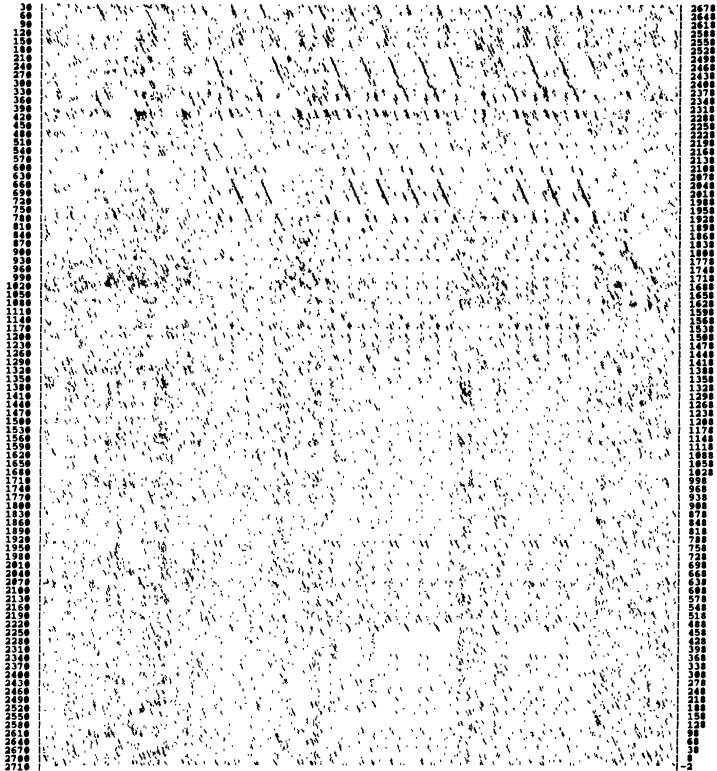


Fig. 9. Dot matrix homology comparison of DNA nucleotide sequence of the HindIII/PstI subfragment (0.535 to 0.548 mu) and the PvuII DNA fragment L (0.920 to 0.944 mu). The position, size, and the base composition of the individual repetitions are given in Figs. 10 and 11. The analysis was performed as described in the legend of Fig. 12.

DNA fragment L for detection of repetitions was performed with computer assistance. The results of these studies which have been described elsewhere (16) indicate that the PvuII CIV DNA fragment L contains many perfect direct repeats and a few short inverted repeat sequences of a size up to 145 bp. The dot matrix analysis of the DNA sequence revealed that in addition to the perfect repetitions mentioned above a cluster of imperfect repetitions with a very complex but rather regular

	H	2072	ACCTCCATAAGTTTACGACCCCTCTGAA-TGTCCTC-GTCACAACGTTGTCTGGGGTTGC-AACGGGG-TCCACGG-TAATGTGAACG-TTCTACCGATT-G	1981
A	L-BOX 1	1508	TGGAGGTATTGAAATGTT-AGGAGACTTAACAGG-CAGTGTGCAACAGCCCCAACG-TTGCCAC-TGGTGCC-ATTACATTAGCAAAGATGGCCAATC	1601
	L-BOX 2	1742CG.....C..A.....G.....T.....A.....C.....A.....	1832
	L-BOX 3	2449G...TG.C...G.C.....A.....	2543
	L-BOX 4	2672C.....G...G.....C.T.....	2766
	L-BOX 5	2915G..C.....G...G...C.A..C...C-T.....	3010
	L-BOX 6	3159C.....G...G...C..T..A..C.T.....	3252
	L-BOX 7	3796C.....A..G...C..T..A..C.T...A.....	3890
	L-BOX 8	4039C.....G...C..A...C..TT.....	4133
	L-BOX 9	4282C.....G...G.....T.....	3374
B	H	1863	ACCTTTATTAGGTTGTGTGGCGAGGGAGTCTATCTGGACGTGTTG	1817
	L	4647	TGG-ACAAATCCAAATACAACCTGCTCCAACAGATAGACCAGC--AAC	4690

Fig. 10. Comparison of DNA nucleotide sequences between the repetitive DNA elements (boxes A and B of Fig. 9) of the EcoRI/PstI subfragment of the EcoRI CIV DNA fragment H to the complementary DNA sequences of the PvuII CIV DNA fragment L as labeled in (A) with L-box 1 to 9 and in (B) with L. Dashes indicate artificial gaps introduced into the DNA sequences to achieve optimal base match. Dots represent identical bases of the DNA sequences of the L-boxes 2 to 9 in comparison to the DNA sequences of the L-box 1. Those bases of the DNA sequences of PvuII CIV DNA fragment L which are not complementary to the corresponding DNA sequences of the EcoRI CIV DNA fragment H (H) are marked with asterisks. The photograph was taken from (15).

structural arrangement are present within the PvuII DNA fragment L (Fig. 12). Four repetitive elements were detected and termed R1 to R4. Three of these repetitive elements (R1, R2 and R3) exist in duplicate (two subunits or boxes (B)). The R4 element appears in 12 boxes. The nucleotide positions and the sizes of the individual boxes of R1 to R4 as described previously are given in Fig. 11 C and Tables 2 and 3.

A comparative analysis of the DNA sequences of the subunits of each repetitive DNA element was carried out and the results are given in Fig. 13. In this study the DNA sequences of the second boxes of the elements R1 to R3 were compared to the corresponding DNA sequences of the first boxes and the differences in base composition

Fig. 11. Diagram of the position, distribution, and structure of the repetitive DNA element detected within the EcoRI CIV DNA fragment H (A) and the PvuII CIV DNA fragment L (C). (B) shows the position of the corresponding regions of the DNA sequences of the PvuII CIV DNA fragment L which are homologous to the particular DNA sequences within the EcoRI CIV DNA fragment H. The positions, sizes, and orientations of the ORFs located in the PvuII CIV DNA fragment L are given in (D). (E) Diagram of the amino acid sequence structure of ORF 5 indicates the positions of the two peptide repetitions (TR1 and 2) and their corresponding domains (U). The consensus sequences found after the comparative analysis of the amino acid sequences of all five ORFs are shown in (F).

are indicated as shown in Fig. 13A to C. To achieve maximal DNA base match, artificial gaps (indicated by dashes) were introduced into the DNA sequences of the individual boxes. In the case of the repetitive DNA element R4 the DNA sequence of box 6 was used as a reference for a comparison with the DNA sequences of other boxes (B1 to B5 and B7 to B12) of type R4 (Fig. 13D). The structural organization of all four repetitive DNA elements throughout the length of the PvuII CIV DNA fragment L is shown schematically in Fig. 11 C. The DNA sequence homology between box 1 and 2 of R1, between boxes 1 and 2 of R2, and between boxes 1 and 2 of R3 was found to be 80%, 85.2%, and 87%, respectively. The DNA sequences of the individual boxes of the repetitive DNA element R4 were analysed in comparison to the DNA sequences of the box 6 and the results are summarized in Fig. 13D.

The complete nucleotide sequence of the HindIII/EcoRI subfragment (0.571 to 0.582 mu; a part of the EcoRI CIV DNA fragment H) which contains inverted repetitive DNA sequences as shown in Fig. 6 was determined as described elsewhere (15). This DNA fragment has a size of 2555 bp (Fig. 14) and a base composition of 24.03% G+C and 74.97% A+T. The nucleotide

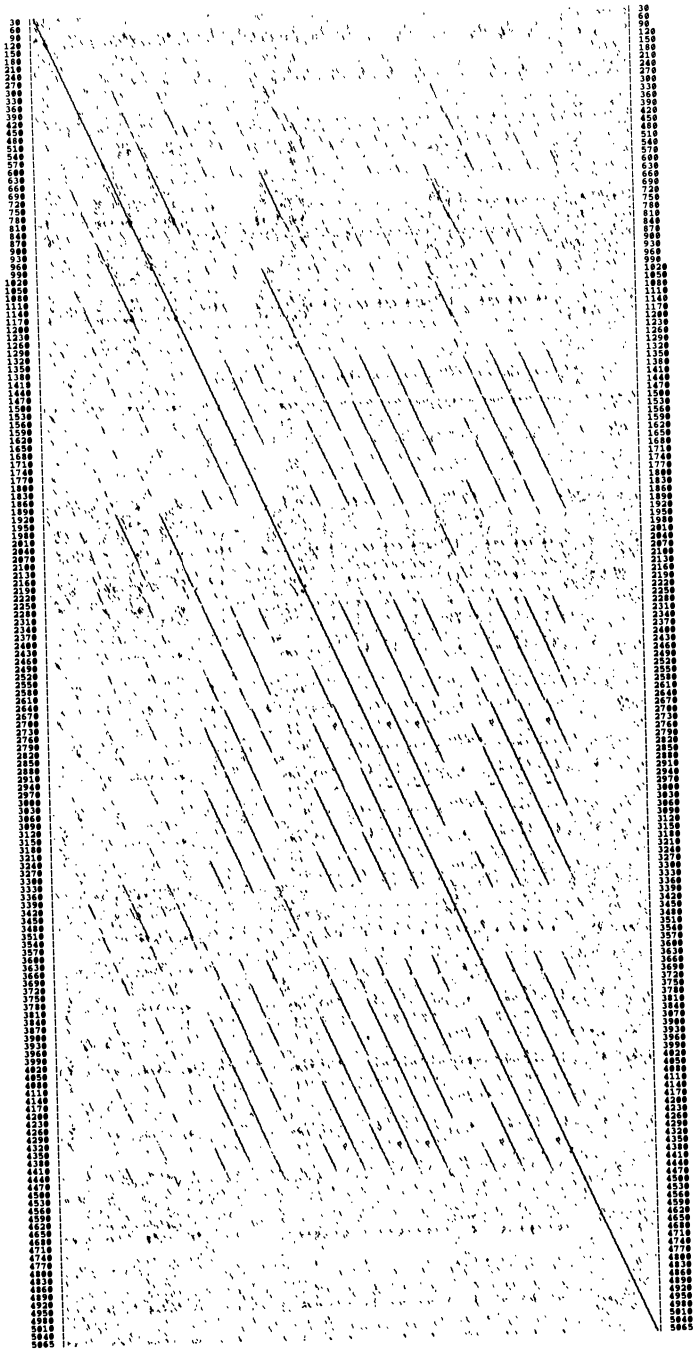


Figure 12

Fig. 12. Dot matrix homology comparison of DNA nucleotide sequence of PvuII CIV DNA fragment L. The position, size, and the base composition of the individual repetitions are given in Table 2 and 3 and Fig. 13. Lines appearing in parallel to the diagonal indicate the presence of tandem repeats at positions earlier in the sequence (to the left of the main diagonal) or later in the sequence (to the right of the main diagonal) or later in the sequence (to the right of the main diagonal). By superimposing a grid over the dot plot rather accurate positions of the homologies were obtained. A program was written for an IBM PC to obtain a plot of the tandem homologies of the sequence allowing a differentiated representation of quality of the matches. A window of 25 bases taken from the sequence is shifted base across the whole sequence and the 100 positions of the best matches are stored. These positions are marked in the dot plot by a subarray of up to six dots to present the different quality of the match. In the plot shown 1 dot represents a match of 13 out of 25 bases, 2 dots 14, etc., and 6 dots a match of 18 bases out of 25 or better. For every new horizontal line of dot plot the window on the sequence was shifted by 5 bases, resulting in a dot matrix of 1012 lines for the analysis of the sequence of 5064 bases.

sequence confirmed the presence of all restriction sites mapped within this fragment. The analysis of the DNA sequence was performed with computer assistance. The search for DNA sequence homologies showed that this part of the EcoRI CIV DNA fragment H contains many perfect direct and inverted repeat sequences (15). The position of three inverted repeats which are able to form stem-loop structures are indicated in Fig. 14. The DNA sequences of the repetition number 2 which are located at the nucleotide positions 304 to 317 and 1011 to 1024 must be responsible for the formation of the stem-loop structure found and measured by electron microscopical analysis (Fig. 6). Only this inverted repeat together with the flanking regions (interruptedly underlined in Fig. 14) allow the construction of a stem of 62 bp and a loop of 694 bases.

Coding capacity of the repetitive DNA sequences

Computer analysis of the 5064 bp DNA sequences of

Table 2: Position and size of the subunits (boxes) of the imperfect repetitive DNA elements (R1 to R4) detected within the PvuII CIV DNA fragment L (5064 bp, 0.920 to 0.944 viral map units)

REPEAT	No. of BOX	POSITION	SIZE(bp)
R1:	1	271 - 838	567
	2	647 - 1215	568
R2:	1	965 - 1882	917
	2	1885 - 2816	931
R3:	1	1032 - 1124	92
	2	3378 - 3466	88
R4:			
Segment 1:	1	1301 - 1540	239
	2	1541 - 1774	233
	3	1775 - 1882	107
Segment 2:	4	2237 - 2481	244
	5	2482 - 2704	222
	6	2705 - 2947	242
	7	2949 - 3191	242
	8	3192 - 3340	148
Segment 3:	9	3588 - 3828	240
	10	3829 - 4071	242
	11	4072 - 4314	242
	12	4315 - 4417	102

the PvuII DNA fragment L was carried out for the detection of ORFs. The results of this study are given in Fig. 15 and Table 4. Five ORFs were identified of sizes from 118 to 333 amino acid residues. The largest one is located between nucleotide positions 3404 to 4403 of the upper DNA strand (Fig. 11 D).

A search for the detection for known canonical promoter and termination signal sequences was carried out and the corresponding results are given in Table 4. Although the classical or slightly modified TATA, CAAT, and GC motifs were found, polyadenylation signals were not observed.

Table 3: Analysis of the DNA sequences of the imperfect repetitive DNA element R4 for detection of the DNA sequence homology between individual boxes

Number of box (position)	size (bp)	^a		Modification compared to box 6	DNA sequence homology (%) compared to DNA of box 6
		Gaps	Total size (bp)		
<u>Segment 1:</u>					
1 (1301-1540)	239	38	277	25	91
2 (1541-1774)	233	44	277	17	94
3 (1775-1882)	107	33	140	12	91 ^b
<u>Segment 2:</u>					
4 (2237-2481)	244	33	277	27	90
5 (2482-2704)	222	55	277	29	90
6 (2705-2947)	242	35	277	0	100
7 (2949-3191)	242	35	277	3	99
8 (3192-3340)	148	31	179	4	98 ^b
<u>Segment 3:</u>					
9 (3588-3828)	240	37	277	49	82
10 (3829-4071)	242	35	277	15	95
11 (4072-4314)	242	35	277	10	96
12 (4315-4417)	102	37	139	4	97 ^b

a Number of introduced gaps necessary for achieving a maximum of DNA base match

b The DNA sequence homology of incomplete repeat boxes 3, 8, and 12 was compared to the DNA sequences of the box 6 at the corresponding size.

The analysis of 333 amino acid residues of ORF 5 revealed an internal homology as reflected in the presence of two perfect repetitions (TR1 and 2) and their structural organization is shown in Fig. 11 E. The first type of repeat (TR1) appears as three domains (U1 to 3). Each domain possesses 50 amino acid residues placed at the amino acid position 100 to 149 (U1), 181 to 230 (U2), 262 to 311 (U3). The second type of repeat (TR2) consists of



Fig. 14. Nucleotide sequence of the HindIII/EcoRI subfragment (0.571 to 0.582 m.u., 2555 bp) of the EcoRI CIV DNA fragment H. The positions of the three inverted repetitions which are able to form a stem-loop structure are indicated. The photograph was taken from (15).

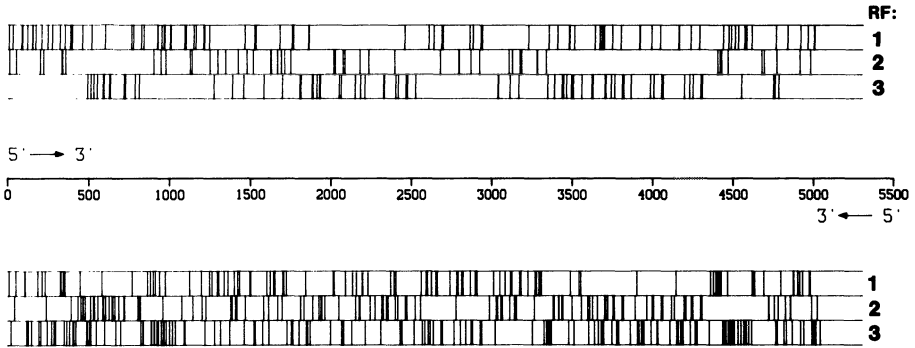


Fig. 15. Diagram of putative reading frames in the DNA nucleotide sequence of the PvuII CIV DNA fragment L on both strands. Vertical lines represent stop codons in the three reading frames. The position and the size of those ORFs that encode proteins with an amino acid sequence larger than 100 residues are listed in Table 4.

cysteine; D, aspartic acid; E, glutamic acid; F, Phenylalanine; G, glycine; H, histidine, I, isoleucine; K, lysine; L, leucine; M, methionine; N, asparagine; P, proline; Q, glutamine; R, arginine; S, serine; T, threonine; V, valine; W, tryptophan; Y, tyrosine. The photograph was taken from (16).

Table 4: Position and size of the possible proteins encoded in the DNA sequences of PvuII CIV DNA fragment L (5064 bp; 0.920 to 0.944 viral map unit) and presumptive transcription start signals

Number of ORFs	Reading frame 5' to 3'	Possible protein			number of amino acids (kD)	Signals (position)
		start (ATG)	stop codon	position		
1	nd 2	521	TAA	902	127 (13.3)	TATA (490) CAAT (406) GCGG (334)
2	rd 3	897	TAA	1275	126 (13.4)	TATTA (838) CAAT (822) CCGG (672)
3	st 1	2104	TGA	2458	118 (12.1)	TATA (2002) CAAT (1983) CCGG (1953)
4	rd 3	2685	TAG	3039	118 (12.1)	TATTT (2645) CAAAT (2622) CCGG (2614)
5	nd 2	3404	TAG	4403	333 (32.4)	TATTA (3367) CAAAT (3330) GGCC (3245) GGCGC (3223) GCGC (3217)

Note, No classical polyadenylation sites AATAAA were detected in 100 bp distance downstream of the termination codons of the individual ORFs.

two domains (U1 and 2) of a size of 74 amino acid residues which are located at the amino acid position 159 to 223 (U1) and 240 to 313 (U2).

It is noteworthy that the glycosylation signals of the type NXS or NXT occur in the different ORFs, e.g. ORF 5 contains at least seven glycosylation signals at amino acid positions 27, 81, 85, 162, 181, 243, and 262. It is interesting that the fourth glycosylation signal at

position 162 is conserved in the amino acid sequences of all of the putative gene products.

Comparative analysis of DNA and amino acid sequences of each ORF was carried out as described elsewhere (16) and the results are shown in Fig. 16. This analysis of the amino acid and DNA sequences of ORF 5 was used as a reference for a comparison with the other ORFs (1 to 4, amino acid and DNA sequences of ORF 5 was used as a reference for a comparison with the other ORFs (1 to 4, Table 4). The homologies of the protein sequence of ORF 5 to the amino acid residues of the other ORFs are not limited to the above region and extended in ORFs 3 and 4 into neighboring sequences of ORF 5 (Fig. 16).

All putative proteins possess a common amino acid consensus sequence which starts and terminates at the amino acid position 160 to 198 of ORF 5:

160-MANL(X)₆ IGSSST(X)₆ L(X)₁ LGS(X)₁ LQISG(X)₂ L(X)₁ VN-198

The analysis of 2555 bp DNA sequences of the HindIII/EcoRI DNA fragment (0.571 to 0.582 mu) for encoded possible proteins revealed the presence of an ORF between the nucleotide positions 1220 and 1721 encoding a putative protein of 167 amino acid residues. As shown in Fig. 17 this putative gene contains all classical or slightly modified transcriptional signals in particular polyadenylation signals.

VIRAL DNA REPLICATION

The analysis of the viral DNA replication revealed that the complete CIV DNA molecule has been detectable between three to four hours after infection as shown in Fig. 18. For the detection of the origins of DNA replication of the viral genome the defined genomic library of CIV was screened using transfection of CF-124

1101 AAACAGTCGTTTCCACTCCTGGAAACCGCGTGGTCTTTTAAATAGTATGTGATTGAAGGGTG
 1161 TGATAAGACAGGAAAATCAACTCAATGCAAATTATTATTA¹⁷²¹AAAAAATATAGAAGTACGTA
 1221 TGATTAATTTTCCAAATAGAACCAACTTTATAGAACACACAAACAGGAAAATTAATAG
 1 M I N F P N R T T L Y R T T Q T G K L I
 1281 ATCAATATTTAAAGGAAAAGAAGATATTCACATTTTATTTTCTAAAAATAGATGGGAAA
 21 D Q Y L K G K E D I H I L F S K N R W E
 1341 TTATCGATAACAATTA¹⁷²¹AAAAACAATATTCTTAATGGTATTACAGTCATTATTGATAGATATT
 41 I I D T I K T N I L N G I T V I I D R Y
 1401 CTTATTCTGGAATTGCGTTTTCTGTTGCTAAAGGTTTAGATTTTCAATGGTGCAAACAAA
 61 S Y S G I A F S V A K G L D F Q W C K Q
 1461 CAGAAAATGGATTGTTAA¹⁷²¹AACTGATATAATTATTATTTAAACAGGACAAACAAAAATA
 81 T E N G L L K P D I I I Y L T G Q T K N
 1521 TGGCATCAAGAAATGGTTATGGAAGTGA¹⁷²¹AATTTATGAAAGAATTGAAATTCAGATAAAG
 101 M A S R N G Y G S E I Y E R I E I Q D K
 1581 TTA¹⁷²¹AAAAATGTTATGAAAAAATGATTGAAATTCATTATGGAACAAAATAAATGCGGATC
 121 V K K C Y E K M I E I P L W N K I N A D
 1641 AGGATGTTTTAATAATTA¹⁷²¹AAAAACAATGAAACTATTATTCAA¹⁷²¹AAATTTTCGTTAGAAA
 141 Q D V L I I K K Q I E T I I Q K F S L E
 1701 ACAACAACTTGAGTATATATGAATAAGTATATGAATAAGTATATGAATAAGTATATGAA
 161 N N K L E Y I 167
 1761 AATTTATAAATTTTATA¹⁷²¹AAAATGAAACCTTTTTTCAAAGTTTATTTAACAATTAAGG
 1821 TATTTAATCAATTAAGGTATTTAATACAACAATGAATACCAGGAAAAAGTCATATTTAA
 1881 TTATAGATTAAATTTTCATA

Fig. 17. DNA and predicted amino acid sequence of the putative gene detected within the DNA sequences of the HindIII/EcoRI (0.571 to 0.582 map units; 2555 bp, see Fig. 10) subfragment of the EcoRI CIV DNA fragment H. The positions of the start codon (ATG nucleotide position 1220) and stop codon (TGA nucleotide position 1721) are indicated. The positions of transcriptional signals upstream and downstream of the start- and termination codons are underlined. The single letter amino acid code is indicated in the legend of Fig. 16.

(19) which were previously infected with CIV. The plasmid rescue experiments were carried out for selection of those recombinant plasmids which were amplified during the viral replication in infected cell cultures. It was found that six recombinant plasmids

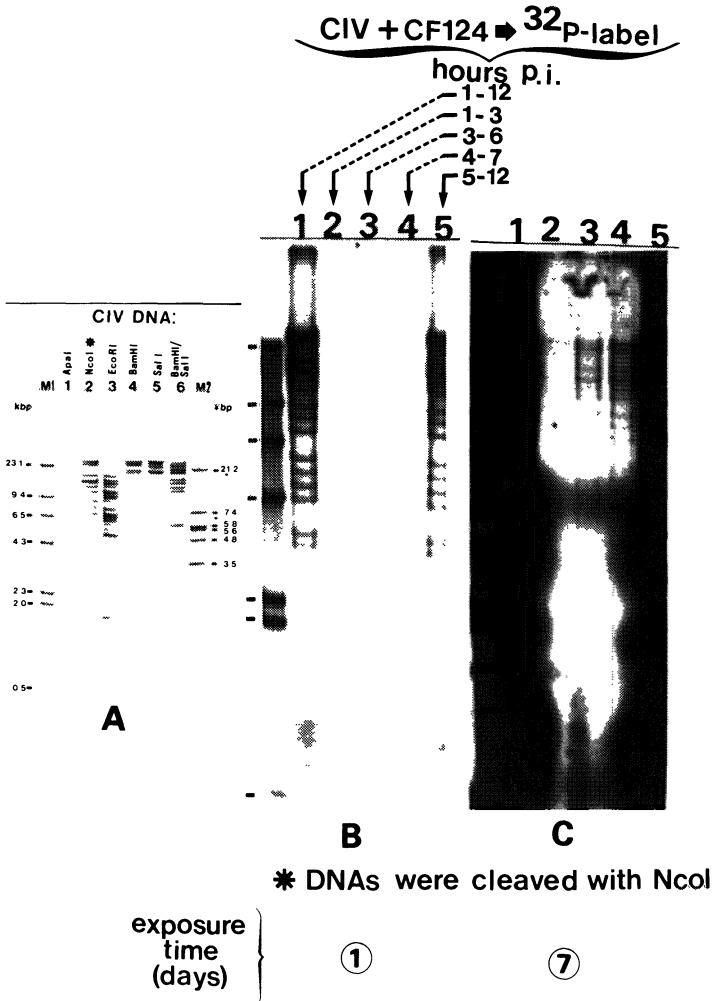


Fig. 18. Autoradiogram of ³²P-labeled CIV DNA (panel A) cleaved with the restriction endonucleases ApaI (lane 1), NcoI (lane 2), EcoRI (lane 3), BamHI (lane 4), SalI (lane 5), and BamHI/SalI (lane 6). Radioactively labeled phage Lambda DNA digested with HindIII (M1) and EcoRI (M2) served as molecular weight marker. Panels B and C show the autoradiogram of radioactively labeled DNA of CIV infected cells after digestion with NcoI. The CF-124 cells were infected with CIV at a multiplicity of infectious dose of about five infectious particles per cell. At different times after infection (1 to 12 hours) the cultures were labeled (1mCi/ml) with phosphorus-32

(as orthophosphatic acid in HCl-free solution) using phosphate free Grace's medium according to (17).

harboring the EcoRI DNA fragments C (13.5 kbp, 0.909 to 0.974 map units (m.u.)), H (9.8 kbp, 0.535 to 0.582 m.u.), M (7.3 kbp, 0.310 to 0.345 m.u.), O (6.6 kbp, 0.196 to 0.228 m.u.), Q (5.9 kbp, 0.603 to 0.631 m.u.), and Y (2.0 kbp, 0.381 to 0.391 m.u.) were able to be amplified under the conditions used. This indicates that the CIV genome possesses at least six DNA replication origins.

CONCLUSION

The genome of Chilo iridescent virus was found to be circularly permuted and terminally redundant, a unique genomic feature among eukaryotic viruses but similar to the structure of the genomes of Frog virus 3 (8, 18), Fish lymphocystis disease virus (9, 10), and Insect iridescent virus type 9 (20). The recent data obtained by the analysis of the genome of Tipula iridescence virus (TIV) shows a variability of the genomic size only (21, 22). However, this result can not yet be considered as an evidence suggesting that the TIV genome could also possess a similar structural arrangement. Consequently, more detailed analysis is necessary to find the real genomic organization of TIV.

The detection of a cluster of tandemly repetitive DNA elements with a complex structural arrangement within the CIV genome is of particular interest. To our knowledge, the extremely complex arrangement of the CIV repetitive DNA elements has no counterpart in other known DNA or RNA viral systems, not even in herpesvirus and poxvirus genomes which contain many tandem repeat DNA sequences (23-25). Furthermore the analysis of the amino acid sequence of the putative protein of the largest ORF identified within the DNA sequences of the repetitive DNA

elements which contains 333 amino acid residues revealed the presence of two perfect peptide repetitions. One containing 50 amino acid residues appears in triplicate and the other with 74 amino acid residues exists in duplicate. No polyadenylation signals were detected downstream of the stop codons of ORFs detected within the DNA sequences of the PvuII DNA fragment L. However, multiple slightly modified polyadenylation signals were detected downstream of a putative gene identified within the EcoRI CIV DNA fragment H (HindIII/EcoRI subfragment, 0.571 to 0.582 mu).

The absence of polyadenylic acid in the majority of virus-specific RNA species was reported for FV3, another member of the family Iridoviridae (26). This observation was confirmed by the analysis of the DNA sequences of the immediate-early ICR169 gene (27) and immediate-early ICR489 gene (28) of FV3. However, the absence of polyadenylation signals described above does not necessarily mean, that none of the viral mRNA species are polyadenylated.

ACKNOWLEDGMENTS

This study was supported by the Deutsche Forschungsgemeinschaft, project II B 6 Da 142/2-1 to 2-4.

REFERENCES

1. Tinsley, T.W., and D.C. Kelly. *J. Invert. Pathol.* 16: 470-472, 1970.
2. Fukaya, M., and S. Nasu. *Appl. Entomol. Zool.* 1: 69-72, 1966.
3. Smith, K. M. (ed.). In: *Virus-insect relationships*, Longman, London, 1976, pp. 102-104.
4. Jensen, D.D., T. Hukutsara, and Y. Tanada. *J. Invert. Pathol.* 19: 276-278, 1972.
5. Kelly, D.C., M.D. Ayres, T. Lescott, J.S. Robertson, and G.M. Happ. *J. Gen. Virol.* 42: 95-105, 1979.
6. Carey, G.P., T. Lescott, J.S. Robertson, L.K. Spencer, and D.C. Kelly. *Virology* 85: 307-309, 1987.

7. Bellet, A.J.D., and R.B. Inman. *J. Mol. Biol.* 25: 425-432, 1967.
8. Goorha R. and Murti, K.G. *Proc. Nat. Acad. Sci. USA* 79: 152-248, 1982.
9. Darai, G., Anders, K., Koch, H.G., Delius, H., Gelderblom, H., Samalecos, C. and Flügel, R.M. *Virology* 126: 466-479, 1983.
10. Darai, G., Delius, H., Clarke, H., Apfel, H., Schnitzler, P. and Flügel, R.M. *Virology* 146: 292-301, 1985.
11. Willis, D.B. In: *Molecular Biology of Iridoviruses* (ed. G. Darai), *Developments in Molecular Virology*, Kluwer Academic Publishers, Boston, 1989, pp. 1-12.
12. Delius H., Darai, G. and Flügel, R.M. *J. Virol.* 49: 609-614, 1984.
13. Schnitzler, P., Soltau, J.B., Fischer, M., Reisner, H., Scholz, J., Delius, H., and Darai, G. *Virology* 160: 66-74, 1987.
14. Soltau, J.B., Fischer M., Schnitzler, P., Scholz, J., and Darai, G. *J. Gen. Virol.* 68: 2717-2722, 1987.
15. Fischer, M., Schnitzler, P., Delius, H., and Darai, G. *Virology* 167: 485-496, 1988.
16. Fischer, M., Schnitzler, P., Scholz, J., Rösen-Wolff, A., Delius, H., and Darai, G. *Virology* 167: 497-506, 1988.
17. Lonsdale, D. *Lancet* 8121(1), 849-851 (1979).
18. Lee, M. H., and Willis, D. B. *Virology* 126: 317-327, 1983.
19. Sohi, S. S. *Can. J. Zool.* 46: 11-13, 1980.
20. Ward, V.K. and Kalmakoff, J. *Virology* 160: 507-510, 1987.
21. Tajbakhsh S., Dove, M.J., Lee, P.E., and Seligy, V.L. *Biochem. Cell Biol.* 64: 495-503, 1986.
22. Tajbakhsh S. and Seligy, V.L. In: *Molecular Biology of Iridoviruses* (ed. G. Darai), *Developments in Molecular Virology*, Kluwer Academic Publishers, Boston, 1989, 98-132.
23. Pickup, D.J., Bastia, D., Stone, H.O., and Joklik, W. K. *Proc. Natl. Acad. Sci. USA* 79: 7112-7116, 1982.
24. Wadsworth, S., Jacob, R.J., and Roizman, B. *J. Virol.* 15: 1487-1497, 1975.
25. Wittek, R. and Moss, B. *Cell* 21: 277-284, 1980.
26. Willis, D.B. and Granoff, A. *Virology* 73: 443-453, 1976.
27. Willis, D., Foglesong, D., and Granoff, A. *J. Virol.* 53: 905-912, 1984.
28. Beckman, B., Tham, T.N., Aubertin, A.M., and Willis, D.B. *J. Virol.* 62: 1271-1277, 1988.

4

PROTEIN COMPOSITION OF CHILO IRIDESCENT VIRUS

M. CERUTTI and G. DEVAUCHELLE

Station de Recherches de Pathologie Comparée, INRA-CNRS,
30380 Saint-Christol-lez-Alès, France.

ABSTRACT

Previous studies on interactions between Chilo iridescent virus (CIV) and cells have shown that several specific biological activities are associated with structural components of the virus particles. This is the case for enzymatic activities (e.g. ATPase, protein kinase and DNase), cell fusion induction, inhibitory activity of cellular macromolecular syntheses and non-genetic reactivation of CIV DNA infectivity. In order to gain insight into viral pathogenesis, precise localization of the CIV polypeptides within the virion and characterization of their related biological properties is indispensable. This was achieved by different techniques: (i) analysis of CIV polypeptides cross-linked by disulfide bridges in two-dimensional gel electrophoresis, (ii) stepwise disruption and stripping of virus particles, (iii) detection of external polypeptides by surface labeling, (iv) detection of proteins involved in nucleoprotein complexes and (v) selective solubilization and reconstitution of the inner viral membrane.

Thus far, up to 43 polypeptides have been identified by two-dimensional SDS-polyacrylamide gel electrophoresis. In contrast with previous reports, the major capsid component was found to be constituted of two proteins, a protein of 150,000 daltons (150 kDa, P150) composed of three identical disulfide-linked polypeptide subunits of

50 kDa (P'50) and a 50 kDa protein (P50). Although differing in some of their properties, these two proteins showed identical migration in SDS-2-ME-PAGE, however they differed in some properties. The accessibility of their sulfhydryl residues was different and radioiodination of the external polypeptides showed only one single intensively labeled spot, corresponding to the P50. However, tryptic peptide analysis showed that P50 and P'50 had a very similar peptide composition. These observations indicated that the trimeric protein P150 was not directly exposed at the surface of the viral particle. In addition, P'50 did not seem to have any affinity for viral DNA.

Thermodynamic analysis of CIV particles suggested that the DNA would be packed into a nucleosome-like structure with a viral core composed of at least six DNA-associated polypeptides. Among the six DNA-binding proteins P12.5 represents the major constituent and the preferred substrate for the virus-coded protein kinase. Preliminary experiments suggested that phosphorylation of P12.5 may result in decondensation of the DNA molecule and contribute to the release of DNA from the viral nucleocapsid at early stages of infection.

Viral inner membrane can be readily solubilized with octylglucoside. Biochemical analysis of the vesicles obtained after action of the detergent, showed that only a few polypeptides were solubilized under these conditions. However, this soluble fraction was found to be of major importance in the first stages of virus infection. The solubilized fraction contained all the factors required to initiate the replication cycle. (i) The so-called "virus-promoting factor" (VPF) induced a full cell-fusion activity and this phenomenon is independent of the capsid virus proteins. (ii) The soluble fraction also contained an inhibitory protein that facilitated viral infection by switching off cellular macromolecular syntheses and (iii) a viral-activation protein factor

that stimulated the transcription of immediate early genes by a cellular polymerase.

INTRODUCTION

The genus Iridovirus which comprises the small Iridoviridae family includes over 50 isolates (1, 2). Chilo Iridescent virus (CIV) or Iridovirus type 6 was first described by Fukaya and Nasu (3) as a pathogen for the larvae of the rice stem borer Chilo suppressalis Walker. Thin sections of the virus particles show an electron-dense irregular core enveloped by a single unit membrane. Subunits uniformly disposed on the external surface of this membrane appeared to be responsible for the typical icosahedral shape of the shell (4).

The viral genome is constituted of a large (209 kbp) linear double-stranded DNA molecule with a circular permutation and a terminal redundancy of about 12% (5). This DNA accounts for approximately 12% of the particle weight (6) and has a GC content of 29% (7).

CIV contains about 9% lipids, sufficient to form a continuous internal lipid bilayer (8). The lipid composition of the viral membrane remains unchanged whenever the virus is propagated, in vivo in larvae of Galleria mellonella, or in vitro in Choristoneura fumiferana cells. It clearly differs from that of the host membrane and is mainly characterized by an abundance of phosphatidylinositol and diglycerides. This observation suggests that the viral lipid membrane is not derived from pre-existing host membranes but is synthesized de novo during viral replication (9).

The polypeptide composition of Iridovirus particles was first analyzed by Kelly and Tinsley (10). About 19 polypeptides in the range of 10 to 213 kDa were resolved in SDS-PAGE. In later studies, Barray and Devauchelle (11) have shown that after solubilization of CIV particles with SDS-2-ME, 16 polypeptides could be resolved ranging

from 7 to 120 kDa with a major species of 51 kDa, whereas after solubilization with SDS-urea, 26 polypeptides could be identified ranging from 10 to 230 kDa. No glycosylated proteins were found by specific staining of the gel or by incorporation of labeled carbohydrates. No phosphorylated polypeptides were detected in the native particle.

A number of enzymatic activities have been reported to be associated with purified CIV particles: a nucleotide phosphohydrolase (12), a protein kinase (13) and a deoxyribonuclease (14).

The cytoplasm was described as the site of Iridoviridae assembly, morphogenesis and DNA synthesis. However, the necessity for a functional cell nucleus was established for invertebrate (15) and vertebrate iridoviridae (16). In previous studies on interactions between CIV and cells, we have shown that inoculation of vertebrate or invertebrate cells with CIV rapidly induces a massive formation of syncytia (17), whereas host cell macromolecular syntheses were drastically depressed (18). These effects which are independent of viral replication were due to one or more structural components of the invading particle.

This review summarizes the results of our studies on polypeptide composition, characterization and localization of some viral structural proteins. The implications of these structural data for morphogenesis of the particle and for the virus physiology are also discussed.

MATERIALS AND METHODS

Virus

CIV was grown in late instar Galleria mellonella larvae. Larvae were infected by intrahemocoelic inoculation of a sterile suspension of CIV. Twelve days later larvae were sacrificed and the virus purified as previously described (10).

SDS-polyacrylamide gel electrophoresis

One-dimensional SDS polyacrylamide gradient gel

electrophoresis was carried out using the discontinuous buffer system described by Laemmli (19). For two-dimensional SDS-polyacrylamide gradient gel electrophoresis, samples were treated with SDS-lysis buffer. They were boiled for 5 min and analyzed in the first dimension on 8-16% linear gradient polyacrylamide gel rods (14 x 0.3 cm). After electrophoresis the gel rods were incubated for one hour in 0.05 M Tris-HCl, pH 6.8, 15% glycerol, 2% SDS and 5% 2-ME and layered on the top of a 8-16% linear gradient slab gel (14 x 18 cm) for the second dimension. The gels were electrophoresed at 150 V (constant voltage) and stained with Coomassie blue R250.

Detection of sulfhydryl residues in CIV polypeptides

Sulfhydryl-containing polypeptides were detected in SDS-PAGE profiles by chemical labeling with N-¹⁴C ethylmaleimide (¹⁴C-NEM). Purified viral suspension in 0.01 M sodium phosphate buffer pH 7.0 was divided into three samples. Sample 1 was consisted to 100 μ l of viral suspension and samples 2 and 3 of 100 μ l of viral suspension plus 20 μ l of 10% SDS. All samples were incubated for 4 hr at 37^oC with 40 μ l (12.5 μ Ci) of ¹⁴C-NEM (2-10 mCi/mmol, Amersham) and were incubated at 37^oC. The reaction mixture was stopped in samples 1 and 2 by addition of 2-ME at 5% final concentration. Sample 3 was heated at 100^oC for 5 min prior to additon of 2-ME. The three labeled viral extracts were treated with SDS-2-ME lysis buffer and analyzed by electrophoresis in one-dimensional polyacrylamide gradient gel. One sample from batch 3 was analyzed by two-dimensional electrophoresis. Slab gels were stained, dried under vacuum and autoradiographed.

Surface labeling of CIV particle

Surface viral polypeptides were labeled with ¹²⁵I using an iodosulfanilic acid-labeling kit (New England Nuclear). Prior to coupling with proteins ¹²⁵I-iodosulfanilic acid was converted to diazonium salt by addition of 0.05 M NaNO₂ and 0.1 M HCl. Five min later

the reaction mixture was neutralized by addition of 0.05 M phosphate buffer pH 7.5. The purified viral suspension was divided into samples. Sample 1 consisted of 2 ml of native CIV. 25 μ l of the neutralized diazonium salt was added to samples 1 and 2 and the reaction mixtures were gently stirred on ice. After 15 min the labeled viral suspension of sample 1 was mixed with SDS-lysis buffer without further analysis. For sample 2, unreacted diazonium salt was eliminated from the native viral suspension by sedimenting the virus sample through a 10-40% (wt/vol) sucrose gradient (13,000 rpm, 30 min) in a Beckman SW27 rotor. Purified virus was then resuspended in SDS-lysis buffer. Both viral suspensions were analyzed by two-dimensional polyacrylamide gel electrophoresis.

DMSO treatment of the viral particle

A purified viral suspension was pelleted at 15,000 rpm for 30 min in a Sorvall SS-34 rotor and resuspended in 140 mM NaCl, 5 mM KCl, 0.7 mM Na₂HPO₄, 5 mM glucose, 20 mM Hepes pH 7.05 and 10% DMSO. After standing overnight at 4°C the viral suspension was layered on top of a 10% sucrose solution and centrifuged at 36,000 rpm in a Beckman T40 rotor for 90 min. The supernatant was extensively dialyzed at 4°C against 50 mM Tris-HCl pH 7.4, 150 mM NaCl.

Identification of DNA-binding proteins

DNA binding properties of the viral proteins were detected by the method described by Bowen et al. (20). Polypeptides were analyzed by electrophoresis on a two-dimensional polyacrylamide gradient slab gel and were transferred onto a nitrocellulose sheet (Schleicher and Schuell BA85, 0.45 μ m). The blots were preincubated for 30 min at room temperature in 1 mM EDTA, 10 mM Tris-HCl pH 7.0, 50 mM NaCl, 0.02% bovine serum albumin fraction V, 0.02% Fricoll 400 and 0.02% polyvinylpyrrolidone 360. The blots were then incubated at 37°C with ³²P-labeled viral DNA (5 μ g/ml, 2 x 10⁵ cpm/ μ g). After 6 hr incubation, blots were rinsed four times with 2 x SSC for 30 min at

room temperature, dried and autoradiographed (Fuji X-ray films).

Solubilization and reconstitution of viral inner membrane

Purified viral particles were resuspended in the following buffer: 25 mM Tris-HCl pH 9.0, 1 M NaCl and 30 mM octylglucoside (Buffer C). After standing overnight at 4°C the viral suspension was loaded on top of a 10% sucrose cushion (6 ml, in buffer C) and centrifuged at 36,000 rpm for 2 hr in a Beckman SW41-Ti rotor. The clear supernatant was extensively dialyzed at 4°C against 50 mM Tris-HCl pH 7.4 150 mM NaCl to remove detergent.

Protein kinase assay

Autophosphorylation of CIV polypeptides by endogenous protein kinase was carried out as previously described (13). Purified CIV was resuspended in the following reaction mixture: Tris-HCl 25 mM pH 8.0, MgCl₂ 20 mM, NP40 0.02%, ATP 2mM and 15 μ Ci of ³²P ATP as substrates. After 1 hr incubation, polypeptides were analyzed on two-dimensional SDS-PAGE. Phosphorylated polypeptides were detected by autoradiography.

RESULTS

Analysis of the CIV polypeptides by two-dimensional polyacrylamide gradient gel electrophoresis

The electrophoretic patterns of CIV polypeptides were compared under reducing and nonreducing conditions. Treatment of CIV particles with 2% SDS leads to the solubilization of about 35 polypeptides designated as: "polypeptides SDS no" with apparent relative molecular weights (M_r) ranging from 300 to 11 kDa. At least, two major polypeptides could be resolved: polypeptide SDS 6 (150 kDa) and SDS 18 (50 kDa). Electrophoretic pattern obtained under reducing conditions showed very significant differences. Viral polypeptides solubilized in these conditions were resolved into molecular species ranging from 200 to 11 kDa, with a major polypeptide mi-

grating at 50 kDa. The relationship between these two different profiles was established by two-dimensional polyacrylamide gradient gel electrophoresis (Fig. 1). Purified CIV suspension was solubilized and electrophoresed under nonreducing conditions in the first dimension and under reducing conditions in the second dimension. Figure 1 shows that some of the viral polypeptides have a particular behaviour. (i) Most of the CIV polypeptides are not sensitive to mercaptoethanol and migrated similarly in both dimensions. They were distributed diagonally in accordance with their molecular size. (ii) Some polypeptides migrated as smaller molecules in the second dimension representing viral polypeptide subunits originally linked with disulfide bonds. At least three proteins behaved in such a way: the major polypeptide SDS 6, which migrated in the first dimension at 150 kDa corresponded to a trimeric form of a 50 kDa polypeptide species (P'50). Similarly, polypeptide SDS 7 (120 kDa) corresponded to a dimeric form a P60 and P12.5 respectively. (iii) Four spots referred to as P81, P79.5, P53 and P49 appeared above the diagonal line of migration. These polypeptides migrated with a lower molecular size in the first dimension and behaved as much larger molecules in the second dimension. This shift suggested a conformational change of the molecule likely due to occurrence of intramolecular disulfide bonds.

Addition of 8 M urea in the lysis buffer and in the first dimension gel did not significantly modify the two-dimensional pattern (Fig. 2). This experiment indicated that the presence of polypeptide P'50 was not the consequence of a non-exhaustive solubilization of the sample. In addition, treatment of CIV with urea led to an extensive solubilization of polypeptide P12.5 (compare panels Fig. 1 and Fig. 2). When gels were electrophoresed without urea, a large proportion of P12.5 was retained on top of the first-dimension gel. After incubation in

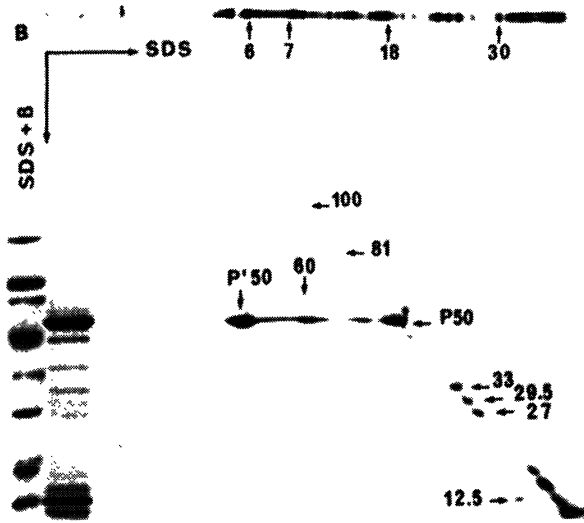


Fig. 1. Two-dimensional SDS-PAGE analysis of CIV proteins and disulfide-linked protein complexes. CIV was fractionated in the first dimension in nonreducing SDS-PAGE and in the second dimension in 2-ME-containing SDS-PAGE.

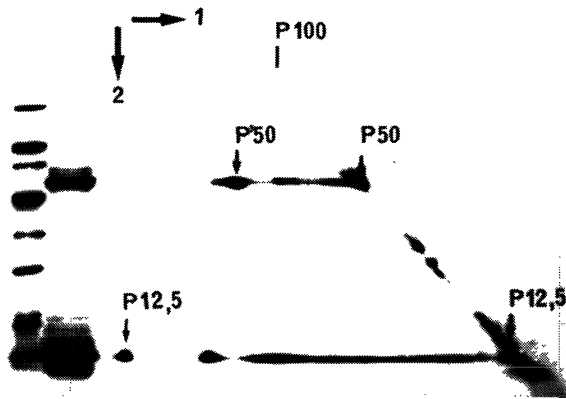


Fig. 2. Two-dimensional electrophoresis pattern of CIV polypeptides after disruption of viral particles with 2% SDS, 5% 2-ME and 8 M urea solution.

reducing buffer, this fraction was partially solubilized and a discrete spot appeared perpendicularly to the top of the first-dimension gel. This experiment showed, that polypeptide P12.5 represented an important proportion of the total virion protein.

Accessibility of sulfhydryl residues in the CIV particle

Sulfhydryl-containing polypeptides were detected by binding with N- ^{14}C ethylmaleimide (^{14}C -NEM) and accessibility of these residues was analyzed after stepwise stripping of the CIV particle. This was achieved in one- and two-dimensional electrophoresis. ^{14}C -NEM labeling was performed in three different samples. When native CIV particles (Sample 1) were incubated with ^{14}C -NEM, one-dimensional autoradiogram (Fig. 3A) only showed a weak labeling of (P50-P'50). The intensity of the (P50-P'50) labeling was significantly increased by 2% SDS treatment of the CIV particle (Sample 2). In addition, ^{14}C -labeling of P60 was observed. When CIV was heated at 100°C for 5 min with 2% SDS (Sample 3) the labeling intensity in the (P50-P'50) zone was even more pronounced, whereas the labeling in the P60 species seemed to remain unchanged. Two polypeptides referred to as P100 and P33, appeared to be highly reactive under the most denaturing conditions (Sample 3). Two-dimensional analysis of sample 3 (Fig. 3B) showed a very significant difference of labeling intensity between P50 and P'50. This difference could not be account for by a difference in the copy number of P50 and P'50 within the virion. Coomassie blue staining of the same gel suggested a stoichiometric ratio of 1:1 for P50 and P'50 (Fig. 1).

Identification of surface viral polypeptides

Surface viral polypeptides were labeled with ^{125}I -iodosulfanilic acid and analyzed by two-dimensional polyacrylamide gel electrophoresis. Iodosulfanilic acid reacts with amino groups of tyrosine and histidine and with sulfhydryl groups of the cell surface proteins (21). It has been shown that diazotized sulfanilic and iodosul-

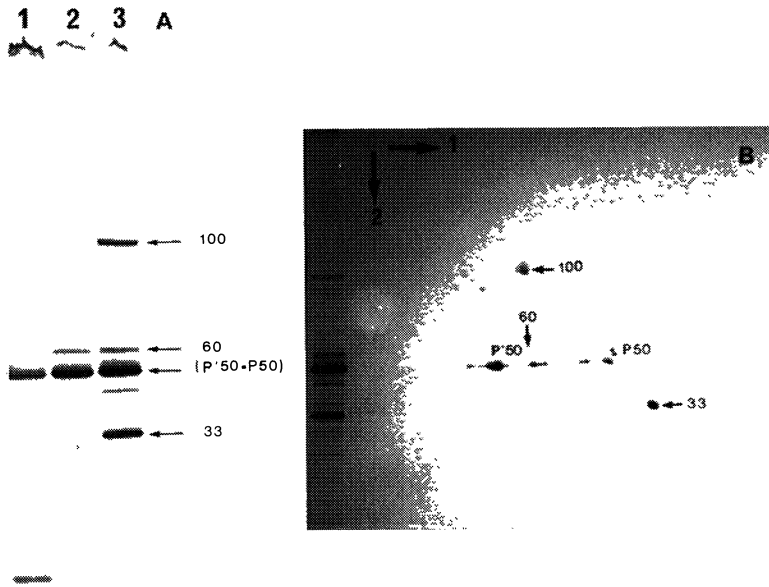


Fig. 3. Sulfhydryl-containing polypeptides of CIV (A) one-dimensional SDS-PAGE pattern of ^{14}C NEM-labeled virus. The viral suspension was aliquoted into three samples. Sample 1 consisted of $100\ \mu\text{l}$ of viral suspension, samples 2 and 3 of $100\ \mu\text{l}$ of viral suspension plus $20\ \mu\text{l}$ of 10% SDS. $40\ \mu\text{l}$ of ^{14}C NEM was added to each sample and further incubated for 4 hr at 37°C . The reaction was stopped in samples 1 and 2 by addition of 2-ME 5% final concentration. Sample 3 was boiled for 5 min prior to addition of 2-ME (B). An aliquot of sample 3 was analyzed in two-dimensional SDS-PAGE containing 2-ME in the second dimension. The polypeptides were visualized by autoradiography.

fanilic acid do not enter the cell membrane (22). In order to specifically label the external polypeptide, iodination has been carried out on native CIV particles and compared with virions disrupted with 2% SDS. As shown in Fig. 4, all the polypeptide spots visible by Coomassie blue staining were found to be labeled. The high labeling level of P100 and P33 (compare Fig. 4A and Fig. 1) was consistent with their reactivity with NEM. P100 and P33

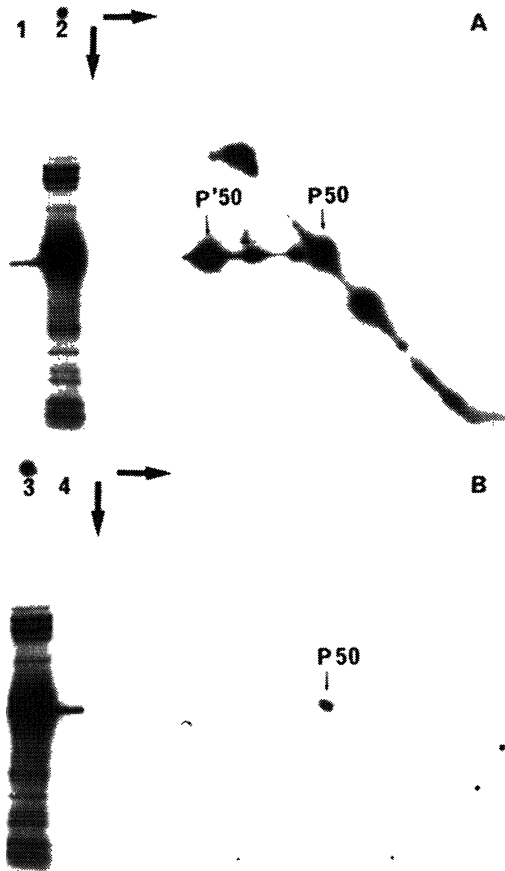


Fig. 4. Identification of surface viral polypeptides. Surface viral polypeptides were labeled with ^{125}I -iodo-sulfanilic acid and analyzed by two-dimensional SDS-PAGE. (A) Autoradiogram of two-dimensional analysis of CIV disrupted by 2% SDS prior to the labeling reaction. (B) Autoradiogram of two-dimensional analysis of native CIV particles. Control electrophoretic patterns of one dimension are indicated along the left sides of two-dimensional profiles. Lanes 1 and 4 represent native CIV; lanes 2 and 3, CIV disrupted by 2% SDS.

are likely to be sulfhydryl-rich polypeptides (Fig. 3). In contrast, iodination of native particles showed one single, intensively labeled spot corresponding to P50 (Fig. 4B). Polypeptide P'50 was barely visible on the

autoradiogram. Polypeptide P50 would thus be the more external component of the virus particle. The P50 polypeptide was selectively solubilized by incubating the CIV suspension with 10% DMSO. As shown in Fig. 5A, P50 was readily solubilized by DMSO treatment, whereas the trimeric form of P'50 (P150) was still found associated with the pellet. Electron microscopic observation of the DMSO extract (Fig. 5B) showed the presence of viral subunits displaying the typical morphology of Iridoviridae capsomers i.e. cylindrical shape with a central hole, and a diameter of about 7 nm (23).

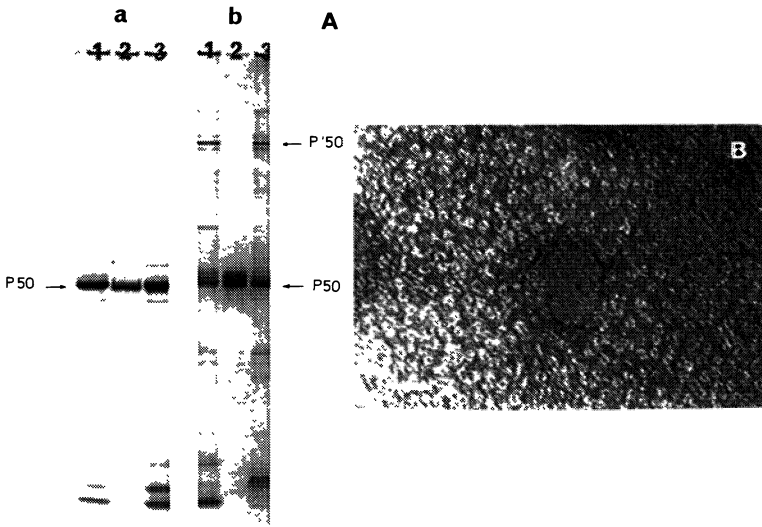


Fig. 5. Selective solubilization of P50 polypeptide by DMSO-containing buffer. After treatment with DMSO, the viral suspension was layered on 10% sucrose and centrifuged at 36,000 rpm for 90 min. (A) Supernatant and pellet was analyzed by one-dimensional electrophoresis under reducing (a) and non-reducing (b) conditions. Lane 1, pellet; lane 2, supernatant; lane 3, native CIV (B) electron microscopy of CIV surface subunits released by DMSO treatment. Negative staining with 1% uranyl acetate. Bar indicates 20 nm.

When viral suspensions were submitted to several cycles of freezing and thawing in the presence of EDTA (Fig. 6A), a new type of viral subunit could be observed (Fig. 6B). These subunits showed an asymmetrical dumbbell-like shape. These subunits were fibrous structures, 10 nm in length, terminated at one end by a sphere of 4 nm in diameter and at the other extremity, by a knob of 2 nm in diameter. The whole dumbbell-like structure is 16 nm in total length, and is reminiscent of the adenovirus penton fiber structure. In the case of adenovirus serotype 3, the fiber capsomer is 11 nm in length, 2 nm in diameter, terminated by a knob of 4 nm and is composed of three subunits of 34.8 kDa (24, 25).

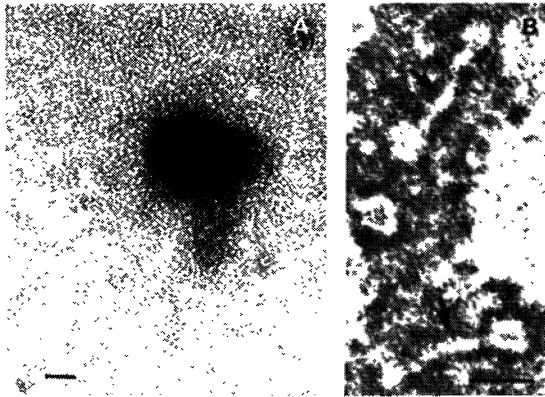


Fig. 6. Electron microscopy of viral subunits released after several cycles of freezing and thawing in the presence of 1 mM EDTA. Negative staining with 1% uranyl acetate. A) Bar indicates 40 nm; B) bar indicates 6 nm.

One can speculate that these fibers correspond to the P150 protein species. A rough estimation of the protein mass of this structure calculated from its physical parameters (length, diameter, volume of spherical extremities and a density of 1.3 for protein) gives a value of 2.5×10^{-19} g for one molecule of fiber. This is in good agreement with a trimeric structure, compound

of 50 kDa subunits. In this hypothesis these fiber structures could represent the covalent P150 trimer, since these subunits resist drastic disruption of the viral capsid.

Comparative analysis of P50 and P'50

Purified CIV particles were solubilized at high ionic strength with octylglucoside and 2-ME. This treatment resulted in solubilization of P50 and P'50 polypeptides. Unsolubilized material was removed by centrifugation through a 10% sucrose cushion containing octylglucoside. After extensive dialysis to eliminate 2-ME and detergent, soluble viral extract was analysed by two-dimensional electrophoresis (Fig. 7A). As a control, virus particles were solubilized by SDS-2-ME and electrophoresed in two-dimensional gels without fractionation. In the control experiment (Fig. 7B), all the virus polypeptides migrated in a diagonal line with a major spot corresponding to overlapping P50-P'50. In contrast with this pattern, two distinct spots (a, b) could be resolved in the supernatant of virus treated with 2-ME and octylglucoside. The spot (a) had the same electrophoretic mobility in both dimensions and appeared in the diagonal line. It could therefore be identified as P50. The second polypeptide (b) migrated above the diagonal line symmetry indicating the presence of intramolecular disulfide bonds (Fig. 7A). A minor 50 kDa species (spot c) was also visible, underneath a 100 kDa spot. One explanation for the occurrence of spots b and c would be that sulfhydryl residues generated with 2-ME from trimeric protein could react with each other to form dimeric structures (spot c) and/or reform more easily with intramolecular disulfide bonds to generate species migrating in spot b. This experiment suggested that P50 and P'50 constituted two distinct structural entities.

Comparative tryptic peptide analysis was carried out on P50 and P'50 polypeptides using ^{125}I -labeled CIV particles. The first-dimension SDS-PAGE gel was treated

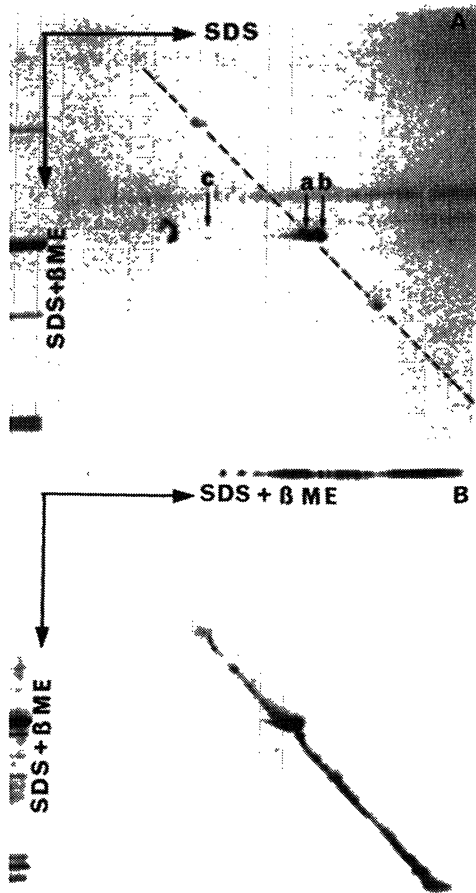


Fig. 7. Two-dimensional SDS-PAGE pattern of octylglucoside, 2-ME solubilized fraction of CIV particles. (A) Purified CIV particles were solubilized in 1 M NaCl containing 30 mM OG and 5% 2-ME. Unsolubilized material was discarded by centrifugation through a 10% sucrose cushion. After extensive dialysis, the soluble viral extract was analyzed by two-dimensional electrophoresis. (B) The reference two-dimensional profile was obtained with purified CIV particles solubilized at each of the two steps by SDS-2-ME lysis buffer. Coomassie blue staining.

with TPCC-trypsin for 20 min at 20⁰ C, and subjected to a second SDS-2-ME-PAGE. The results in Fig. 8 show that P50 and P'50 had a similar peptide composition, suggesting

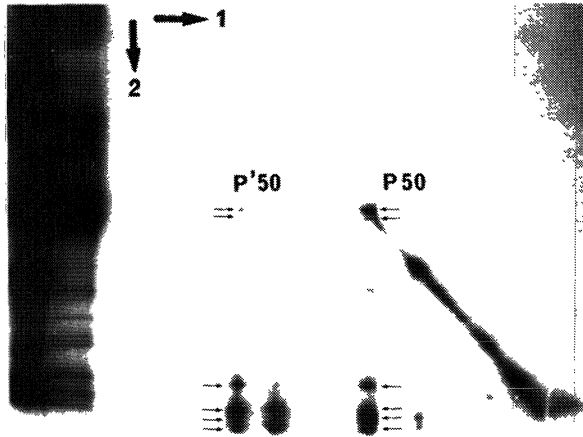


Fig. 8. Tryptic peptide analysis of P50 and P'50 by two-dimensional SDS-PAGE. ^{125}I -labeled virus was first electrophoresed in a cylindrical gel by the standard SDS-PAGE method. The first dimensional gel was treated with trypsin solution (DPCC-treated trypsin, Sigma; 1 mg/ml, 10 mM Tris-HCl pH 7.6, 5 mM CaCl_2 , 140 mM NaCl) for 20 min at 20°C , and subjected to second dimension SDS-PAGE. Proteolytic cleavage products migrated under the diagonal line as shown by autoradiography.

structural identity of the two polypeptides.

It was previously reported that the major CIV protein might be composed of a single species of polypeptide subunits (10, 26). Our observations confirmed that the major protein of CIV is in fact constituted of identical polypeptides, of which the subunits are differently arranged. One component would be a trimeric 150 kDa protein composed of three identical subunits linked by disulfid bonds. Considering the stoichiometry ratio of 1:1 for P50 and P'50 (Fig. 1 and Fig. 7A), it is reasonable to postulate that the second component of the major capsid protein of CIV is also a trimer composed of three P50 subunits interacting with non-covalent bonds. Radiolabeling of external polypeptides indicated that polypeptide P50, but not polypeptide P'50 was directly

exposed at the surface of the viral particle.

Identification of viral DNA-binding protein(s)

Viral nucleoproteins were identified using the method for detecting proteins with a DNA-binding capacity (20). Purified virus was electrophoresed in two-dimensional polyacrylamide gradient slab gels and the polypeptides transferred onto nitrocellulose sheets and hybridized with ^{32}P -labeled CIV DNA. At least six polypeptides (P81, P60, P29.5, P18, P15, and P12.5) showed an affinity for CIV DNA (Fig. 9). All these DNA-protein interactions were found to be very stable, and adsorbed DNA could not be released even after repeating washings of the blots with 2 x SSC. Polypeptide P150 did not seem to have any affinity for viral DNA at least under our conditions. It is interesting to note that among the six DNA-binding proteins, the polypeptide P12.5 represented a major component of the CIV particle, suggesting an important role for this polypeptide in the compaction of the genomic DNA molecule within the virus particle. This property may explain the unusual behaviour of this polypeptide in the two-dimensional PAGE (Fig. 1).

Phosphorylation of viral polypeptides by endogenous protein kinase

Monnier and Devauchelle (13) have shown that viral protein kinase is able to phosphorylate endogenous polypeptides and particularly low molecular weight polypeptides. Autophosphorylation experiments have been carried out in optimized conditions for the viral protein kinase, namely in 25 mM Tris-HCl pH 8.0, 20 mM MgCl_2 , 0.02% NP40, 2 mM ATP in the presence of ^{32}P -ATP. After 1 hr incubation at 30°C, viral extracts were analyzed in two-dimensional gels. As shown in Fig. 10, polypeptide P12.5 constituted the preferential substrate for the viral kinase. The possible consequence of the phosphorylation process of P12.5 on its DNA binding capacity was

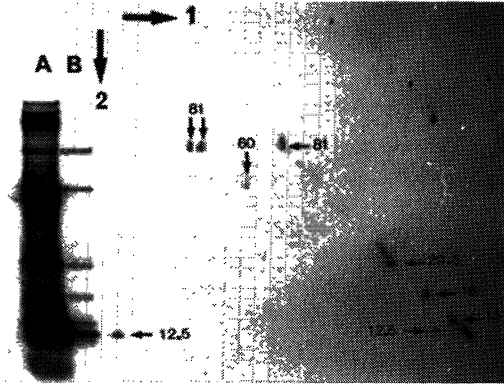


Fig. 9. DNA-binding proteins of CIV. Proteins were analyzed by two-dimensional SDS-PAGE and blotted onto nitrocellulose. Blots were incubated with ^{32}P -labeled CIV DNA solution (10^6 cpm/ml). Protein-bound DNA was detected by autoradiography. Lane A, ^{125}I -labeled CIV; lane B, unlabeled CIV.

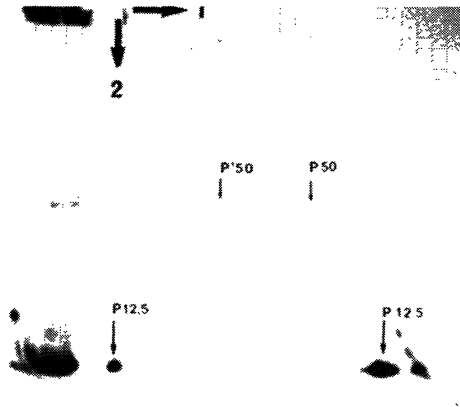


Fig. 10. Phosphorylation of viral polypeptides by endogenous protein kinase. CIV was incubated for 1 hr at 30°C in 25 mM Tris-HCl pH 8, 20 mM MgCl_2 , 0.02% NP40, 2 mM ATP in presence of ^{32}P -ATP (15 μCi). Viral extract was analyzed by two-dimensional SDS-PAGE and autoradiography.

investigated in the following experiment. CIV suspension was incubated as described above, but in the presence of unlabeled ATP. After 1 hr incubation at 30°C, polypeptides were analyzed by two-dimensional polyacrylamide gel electrophoresis, transferred onto a nitrocellulose sheet and hybridized with ³²P-CIV DNA. No apparent change in DNA-binding property of the phosphorylated polypeptides was evidenced on the autoradiography (not shown).

Solubilization and reconstitution of the viral membrane

Purified virus suspension was treated with 30 mM octylglucoside in 1 M NaCl (buffer OG). After standing overnight at 4°C, insoluble material was discarded by centrifugation (35,000 rpm for 2 hr at 4°C in a SW 41-Ti rotor) through a 10% sucrose cushion in buffer OG. The clear supernatant was extensively dialyzed to remove salt and detergent allowing the reconstitution of the viral membrane. The slightly opalescent suspension which was recovered was examined by electron microscopy. Negative staining showed viral vesicles of different size varying in diameter from 50 to 200 nm. Viral subunits were hardly indistinguishable on the vesicle surface. Thin sections of reconstituted materials (Fig. 11) showed single-shelled vesicles with a single unit membrane. From biochemical analyses it was found that about 86% of viral phospholipids and only 4% of total proteins were recovered in this fraction. As shown in Fig. 12, octylglucoside and high ionic strength treatment led to the selective solubilization of at least five polypeptides, P53, P46.5, P15, P11. Under these conditions, polypeptides P50 and P'50 remained strongly bound to the core fraction, resulting in the formation of delipidated CIV particles. These observations suggested the existence of preferential interactions between capsid polypeptides and core polypeptides. It should be noted that the major component of the membrane fraction - polypeptide P11 -

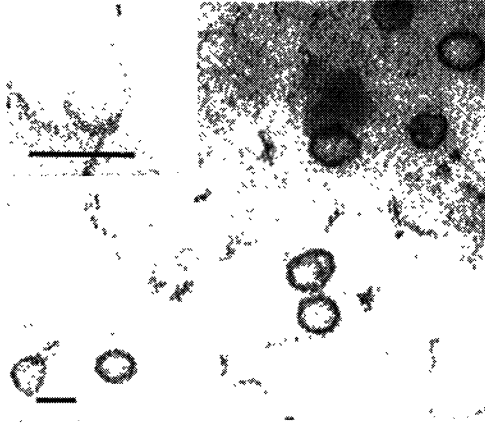


Fig. 11. Electron microscopy of thin sections of pelleted vesicles. Inset: magnification of characteristic vesicle. The three-layered membrane is visible. Bar indicates 100 nm.

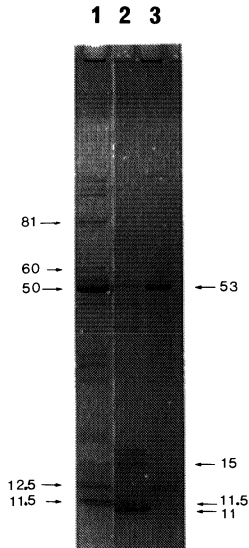


Fig. 12. SDS-gradient polyacrylamide gel electrophoresis of vesicles obtained after treatment of CIV with octylglucoside. Lane 1: native CIV, lane 2: vesicles, lane 3: residual pellet.

represents a very minor component of the native virus particle. In order to further characterize the association between lipids and viral polypeptides, lipophilic polypeptides were selectively extracted from CIV particles (27) with acidic chloroform-methanol (28). Five polypeptides of 11, 12.5, 16, 18, and 50 kDa, were thus identified. While polypeptides of 50 kDa, 16 kDa and 18 kDa were strongly associated with phospholipids such as phosphatidylinositol and phosphatidylcholine, preliminary experiments suggested that the polypeptide of 11 kDa would be covalently linked with a fatty acid, probably palmitic acid (data not shown).

Contrasting with a rather simple polypeptide pattern, various biological activities were found associated with the membrane fraction. These include cell fusion induction, inhibitory activity of host cell macromolecular syntheses, and transcription activating factor(s). Analysis of reconstituted vesicles by isopycnic centrifugation in sucrose gradients showed that although differing in size, the vesicles sedimented as a sharp peak at a density of 1.10-1.13. The observed density could be modified by addition of exogenous lipids e.g. cellular lipids, during the reconstitution (data not shown).

Incubation of permissive cells (Cf124 cells) with vesicles showed that this fraction was infectious (29). This infectivity was very low, and could only be detectable after two serial passages in permissive cells. When vesicles were prepared from ³H-methyl-thymidine-labeled virus, DNA was found to cosediment with the vesicles (Fig. 13). Extraction and purification of this vesicular DNA confirmed the presence of large subgenomic DNA fragments (about 75 kbp). Digestion with restriction endonuclease demonstrated that this DNA did not correspond to a particular fragment but to a population of DNA fragments of homogenous size, arising from various

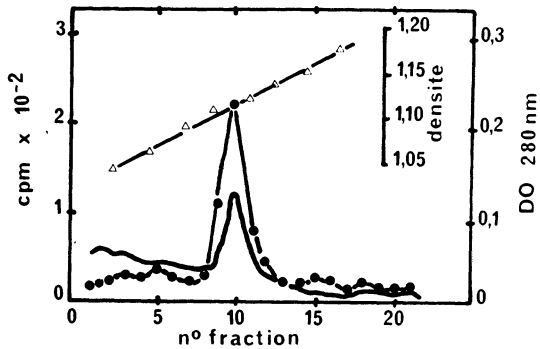


Fig. 13. Isopycnic centrifugation of vesicles reconstituted from ³H-methyl-thymidine-labeled CIV. Samples were layered on a 10-60% sucrose gradient in 50 mM Tris-HCl pH 7.4, 150 mM NaCl. The gradient was centrifuged at 4° C in a SW41-Ti Beckman rotor at 38,000 rpm for 24 hr. Fractions were collected from the top of the gradient and aliquots were used for radioactivity measurements.

regions of the viral genome. However, purified viral DNA was not infectious. The presence of DNA in the vesicles could not therefore account for the observed infectivity.

Experiments of nongenetic reactivation of purified CIV DNA by UV-irradiated virus suggest that one (or more) structural component(s) of CIV particles must be involved in the first step of the viral infection (29). It can be supposed that the vesicle suspensions composed of a population of vesicles that differ in their DNA content, also contain some "activating-protein factor". Infectivity of such suspensions would thus be the result of both a recombination event between large overlapping DNA fragments and the presence of viral protein factor(s).

The presence of the large subgenomic DNA fragments in the vesicular fraction prompted us to look for the presence of DNA-binding proteins in this fraction. One can postulate that some specific regions of the DNA molecule present a high affinity for membrane component(s), so that DNA molecules remain tightly bound to the membrane via one (or more) anchorage point(s) during the

octylglucoside solubilization process. During dialysis, DNA molecules would be mechanically cleaved and randomly packed into the vesicles. Fig. 14 showed that at least two membrane associated polypeptides (P20a and P20b) displayed a very high affinity for viral DNA. However, these DNA-binding proteins did not constitute major DNA-binding proteins in the native particle. At least two hypotheses can be formulated: (i) these proteins might be involved directly or indirectly in the activation process, possibly enhancing transcription of immediate early viral genes, or (ii) these proteins might play a role in the morphogenesis process.

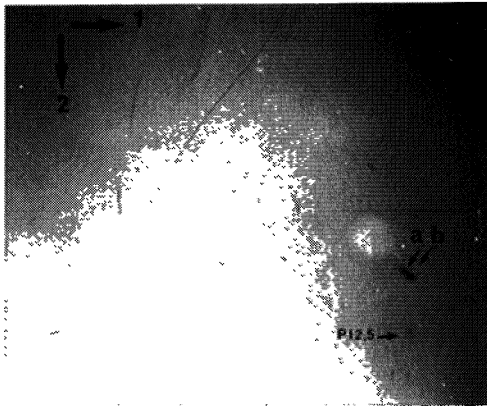


Fig. 14. Identification of DNA-binding proteins in the vesicle fraction by Western blotting as described in Materials and Methods. Protein-bound DNA was detected by autoradiography.

Very little is known about assembly of Iridoviridae particles in host cell cytoplasm (30). The earliest recognizable intermediate structure is an incomplete icosahedral structure located on the edges of a virogenic stroma. As the shell enlarges, it appears to sequester a portion of the virogenic stroma (28). One hypothesis is that the inner membrane might function to segregate viral genomes from the virogenic stroma (31). Such a hypothesis

has also been postulated in the case of poxvirus (20), where the membrane acts as a mesosome-like structure.

Enzymatic activities associated with purified CIV particles

CIV particles contain at least three enzymatic activities firmly associated with purified virions. A nucleotide phosphohydrolase which requires Mg^{++} for activity, hydrolyses preferentially ATP and dATP to yield ADP and inorganic phosphate (12). A protein kinase (13) was found to phosphorylate some low molecular weight polypeptides "in vitro", and displayed a high preference for basic proteins as exogenous substrate: protamine was phosphorylated at serine and threonine residues. The enzyme was c-AMP independent and phosphorylation rates were higher with ATP than with GTP. A deoxyribonuclease cleaved DNA(s) from different origins, including CIV DNA (14). So far, none of these activities have been localized in the virus particle.

CONCLUSION

Different polypeptide patterns have been published for members of the Iridovirus group (10, 32). These studies demonstrated the high complexity of the polypeptide content of these viruses but no observations were reported on the possible presence of disulfide-linked protein complexes. All isolates of Iridovirus appeared to be serologically related to some extent, with the exception of CIV and possibly iridescent virus type 24 (33). However, electrophoretic patterns of structural polypeptides obtained from these different isolates are closely related, with a common major structural polypeptide of about 50-55 kDa. Unfortunately, no experiments were reported on the behavior of these major polypeptides under nonreducing conditions. It is interesting to note that

Iridovirus type 2 (Sericesthis iridescent virus, SIV) possesses two major structural polypeptides of 53 kDa and 55 kDa respectively (34). Coomassie blue staining suggests that these two polypeptides are present in equimolar ratio within the virus particle.

The results presented here strongly suggest that the major capsid component of CIV is in fact, a multimeric protein edifice constituted of several polypeptide subunits of 50 kDa, structurally identical, but differently arranged and exposed. The resulting structure would be formed of two trimeric proteins, one maintained by covalent disulfide bridges ($P'50 \times 3$), the other one by noncovalent bonds ($P50 \times 3$). This latter trimer would be externally exposed at the surface of the virion. Our structural model was based on the following data: (i) both P50 and P'50 polypeptides show identical mobility in SDS-2-ME-PAGE, identical peptide finger-prints and are present in equimolar ratio within the virus particles, (ii) however, the accessibility of their sulfhydryl residues is totally different, as well as (iii) their solubilization with DMSO. This is reminiscent of the data reported for phage Q in which intermolecular disulfide links between identical protein subunits leads to the formation of two distinct protein entities (35).

The phageQ capsid is estimated to consist of 12 pentamers and 20 hexamers which are detected as distinct morphological and biochemical entities. However, both are composed of identical proteins subunits stabilized by intermolecular disulfide bonds. In that case, as in the case of CIV capsid polypeptides, it remains to be determined whether the disulfide bonds are formed before or after virus assembly. Two hypotheses can be formulated to explain the structural model we propose for CIV capsomeric protein. (i) Some discrete and undetectable post-translational modifications of P50/P'50 might result in structural changes rendering some thiol residues acces-

sible or bound in the protein. The one species with accessible thiol groups might form the covalently bound trimeric protein P150. The species with bound thiol group(s) would trimerize via noncovalent hydrophobic Van der Waal's bonds. (ii) Trimerization of P'50 subunits via disulfide bonds might generate new binding sites on the trimeric protein available to three additional P50 subunits linked to the trimer by noncovalent bounds. Such a mechanism of stepwise binding of additional protein subunits has already been described in morphogenesis of t-even bacteriophages (36). These two hypotheses are not mutually exclusive.

More and Kelly (26) have isolated by preparative SDS-2-ME-PAGE the major structural polypeptide of Iridovirus types 2, 6 and 9. While proteins of each virus have a slightly different M_r amino acid analysis indicated a very similar composition, with no particular enrichment in either hydrophobic, hydrophylic or basic amino acids. In addition, N-terminal analysis of the three polypeptides gave a single N-terminal (proline), suggesting that the proteins are homogeneous.

These apparently conflicting observations suggest that: (i) P50 and P'50 constitute two closely related but distinct polypeptide entities deriving from a common precursor protein. (ii) Polypeptides P50 and P'50 possess an identical primary amino acid sequence. Discrepancies between these two different polypeptide entities could be explained either by polypeptide modification at the post-translational level (although no glycosylated, acylated or phosphorylated proteins were detected in native CIV particles) or by differences in the folding of the polypeptide which would be directly related to the location of this polypeptide during morphogenesis.

In the case of FV3, ultrastructural and biochemical studies suggest that capsomers are composed of trimers of VP48. FV3 capsid subunits have the same mobility in SDS-

gels under nonreducing or reducing conditions, implying that the trimer assembly does not occur via disulfide bonds. The interpeptide bonds responsible for the cohesion of the trimers is therefore noncovalent in nature and involve Van der Waal's links (37).

Several authors have reported the presence of disulfide-linked proteins in a number of unrelated viruses. The importance of these proteins in biological activities (38, 39), structure and morphogenesis (40, 41) of the viruses is well known. In the case of CIV particles, there is no evidence for the implication of such complexes in biological activities. However, it seems that these structures are of great importance for CIV capsid stability. Analysis of delipidated particles obtained after OG treatment, shows that polypeptides P50 and P'50 remain strongly bound to the core fraction, suggesting the existence of preferential interactions between capsid and core polypeptides. Addition of 2-ME to these delipidated particles leads to the solubilization of P50 and P'50. This experiment shows the importance of the underlayer of trimeric complex P150 in capsid stability.

The viral inner membrane has been solubilized with octylglucoside. Biochemical analysis of the reconstituted viral membrane obtained after dialysis of the detergent shows that only a few polypeptides have been selectively solubilized under these conditions. However, the biological importance of this fraction in the first stage of infection is demonstrated by the observation that this fraction contains all the main "promoting events" required to initiate the replication cycle: (i) a cell fusion activity, independent of the capsid proteins, leading to a rapid fusion between viral and cellular membranes, (ii) an inhibitory protein which facilitates viral infection by switching off the macromolecular syntheses and (iii) an "activating factor" stimulating the transcription of immediate early genes by a cellular RNA polymerase.

Thermodynamic investigation of CIV by means of UV-

spectroscopy and microcalorimetry shows that the CIV DNA denaturation pattern resembles that of nucleosomal structures (42). At least six polypeptides have been found to possess an affinity for CIV DNA. It is interesting to note that P12.5, which probably represents the essential component of the viral core, constitutes the preferential substrate for the viral protein kinase. Preliminary results suggest that DNA-binding property of this polypeptid would not be modified upon phosphorylation. However, it seems that its solubility in 2% SDS is significantly increased. It can be hypothesized that endogenous protein kinase activity results in decondensation of the DNA molecule, thus contributing to the release of DNA from the nucleocapsid at the first step of infection. In this respect, it would be interesting to know whether this highly preferential phosphorylation occurs "in vivo" during the virion uncoating. Further investigation is necessary to confirm the functional role of the endogenous kinase. Many investigators have proposed possible functions such as phosphorylation of viral or host-cell protein via endogeneous viral kinase activity. These proposed functions include regulation of viral genome replication and transcription, virion uncoating, modification of host-cell protein(s) which may contribute to the shutdown of the cell macromolecular synthesis and virion assembly.

Our findings clearly show that different types of interactions and organizations are involved in the structure of the CIV particle. A tentative model for CIV structure could be a central DNA genome packed into a nucleosomal-like structure, with at least six DNA-associated proteins constituting the viral core. The core structure would be surrounded by a membrane containing a P150-3xP50 complex, with the P150 trimer oriented inward and the P50 polypeptides being more exposed at the surface of the particle. Preferential interaction between the capsid protein trimer P150 and the core polypeptides

might be responsible for the stability of the whole particle, resulting in the typical icosahedral shape of the shell.

We acknowledge Professor P. BOULANGER for helpful discussions and for critical reading of the manuscript, G. KUHL for the preparation of illustrations and M. DALVERNY for manuscript preparation.

REFERENCES

1. Kelly, D.C. In: Current topics in microbiology and immunology (Ed. D.B. Willis), Springer Verlag Berlin, Heidelberg, New York, Tokyo, No.116, 1985, pp. 23-35.
2. Hall, D.W. In: Viral insecticides for biological control (Eds. K. Maramorosch and K. Sherman), 1985, pp. 163-196.
3. Fukaya, M. and Nasu, S. Appl. Ent. Zool. 1: 69-72, 1966.
4. Stoltz, D.B. J. Ultrastr. Res. 43: 58-74, 1973.
5. Delius, H., Darai, G. and Flügel, R.M. J. Virol. 49: 609-614, 1984.
6. Bellett, A.J.D. Adv. Virus Res. 13: 225-246, 1968.
7. Bellett, A.J.D. and Inmann, R.B. J. Mol. Biol. 25: 425-532, 1967.
8. Kelly, D.C. and Vance, D.E. J. Gen. Virol. 21: 417-423, 1973.
9. Balange-Orange, N. and Devauchelle, G. Arch. Virol. 73: 363-367, 1982.
10. Kelly, D.C. and Tinsley, T.W. J. Invertebr. Pathol. 19: 273-275, 1972.
11. Barry, S. and Devauchelle, G. Can. J. Microbiol. 25: 841-849, 1979.
12. Monnier, C. and Devauchelle, G. J. Virol. 19: 180-186, 1976.
13. Monnier, C. and Devauchelle, G. J. Virol. 35: 444-450, 1980.
14. Abdali, A. Thèse 3ème cycle - Université de Rouen, 1986.
15. Lea, M.S. J. Invertebr. Pathol. 46: 219-230, 1985.
16. Goorha, R. J. Virol. 43: 519-528, 1982.
17. Cerutti, M. and Devauchelle, G. Arch. Virol. 61: 149-155, 1979.
18. Cerutti, M. and Devauchelle, G. Arch. Virol. 63: 297-303, 1980.
19. Laemmli, U.K. Nature 227: 680-685, 1970.
20. Bowen, B., Steinberg, J., Laemmli, U.K. and Weintraub, H. Nucl. Acid Res. 8: 1-20, 1980.

21. Carraway, K.L. *Biochem. Biophys. Acta* 415: 379-410, 1975.
22. Tinberg, H.M., Melnick, R.L., Maguire, J. and Packer, L. *Biochem. Biophys. Acta* 345: 118-128, 1974.
23. Guerillon, J., Barray, S. and Devauchelle, G. *Arch. Virol.* 73: 161-170, 1982.
24. Norrby, E., Marusyk, H.L. and Hammarskjöld, M.L. *Virology* 38: 477-482, 1969.
25. Signas, C., Akusjarvi, G. and Pettersson, U.J. *Virol.* 53: 672-678, 1985.
26. Moore, N.F. and Kelly, D.C. *J. Invertrebr. Pathol.* 36: 415-422, 1980.
27. Orange, N. and Devauchelle, G. *FEMS letters* 48: 1-64, 1987.
28. Gregoriades, A. *Virology* 54: 369-383, 1973.
29. Cerutti, M., Cerutti, P. and Devauchelle, G. *Virus Res.* (in press).
30. Stoltz, D.B. and Summers, M.D. *J. Ultrastr. Res.* 40: 581-598, 1972.
31. Devauchelle, G. *Virology* 81: 237-247, 1987.
32. Krell, P. and Lee, P. *Virology* 60: 315-326, 1974.
33. Kelly, D.C., Ayres, M.D., Lescott, T., Robertson, J. S. and Happ, G. *Gen. Virol.* 42: 95-105, 1979.
34. Elliott, R.M., Lescott, T. and Kelly, D.C. *Virology* 81: 309-316, 1977.
35. Takamatsu, H. and Iso, K. *Nature (London)* 298: 819-824, 1982.
36. Kellenberger, E. *Bopsystems* 12: 201-223, 1980.
37. Darcy-Tripier, F., Nermut, M.V., Brown, E., Monnemacher, H. and Braunwald, J. *Virology* 149: 44-54, 1986.
38. Neurath, A.R., Vernon, S.K., Hartzell, R.V. and Rubin, B.A. *J. Gen. Virol.* 19: 9-20, 1973.
39. Sarmiento, M. and Spear, P.G. *J. Virol.* 29: 1159-1167, 1979.
40. Yoshinaka, Y., Katoh, I. and Luftig, R.B. *Virology* 126: 274-281, 1984.
41. Ichihashi, Y., Oie, M. and Isuruhara, T.J. *Virol.* 50: 929-938, 1984.
42. Klump, H., Beaumais, J. and Devauchelle, G. *Arch. Virol.* 75: 269-276, 1983.

5

INSECT IRIDESCENT VIRUS TYPE 9 AND TYPE 16

J. KALMAKOFF, N. McMILLAN AND S. DAVISON

Department of Microbiology, University of Otago, P.O. Box 56, Dunedin, New Zealand

ABSTRACT

Insect iridescent viruses type 9 from Wiseana spp. (WIV) and type 16 from Costelytra zealandica (CzIV) were compared with respect to their viral proteins, antigens and physical DNA maps. Analysis by SDS-PAGE showed that WIV and CzIV had major polypeptide bands at 52K and 53K respectively. Using HRPO-labelled antibodies and surface iodination by ^{125}I , several coat-surface proteins were determined. These were the 129K, 99K, 52K and 33K proteins for WIV and 117K, 97K, 53K and 37K proteins for CzIV. The genome size for WIV and CzIV was 192.5Kbp and 168.5Kbp respectively. Comparison of the DNA by REN mapping and DNA hybridizations showed that although the viruses are related there are distinct differences. When ^{32}P -labelled CzIV DNA was hybridized to Southern blotted WIV DNA, a 24Kbp region of non-homology was found (12.5% of the genome). When ^{32}P -labelled WIV DNA was hybridized to CzIV DNA, a 67Kbp (or 39.7%) region of non-homology with CzIV was found. A partial amino acid sequence of the major protein from WIV was obtained and an oligonucleotide probe was synthesized. The probe was used to locate the position of the VP52 gene on the DNA map.

INTRODUCTION

Wiseana iridescent virus (WIV) was first discovered by Jimmie Robertson (on secondment from Oxford, UK) at Tennyson Inlet, Nelson, New Zealand in 1969. It was first reported by Kalmakoff and Robertson (1), and being the ninth insect iridescent virus to be found, it was classified by the interim nomenclature of Tinsley and Kelly (2) as type 9. The larvae of Wiseana spp. are lepidopteran pests of pastures in New Zealand and cause substantial annual loss (\$10-30 million) of pasture production. Based on the iridescence of the larvae, virus infection rates as high as 30% were found in the field. This is a low estimate since it has been subsequently shown (3) that many infected larvae do not show any iridescence. Despite this high infection rate, the virus was not detected in any other site.

A total of 34 localities in the South Island, NZ, were extensively sampled for virus diseases during the 1969-1971 period, but no other infections were found. In 1985 another 10 localities were sampled for virus diseases using a ^{32}P -labelled DNA probe and the dot-blot assay as the detection system (4), but no further isolates of WIV were obtained. The ecology of WIV needs further study before any comments on the natural spread and pathogenicity of WIV in its host can be made.

Costelytra zealandica iridescent virus (CzIV) was discovered in 1972 in grass grub larvae from a scenic reserve in South Canterbury, New Zealand (5). It was designated type 16 according to the interim nomenclature scheme. This coleopteran host is the other major insect pest of New Zealand pastures. Both Costelytra zealandica and Wiseana spp. often occupy similar pasture environments and the initial studies were made to determine if these two viruses were the same virus growing in different hosts. Serological studies showed that CzIV was clearly distinguishable from WIV and from other iridescent viruses. WIV showed some serological relationship to Tipula iridescent virus (TIV), Sericesthis iridescent virus (SIV) and CzIV. Subsequent work (6) demonstrated that WIV and CzIV are distinctly different viruses since they have a different host range, different DNA restriction endonuclease patterns and different DNADNA homologies (see below). As with WIV, no other isolation of CzIV has been made from grass grubs, despite extensive sampling of larval populations from different localities during the intervening years. It could be that the virus occurs only in isolated areas of native bush and grassland. The use of sensitive and specific labelled DNA probes for detection of subclinical infections should help to elucidate the natural ecology of these two iridescent viruses.

Previous work

There have been relatively few published reports on type 9 and type 16 iridescent viruses. Work in the 1970's by Kelly and Avery (7) and Kalmakoff et al (5) was concerned with the DNA homology and serological relationships using a limited range of viruses. The results of that work are summarized in Table 1.

Tests with antiserum to type 9 (WIV) virus showed that there was some serological relationship between type 9 type 1 (TIV), type 2 (SIV) and type 16 (CzIV). With antiserum to type 16 (CzIV) there was little serological relationship to the other iridescent viruses tested. Type 6 (CIV) showed no serological relationship with any of the other iridescent viruses. Type 9 was 100% homologous to type 18 in both DNA and serological comparisons and these two viruses are probably the same virus. Type 18 was isolated from a scarabaeid larvae Opagonia

Table 1. % Serological or DNA Homology

Antigens or unlabelled DNA	Antiserum or labelled DNA fragments						
	Type 1 aTIV*	Type 9 aWIV	WIV	Type 16 aCzIV	Type 6 aCIV	CIV	Type 2 SIV
type 1 (TIV)	100	50	NT	6	0	NT	NT
type 2 (SIV)	25	50	45	0	0	0	100
type 6 (CIV)	0	0	0	0	100	100	0
type 9 (WIV)	12	100	100	3	0	0	26
type 16 (CzIV)	25	50	NT	100	0	NT	NT
type 18 (OIV)	NT	100	100	NT	NT	NT	28

* aTIV refers to antiserum prepared against type 1 (TIV) virus. The % serological homology was determined as a % of the reciprocal end points of the precipitin end points in agar gels (5). The % DNA homology data is from Kelly and Avery (7). NT = Not Tested.

sp. from the same locality as type 9 in New Zealand in 1969 (8). Type 19, which was isolated from the coleopteran host Odontria striata, is very likely the same virus as type 16, which was isolated from a similar coleopteran host Costelytra zealandica. These two insect hosts are difficult to distinguish from each other and often occur as mixed populations in the same locality. Type 9 virus shows some DNA homology (45%) and serological homology (50%) with type 2 virus isolated from a scarabaeid, Sericesthis pruinosa from New South Wales in Australia (7).

A comparison of the structural polypeptides of type 9 and two other viruses, type 2 and type 6 was carried out by Moore and Kelly (9) using PAGE. They found similarities in the three viruses with one major polypeptide representing 40% of the total virus protein and 20 other minor polypeptides. ¹²⁵I labelling by the lactoperoxidase or the chloramine T method indicated that the major protein was located on the outside of the virus. By dansylation of the isolated major band and hydrolysis, the N-terminal was found to be proline for the 3 viruses. This does not agree with our results (see below), since the N-terminal of the major protein was found to be blocked. Their major protein band may have contained a number of polypeptides with one having an unblocked N-terminal.

Host range

In order to investigate further the relatedness of WIV and CzIV, a host range study was carried out using a number of common insect hosts. Viruses were introduced by intrahemocoelic injection into the proleg region of 2nd-4th instar larvae of 10 lepidopteran and 2 coleopteran hosts. The larvae were incubated

for 10 days and the virus was isolated from infected larvae and the larvae were examined either for iridescence or the presence of viral DNA (WIV) or by electron microscopy (CzIV).

It was found that 8 of the 12 hosts were infected with WIV and 3 of 8 hosts were infected with CzIV (Table 2). It is interesting to note that both viruses may have replicated in Lasperyrasia pomonella and Odontria spp - a lepidopteran and coleopteran host respectively. However, while virus was seen under EM or viral DNA was detected, no iridescent pellet was observed. This result may indicate an incomplete replicative cycle in these alternative hosts.

Table 2. Host Range of WIV and CzIV

Host	WIV ^a	CzIV ^b
<i>Galleria mellonella</i>	+	-
<i>Heliothis armigera</i>	+	-
<i>Planotortrix excessana</i>	+	-
<i>Lasperyrasia pomonella</i>	+	+
<i>Ctenopseutis obliquana</i>	-	ND
<i>Mithimna separata</i>	-	-
<i>Agrotis ipsilon</i>	-	ND
<i>Epiphyas postvittana</i>	+	ND
<i>Bombyx mori</i>	+	-
<i>Costelytra zealandica</i>	-	+
<i>Odontria</i> spp.	+	+
<i>Wiseana</i> spp.	+	ND

a = Iridescent pellet and Viral DNA detected (10); b = Virus detected by EM; ND = Not done

THE PROTEINS OF WIV and CzIV

In order to characterize the similarities and differences in the proteins of WIV and CzIV, the viruses were compared by polyacrylamide gel electrophoresis (PAGE). The virus particles were disrupted by boiling in a buffer containing SDS and β -mercaptoethanol prior to loading onto a 10% gel. Between 27 and 30 polypeptides were detected by silver staining (Fig 1). This is more than the 15-20 polypeptides previously reported for WIV (9). On a 15% gel an additional 7-9 polypeptides could be identified. The molecular weights ranged from 7K to 147K (Table 3). Other iridescent viruses (types 1, 2, 6, 9, 22 and 25) have been shown to have between 15 and 28 polypeptides (10,11,12). It was also found that by combining the results from polyacrylamide gels at 10% and 15% a more accurate assessment of the size and number of higher and lower molecular weight bands was obtained.

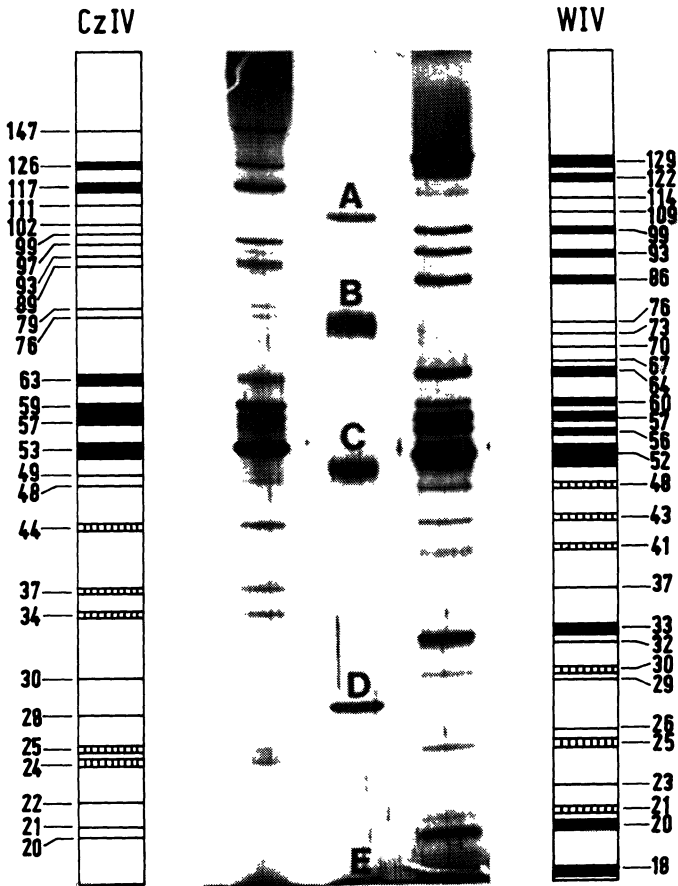


Fig. 1. Polyacrylamide gel electrophoresis (PAGE) of the polypeptides of WIV and CzIV. The polypeptides were detected by silver staining, the diagrams indicate the positions of some minor bands. The molecular weight markers are: A) Phosphorylase B (97K). B) Bovine Serum Albumin (66K). C) Ovalbumin (43K). D) Carbonic Anhydrase (31K). E) Soybean trypsin inhibitor (22K).

The polypeptide profiles of WIV and CzIV were different, although the estimated total molecular weights of all polypeptides was similar. If one assumes that no aggregation of protein occurs in the electrophoresis system, the total molecular weight for WIV and CzIV proteins was 1.82×10^6 and 1.86×10^6 respectively. The minimum DNA required to code for the proteins of WIV would be 49Kbp. If one takes the average molecular weight of an amino acid as being 120 and the total DNA as being 190Kbp (13), a minimum of 24% of the viral genome

Table 3. Molecular Weights of the Proteins of WIV and CzIV

Band number	WIV MW x 10 ⁻³	CzIV MW x 10 ⁻³
1	129	147
2	122	126
3	114	117
4	109	111
5	99	102
6	93	99
7	86	97
8	76	93
9	73	89
10	70	79
11	67	76
12	64	63
13	60	59
14	57	57
15	56	53
16	52	49
17	48	48
18	43	44
19	41	37
20	37	34
21	33	30
22	32	28
23	30	25
24	29	24
25	26	22
26	25	21
27	23	20
28	21	18
29	20	17
30	18	14
31	16	12
32	14	11
33	12	10
34	9	9
35	8	8
36	7	7

is involved in coding for the viral structural proteins. Similarly the minimum DNA required to code for the protein of CzIV would be 50Kbp or 27% of the viral genome (the DNA of CzIV is 170kb, see below). This agrees with the observations of Kelly and Tinsley (14) that both CIV and SIV use 30% of their genome to direct virion polypeptide synthesis and with the estimate of Krell and Lee (12) of 25% for TIV.

The molecular weight of the major band was 52K and 53K for WIV and CzIV respectively. This was in agreement with previously reported results which have found the major protein bands of iridescent viruses to be in the 50K-55K range (11,15). This band has been estimated to comprise 40% of the viral proteins (9).

Virus Surface Proteins

In an attempt to identify the WIV surface proteins, antibodies to the viral surface proteins were isolated. Polyvalent WIV antisera was incubated with intact WIV. Antibodies not attached to the virus surface were removed by pelleting the virus-antibody complex by centrifugation. The antibodies attached to the surface of the virus were dissociated by incubation with a low pH glycine buffer. These coat-surface specific antibodies were conjugated to horse-radish peroxidase (HRPO) and used in a Western blot of SDS-PAGE separated proteins. These antibodies reacted only with the 129K and 99K polypeptides (see summary figure below). However, if the virus sample was not reduced by β -mercaptoethanol prior to separation by SDS-PAGE, the coat-surface specific antibodies also reacted with the major polypeptide which under non-reducing conditions banded at the 50K position. Antigenic sites on the major band appear to be denatured by the reducing conditions.

The WIV coat-specific antisera did not cross react with any CzIV polypeptides. As CzIV has a different host range from WIV (see above) and the host range is possibly determined by antigenic determinants on the surface of the virus, then one would expect there to be only limited antibody cross-reactivity between the coat-surface proteins.

Further evidence of the surface location of the 129K and the 99K proteins came from analysis of the insect homogenate supernatant after virus had been extracted by high speed centrifugation. This supernatant should contain both insect and virus soluble proteins. After SDS-PAGE separation of these proteins and Western blot analysis using the polyvalent WIV antiserum as a probe, only proteins corresponding to the 129K and 99K polypeptides were detected (once again the antigenic sites of the major protein band may have been antigenically denatured by the reducing conditions). Since the 129K and 99K polypeptides are coat proteins and react with the environment, it was not surprising to find them in the high speed supernatant.

Major Band Analysis

After electrophoresis of total WIV proteins on a preparative SDS-gel, the major 52K polypeptide was excised and allowed to diffuse into a buffer. The purity of this isolated protein was checked by running it by PAGE (Fig 2).

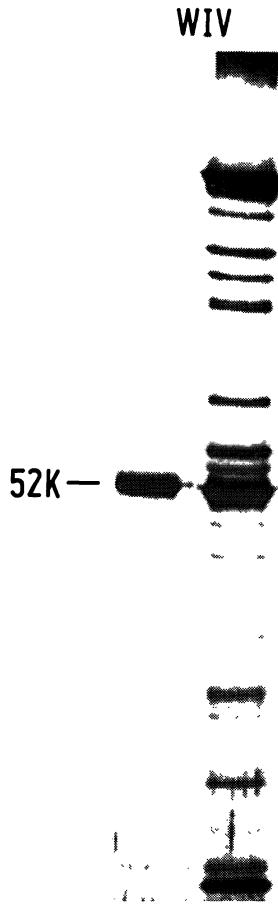


Fig. 2. PAGE of total WIV polypeptides and the purified major 52K WIV polypeptide. The major 52K polypeptide was excised from a preparative SDS-gel and eluted into buffer. The purified 52K polypeptide was rerun along with whole virus.

Antibody to the 52K polypeptide was raised by immunizing a rabbit by intramuscular injections at 3 weekly intervals. This antibody was conjugated to HRPO and by Western blotting was found to be strongly immunoreactive to the major 52K WIV polypeptide and also to the 129K, 99K, 60K and 56K polypeptides (Fig 3).

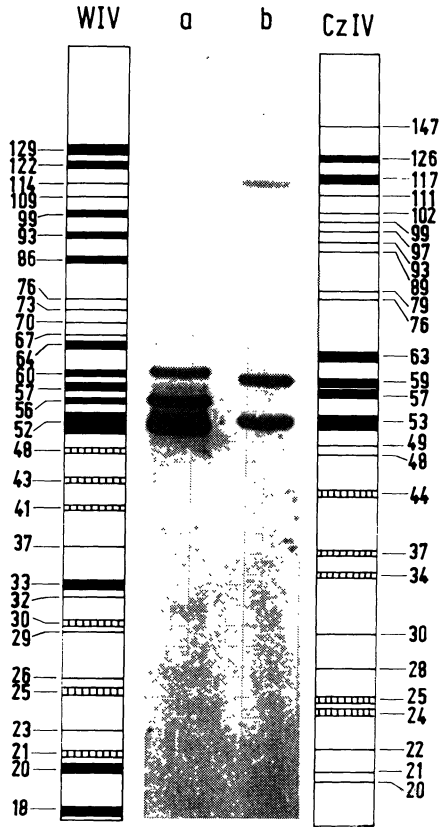


Fig. 3. Western blot of WIV (a) and CzIV (b) using CzIV antibodies to purified 52K polypeptide. The polypeptides of WIV and CzIV virions were separated by PAGE in a 10% polyacrylamide slab gel and the fractionated proteins were electrophoretically transferred to a nylon membrane. The blot was then reacted with HRPO-labelled rabbit antiserum raised against the WIV 52K polypeptide.

The reaction with the 129K and 99K coat proteins is in agreement with the findings of Cerrutti and Devauchelle (16). They found that under reducing conditions CIV had a 150K polypeptide that fractionated to a 50K monomeric form (the same molecular weight as the CIV major polypeptide). It would appear that in WIV the 129K polypeptide can be fractionated to a monomeric form which is contained in the 52K band. The antibodies against the 52K polypeptide of WIV also reacted with the 53K, 59K and 117K polypeptides of CzIV. It was interesting to note that the major 52K band of WIV is antigenically related to the 53K band of CzIV. This antibody cross-reaction was not shown when antiserum to whole virus was used.

125-I Labelling of Surface Proteins

Virus ^{125}I labelling was carried out by using the lactoperoxidase method (9). Lactoperoxidase has a molecular weight of 78K and catalyzes the iodination of the tyrosine residues. The enzyme is presumably too large to penetrate the virus and label any internal proteins.

The polypeptides that were iodinated when intact WIV and CzIV were labelled with ^{125}I are shown in Figure 4.

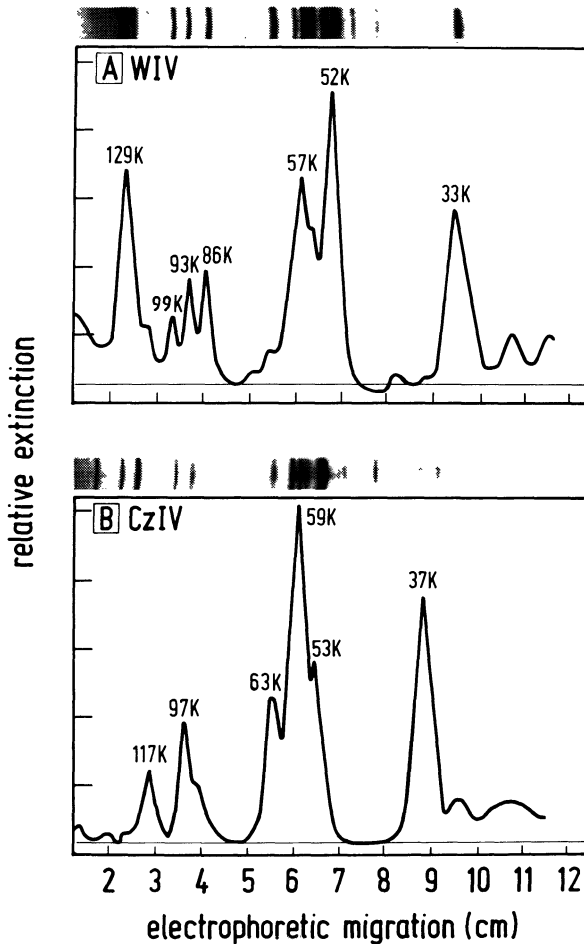


Fig. 4. The densitometer scans of a 10% polyacrylamide gel containing the iodinated proteins of intact WIV (A) and CzIV (B). Before PAGE the viruses were banded on 5-40% (w/v) sucrose gradients to remove any disrupted virus. Included above are SDS-PAGE gels of whole virus (silver stained).

Several WIV and CzIV polypeptides appeared to be at the surface of the virus. For WIV the major 52K band and a smaller 33K polypeptide were labelled as has been previously reported (9). We also found the 129K and 99K polypeptides of WIV to be labelled along with the 93K, 86K and 57K polypeptides. The labelling of the 129K and 99K polypeptides agrees with the Western blotting result using coat-surface specific antibodies. For CzIV six polypeptides were labelled. In comparison to WIV it is likely that the surface proteins of CzIV are the 117K, 97K, 53K and 37K polypeptides. The other two polypeptides, the 63K and 59K, are probably internal proteins labelled by the lactoperoxidase method. It has been previously reported that the 50K monomeric form of a 150K polypeptide in CIV can be ^{125}I surface labelled (16). This result corresponds with the labelling of the 129K polypeptide of WIV and 117K polypeptide of CzIV. Because of the similarity in iridescent viruses found so far, it is possible they all have high molecular weight proteins exposed on the surface of the virus.

Serological Relationship

Antibody to disrupted WIV virions was raised in rabbits and the purified IgG was conjugated to HRPO. These conjugated antibodies were used to detect 11 of the WIV polypeptides and 16 CzIV polypeptides previously separated by PAGE and Western blotted (Fig 5).

This cross-reactivity to CzIV proteins would indicate that CzIV was antigenically related to WIV. However CzIV antiserum raised against whole CzIV did not cross-react with any WIV polypeptides (Fig 6). This experiment was repeated using CzIV antisera raised in three different rabbits to confirm that the result was not due to the response of one particular rabbit. This lack of cross-reactivity of CzIV antisera has also been demonstrated by precipitin end points and intragel cross absorption tests (see above). No explanation for this anomalous result can yet be made.

The strongest immunoreactive polypeptides of WIV were the 129K, 99K and 56K. WIV antisera was not immunoreactive to the major WIV 52K and CzIV 53K polypeptides. This result could be due to the β -mercaptoethanol denaturing the antigenic sites within these proteins (17,18), since the WIV 52K polypeptide was immunoreactive in unreduced conditions.

Partial Amino Acid Sequence of the Major Band

Amino acid sequence analysis was performed on the major protein bands of WIV and CzIV with a view to constructing a synthetic oligonucleotide probe to use for mapping the gene that codes for a coat protein. The total virus proteins were separated on a 10% SDS-PAGE. Following electrophoresis the separated

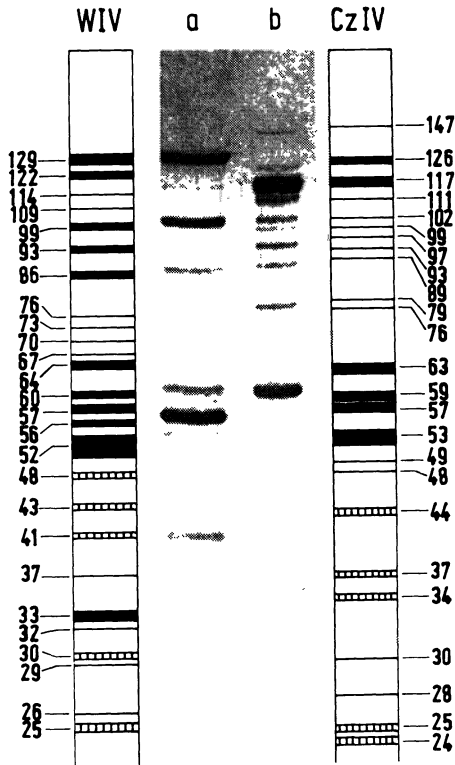


Fig. 5. Western blot and detection of WIV and CzIV antigens by HRPO-labelled antibodies. The virus polypeptides were detected as described for Figure 3. Rabbit antiserum was raised against WIV virions.

proteins were electroblotted onto polyvinylidene difluoride membrane. Protein bands were visualized on the membrane with amido black stain and the major bands were excised for analysis. The major 52K polypeptide of WIV was found to be blocked at the N-terminus. An *in situ* cyanogen bromide digest was performed and from this a 10K and 16K portion of the major band of WIV and CzIV respectively were used for sequence analysis. The amino acid sequence from WIV was found to have little sequence homology with CzIV (50% homology over a 4 amino acid region, Table 4). Since different fragments of the major protein of WIV and CzIV were analysed, this lack of homology was not surprising. The Protein Identification Resource (PIR) database was searched for amino acid sequence homology and showed that the WIV sequence had homologies with

poliovirus capsid protein and with Black Beetle virus coat protein. This information suggested that there may be some amino acid sequence homology among virus coat proteins.

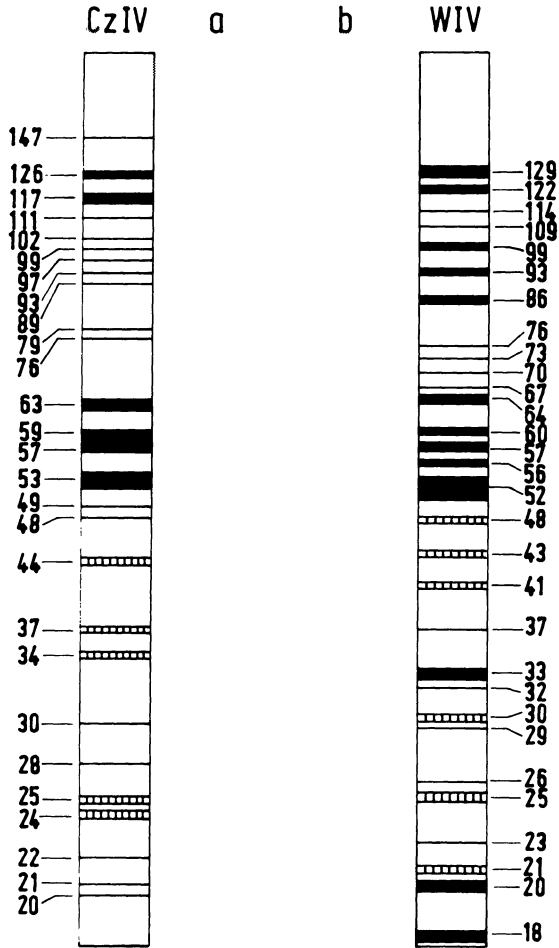


Fig. 6. Western blot and detection of WIV and CzIV antigens by HRPO-labelled antibodies. The virus polypeptides were detected as described for Figure 3. Rabbit antiserum was raised against CzIV virions.

Table 4. PIR Database Protein Sequence Homology

WIV:	A I E D I L E Q V Q T A P C Q N Y N P L
POLIOVIRUS:	W I V D I T S Q V Q T E R N I N R A M T
IDENTITY:	70% Homology over 10 amino acids
WIV:	A I E D I L E Q V Q T A P C Q N Y N P L
BLACK BEETLE VIRUS	E F S D I L E G I Q T L P P A N V T V A
IDENTITY:	58% Homology over 12 amino acids
WIV:	A I E D I L E Q V Q T A P C Q N Y N P L
CzIV:	I S N I T S G F I D I A T F D E
IDENTITY:	50% Homology over 4 amino acids

The single amino acid letter codes of PIR (19) were used.

Summary of the Protein Study

Most of the research on the composition and structure of iridescent viruses was carried out on CIV and TIV. In CIV a lipid membrane surrounds the inner core and makes up about 9% of the virion (20). Protein units spread through the single unit membrane, attaching the core polypeptides to the capsid polypeptides; this may be an explanation for the high stability of the viruses (16). TIV has been shown to be a lattice of hexagonally packed units (21), composed of 1472 triangular and pentangular subunit aggregates (22,23). The composition and structure of WIV and CzIV will probably be similar to that of these other iridescent viruses.

The results of the present study are summarized in Figure 7. There are many proteins involved in the surface structure of these viruses. The major 52K polypeptide of WIV is partially exposed at the surface of the virus as shown by ¹²⁵I labelling (Fig 7D) and the reaction with HRPO-labelled coat-surface specific antibodies when polypeptides were run on a non-reducing SDS-PAGE gel. The 129K and 99K polypeptides are coat-surface proteins as shown by ¹²⁵I labelling (Fig 7D) and coat-surface specific antibody experiments (Fig 7B).

WIV and CzIV are antigenically related since the WIV antisera cross-reacted with the CzIV polypeptides (Fig 7F). Antibodies prepared against whole WIV were reactive neither to the WIV major 52K polypeptide (Fig 7A) nor to the CzIV major polypeptide (Fig 7F). This may have been due to the antigenic sites being denatured by the detergents in the SDS gels or by the reducing conditions.

When the purified 52K band was used to immunise a rabbit it was found to be immunoreactive (Fig 7C). These antibodies reacted not only with the 52K polypeptide but also cross-reacted with the 129K and 99K coat proteins, thus demonstrating the antigenic relatedness between these three virus surface

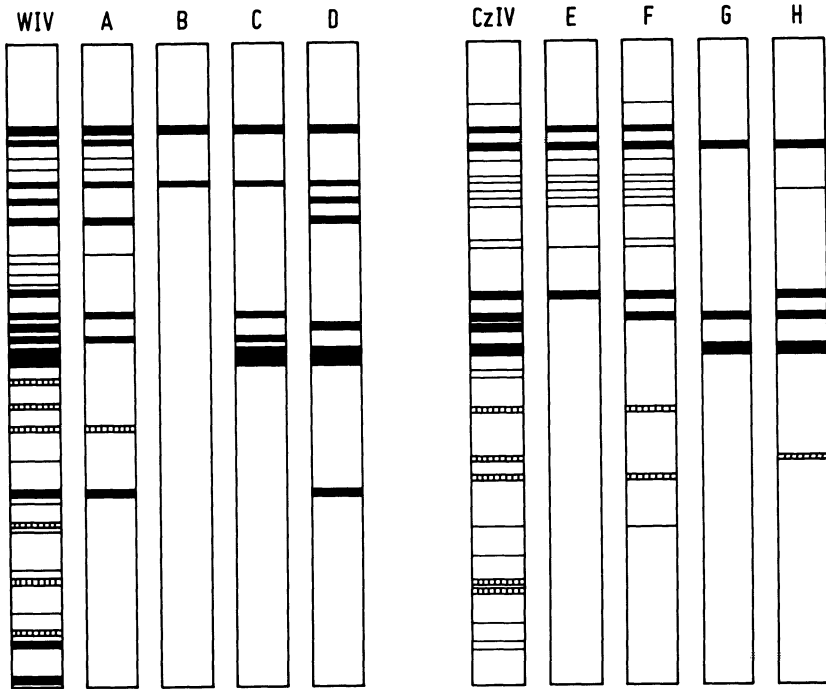


Fig. 7. Summary diagram of the WIV and CzIV polypeptide study.

- Lane A: WIV polypeptides detected by HRPO-labelled antibodies prepared against whole disrupted WIV.
- Lane B: WIV polypeptides detected by HRPO-labelled antibodies to surface proteins.
- Lane C: WIV polypeptides detected by HRPO-labelled antibodies prepared against the WIV 52K polypeptide.
- Lane D: 125 -I labelled WIV polypeptides using lactoperoxidase.
- Lane E: CzIV polypeptides detected by HRPO-labelled antibodies prepared against whole disrupted CzIV.
- Lane F: CzIV polypeptides detected by HRPO-labelled antibodies prepared against whole disrupted WIV.
- Lane G: CzIV polypeptides detected by HRPO-labelled antibodies prepared against the WIV 52K polypeptide.
- Lane H: 125 -I labelled CzIV polypeptides using lactoperoxidase.

proteins. Antibodies to the WIV major band also cross-reacted with the 53K CzIV major polypeptide, the 59K polypeptide and with the high molecular weight 117K CzIV polypeptide (Fig 7G). Since the 117K and the 59K polypeptides were 125 -I labelled (Fig 7H), they are probably surface proteins of CzIV.

THE DNA OF WIV AND CzIV

The genome of iridescent viruses is a single-copy, double-stranded, linear DNA molecule and ranges in size from 98 to 216Kbp (10). Frog Virus 3 (FV3), Fish Lymphocystis Disease Virus (FLDV) and insect iridescent virus Type 6 (CIV) are the best characterized of these viruses. An important step to understanding the relationship of the insect iridescent viruses at the molecular level is the construction of restriction endonuclease (REN) maps of the DNA. At present there are only two DNA restriction maps available; these are Type 6 (24) and Type 9 (13). The physical map for iridescent virus Type 16 (CzIV) using the REN's BamHI and PstI is presented below.

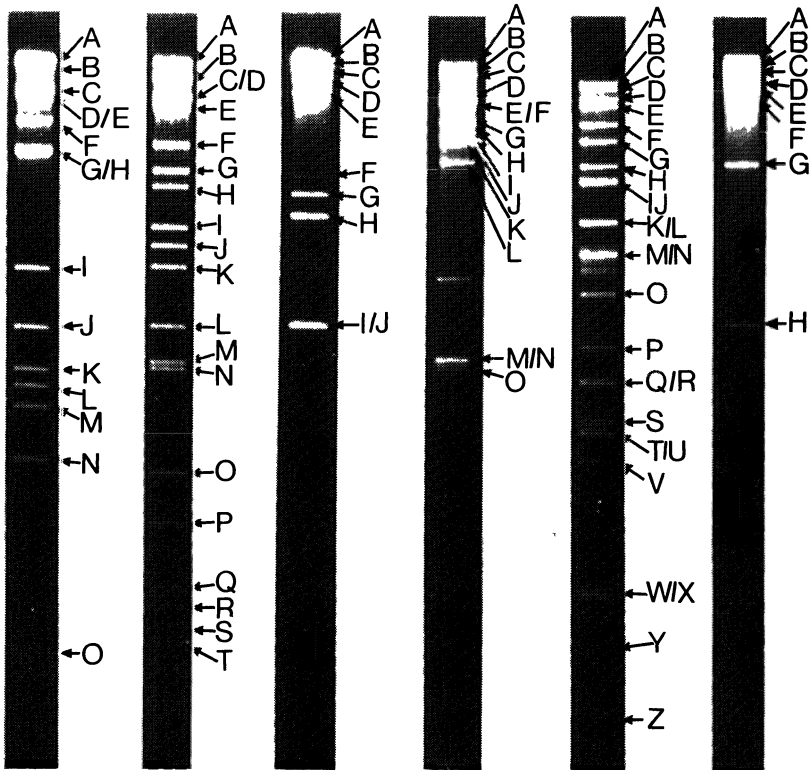


Fig. 8. Restriction endonuclease digestions of CzIV (Lanes 1-3) and WIV DNA (Lanes 4-6). The DNA was separated by electrophoresis on 0.6% agarose. Lanes (1) BamHI; (2) KpnI; (3) PstI; (4) BamHI; (5) EcoRI and (6) PstI.

Restriction Endonuclease Analysis

The DNA from WIV and CzIV was characterized using the REN's BamH1, Kpn1 EcoR1 and Pst1 (Fig 8). The fragments produced were sized using lambda DNA as standards and the results are given in Table 5.

Table 5. Restriction Fragment Sizes of WIV and CzIV

	WIV			CzIV		
	BamH1	EcoR1	Pst1	BamH1	EcoR1	Pst1
A	27.11	18.78	49.87	32.39	30.68	36.28
B	21.45	17.48	35.96	29.37	22.85	32.99
C	20.04	16.17	27.02	18.23	17.42	26.81
D	15.15	14.84	25.73	16.79	16.32	22.53
E	13.99	13.78	20.35	16.73	14.04	18.14
F	13.93	11.67	17.67	12.30	10.28	8.32
G	11.67	10.21	8.97	9.59	8.48	7.77
H	11.23	8.56	4.43	9.59	7.68	6.74
I	10.40	8.06	1.83	5.46	6.53	4.45
J	10.39	7.87	0.62	4.36	6.13	4.21
K	9.72	6.59		3.84	5.63	
L	8.74	6.59		3.62	4.52	
M	3.94	5.75		3.37	4.02	
N	3.93	5.76		2.84	3.92	
O	3.83	4.90		1.50	2.82	
P	2.23	4.11			2.34	
Q	1.98	3.64			1.87	
R	1.97	3.64			1.81	
S	0.77	3.24			1.65	
T		3.23			1.59	
U		3.20			0.63	
V		2.86			0.57	
W		1.88			0.50	
X		1.88				
Y		1.55				
Z		1.23				
a		1.14				
b		0.89				
c		0.83				
d		0.75				
e		0.55				
f		0.55				
g		0.24				
h		0.22				
	192.45	192.45	192.45	169.99	172.28	168.46

Note: Values are derived from a combination of computer modelling values and physical measurements.

For geographically close and ecologically similar viruses, the REN patterns are quite different. Although the numbers of fragments are similar for BamHI (19 and 15 for WIV and CzIV respectively), EcoRI (32 and 28), and PstI (10 for both), similarities in fragment sizes were not common, indicating a more distant relationship than might be expected.

The genome sizes, calculated using the REN fragment sizes, indicate WIV and CzIV are different viruses. WIV has a genome size of 192.5 Kbp while CzIV has a size of 168.5Kbp. The genome sizes for other iridescent viruses are 209Kbp for Type 6 (24), 146–174Kbp for Type 1 (25), 197–216Kbp for Type 22 DNA (26) and 143.7Kbp for Southern Mole cricket iridescent virus (27). There is a wide variation in genome size within the insect iridescent virus genus and it is larger than its vertebrate counterpart e.g. FV3 is 107Kbp (28) and FLDV 98Kbp (29). This larger genome size may account for the wide host range exhibited by the insect iridescent viruses (30).

Ward and Kalmakoff (10) compared the EcoRI patterns from 5 iridescent viruses (Types 1, 6, 9, 16 and 22) and found them to be distinctly different. This indicated that the insect iridescent viruses were probably not closely related to each other.

Physical Mapping of the DNA

Physical maps were constructed by cloning REN fragments of DNA into the plasmid vectors pUC8, pUC19 and pBR328, using the *E. coli* hosts JM83, JM83, and HB101 respectively. The cloned fragments were used for multiple REN digests and hybridization to Southern blots of genomic DNA. The WIV map was constructed using the REN's BamHI, EcoRI and PstI (Fig 9), while CzIV was mapped using BamHI and PstI (Fig 10). KpnI data is 90% complete for CzIV (data not shown) and was used in the construction of the map.

All other iridescent virus genomes which have been physically mapped (FV3, FLDV and CIV) have been shown to be terminally redundant and circularly permuted and although the molecules are physically linear the maps are circular (31,32,33). Results indicate WIV to be circularly permuted as no end points could be found during cloning and mapping procedures (13). The mapping data from CzIV also indicated it was circularly permuted.

FEATURES OF THE DNA MAPS

Repeat Sequences

During mapping it was found that CzIV DNA contained elements of repeated

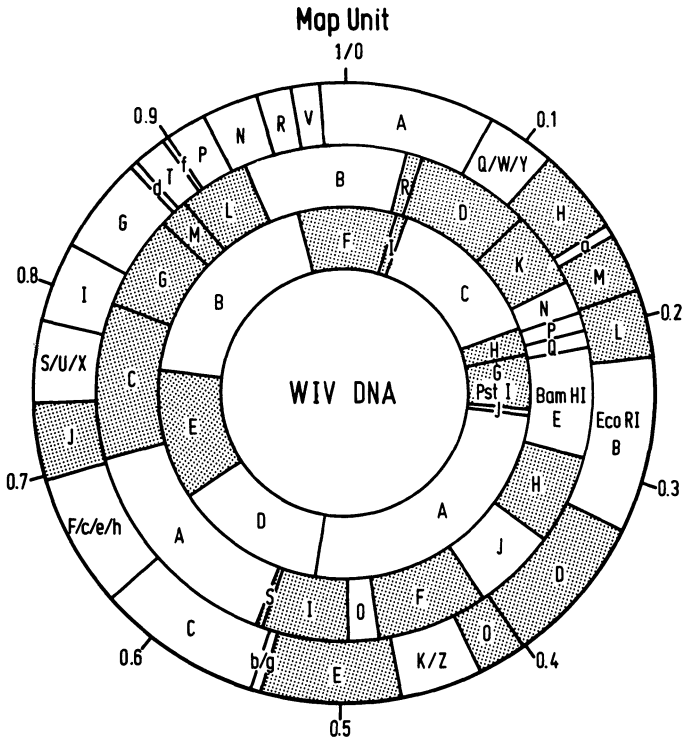


Fig. 9. Physical map of the genome of WIV. The restriction enzymes BamHI, EcoRI and PstI were used in cloning procedures. Shaded areas represent cloned fragments.

DNA sequences within a particular region of the genome. This confirms what had previously been found in WIV (13). For example, the Kpn H fragment (7.7Kbp) hybridized to Bam D and J and Pst G and J. However, it also hybridized to Pst H and B. The Kpn H fragment probably also hybridized to repeat sequences in Bam D and E but this would not be seen as Bam D/E co-migrate (a double) and therefore masked each other.

Repeat sequences or repetitive DNA are not new in molecular virology. They have been found in nuclear polyhedrosis virus, adenovirus, herpes virus, and poxvirus (34,35,36,37). Various functions have been assigned to these repeat sequences, such as host range and replicative functions. All other iridescent virus genomes studied have been found to contain repeat sequences e.g. insect iridescent viruses Types 1, 6 and 9, FV3 and FLDV (13,24,25,29,31). Both WIV and CzIV appear to have more extensive repeat regions than other iridescent viruses. WIV

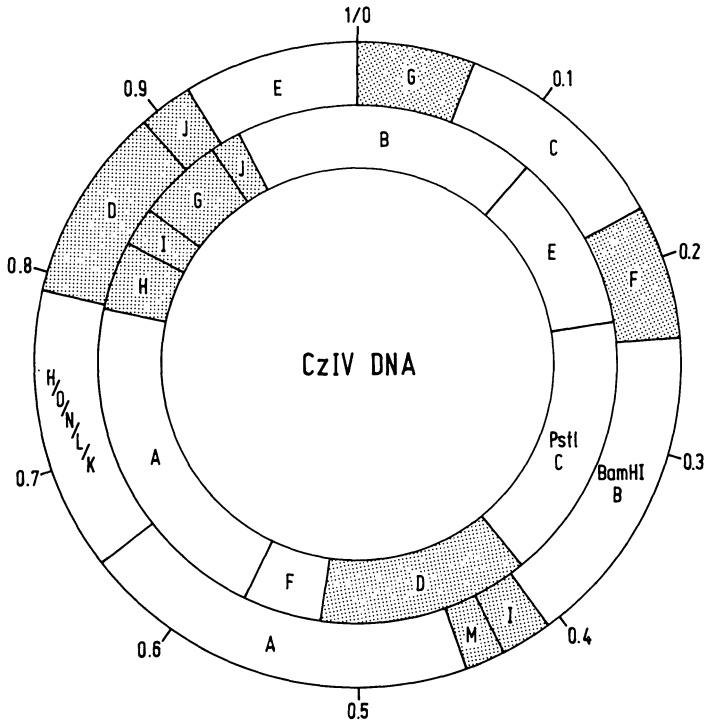


Fig. 10. Physical map of the genome of CzIV. The restriction enzymes BamHI and PstI were used in cloning procedures. Shaded areas represent cloned fragments.

repeats account for 25% of the genome and 39% for CzIV (finer mapping will probably reduce this). Ward and Kalmakoff (13) indicated that more than one type of repeat was present in WIV and this also seems to be the case with CzIV (unpublished data).

Homology

In an effort to detect the DNA homology between WIV and CzIV, hybridization of whole genomic digests was carried out. DNA was cut with the REN's BamHI, EcoRI and PstI, separated by agarose gel electrophoresis and Southern blotted onto nylon membranes. ^{32}P -labelled DNA was then hybridized to these blots. To quantitate the result of the hybridization, changes in the stringency conditions were employed according to the formula (38):

$$TM = 8.15 + 16.6(\log M) + 0.41(\%G+C) - 0.71(\% \text{ formamide})$$

Stringency changes were achieved by altering the concentration of the solvent formamide from 50% to 20% in the hybridization mix. This results in

stringency changing from 85% (50% formamide, 42°C) to 68% (20% formamide, 42°C) i.e. a greater base pair mismatch is allowed as formamide concentration decreases.

32P-CzIV/WIV Hybridization

It was found that when ^{32}P -CzIV DNA was hybridized to WIV DNA, certain REN fragments of WIV DNA did not hybridize at either stringency condition. These fragments were identified as Pst G and H; Bam N, M and P; and Eco L. Individual hybridization experiments (50% formamide) with the WIV cloned fragments Eco L, Bam N, and Eco a show that no homology occurs. When compared to the physical map, 5 of these 6 bands were found to be in the same area of the genome (Fig 11). These areas of non-homology flanked the WIV DNA repeat regions.

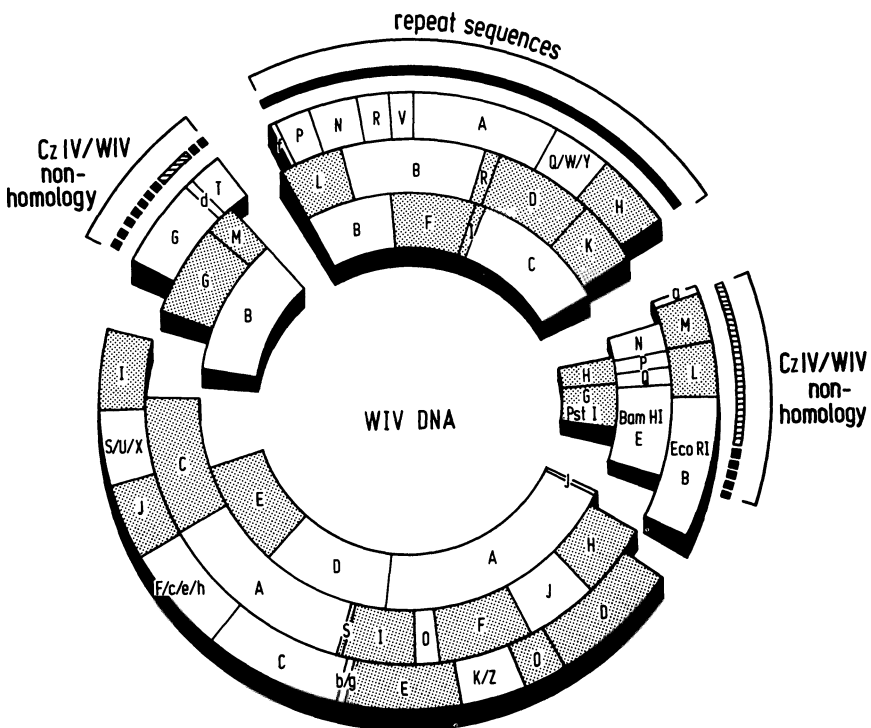


Fig. 11. Features of the WIV map. Location of the WIV repeat sequences, CzIV area of non-homology and the major virus protein VP52 on the physical map of WIV. Dotted lines indicate possible range of regions of non-homology and repeats. VP52 is located in the area common to the fragments Eco A and Bam D.

The difference in genome size between WIV and CzIV is 24Kbp, and the areas of non-homology to CzIV on the WIV genome equal 23.4Kbp. We expect that finer mapping will result in the remaining difference (0.6Kbp) being found.

32P-WIV/CzIV Hybridization

When the reciprocal experiment was carried out it was found that at 68% stringency (20% formamide, 42°C) all of the CzIV genome was homologous to the labelled WIV DNA, but at 85% stringency (50% formamide, 42°C) only one large area of the CzIV genome showed homology (Fig 12). This area, spanning Pst A to D, comprises 67Kbp, or 39.7% of the genome and is also not in the repeat regions.

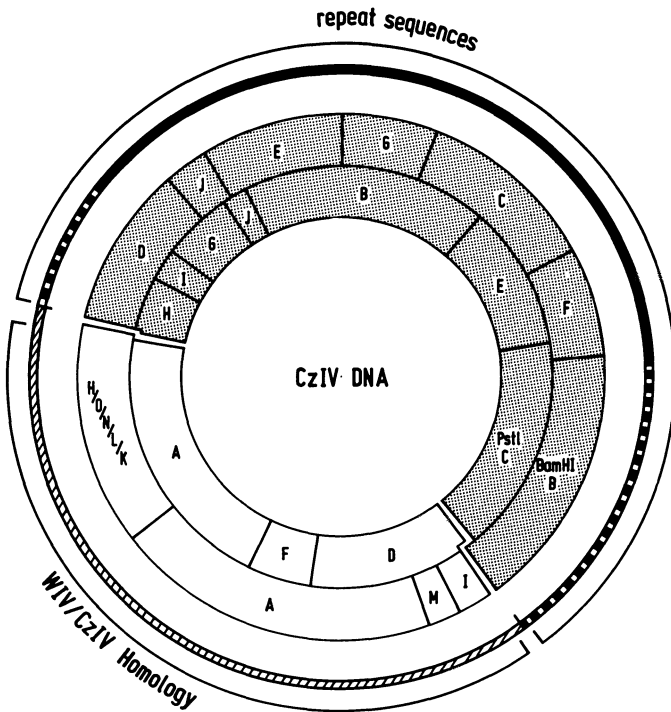


Fig. 12. Features of the CzIV map. Location of the CzIV repeat regions and WIV non-homology regions on the physical map of CzIV.

WIV Coat Protein Gene

Investigations into the structural proteins of WIV were described in the previous section and indicated that the 52K protein band on SDS-PAGE was the major structural protein. For mapping purposes this protein was designated VP52. A 10K polypeptide, cleaved by cyanogen bromide from this protein, was isolated and sequenced. From this sequence an oligonucleotide was synthesized with redundancies in the third code position as indicated below.

TGC CAA AAC TAC AAC CC
 . . T . . G . . T . . T . . T . .

After end-labelling with ^{32}P , this oligonucleotide probe hybridized to WIV DNA fragments Bam D, Eco A, Pst C and Pst F (Fig 9). It was concluded that the most probable location for this gene, VP52, was between 0.05 and 0.08 map units. The hybridization of Pst F was considered non-specific, as neither Bam B nor Bam R hybridized. Previous work has indicated that all insect iridescent viruses have a major protein band between 50K and 55K. This protein may provide a useful zero point on physical DNA maps of the insect iridescent viruses, similar to that used for the polyhedrin gene of baculoviruses. In this way DNA maps can be oriented in a similar manner and comparisons of genetic organization made more meaningful.

REFERENCES

1. Kalmakoff, J. and Robertson, J.S. Proc. Univ. Otago Med. School 48: 16-18, 1970.
2. Tinsley, T.W. and Kelly, D.C. J. Invertebr. Pathol. 16: 470-472, 1970.
3. Moore, S.G. Virus diseases of two insect pests of pastures: Potential for biological control. Ph.D. Thesis, University of Otago, Dunedin, New Zealand, 1973.
4. Ward, V.K., Fleming, S.B. and Kalmakoff, J. J. Virol. Methods 15: 65-73, 1987.
5. Kalmakoff, J., Moore, S.G. and Pottinger, R.P. J. Invertebr. Pathol. 20: 70-76, 1972.
6. Ward, V.K. Characterisation of two *Wiseana* spp. viruses. Ph.D. Thesis, University of Otago, Dunedin, New Zealand, 1987.
7. Kelly, D.C. and Avery, R.J. Virology 57: 425-435, 1974.
8. Fowler, M. and Robertson, J.S. J. Invertebr. Pathol. 19: 154-155, 1972.
9. Moore, N.F. and Kelly, D.C. J. Invertebr. Pathol. 36: 415-422, 1980.
10. Ward, V.K. and Kalmakoff, J. Insect Iridoviridae. In: Invertebrate Viruses (Ed. E. Kurstak), CRC Press, Inc., Boca Raton, USA. 1989 (in press).
11. Elliot, R.M., Lescott, T. and Kelly, D.C. Virology 81: 309-316, 1977.
12. Krell, P. and Lee, P.E. Virology 60: 315-326, 1974.
13. Ward, V.K. and Kalmakoff, J. Virology 160: 507-510, 1987.
14. Kelly, D.C. and Tinsley, T.W. J. Invertebr. Pathol. 19: 273-275, 1972.
15. Kelly, D.C., Ayers, M.D., Lescott, T., Robertson, J.S. and Happ, G.M. J. gen. Virol. 42: 95-105, 1979.
16. Cerrutti, M. and Devauchelle, G. Virology 145: 123-131, 1985.

17. Reynolds, J.A. and Tanford, C. Proc. Natl. Acad. Sci. (USA) 66: 1002-1007, 1970.
18. Waehnedlt, T.V. Biosystems. 6: 176-187, 1975.
19. Protein Identification Resource, National Biomedical Research Foundation, Georgetown University Medical Center, Washington D.C., USA.
20. Kelly, D.C. and Vance, D.E. J. gen. Virol. 21: 417-423, 1973.
21. Wrigley, N.G. J. gen. Virol. 5: 123-134, 1969.
22. Wrigley, N.G. J. gen. Virol. 6: 169-173, 1970.
23. Manyakov, V.F. J. gen. Virol. 36: 73-79, 1977.
24. Schnitzler, P., Soltau, J.B., Fischer, M., Reisner, H., Scholtz, J., Delius, H. and Darai, G. Virology 160: 66-74, 1987.
25. Tajbakhsh, S., Dove, M.J., Lee, P.E. and Seligy, V.L. Biochem. Cell Biol. 64: 495-503, 1986.
26. Hibbin, J.A. and Keely, D.C. Arch. Virol. 68: 9-18, 1981.
27. Boucias, D.G., Maruniak, J.E. and Pendland, J.C. J. Invert. Pathol. 50: 238-245, 1987.
28. Lee, M.H. and Willis, D.B. Virology 126: 317-327, 1983.
29. Darai, G., Delius, H., Clarke, J., Apfel, H., Schnitzler, P. and Flugel, R.M. Virology 146: 292-301, 1985.
30. Smith, K.M., Hills, G.J. and Rivers, C.F. Virology 13: 233-241, 1961.
31. Goorha, R. and Murti, K.G. Proc. Natl. Acad. Sci. (USA) 79: 248-252, 1982.
32. Darai, G., Anders, K., Koch, H.G., Delius, H., Gelderblom, H., Samalecos, C. and Flugel, R.M. Virology 126: 466-479, 1983.
33. Delius, H., Darai, G. and Flugel, R.M. J. Virol. 49: 609-614, 1984.
34. Arif, B.M. and Doerfler, W. EMBO J. 3: 525-529, 1984.
35. Garon, C.F., Berry, K.W. and Rose, J.A. Proc. Natl. Acad. Sci. (USA) 69: 2391-2395, 1972.
36. Roizman, B. Cell 16: 481-491, 1979.
37. Wetlek, R. and Moss, B. Cell 21: 277-284, 1980.
38. Howey, P.M., Israel, M.A., Law, M. and Martin, M.A.J. Biol. Chem. 254: 4876-4883, 1979.

6

VIRUS-CYTOSKELETON INTERACTION DURING REPLICATION OF FROG VIRUS 3

K. G. MURTI AND R. GOORHA

Department of Virology and Molecular Biology, St. Jude Children's Research Hospital, Memphis, Tennessee 38101, USA

ABSTRACT

Frog virus 3 (FV3) induces selective and sequential changes in the eukaryotic cytoskeleton. Morphologically, the virus disrupts the microtubules, reorganizes the intermediate filaments, and disrupts and reorganizes the microfilaments. Biochemically, the virus selectively inhibits tubulin synthesis, increases the phosphorylation of vimentin, and modifies actin in an unknown manner. Functionally, the virus uses intermediate filaments in compartmentalizing viral genomes and viral proteins, and microfilaments in virus release. By studying how FV3 modulates the cytoskeleton for its own replication we may learn the roles of cytoskeleton (i) in the compartmentalization and movement of intracellular proteins and (ii) in the contractile mechanisms operative in virus release.

INTRODUCTION

It is now well established that eukaryotic cells contain fibrous elements which interact to form a highly integrated network termed the cytoskeleton (1-9). The principal constituents of the cytoskeleton are three types of filaments: the microtubules, the intermediate filaments (IF), and the microfilaments (1-9). The three types of filaments have been well characterized both morphologically and biochemically. Microtubules are hollow tubes measuring 22 to 26 nm in diameter (1). Each microtubule contains protofilaments which in turn are composed of heterodimers of tubulin (1). IF are wavy filaments measuring 7 to 11 nm in diameter (2). At present, five classes of IF have been identified

(2, 3). They are keratin filaments of epithelial cells, neurofilaments of neurons, glial filaments of cells of glial origin (e.g., astrocytes), desmin filaments of muscle cells and vimentin filaments of cells of mesenchymal origin. Though morphologically similar, each class of IF contains distinct proteins (2, 3). Microfilaments measure 4 to 8 nm in diameter and contain subunits of actin (4). Considerable information is now available on the biochemistry of all three types of filaments and their associated proteins, their patterns of organization in different cell types, and the dynamics of their assembly and disassembly (1-13).

The components of cytoskeleton have been implicated in a variety of cellular functions. The actin-containing microfilaments have been assigned a role in cellular contractile and motile phenomena, including chromosome movement, cytokinesis, cell motility, budding of viruses, exocytosis, and phagocytosis (13-18). Some recent studies have demonstrated actin to be a major component of the nucleus (19, 20) and that it promotes the transcriptional activity of lampbrush chromosomes in amphibian oocytes (21). It is also believed that actin is an initiation factor for RNA polymerase II (22). Microtubules are the constituents of motile structures such as cilia and flagella. Therefore, they are thought to have a role in cell motility, chromosome movement, axonal transport, movement of pigments and granules, and movement of the cell membrane (1, 9, 23, 24). Recently, tubulin and its associated proteins have been found to stimulate the transcription and replication of RNA viruses, Sendai virus and vesicular stomatitis virus (25, 26). It appears from the above that microtubules, microfilaments and their associated proteins perform several cellular functions and that some of these functions are unrelated to their conventional "cytoskeletal" roles. The list of their functions may continue to grow as research expands into newer model systems.

By contrast, IF perhaps are the most studied cytoskeletal filaments in recent years but their function is least understood. Typically, they form an intricate and extensive network that stretches from the nucleus to the plasma membrane. IF subunit

proteins form a family of proteins that appears to include the nuclear lamins, the major structural proteins of the nuclear envelope complex (27-29). The expression of IF subunit proteins is closely linked to development and cellular differentiation (3). Initially, it was proposed that IF are involved in the determination of cell morphology, organelle placement and movement, and cell motility (29-38). The fact that IF connect nuclear lamina at one end and membrane skeleton on the other led some to speculate that IF play a general role in the spatial organization of cytoplasmic matrix or in the active or passive transport of macromolecules between nucleoplasmic and cytoplasmic compartments (39). However, a number of studies using the intracellular injection of anti-intermediate filament antibodies to disrupt normal IF organization have so far failed to reveal any obvious effects on the above or other cellular functions (40-42). One suggestion is that the true function of IF is unrelated to their "cytoskeletal" role, but arises from their ability to bind with high affinity to nucleic acids (30, 43). In this view, soluble IF subunit proteins, which exist at a very low concentration within the cell, would act as regulators of gene expression. Thus, there is no definitive evidence supporting a functional role of IF in the cell life cycle.

Traditionally, animal viruses have provided simple model systems to understand a variety of cellular functions (e.g., methylation, capping, polyadenylation of mRNA, split genes). The virus model systems are attractive for three reasons. First, the viruses, upon infection, divert cellular machinery to perform a few defined functions, thereby illuminating the machinery involved in those functions. Second, the process of virus infection provides a synchronous phenomenon in which the sequential structural and functional changes can be analyzed for an understanding of the "cause and effect". Third, the ease with which the small viral genomes can be manipulated makes it possible to use a genetic approach by using temperature-sensitive (ts) mutants to deduce the functional interaction between viral and cellular molecules. There have been many reports suggesting a role for cytoskeleton in virus

macromolecular synthesis, virus assembly, and transport (for the only review on the subject, see 44). But the potential of animal virus model systems in analyzing the function of the cytoskeleton has not been fully exploited.



Fig. 1. Overview of FV3-infected normal rat kidney cell at 8 hr post-infection as seen by High Voltage (1000 kv) Electron Microscope. Note the assembly sites (AS) close to the nucleus (N).

For the past six years, we have used frog virus 3 (FV3) as a model system to explore the roles of cytoskeleton and the molecular basis for such roles (45-50). In the next section we describe this model system, what we have learned from it thus far, and how we can utilize it to reveal function(s) of the cytoskeleton.

FV3 is a well characterized icosahedral animal DNA virus which belongs to the family *Iridoviridae*. The virus replicates in a variety of tissue culture cells of piscine, amphibian, avian and mammalian (including human) origin (reviewed in 51). The genome is a double-stranded linear DNA of MW 100×10^6 (52) which is circularly permuted and terminally redundant (53). A number of temperature-sensitive mutants have been obtained and placed in 12 complementation groups (54). Purified FV3 particles contain more than 35 structural proteins, including 5 enzyme activities, viz., nucleotide phosphohydrolase, ribonuclease, deoxyribonuclease, cyclic AMP-independent protein kinase, and protein phosphatase (55). The virus utilizes both the nucleus and the cytoplasm for its nucleic acid synthesis but assembles in discrete sites in the cytoplasm termed assembly sites (Fig. 1). The assembly sites are devoid of cellular components such as ribosomes, polysomes, mitochondria, vesicles, etc., but are encircled by IF (45, 57). The viral genomes made in the nucleus and the viral proteins made in the cytoplasm are transported to the assembly site and assembled into virions (58). The virions move from the assembly site to the plasma membrane and are released by budding (45, 47).

FV3-INDUCED CYTOSKELETAL CHANGES

Soon after infection, FV3 induces dramatic organizational changes in all three classes of cytoskeletal filaments: the microtubules, the intermediate filaments, and the microfilaments. The organizational changes in the filaments are preceded by or coincident with extensive biochemical changes in the filament proteins. The changes are relevant to FV3 replication, since treatment of cells with heat-inactivated FV3 or mutants of FV3 defective in virus replication do not induce these alterations. In the following sections, we describe in detail the morphological and

biochemical changes in every class of cytoskeletal filaments and comment on their relevance to FV3 replication.

Microtubules

When examined by immunofluorescence microscopy with antitubulin antibodies, uninfected baby hamster kidney (BHK) cells show a pattern of organization of microtubules typical of normal mammalian tissue culture cells (23). The microtubules radiate from a focal point near the nucleus and extend to the cell periphery (Fig. 2A). In FV3-infected BHK cells, the pattern of microtubule organization remains normal until 6 hr. At about this time the virus assembly sites appear and the number of microtubules begins to decrease (Fig. 2B). By 10 hr a drastic reduction in the number of microtubules occurs and a few microtubules are seen in the vicinity of the assembly sites (Fig. 2C). Thus the microtubules appear to decrease progressively in the course of FV3 infection.

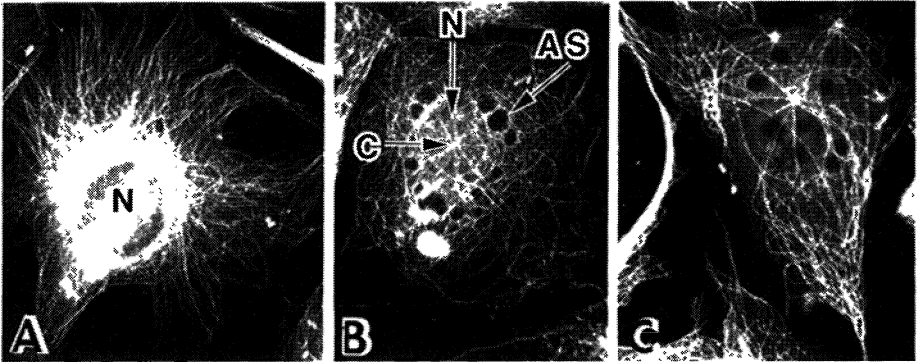


Fig. 2 Indirect immunofluorescence with tubulin antibodies on FV3-infected BHK cells. A) uninfected cell, B) 6 hr post-infection, and C) 10 hr post-infection. (AS) virus assembly sites. (N) nucleus. (C) focal point.

To determine whether the observed reduction of microtubules is due to inhibition of tubulin synthesis or due to degradation of microtubules, the following experiment was done. Uninfected and 3 hr-infected BHK cells were labeled with [35 S]-methionine for 1 hr

and the cell lysates were analyzed by two-dimensional gel electrophoresis (48). A comparison of the amount of tubulin in infected and uninfected cells showed an 80% reduction in tubulin synthesis in infected cells. Thus these results showed that the reduction of microtubules seen by immunofluorescence in infected cells is at least partially due to a severe inhibition of tubulin synthesis. The significance of microtubule reduction is not known but a similar phenomenon is noted in cells infected with herpesviruses (78, 79).

The progressive reduction of microtubules in FV3-infected cells suggests that microtubules may not have a role in FV3 replication. To further examine this, we studied FV3 assembly and growth in BHK cells treated with the microtubule-depolymerizing drug, colchicine. In these experiments the cells were pretreated with 10 $\mu\text{g/ml}$ or 40 $\mu\text{g/ml}$ of the drug to depolymerize the microtubules and then infected with FV3 in the presence of the drug. When examined by immunofluorescence and electron microscopy, these cells showed normal assembly sites (50). The virus production was also unaffected in these cells as revealed by plaque assay (50). These results suggest that microtubules have no function in any aspect of FV3 replication.

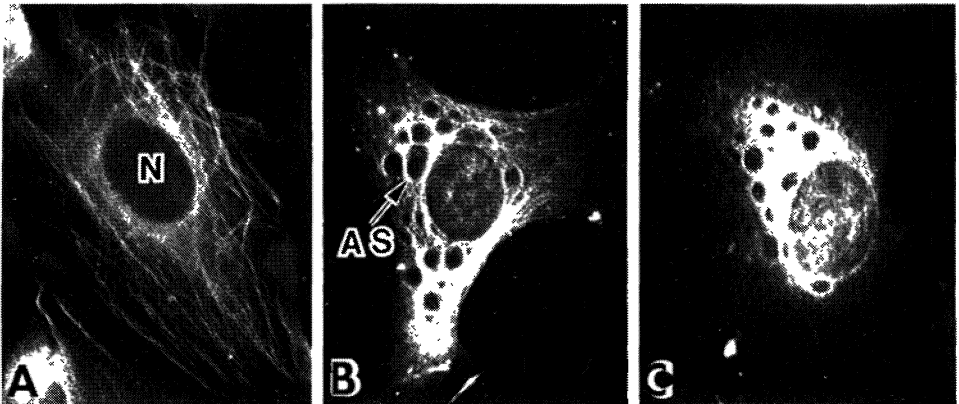


Fig. 3. Indirect immunofluorescence with antivimentin antibodies on BHK cells. A) uninfected cells, B) cells infected with FV3 for 6 hr, and C) for 8 hr. Abbreviations as in Fig. 2.

Intermediate Filaments

The organization of IF in uninfected and infected BHK cells was compared by means of immunofluorescence, using antibodies

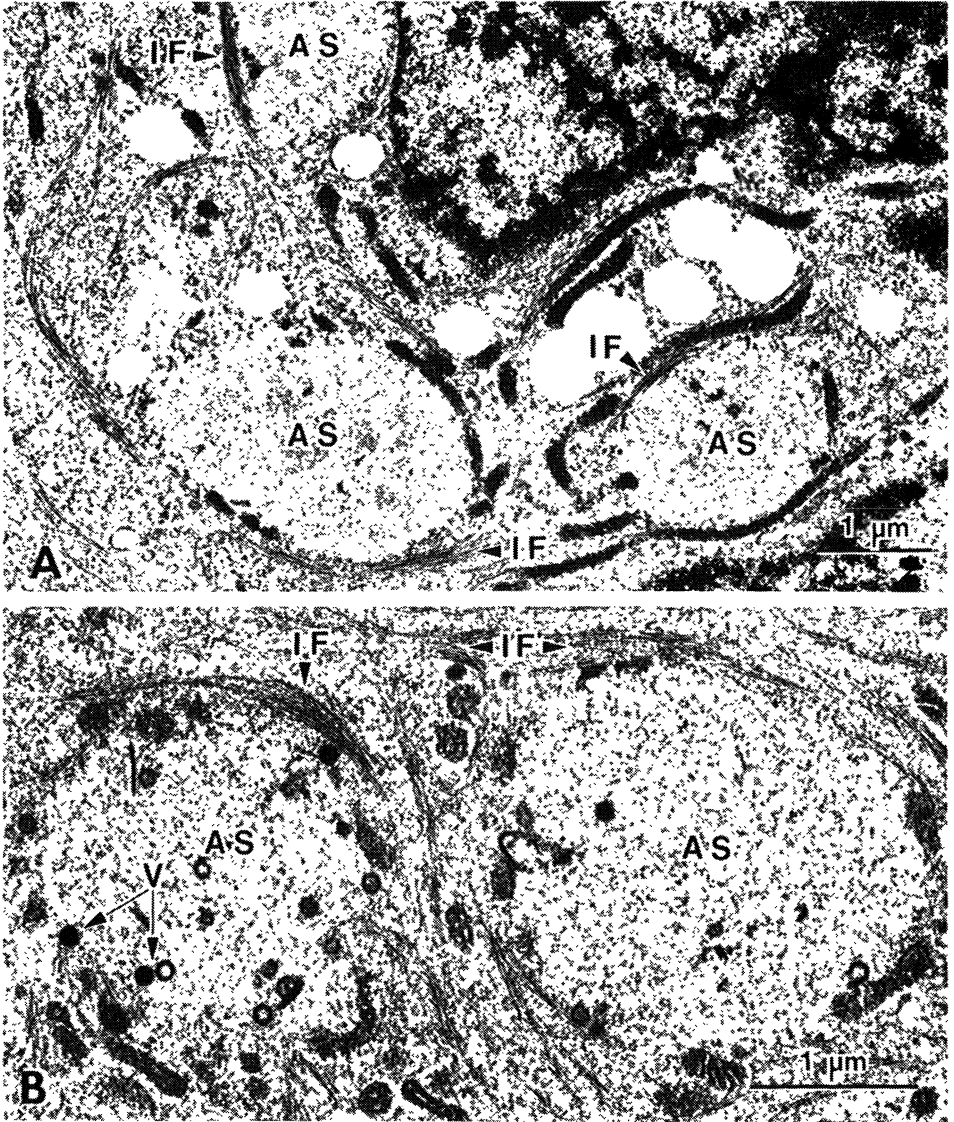


Fig. 4. Electron micrograph of FV3-infected fathead minnow cell at 4 hr (A) and at 6 hr (B). Note the bundles of intermediate filaments (IF) surrounding the virus assembly sites (AS).

against vimentin (IF protein). In uninfected cells, the pattern resembles that previously reported (59). The filaments emanate from the perinuclear region and extend into the cytoplasm (Fig. 3A). In FV3-infected cells, changes in the organization of IF begin at 6 hr. The filaments retract from the cell periphery and outline certain discrete bodies in the cytoplasm (Fig. 3B). At 8 hr, all of the fluorescence is concentrated around the discrete bodies, which are now located near the nucleus (Fig. 3C). That the discrete bodies are viral assembly sites is demonstrated by electron microscopic observations of infected cells. In electron micrographs bundles of IF are seen surrounding each virus assembly site at earlier (Fig. 4A) and later (Fig. 4B) times after infection. Thus, IF appear to reorganize to surround the virus assembly sites during FV3 infection.

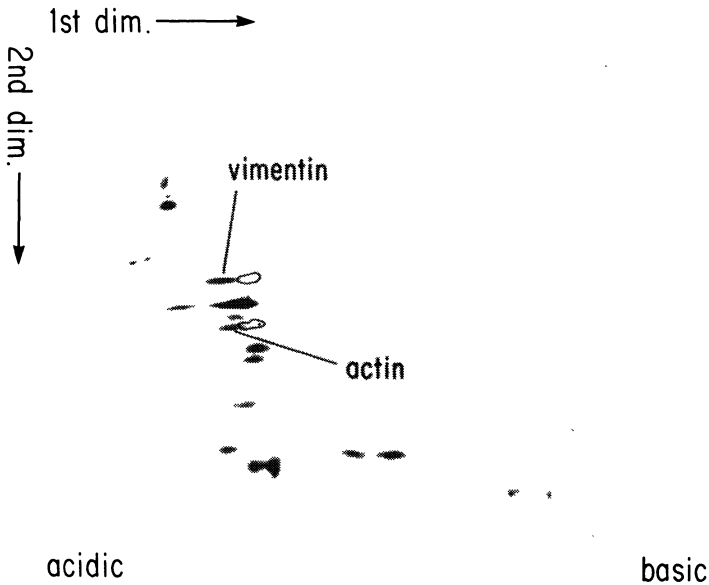


Fig. 5. Two-dimensional gel analysis of vimentin and actin in FV3-infected cells. FV3-infected BHK cells were labeled with ^{35}S methionine at 6 hr post-infection and the proteins were analyzed. Areas outlined in black represent the position of markers.

To determine the molecular basis for the organizational changes in IF, we examined the qualitative and quantitative changes in vimentin of FV3-infected cells by two-dimensional gel electrophoresis. There was no decrease in the synthesis of vimentin in FV3-infected cells but the vimentin of infected cells was more acidic than its counterpart in uninfected cells (Fig. 5). The shift in the mobility of vimentin might have been due to a post-translational modification of the protein such as phosphorylation (60). To determine if this was so, we labeled FV3-infected BHK cells at 3 hr post-infection with ^{32}P and subjected

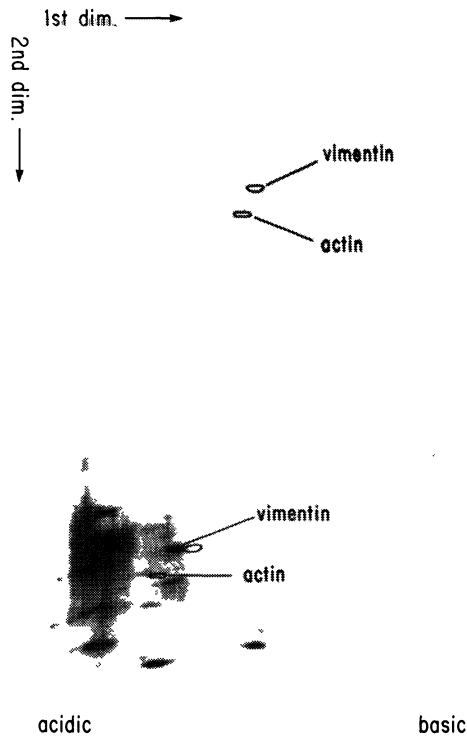


Fig. 6. Increased phosphorylation of vimentin in FV3-infected BHK cells. The infected cells were labeled at 3 hr with $^{32}\text{PO}_4$ for 1 hr and the labeled proteins were analyzed by 2-D gel electrophoresis. Upper panel, uninfected cells. Lower panel, infected cells.

the cell extracts to two-dimensional electrophoresis. The results showed a dramatic increase in the phosphorylation (more than four-fold) of vimentin by 4 hr post-infection (Fig. 5). Pulse-chase experiments showed no detectable differences in the turnover of ^{32}P -labeled vimentin, suggesting that the observed increase in the phosphorylation of vimentin in infected cells is not due to a

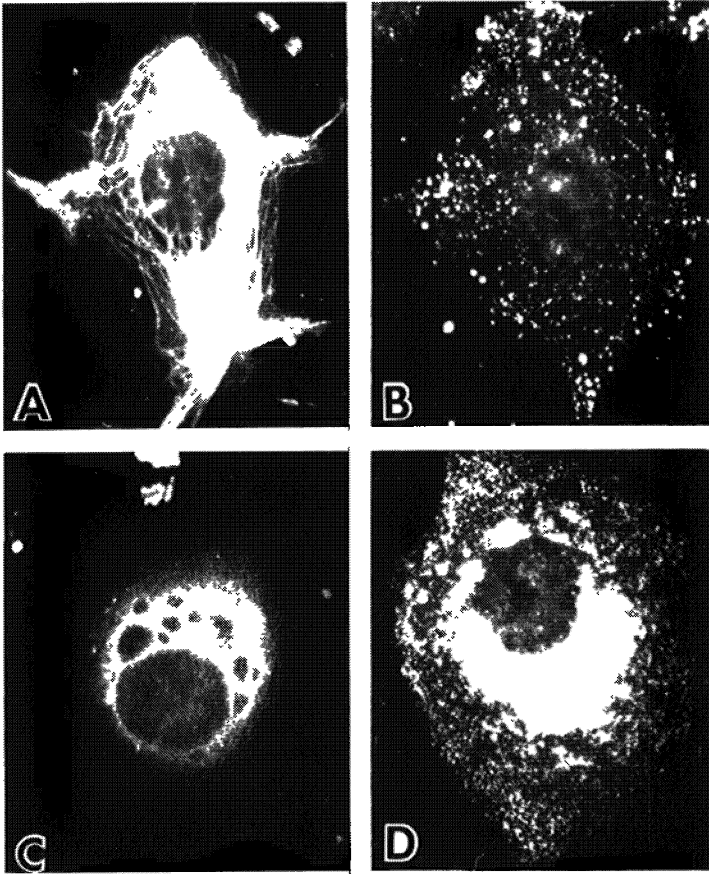


Fig. 7. Immunofluorescence analysis of ts 9467-infected BHK cells labeled with antivimentin (A, C) or anti-FV3 (B, D) antibodies at 7 hr post-infection. At 30°C (A, B), the IF network was unchanged (A) and the assembly sites were not formed (B). At 25°C (C, D) the IF reorganized (C) and the assembly sites are formed (D). AS, assembly site, N, nucleus, IF, intermediate filaments.

decreased rate of dephosphorylation. Thus, the observed changes in vimentin precede the reorganization of IF which occurs before the assembly site formation.

The increased phosphorylation of vimentin in FV3-infected cells is interesting, especially in view of the proposal that phosphorylation modulates the organizational changes in IF (1, 10). To determine if phosphorylation of vimentin, IF reorganization, and assembly site formation are all interconnected, we studied cells infected with a ts mutant of FV3, ts 9467 (61). This mutant, at the nonpermissive temperature of 30°, makes early viral proteins but neither reorganizes IF nor forms the assembly sites. Upon shift to the permissive temperature (25°), the normal course of events occur. In biochemical studies with BHK cells infected with ts 9467, we found that at the nonpermissive temperature vimentin is not phosphorylated. An examination of these cells by means of immunofluorescence with antibodies against vimentin and FV3 revealed an organization of IF typical of uninfected cells and the absence of assembly sites (Fig. 7A, B). Upon shift to the permissive temperature, the vimentin was phosphorylated, the IF reorganized, and normal assembly sites formed (Fig. 7C, D). It appears then from the above studies that phosphorylation of vimentin is necessary for IF reorganization, which in turn is essential for assembly site formation.

To study the functional significance of the association between IF and FV3 assembly sites, we disrupted the organization of IF in BHK cells either by drugs or by antivimentin antibody microinjection and studied the effect of such disruption on FV3 assembly.

Of all the drugs that have been reported to affect IF organization, those that act on microtubule organization appear to be the most effective. The primary effect of the drug colchicine is to depolymerize microtubules (1). In response to microtubule depolymerization, the IF collapse (37, 62). The collapse is presumably due to the dependence of organization of IF on an intact microtubule system (63). Colchicine, as previously noted, had no effect on IF reorganization around FV3 assembly sites, nor affected

virus growth (50). A second drug, taxol promotes microtubule assembly (64, 65) and while doing so induces dramatic changes in the organization of microtubule and IF (66). In FV3-infected BHK cells taxol prevented the reorganization of IF around assembly sites. The assembly sites formed in the presence of taxol were not clearly demarcated from the rest of cytoplasm, contained cell components such as mitochondria, polysomes and microtubules, and reduced accumulation of proteins. The drug at a concentration of 50 μM also reduced the virus yield by about 80% (50). Thus a block in IF reorganization around FV3 assembly site seems to interfere with FV3 assembly and growth.

As an independent test of the role of IF reorganization in the formation and maintenance of FV3 assembly sites, we examined the effect of antibody-induced disruption of IF on FV3 replication. It has been shown that intracellular injection of antivimentin antibodies causes vimentin-type IF to collapse in a variety of cell types (67). To test the effect of antivimentin-induced collapse of IF on FV3 assembly, BHK cells were infected with FV3 2 hr after antibody injection. When examined by immunofluorescence 8 hr later, the cells showed collapsed masses of IF near the nucleus and several diffuse assembly sites scattered in the cytoplasm (50). When these cells were examined by electron microscopy, the assembly sites were seen as irregular fibrous structures often attached to the collapsed mass of IF (Fig. 8). As in taxol-treated cells, the assembly sites were indistinct, contained microtubules and polysomes, and showed fewer assembled virions than in serum-injected controls. To quantitate virus production in antivimentin-injected cells and serum injected (control) cells, five assembly sites from each group of cells were serially sectioned and the total number of virus particles in the assembly sites was counted in the electron microscope. The assembly sites of antivimentin-injected cells contained 281 mature virions while those of serum-injected cells had 953 mature virions. Thus, there appears to be a 70% inhibition of virus production in antivimentin-injected cells. In general, the effect of antivimentin injection on viral assembly

site morphology and virus growth was very much like that observed in taxol-treated cells.

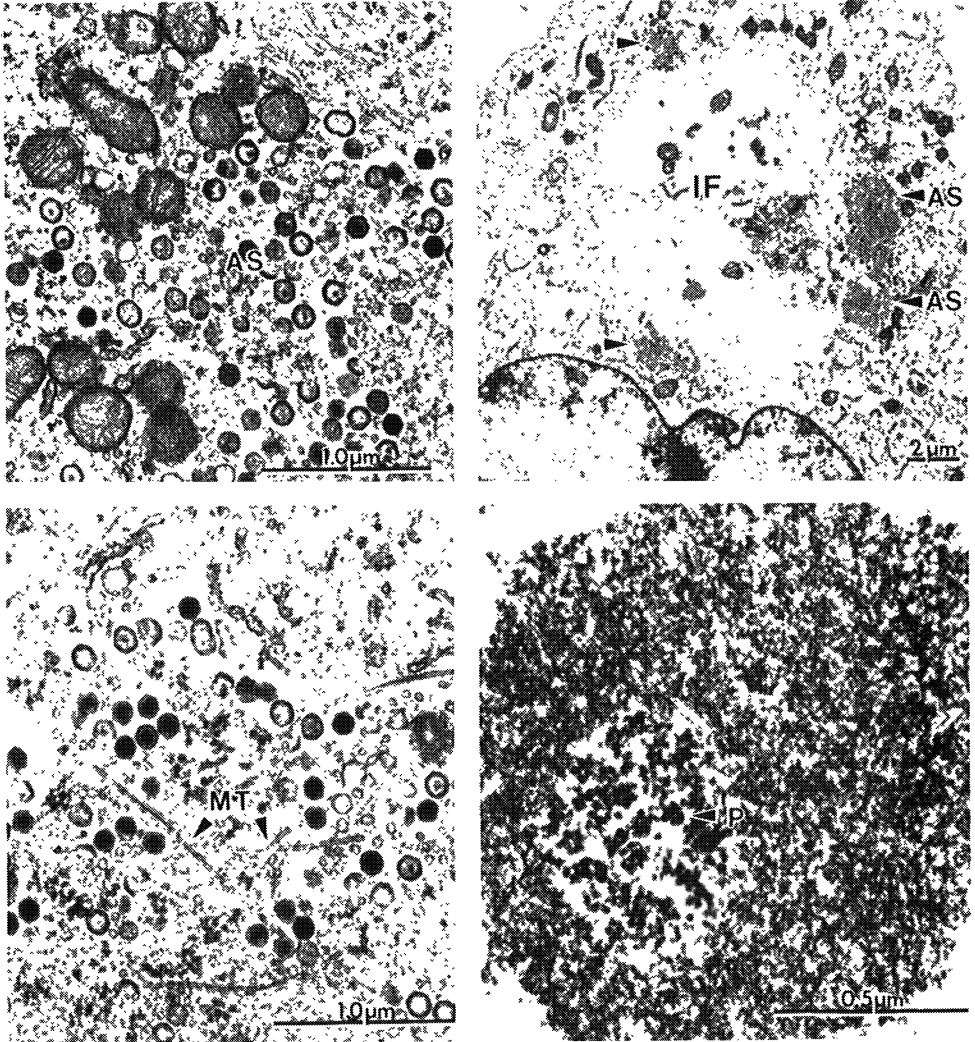


Fig. 8. Electron micrographs of FV3 assembly sites of BHK cells microinjected with antivimentin antibodies and infected with FV3. The assembly sites (AS) were not clearly demarcated from the cytoplasm (panel A) and were often found attached to the collapsed mass of intermediate filaments (panel B). The sites also contained microtubules (MT, panel C) and polysomes (P, panel D).

The taxol and microinjection studies described above have shown that IF play a crucial role in FV3 assembly. Both taxol and antivimentin microinjection prevented the reorganization of IF around FV3 assembly sites. The failure of IF to surround the assembly site led to (i) intrusion of cell components into the assembly site, (ii) reduced accumulation of viral proteins, and (iii) about 80% inhibition of virus growth. Thus, IF appear to be necessary to produce and/or maintain the structural integrity of the viral assembly sites, but they are not strictly required for the assembly of mature virions. The disorganized assembly sites that are formed in the absence of the circumferential IF system do produce mature virions, but they do so with dramatically lower efficiency than normal IF-associated assembly sites. This implies that in FV3-infected BHK cells, IF appear to help organize a region of the cytoplasm, the viral assembly site, into a more efficient three-dimensional ensemble of interacting viral components. A subsequent study has suggested that in murine 3T3 cells the IF similarly compartmentalize lipid globules for adipogenesis (68).

A variety of animal viruses are shown to interact with the cytoskeleton for their assembly and transport (for a review, see 44). Two viruses of the family *Reoviridae*, which assemble in cytoplasmic factories, have also been shown to interact specifically with the IF (69, 70). The functional interaction between FV3 and IF demonstrated here, however, constitutes the first direct experimental evidence that the IF play an active role in virus assembly.

Microfilaments

To compare the organization of microfilaments in infected and uninfected cells, the cells were examined in the fluorescence microscope after labeling with rhodamine-conjugated phalloidin (50). Phalloidin is a small stable compound that forms a complex with actin (71). The uninfected BHK cells show a few thick bundles of microfilaments (stress fibers) and many finer filaments running parallel to the long axis of the cell (Fig. 9A). In infected cells, at the time of assembly site formation (i.e., 6 hr), the

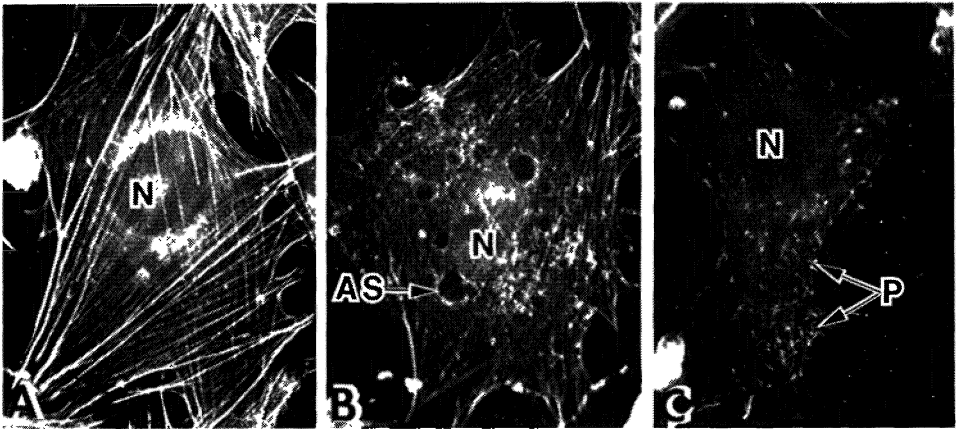


Fig. 9. Immunofluorescence with rhodamine-conjugated phalloidin on BHK cells. (A) uninfected cells, (B) FV3-infected cells at 6 hr, and (C) at 10 hr. P, microvillus-like projections, AS, assembly site, N, nucleus.

stress fibers disappear, the thin filaments persist, and the entire cell exhibits particulate fluorescence (Fig. 9B). At 10 hr (Fig. 9C), the cell surface contains many actin-positive microvillus-like projections. That the microvillus-like projections appear at the time of virus release is dramatically illustrated by a scanning electron microscopic study of the surfaces of FV3-infected BHK cells at various times after infection (Fig. 10). At 3 hr after the adsorption of the virus, the cell surface exhibits few projections (Fig. 10A). At 7 hr after infection or at a time when the virus begins to appear at the cell surface, the number of projections increases (Fig. 10B). At a time when the virus is released in abundance, the number of projections greatly increases (Fig. 10C) and each projection possesses a series of bulges, each of which presumably contains a single virus particle (Fig. 10C, inset). Thus, it appears that FV3 is released through microvillus-like projections formed *de novo*. The microvillus-like projections contain microfilaments and virus particles in the process of budding. Thin sections of virus-infected cells viewed by transmission electron microscopy (Fig. 11) support this contention.

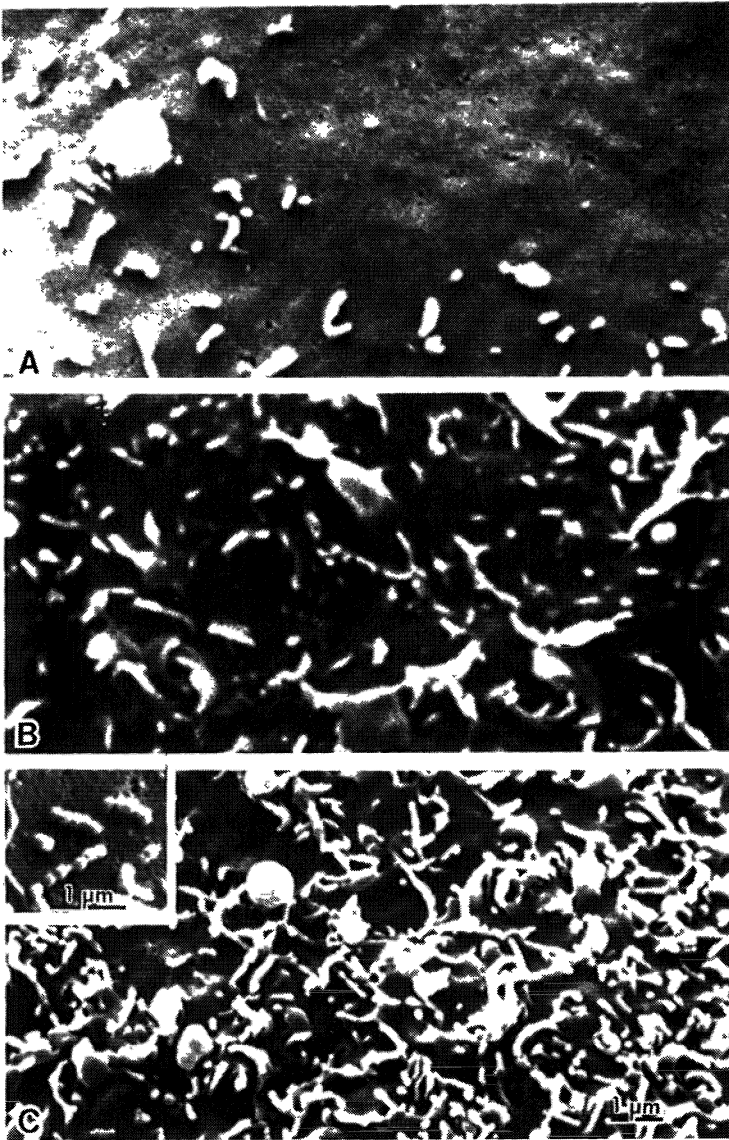


Fig. 10. Scanning electron micrograph of the surface of BHK cells infected with FV3 for 3 hr (A), 7 hr (B), and 15 hr (C). Note the progressive increase in the number of microvillus-like projections with time. The inset shows a highly magnified view of microvillus-like projections containing virions.

Electron micrographs of FV3-infected cells late in infection show microvillus-like projections enclosing one to several virions. In addition, bundles of microfilaments are also seen lining the plasma membrane and extending into these projections.

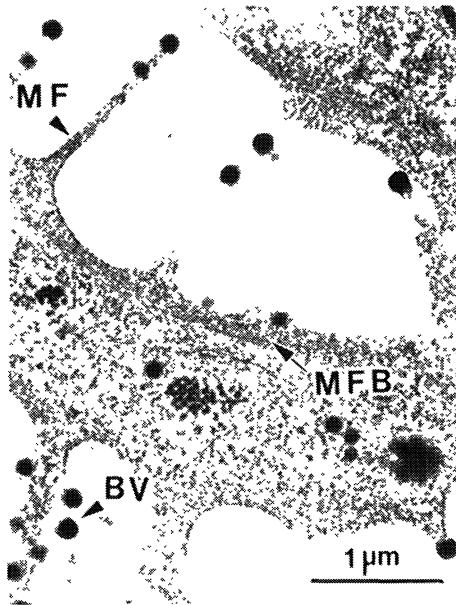


Fig. 11. Electron micrograph of a portion of fathead minnow cell infected with FV3 for 8 hr. MFB, microfilament bundles. MF, microfilaments. BV, budding virions.

Biochemical studies have shown that actin, the constituent protein of microfilaments, exhibits qualitative changes in FV3-infected cells. Unlike tubulin, actin continued to be synthesized in infected cells at normal levels but showed a change in its isoelectric point. At about 4 hr after infection, the actin moved towards the acidic pH range in two-dimensional gels, and by 6 hr post-infection most of the newly synthesized actin was more acidic than its counterpart in uninfected cells (Fig. 5). The change in the mobility of actin was not due to phosphorylation since actin in infected cells was not labeled by ^{32}P (Fig. 6). It is not known whether the observed shift in actin is due to a post-translational

modification or whether the phenomenon represents the synthesis of a new isoform (e.g., α -actin) of actin. In either case, the process must occur during virus replication, since actin synthesized before infection did not show any change in mobility. It is interesting to note that changes in actin precede the formation of the microvillus-like structures utilized in virus release.

To determine the role of microfilaments in FV3 release, we have studied the effect of disruption of microfilaments by cytochalasins on virus release. Cytochalasin B (CB) is known to disrupt microfilaments by inhibiting the polymerization of actin monomers (72, 73). Cytochalasin D (CD), on the other hand, disrupts microfilament function by binding to myosin (72, 74). Among the two drugs, CB is known to perturb sugar metabolism by inhibiting hexose transport (75), while CD causes only minor, if any, inhibition of hexose transport (72). The secondary effect of these drugs on sugar metabolism is important to consider since the production of several viruses depends on glycosylation of viral proteins (76, 77). However, since none of the FV3 proteins are glycosylated (51), the effect of cytochalasins on glycosylation may not be relevant to the current study.

To determine the effect of CB and CD on virus yield, BHK cells were adsorbed with FV3, the drugs were added to the cell cultures at various concentrations, and the quantity of infectious virus produced and released at 48 hr post-infection was determined by plaque assay. With FV3, like measles virus (77), only a fraction of the infectious virions are released from the cell (released virus), while a major fraction of infectious virions remains associated with the cell (cell-associated virus). This is highly advantageous in drug studies since a quantitation of the two fractions of the virus in drug-treated and control cultures will permit us to determine if the block is at the level of production or release of the virions. At a concentration of 30 $\mu\text{g/ml}$, CB inhibited the release of FV3 by 80%, while CD, at a concentration of 2 $\mu\text{g/ml}$ inhibited virus release by 99%. The inhibition of virus release by both CB and CD were not due to decreased production of

the virus, since there was no reduction in the titers of cell-associated virus. In fact, the decrease in the amount of released virus was coincident with an increase in the cell-associated virus, suggesting that virus that failed to release accumulated within the cell.

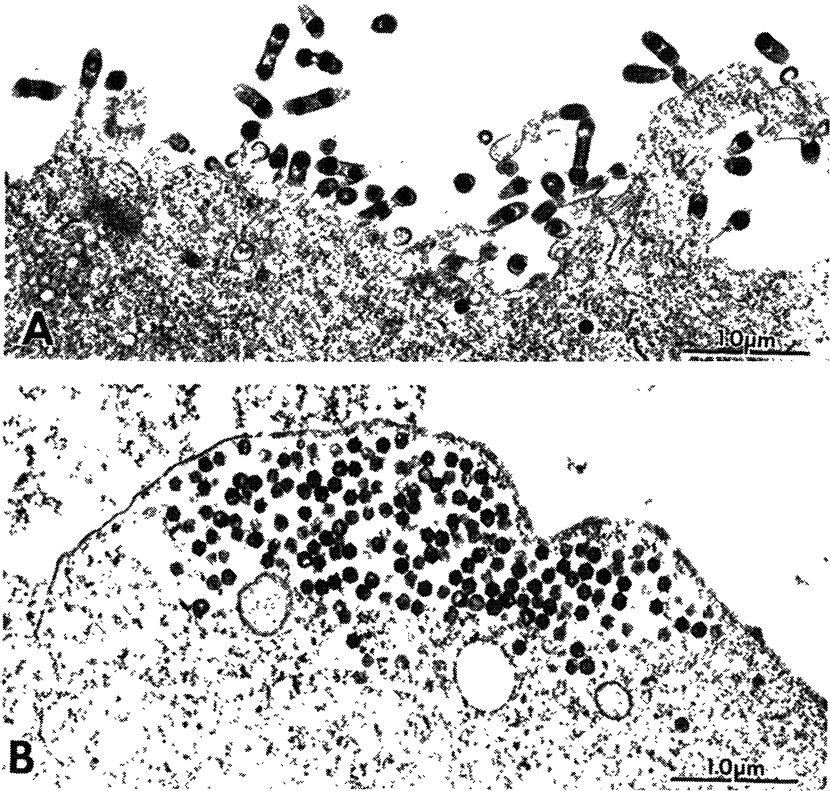


Fig. 12. (A) Electron micrograph of a portion of FV3-infected BHK cell at 24 hr post-infection. Note the budding virions. (B) A cell infected with FV3 in the presence of cytochalasin D ($2 \mu\text{g/ml}$) for 24 hr. The infection was carried out in the presence of CD ($2 \mu\text{g/ml}$) for 24 hr and the cells were fixed and processed. Note the accumulation of a large number of virus particles beneath the plasma membrane and the absence of microvillus-like structures on the plasma membrane.

The results of CB and CD studies suggested that the drugs affected either the traverse of virions from the assembly site to the plasma membrane, or the release of virions at the cell surface, or both. In an effort to determine which of these possibilities is true, we have examined the CB and CD treated, FV3-infected cells by electron microscopy. The untreated control cells showed numerous microvilli bearing virus particles at the cell surface (Fig. 12A). The cells treated with CB or CD had no microvilli and the virions accumulated in large numbers beneath the plasma membrane (Fig. 12B). The results suggest that both CB and CD inhibit the release but not the traverse of the virions.

The reason for the suppression of virus release by CB and CD appears to be the failure of the cell to form the microvillus-like structures through which the virus exits. Since CB binds to actin (72, 73) and CD binds to myosin (72, 74), it appears that the formation of the microvilli-like structures involves the actomyosin complex. In general, the results of cytochalasin studies with FV3 agree with those with measles virus (77). In summary, all of our above studies with FV3-infected cells strongly favor an active role for microfilaments in virus release.

CONCLUSION

A variety of animal viruses are now known to interact with the eukaryotic cytoskeleton for protein synthesis, assembly and transport (44). A study of this interaction will shed light not only on the role of cytoskeleton in virus replication but also on the function of cytoskeleton in normal cells. The studies with FV3 have shown that IF are important in maintaining the structural and functional integrity of virus assembly site and that microfilaments are essential for virus release. The functional interaction between IF and FV3 demonstrated here constitutes the first direct demonstration that IF play a role in a biological event. Future studies will elucidate the molecular basis of the function of IF in FV3 replication; the knowledge in turn may provide the intellectual framework for understanding the function of IF in normal (uninfected) cells.

ACKNOWLEDGEMENTS

We thank Mrs. Kathy Troughton and Mrs. Ramona Tirey for expert technical assistance, and Ms. Glenith D. White for typing the manuscript. This work was supported by research grants from American Cancer Society #CD-253B (KGM), National Institutes of Health GM 23638 (RG), National Institutes of Health Cancer Center Support (CORE) grant, and by American Lebanese Syrian Associated Charities.

The authors thank Rockefeller University Press for permission to use Figs. 2, 3, 4, 9 and 11 (ref. 45), Academic Press for Figs. 1, 5, 8, 10 and 12 (refs. 46, 47, 50), Cambridge University Press for Fig. 7 (ref. 49), and Springer-Verlag for Fig. 6 (ref. 48).

REFERENCES

1. Olmsted, J.B. and Borisy, G.G. *Ann. Rev. Biochem.* 43:507-540, 1973.
2. Lazarides, E. *Ann. Rev. Biochem.* 51:219-250, 1982.
3. Steinert, P.M. and Roop, D.R. *Ann. Rev. Biochem.* 57:593-625, 1988.
4. Groeschel-Stewart, U. *Int. Rev. Cytol.* 65:193-254, 1980.
5. Schliwa, M. *In*: *The Cytoskeleton, An Introductory Survey*, Springer-Verlag, New York, 1986.
6. Borisy, G.G., Cleveland, D.W. and Murphy, B.D. *In*: *Molecular Biology of the Cytoskeleton*, Cold Spring Harbor Laboratory, New York, 1984.
7. Bershadsky, A.D. and Vasiliev, J.M. *In*: *Cytoskeleton*, Plenum Publishing Corporation, New York, 1988.
8. *Cold Spring Harbor Symposia on Quantitative Biology*, Vol. XLVI, Parts 1 and 2, 1982.
9. Roberts, K. and Hyam, J.S. *In*: *Microtubules*, Academic Press, New York, 1979.
10. Inagaki, M., Nishi, Y., Nishigawa, K., Malsugama, M., and Sato, C. *Nature* 328:649-652, 1987.
11. Cleveland, D.W. *Cell* 28:689-691, 1982.
12. Kirschner, M.W. *Int. Rev. Cytol.* 54:1-71, 1978.
13. Pollard, T. *J. Cell. Biol.* 91:1565-1655, 1981.
14. Clarke, M. and Spudich, A. *Ann. Rev. Biochem.* 46:797-822, 1977.
15. Damsky, C.H., Sheffield, J.B., Tuszynski, G.P. and Warren, L. *J. Cell. Biol.* 75:593-605, 1977.
16. Berl, S., Puskin, S. and Nicklas, W.J. *Science* 179:441-446, 1973.
17. Sanger, J.W. *Proc. Natl. Acad. Sci. USA* 72:2451-2455, 1975.
18. Stossel, T.P. and Hartwig, J.M. *J. Cell. Biol.* 68:602-619, 1976.

19. Douvas, A.S., Harrington, C.A. and Bonner, J. Proc. Natl. Acad. Sci. USA 72:3902-3906, 1975.
20. LeStourgeon, W.M. In: The Cell Nucleus, Vol. 6, (Ed. H. Busch), Vol. 6, Academic Press, New York, 1978, pp. 305-326.
21. Scheer, U., Hinssen, H., Franke, W.W. and Jokusch, B.M. Cell 39:111-122, 1984.
22. Egly, J.M., Miyamoto, N.G., Moncollin, W. and Chambon, P. EMBO J. 3:2363-2371, 1984.
23. Brinkley, B.R., Fuller, G.M. and Highfield, D.P. Proc. Natl. Acad. Sci. USA 72:4981-4985, 1975.
24. Schnapp, B.J., Vale, R.D., Sheetz, M.P. and Reese, T.S. Cell 40:455-462, 1985.
25. Moyer, S.A., Baker, S.C. and Lessard, J.L. Proc. Natl. Acad. Sci. USA 83:5405-5409, 1986.
26. Hill, V.M., Harmon, S.A. and Summers, D.F. Proc. Natl. Acad. Sci. USA 83:5410-5413, 1986.
27. McKeon, F.D., Kirschner, M.W. and Caput, D. Nature 319:463-468, 1986.
28. Aebi, U., Cohn, J., Buhle, L. and Gerace, L. Nature 323:560-564, 1986.
29. Goldman, A.E., Mard, G., Steinert, P.M., Yang, H.S. and Goldman, R.D. Proc. Natl. Acad. Sci. USA 83:3839-3843, 1986.
30. Traub, P. In: Intermediate Filaments, Springer-Verlag, Berlin, 1985.
31. Blöse, S.H. Eur. J. Cell Biol. 22:373, 1980.
32. Wang, E. and Choppin, P.W. Proc. Natl. Acad. Sci. USA 78:2363-2367, 1981.
33. Wang, E. and Goldman, R.D. J. Cell Biol. 79:708-726, 1978.
34. Wang, E., Cross, R.K. and Choppin, P.W. J. Cell Biol. 83:320-337, 1979.
35. Zieve, G.W., Heidemann, S.R. and McIntosh, J.R. J. Cell Biol. 87:160-169, 1980.
36. Dulbecco, R., Allen, R., Okada, S. and Bowman, M. Proc. Natl. Acad. Sci. USA 80:1915-1918, 1983.
37. Goldman, R.D. and Knipe, D.M. Cold Spring Harbor Symp. Quant. Biol. 37:523-533, 1972.
38. Menko, A.S., Toyama, Y., Boettiger, D. and Holtzer, H. Mol. Cell Biol. 3:113-125, 1983.
39. Geiger, B. Nature 329:392-393, 1987.
40. Gawlitta, W., Osborn, M. and Weber, K. Eur. J. Cell Biol. 26:83-90, 1981.
41. Klymkowsky, M.W. Nature 291:249-251, 1981.
42. Lin, J.J.-C. and Feramisco, J.R. Cell 24:185-193, 1981.
43. Kihn, S., Vargias, C.E. and Traub, P. J. Cell Sci. 87:543-554, 1987.
44. Luftig, R.B. J. Theor. Biol. 99:173-191, 1982.
45. Murti, K.G. and Goorha, R. J. Cell. Biol. 96:1248-1257, 1983.
46. Murti, K.G., Porter, K.R., Ulrich, M., Goorha, R. and Wray, G. Exp. Cell Res. 154:270-282, 1984.
47. Murti, K.G., Chen, M. and Goorha, R. Virology 142:317-325, 1985.
48. Murti, K.G., Goorha, R. and Chen, M. Curr. Top. Microbiol. Immunol. 116:107-131, 1985.

49. Chen, M., Goorha, R. and Murti, K.G. *J. Gen. Virol.* 67:915-922, 1986.
50. Murti, K.G., Goorha, R. and Klymkowsky, M.W. *Virology* 162:264-269, 1988.
51. Goorha, R. and Granoff, A. *Comp. Virol.* 14:347-399, 1979.
52. Murti, K.G., Goorha, R. and Granoff, A. *Virology* 116:275-283, 1982.
53. Goorha, R. and Murti, K.G. *Proc. Natl. Acad. Sci. USA* 79:248-252, 1982.
54. Goorha, R., Willis, D.B., Granoff, A. and Naegele, R.F. *Virology* 112:40-48, 1981.
55. Willis, D.B., Goorha, R. and Chinchar, V.G. *Curr. Top. Microbiol. Immunol.* 116:77-106, 1985.
56. Murti, K.G., Goorha, R. and Granoff, A. *Adv. Virus Res.* 30:1-19, 1985.
57. Darlington, R.W., Granoff, A. and Breeze, D.C. *Virology* 29:149-156, 1966.
58. Goorha, R., Murti, K.G., Granoff, A. and Tirey, R. *Virology* 84:32-51, 1978.
59. Hynes, R.O. and Destree, A.T. *Cell* 13:151-163, 1978.
60. Evans, R.M. and Fink, L.M. *Cell* 29:43-52, 1982.
61. Willis, D.B., Goorha, R. and Granoff, A. *Virology* 98:328-335, 1979.
62. Blose, S.H. and Chacko, S. *J. Cell Biol.* 70:459-466, 1976.
63. Goldman, R.D., Milsted, A., Schloss, J.A., Starger, J. and Yerna, M.J. *Annu. Rev. Physiol.* 41:703-722, 1979.
64. Schiff, P.B. and Horwitz, S.B. *Proc. Natl. Acad. Sci. USA* 77:1561-1565, 1980.
65. DeBrabander, M., Guens, G., Nuydens, R., Willebrords, R. and DeMey, J. *Proc. Natl. Acad. Sci. USA* 78:5608-5612, 1981.
66. Geuens, G., DeBrabander, M., Nuydens, R. and DeMey, J. *Cell Biol. Int. Rep.* 7:35-47, 1983.
67. Klymkowsky, M.W. *Nature (London)* 291:249-251, 1981.
68. Franke, W.W., Hergt, M. and Grund, C. *Cell* 49:131-141, 1987.
69. Sharpe, A.H., Chen, L.B., and Fields, B.N. *Virology* 12:399-411, 1982.
70. Eaton, B.T., Hyatt, A.D. and White, J.R. *Virology* 157:107-116, 1987.
71. Langsfeld, A., Low, I., Wieland, T., Dancker, P. and Hasselbach, W. *Proc. Natl. Acad. Sci. USA* 71:2803-2807, 1974.
72. Tannenbaum, J., Tannebaum, S.W. and Godman, G.C. *J. Cell. Physiol.* 91:239-248, 1977.
73. Lin, D.C., Tobin, K.D., Grumet, M. and Lin, S. *J. Cell Biol.* 84:455-460, 1980.
74. Puszkin, E., Puszkin, S., Lo, L.W. and Tannenbaum, S.W. *J. Biol. Chem.* 248:7754-7761, 1973.
75. Kletzien, R.F. and Perdue, J.F. *J. Biol. Chem.* 248:711-719, 1973.
76. Griffin, J.A. and Compans, R.W. *J. Exp. Med.* 150:379-391, 1979.
77. Stallcup, K.C., Raine, C.W. and Fields, B.N. *Virology* 124:59-74, 1983.

78. Dienes, H.P., Hiller, G., Muller, S. and Falke, D. Arch. Virol. 94:15-28, 1987.
79. Pfeiffer, G., Willitzki, D., Weder, D., Becker, B. and Radsak, K. Arch. Virol. 76:153-159, 1983.

7

THE DNA-METHYLASE OF FROG VIRUS 3

KARIM ESSANI

Department of Virology and Molecular Biology, St. Jude Children's Research Hospital, Memphis, Tennessee 38101, USA

ABSTRACT

The DNA of frog virus 3 (FV3) replicates in two stages. During the first stage, genome sized DNA is synthesized in the nucleus of infected cells. This is followed by a second stage of DNA replication in the cytoplasm where concatemeric viral DNA is synthesized. FV3 DNA is methylated in the cytoplasm by a virus-coded DNA-methylase. It has been shown that more than 20% cytosine residues are methylated at the 5-carbon position. FV3 DNA is completely resistant to cleavage by a restriction endonuclease HpaII, a methylation-sensitive enzyme that recognizes the sequence CCGG, while readily restricted by another restriction enzyme MspI (an isoschizomer of HpaII), suggesting that every cytosine residue in the sequence of CpG is methylated. A number of DNA-methylase negative mutants have been derived from FV3 to elucidate the structure and function of this enzyme. Detailed genetic and biochemical studies involving one such mutant have revealed that the FV3 DNA-methylase, unlike other animal DNA-methylases, requires at least two polypeptides for its catalytic activity.

INTRODUCTION

It has long been known that bacterial DNA methylation provides a molecular basis for the modification of resident DNA to protect it from degradation with restriction endonucleases present in the bacterial cells. It, therefore, serves as a primitive and yet sophisticated immune mechanism to protect bacterial cells from invading foreign DNA. It is also known that bacterial DNA methyl-

ation plays a vital role in DNA post-replicative mismatch repair. In order to carry out these and perhaps other biological functions, bacterial DNA-methylases are endowed with a great degree of specificity. On the contrary, one finds DNA-methylases in animal cells that have not shown to demonstrate such specificities. Although there is an increasing body of evidence to inter-relate DNA methylation and gene activity (1), it is not clear how animal DNA-methylases recognize sequences to be methylated. Since the pattern of DNA methylation in animal cells is tissue or organ specific, it is reasonable to postulate that animal DNA-methylases function cooperatively with yet unknown proteins that equip them with the required specificities (2). Since FV3 DNA is heavily methylated in a fashion identical to animal cell DNA in terms of sequences, we expect that FV3 DNA-methylase will serve as a useful model to explore the enzymology of DNA-methylation in eukaryotic cells. Dawn Willis and her associates have described in a separate chapter in this monograph what role DNA methylation plays in transcription of FV3 DNA. I will, therefore, limit this chapter to the little known enzymology of this important enzyme that has just recently started to emerge.

In the process of generating restriction maps of FV3 DNA, Willis and Granoff (3) noticed that the FV3 DNA was completely resistant to cleavage by a methylation-sensitive HpaII, a restriction endonuclease that recognizes the sequence CCGG (4). It was particularly interesting because FV3 DNA contains 55% CG. The restriction endonuclease MspI is an isoschizomer of HpaII and it also recognizes the sequence CCGG, but is not methylation-sensitive. If the internal C in the sequence CpG is methylated, the DNA will remain resistant to HpaII while readily cleavable by MspI (5). This kind of analyses using a number of restriction endonucleases established that every single C residue in the sequence CpG was methylated in FV3 DNA. During these studies, Willis and Granoff (3) also used isoschizomers MboI, DpnI and Sau3A and demonstrated that adenine residues in FV3 DNA were not methylated. This finding was consistent with the DNA from animal cells where 0.5-10% of cytosine residues are methylated in the form

of 5-methylcytosine (6). The amount of 5-methylcytosine present in FV3 DNA was also quantitative and compared with that in the host cell DNA. The purified [^{32}P]-labeled DNA from FV3 virions and from the nuclei of uninfected FHM (host) cells was subjected to thin layer chromatography (TLC) analysis for nucleotide monophosphates. It was shown that the relative proportion of 5-methylcytosines in FV3 DNA was much greater than in FHM cell DNA. More precise studies established that over 21.9% cytosine residues in FV3 DNA and only 6.2% cytosine residues in FHM cell DNA were methylated in the form of 5-methyl cytosines (3).

FV3 DNA is methylated in the cytoplasm of infected cells.

Since FV3 DNA synthesis in infected cells occurs in two stages, involving the nucleus and cytoplasm of infected cells (7), and since eukaryotic DNA-methylases are located in the nucleus of cells, it was interesting to see where FV3 DNA is methylated. It was determined by computing the percentage of 5-methylcytosine in the DNA from both cellular compartments in a pulse-chase experiment. The infected cells were pulsed at 3.5 hours post-infection (hpi) for 30 minutes with 6- ^{3}H -uridine to label the precursor of both forms of cytosines (8) and chased in the presence of unlabeled deoxycytosine and thymine. Soon after pulse, 83% of the cytosines were present in the nucleus of the infected cells and only 2% of these cytosines were in the form of 5-methylcytosine. Cytoplasm from these cells contained 17% of the total labeled cytosines and 18% of these were in the form of 5-methylcytosines. As the chase prolonged for 2 hours, a gradual movement of newly synthesized viral DNA was observed from the nucleus to the cytoplasm where cytosines were methylated (9). This was further confirmed by HpaII and MspI digestion of viral DNA isolated from the cytoplasm and nucleus of infected cells. Taken together these experiments convincingly proved that FV3 DNA methylation is a post-replicative event and occurs in the cytoplasm of infected cells.

FV3 DNA-methylase is virus-coded.

There are basically two lines of evidence that establish that

the enzyme methylating FV3 DNA is encoded by the virus DNA. First, we do not see any DNA-methylase activity in the cytoplasm of uninfected cells; and secondly, there are now several mutants derived from FV3 that failed to induce DNA-methylase. Willis and her coworkers (9) have monitored the kinetics of induction of FV3 DNA-methylase activity in an elaborate time-course experiment where a DNA-methylase negative mutant and a DNA synthesis inhibitor (cytosine arabinoside, AraC) was used. These experiments showed that DNA-methylase activity in the cytoplasm of infected cells increased as a consequence of time and the maximum being attained at 3 hpi and had decreased substantially at 6 hpi. A significant increase in the enzyme activity was observed in the absence of viral DNA synthesis, and DNA-methylase negative mutant failed to induce any DNA-methylase activity. These data provide evidence that the DNA-methylase activity is an early virus-coded function. Why does the host DNA-methylase during the first phase of virus DNA replication in the nucleus not methylate the viral DNA? Although no direct experimental data is available, it is a reasonable assumption that, like other macromolecular synthesis, host DNA-methylase is also inhibited. Secondly, some available data (9) suggest that the substrate specificity of host DNA-methylase is different from viral DNA-methylase. Unlike host DNA-methylase, FV3-induced DNA-methylase prefers double stranded DNA substrate. Comparative substrate specificities of FV3-induced DNA-methylase, using both naturally occurring and synthetic DNAs, have been carried out (9). These experiments have shown that almost every unmethylated DNA molecule tested was actively methylated *in vitro*, by FV3-induced DNA-methylase. Among these a synthetic DNA, poly(dC-dG).poly(dC-dG), was a far superior substrate than any of the naturally occurring DNA.

Purification of FV3-induced DNA-methylase.

Initially, a genetic approach was employed to identify the polypeptide(s) associated with DNA-methylase activity in the infected cells. Comparison of both structural and unstructural polypeptides of an FV3 DNA-methylase negative mutant (AzaC^F),

containing unmethylated genomic DNA, and wild-type FV3 revealed a nonstructural 26 kDa polypeptide in AzaC^r infected cells that demonstrated altered mobility in SDS-polyacrylamide gels. Spontaneous revertants isolated from the AzaC^r mutant regained the normal migration pattern of this polypeptide and DNA-methylase activity. The genomic DNA of revertants, unlike AzaC^r, was also methylated (10). These observations strongly suggested that the 26 kDa polypeptide is associated with DNA-methylase activity. To further evaluate the nature of this relationship, DNA-methylase from FV3-infected cell cytoplasm was purified to apparent homogeneity, as judged by SDS-polyacrylamide gel. The purification scheme involved ssDNA chromatography followed by dye-ligand chromatography and is shown in Fig. 1.

SDS-PAGE analysis of purified enzyme activity resolved three major polypeptides (30 kDa, 26 kDa and 18 kDa) which constitute 90% of the total protein loaded onto such gels. Hübscher and coworkers (11) described a relatively simple technique to identify polypeptides associated with DNA-methylase activity. Substrate DNA is mixed with the polyacrylamide gel mixture prior to polymerization, gels are loaded and run in a manner identical to that of Laemmli (12). The gel is then treated with [³H]-S-adenosylmethionine that serves as a donor of methyl groups. Following proper washing and autoradiography, the polypeptide band with DNA-methylase activity will be visible. In our case, none of the three polypeptides demonstrated any enzyme activity, indicating that perhaps unlike any other known eukaryotic DNA-methylase, FV3 DNA-methylase requires more than one polypeptide for its catalytic activity. This notion was tested by eluting the three polypeptides and testing them singly or in combination for DNA-methylase activity. None of the individual polypeptides showed any enzyme activity. However, DNA-methylase activity was reconstituted when 26 kDa and 18 kDa polypeptides were mixed. These results support the conclusion that FV3 DNA-methylase requires 2 polypeptides for catalytic activity (13). Although these results were unexpected, as almost all known eukaryotic DNA-methylases consist of a single polypeptide, they did not surprise us. FV3 in many respects proves

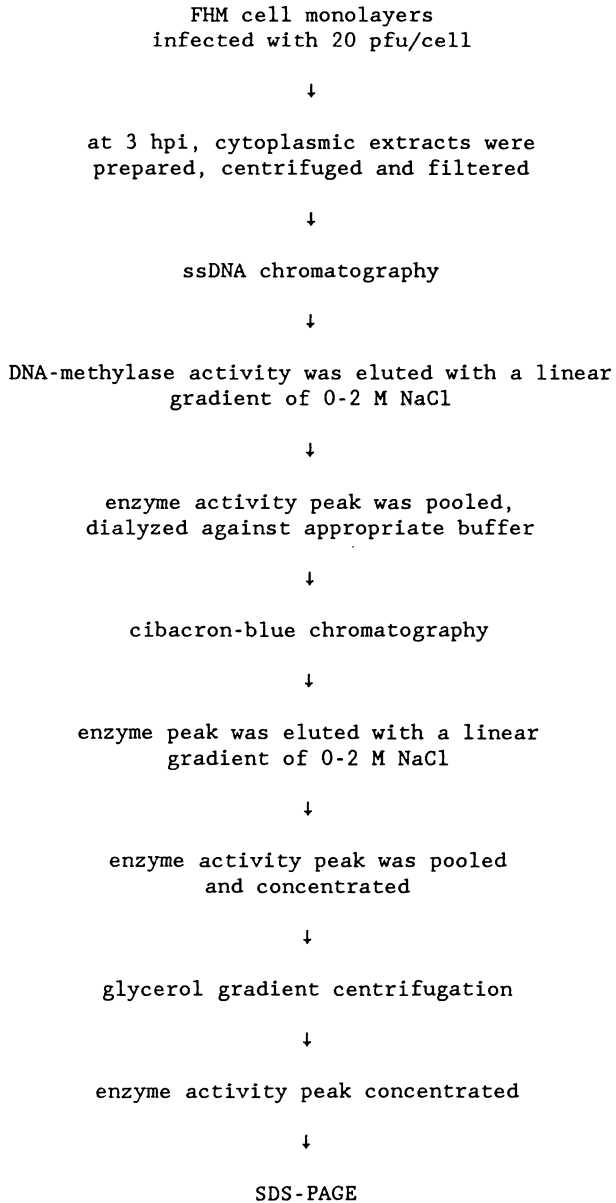


Fig. 1. Purification scheme for FV3-induced DNA-methylase.

to be an intermediate between prokaryotes and eukaryotes (14). Many bacterial restriction-modification systems consist of three polypeptides, two of which are required for DNA-methylase activity and the third serves as an endonuclease (15). It was, therefore, of great interest to see if our DNA-methylase preparation contained any endonuclease activity. Using PM2 DNA, we found that indeed such endonuclease activity was present in the FV3-induced DNA-methylase preparation. However, unlike DNA-methylase activity, we were unable to reconstitute endonuclease activity.

Functions of DNA-methylation in FV3 replication.

The function of DNA-methylase in the replication cycle of FV3 is far from being clear, although we know that it does play a role in the replication cycle. An inhibitor DNA-methylase, 5-azacytidine, can significantly reduce (100-fold or more) the production of mature virions (16). However, inhibition of DNA-methylation by 5-azacytidine does not effect RNA or protein synthesis in any detectable way. This observation led to the suggestion that in FV3 DNA methylation does not play a direct role in FV3 gene expression. This notion is supported by another piece of data from Goorha's laboratory (17) that DNA-methylase negative mutants do not show any abnormal behavior as far as sequential expression of FV3 genes is concerned. Electron microscopic examination of FV3-infected cells treated with 5-azacytidine, revealed viral particles at the periphery of assembly sites that lack DNA, suggesting that DNA methylation may help package the genomic DNA into virions (16). It has been suggested that unmethylated DNA becomes susceptible to viral endonuclease nicking and nicked DNA in case of T4 bacteriophage is not packaged (18). The obvious question arises of how DNA-methylase negative mutants survive. If their genomic DNA is not methylated, Goorha and Antol (17) have provided an answer to this question. Genetic analyses of these mutants have shown all FV3 DNA-methylase mutants lack endonuclease activity.

CONCLUSIONS

FV3 is unique among animal viruses and cells to boast such a highly degree of DNA methylation, and provides an exceptional opportunity to elucidate functional aspects of DNA methylation in animal cells. One of the most intriguing aspects of a high degree of methylation in FV3 DNA is related to transcription, particularly when FV3 uses host polymerase (19) which is refractory to transcription (1) under normal conditions. Dawn Willis has dealt with this question in one of the companion chapters in this monograph. The purpose of this chapter is to bring practical elements of newly emerging FV3 DNA-methylase enzymology together. We now have a purified enzyme to look into its characteristics without interference from other cellular or viral proteins. N termini of cyanogen bromide-generate peptides from 26 kDa and 18 kDa polypeptides have now been sequenced, and using degenerate probes we are in the process of locating the gene(s) coding for this important enzyme. The enzymology of animal DNA-methylases, in general, is in its infancy. Although there are some scattered reports concerning purification of DNA-methylases from animal cells and tissues, only in one instance the cloning and sequencing of a DNA-methylase from mouse cells (20) has been achieved. I hope in coming years FV3 will continue to provide new and exciting information.

ACKNOWLEDGEMENTS

This work was supported by research grants CA 07055 and GM 23638 and Cancer Center Support (CORE) grant CA 21765 from National Institutes of Health, and by the American Lebanese Syrian Associated Charities.

REFERENCES

1. Cedar, H. *Cell* 53:3-4, 1988.
2. Gilbert, W. *In*: *Biochemistry and Biology of DNA Methylation* (Eds. Cantoni, G.L. and Razin, A.), Alan R. Liss, Inc., New York, 1985, pp. 313-315.
3. Willis, D.B. and Granoff, A. *Virology* 107:250-257, 1980.

4. Roberts, R.J., Myers, P.A., Morrison, A. and Murray, K. J. Mol. Biol. 102:157-165, 1976.
5. Waalwijk, C. and Flavell, R.A. Nucl. Acids Res. 5:3231-3236, 1978.
6. Vanyushin, B.F., Mazin, A.L., Vasilyev, V.K. and Belozensky, A.N. Biochem. Biophys. Acta 299:397-403, 1973.
7. Goorha, R. J. Virol. 43:519-528, 1982.
8. Bird, A.P., Taggart, M.H. and Smith, B. Cell 17:889-901, 1979.
9. Willis, D.B., Goorha, R. and Granoff, A. J. Virol. 49:86-91, 1984.
10. Essani, K., Goorha, R. and Granoff, A. Virology 161:211-217, 1987.
11. Hübscher, U., Pedrali-Noy, G., Knust-Kron, B., Doerfler, W. and Spadari, S. Anal. Biochem. 150:442-448, 1985.
12. Laemli, U.K. Nature (London) 227:680-685, 1970.
13. Essani, K., Goorha, R. and Granoff, A. Gene (in press).
14. Granoff, A. In: Progress in Medical Virology (Eds. Melnick, J.L. and Hummeler, K.), Vol. 30, S. Karger, Basel, Switzerland, 1984, pp. 187-198.
15. Bickle, T. In: Nucleases (Eds. Linn, S.M. and Roberts, R.J.), Cold Spring Harbor Laboratory, New York, 1982, pp. 85-108.
16. Goorha, R., Granoff, A., Willis, D.B. and Murti, K.G. Virology 138:94-102, 1984.
17. Goorha, R. and Antol, K. Virology (in press).
18. Zachary, A. and Black, L.W. J. Mol. Biol. 149:641-658, 1981.
19. Goorha, R. J. Virol. 37:496-499, 1981.
20. Bestor, T., Laudano, A., Mattaliano, R. and Ingram, V. J. Mol. Biol. 203:971-983, 1988.

8

TRANSCRIPTION OF FROG VIRUS 3

DAWN B. WILLIS¹, JAMES P. THOMPSON² AND WILLIAM BECKMAN³

Department of Virology and Molecular Biology, St. Jude Children's Research Hospital, Memphis, Tennessee 38101, USA

ABSTRACT

Frog virus 3 (FV3) genes are expressed in infected cells in an orderly stepwise fashion that resembles the pattern of temporal gene activation that occurs during cellular development. To carry out this sequential and quantitative regulation of transcription, FV3 produces a cascade of trans-acting regulatory proteins that (i) cause a switch-off of host cell transcription; (ii) cooperate with host cell RNA polymerase II to initiate transcription from specific viral sequences; and (iii) enable the host polymerase to transcribe highly methylated promoters that are normally refractory to transcription.

INTRODUCTION

Gene expression in cells infected with frog virus 3 is sequentially ordered and coordinately regulated to produce at least three different classes of mRNA in a multi-tiered temporal cascade (1). Immediately after infection, host cell DNA, RNA, and protein synthesis are switched-off by a heat-stable virion protein, but there is no inhibition of viral macromolecular synthesis in cells subsequently infected with active virus (2). The ability to incorporate radioactive isotopes into virus-specific macromolecules without any background incorporation into cellular compounds has

¹ Present address: American Cancer Society, Atlanta, GA, USA

² Present address: University of Tennessee, Memphis, TN, USA

³ Present address: University of Delaware, Newark, DE, USA

proved very useful by allowing us to distinguish up to 47 bands of FV3 specific mRNAs on denaturing acrylamide and agarose gels (1). In contrast to all other animal DNA viruses, the majority of FV3 mRNAs do not contain variable length poly(A) tails (3), the absence of which also contributed to the high degree of resolution of viral mRNAs seen on such gels.

Although FV3, and indeed all iridoviruses, were originally thought to be cytoplasmic DNA viruses closely related to the poxvirus family (4), no one was ever able to show convincingly that the virions possessed any DNA-dependent RNA polymerase activity (reviewed in 5). On the other hand, naked FV3 DNA was not infectious (6) as was the DNA from the strictly nuclear viruses that uses the host polymerase. In addition, purified FV3 DNA could be non-genetically reactivated by UV-, but not heat-inactivated virus, a phenomenon that implied the direct participation of a virion-associated protein in the transcription process (6).

Then Goorha (7) described a two-stage process in the replication of FV3 DNA, with the synthesis of unit-length genomes in the nucleus followed by the transport of the newly-synthesized DNA into the cytoplasm, where concatemer formation and packaging into virions took place. At about the same time, Goorha (8) also showed that a functional host RNA polymerase II was required for immediate-early FV3 transcription. It thus became clear that both the host RNA polymerase II and a virion-associated protein were required to initiate FV3 immediate-early (IE) transcription. In addition, other viral proteins, induced after infection, were necessary for the progression from IE transcription to the delayed-early (DE) stage, and from there to the late stage of transcription (9).

Another interesting problem in the control mechanisms of FV3 transcription came to light with the demonstration that the viral genomic DNA was methylated at every cytosine residue in the dinucleotide sequence dCp dG (10). The conventional dogma stated that transcription by eukaryotic RNA polymerase II was inversely proportional to the degree of methylation of critical regions of the promoter (11). If FV3 used the host RNA polymerase II for

transcription, either the immediate-early promoters were unmethylated, or the virus had evolved some mechanism for overriding the normal inhibitory effect of DNA methylation on transcription by RNA polymerase II.

Thus, not only does FV3 display a temporal regulation of transcription that depends on specific promoter sequences and trans-acting viral proteins, it has also evolved a mechanism involving another trans-acting protein that allows the host RNA polymerase II to transcribe RNA from highly methylated DNA templates (1986).

TEMPORAL REGULATION OF FV3 TRANSCRIPTION

Based on the time of synthesis after infection, FV3 mRNAs can be subdivided into 3 classes: immediate-early (IE), delayed-early (DE), and late (1). The IE class of FV3 mRNA consists of those RNA species synthesized in the presence of protein synthesis inhibitors such as cycloheximide, and represents at least one-third of the transcribable genome (13). The same IE mRNAs are seen in cells infected at the non-permissive temperature of 37° C (14), implying that a temperature-sensitive virus-induced protein is required for the progression from IE to DE mRNA synthesis.

Transcriptional mapping has confirmed that the various classes of FV3 mRNAs, as well as mRNAs within classes, are transcribed from separate promoters. For example, the message for the major capsid protein (a late gene) lies snugly nestled between two IE genes (15). More recently, data from the laboratories of Aubertin (16) and Goorha (personal communication), who have probed Northern blots of RNA from FV3-infected cells with cloned radioactive viral restriction fragments, support the idea that a more extensive region of the viral genome is transcribed in the presence of cycloheximide than previously determined by hybridization techniques (13). Also, there is a complex pattern of transcription that may involve overlapping genes (16). To date, however, there is no evidence of splicing from larger primary transcripts.

Sequencing of three FV3 IE genes has revealed a consensus between two of the promoters, but not a third (17; A. M. Aubertin

personal communication). However, part of the IE homology may reside in secondary structure that is not readily apparent from the primary nucleotide sequence.

Immediate-early gene ICR 169. The first FV3 gene to be cloned and sequenced was the gene encoding a prominent immediate-early protein of molecular weight 18 kD (18). This gene was given the name ICR 169 because it was transcribed into an Infected Cell RNA of 169 kD. It was selected for study because, although it was synthesized at maximum rate throughout infection, it was subject to a very precise post-transcriptional control (2). The function of this gene remains unknown, but one can assume that it is a very important protein since its mRNA is made in such huge quantities, and the synthesis of its protein product is so tightly regulated.

By S1 mapping techniques, we demonstrated that the start site of transcription of ICR 169 was positioned 29 nucleotides 3' of an AT-rich region, TATTTTA (18). An open reading frame of 471 nucleotides, coding for a protein of approximately 18 kD, mapped 18 nucleotides downstream of the transcriptional start site. When the clone containing the entire coding region (but no transcriptional control signals) of the 18 kD protein was ligated into the bacterial transcription vector SP6, the transcript made under the direction of the bacterial SP6 RNA polymerase could be translated in vitro in a reticulocyte lysate to produce a protein that corresponded in molecular weight to the authentic FV3 18 kD protein (unpublished results.)

If 78 bp of the promoter for ICR 169 (containing no coding sequences) was placed immediately 5' to the gene coding for the bacterial enzyme chloramphenicol acetyltransferase (CAT), and the chimeric plasmid (p169P-CAT) was transfected into fathead minnow (FHM) cells, CAT synthesis did not take place unless the transfected cells were subsequently infected with FV3 (19). As shown in Fig. 1, the kinetics of CAT synthesis after FV3 infection were identical to those of the authentic IE gene product, appearing at 2 h and peaking at 4 h post-infection (hpi). Other experiments verified that both a virion-associated trans-acting protein and

host RNA polymerase II were required for CAT mRNA synthesis from the ICR 169 promoter (19).

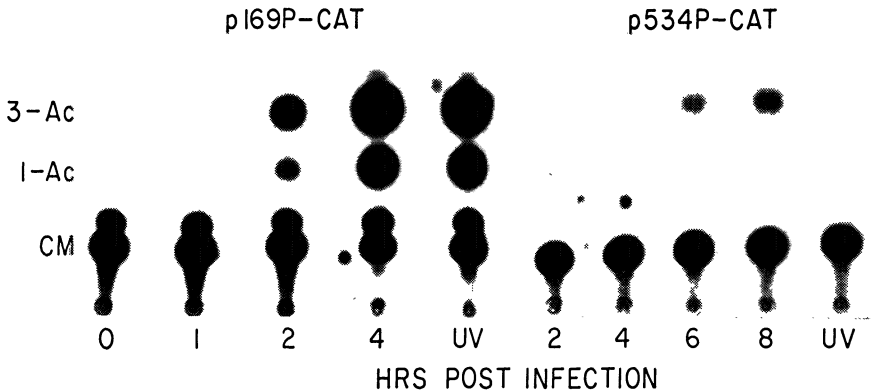


Fig. 1. Kinetics of induction of CAT activity under the direction of immediate-early (p169P-CAT) or late (p534P-CAT) FV3 promoters. FHM cells were transfected with 10 ug/90 mm dish plasmid DNA by CaPO_4 co-precipitation (Willis and Granoff, 1985). After 24 h at 30°C , the cells were infected with active or UV-inactivated FV3 at the same temperature, and samples were taken for the assay of CAT enzyme (Gorman et al., 1982) at the indicated times after infection. The sample treated with UV-inactivated FV3 was assayed at 4 hpi (p169P-CAT) or 8 hpi (p534P-CAT). CM = unacetylated chloramphenicol. 1-Ac and 3-Ac = acetylated chloramphenicol.

The specific sequences within the promoter that respond to the FV3 trans-acting protein have now been identified (20, 21). Deletion of the TATTTTA box did not abolish the induction of transcription by FV3, although CAT synthesis was reduced to 15% of what was seen with the wild-type promoter. The major effect (determined by S1 nuclease mapping) was a repositioning of the start site of transcription to a cryptic promoter within the CAT coding region (20). The amount of RNA actually synthesized was not reduced; therefore, the decreased activity of the CAT enzyme probably reflected a lessened activity of the shortened CAT protein.

Further mutations have shown that the critical region for FV3 induction of CAT activity lies within the 14-base sequence (CAGGGGAATTGAAA) immediately preceding the TATA box (21). When this area was deleted or altered by point mutation, both CAT enzyme and CAT mRNA syntheses declined drastically. Sequencing of two additional IE genes has shown that this same sequence is present in two of them (22), but not another (ICR 489, see below).

Another interesting comparison can be made between the nucleotide sequence of the 169 promoter and the sequence of some well-known viral and cellular enhancers. The GGGGAAT motif is present in SV40, HIV, IgG kappa chain and MHC class I enhancers (23); all of these promoters are known to bind to a specific nuclear protein. When a binding of nuclear proteins from uninfected HeLa cells to radioactively labeled oligonucleotides corresponding to the 169P or MHC-1 promoters was carried out, we observed that the 169P sequence competed with the MHC-1 sequence for binding to a 82 kD protein. A point mutant of the 169 promoter (GGTGAAT), however, did not compete for binding. Since there was no discernible difference between the binding observed in extracts from either control or FV3-infected cells, and no binding to the cis-responsive sequence by LiCL-Nonidet P40 extracted virion proteins, the role of the virion trans-acting protein still remains obscure. There are precedents with herpesvirus (24) and adenovirus (25) that viral gene products can increase the activity of the cellular transcription factors, so perhaps the FV3 factor acts in an analogous manner.

Immediate-early gene ICR 489. The gene coding for ICR 489 first attracted our interest because it was produced in such abundance in infected cells treated with cycloheximide (13). This increased synthesis in the absence of viral protein synthesis implied that, during a normal infection, the gene encoding ICR 489 was negatively regulated by an early viral protein. Transcriptional mapping of this gene (16) placed it immediately downstream from the gene for the major capsid protein, which is not synthesized early in infection. Although ICR 489 is an immediate-early mRNA, the sequence of its promoter bears no resemblance to

that of ICR 169 (17), but instead contains a region that is remarkably like the eukaryotic CG box that binds the cellular transcription factor Spl (26), and a CCAAT box, also shown to bind a cellular transcription factor (27).

When 486 bp of the ICR 489 promoter was placed 5' of the CAT gene and the resulting plasmid was transfected into FHM cells, we observed CAT synthesis only when the cells were subsequently infected with FV3 (17). As expected from an immediate-early promoter, CAT enzyme appeared within two hr after infection and was also produced when the cells were treated with UV-inactivated virus. In contrast to what was observed with the synthesis of authentic ICR 489, the amount of 489PCAT mRNA produced was not substantially increased in infected cells in which protein synthesis had been inhibited, or in cells treated with UV-inactivated virus. Removal of the GC and CCAAT boxes by controlled exonuclease digestion eliminated the response of the ICR 489 promoter to the virion trans-acting factor (unpublished results), suggesting that, as with ICR 169, the virion factor increases the activity of an established--but different--cellular transcription factor. It remains to be shown whether or not the virion trans-acting factor(s) consists of one or several proteins.

Aubertin (22) has made the interesting observation that, late in FV3 infection, a number of small RNA molecules are synthesized that are complementary to the 5' sequence of the ICR 489 mRNA; she suggests that this "anti-sense" RNA may act as a barrier to synthesis in the sense direction. Another possibility is that the synthesis of mRNA coding for the major capsid protein (ICR 534, see below), which takes place from the same strand as ICR 489 and terminates within the ICR 489 promoter, prevents the initiation of ICR 489 synthesis. Much work remains to be done on this highly interesting gene; what is clear is that the hypothesis that all immediate-early genes contain identical cis-responsive sequences for a single virion trans-acting protein, while intellectually appealing, is not correct.

Delayed-early FV3 mRNA. As discussed earlier, when viral protein synthesis is blocked, a specific subset of viral mRNAs (the

immediate-early) is produced in response to a virion trans-acting protein. If, in place of a protein synthesis inhibitor, the amino acid analog fluorophenylalanine (FPA) is added, another subset of early viral messages (the delayed-early, or DE) is synthesized, but neither viral DNA synthesis nor late viral mRNA synthesis takes place. We believe this reflects the fact that one of the immediate-early proteins is a trans-acting factor for turning on DE mRNA, and that this protein does not contain phenylalanine in a critical position.

Although many of the interesting viral functions (particularly those dealing with DNA synthesis and methylation) are probably delayed-early proteins, none of this group has been mapped and sequenced to date. However, two putative genes--those coding for DNA polymerase and thymidine kinase--have been localized via DNA sequence homology with similar enzymes to specific FV3 restriction fragments (Goorha and Willis, unpublished observations), and information concerning the regulatory sequences in the promoters of these genes should soon be forthcoming.

Late FV3 gene ICR 534. As with other DNA viruses, late viral mRNA synthesis in FV3-infected cells does not usually occur until after DNA replication (1). However, late FV3 proteins can be synthesized in the absence of DNA replication (9), and temperature-sensitive mutants have been isolated that synthesize DNA, but no late viral mRNA (28). Therefore, a specific delayed-early FV3 protein appears to be required for initiating late mRNA synthesis independently of DNA replication. The gene coding for the 55 kD major late capsid protein, ICR 534, has been mapped and a preliminary sequence determined (15). This gene lies between two immediate-early genes, the downstream one being ICR 489; in fact, the terminus of ICR 534 transcripts lies within the promoter for ICR 489. This location in itself guarantees that ICR 534 is not part of a late gene "cluster," and therefore its cis-responsive sequences must contain the areas of regulation by the FV3-induced trans-acting protein.

We have narrowed the cis-responsive region to a 95 bp sequence immediately 5' to the transcriptional start site; when this 95 bp

sequence was placed in proper orientation 5' to the CAT coding sequence (p534P-CAT) and transfected into FHM cells, we observed CAT activity in response to FV3 infection (Fig. 1). The kinetics of CAT synthesis directed by the 534 late promoter was clearly different from that of CAT under the control of the IE 169 promoter (Fig. 1). No CAT activity was detected until 4 hpi, and the peak did not occur until 8 hpi. In addition, no CAT was made when the transfected cells were treated with UV-inactivated FV3 (Fig. 1), and no CAT mRNA was synthesized in the presence of cycloheximide (results not shown). The ICR 534 late promoter contains an identical TATTTTA sequence to that found in the immediate-early ICR 169 promoter, but the 5' region is completely different (A. Aubertin, personal communication). Therefore, the sequences that give ICR 534 its "late" phenotype reside in the 64 bases of the 5' region immediately preceding the TATTTTA site. Further studies, e.g., 'site-directed mutagenesis,' will be required to pinpoint the precise late cis-responsive sequences and identify the virus-induced DE trans-acting protein that interacts with them. Also, the regulatory regions of other late FV3 genes need to be sequenced in order to determine what, if any, features they have in common.

ROLE OF DNA METHYLATION IN FV3 TRANSCRIPTION

Several years ago, our laboratories reported that the genome of FV3 was highly methylated--every cytosine in the dinucleotide sequence dCpdG appears to exist as 5-methyl cytosine (10). This methylation is carried out post-replicatively in the cytoplasm by a virus-induced DNA methyltransferase--the first reported DNA methyltransferase to be coded for by a eucaryotic virus (29). Since Goorha (8) had shown that FV3 IE mRNA was synthesized in the nucleus by the host RNA polymerase II, and several investigators had reported on the inability of RNA polymerase II to function on a methylated DNA template (11), the question immediately presented itself of how the host enzyme was able to transcribe the highly methylated FV3 genome.

Induction of a trans-acting factor for the transcription of methylated DNA. To determine if FV3 induced a trans-acting factor

that facilitated the transcription of methylated DNA, we made use of the plasmid pAd12-ElACAT, constructed by Kruzcek and Doerfler (30). These authors had placed the adenovirus 12 ElA promoter 5' to the CAT coding sequence, and shown that methylation in vitro of the plasmid with the bacterial methylases HpaII and HhaI rendered it resistant to transcription after transfection into HeLa cells. We repeated this experiment, and in addition, we infected cells transfected with the methylated pAd12-ElACAT with FV3 24 hr after transfection. We observed CAT activity within four hpi (Fig. 2).

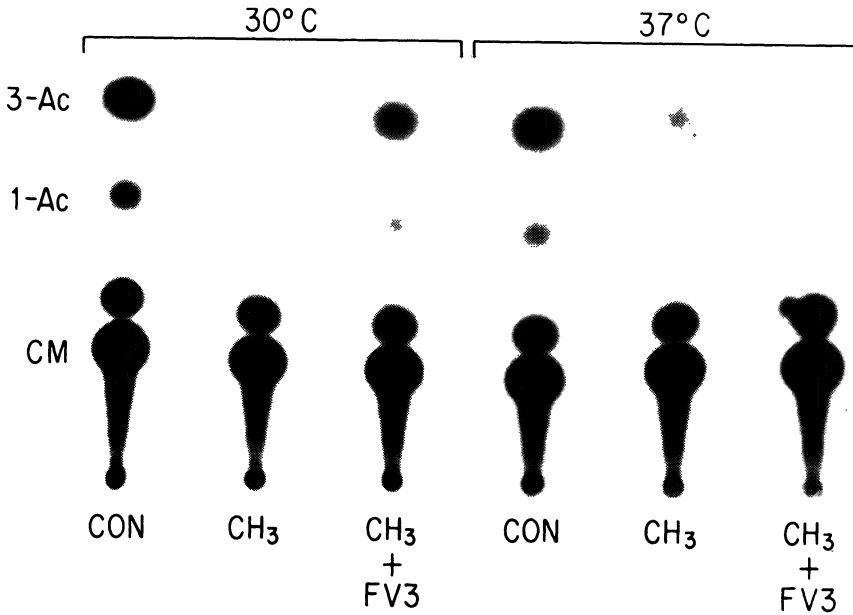


Fig. 2. Infection with FV3 induces a factor that overcomes the inhibition of DNA methylation on transcription. HeLa cells were transfected as described in the legend to Fig. 1 with unmethylated pAd12-ElACAT (CON) or methylated pAd12ElACAT (CH₃) and duplicate samples were incubated for 24 h at 37° C. One dish from each set was infected with FV3 and incubated at either 30° C or 37° C for 4 h before the assay of CAT activity (Gorman et al., 1982).

This override of the customary inhibition of transcription by methylation was observed only at 30° C, the optimum temperature for the virus, and not at 37° C, the optimum temperature for the HeLa cells. No CAT mRNA was synthesized in the absence of protein

synthesis, or in cells treated with UV-inactivated FV3 (12), suggesting that, unlike the trans-acting factor that is required to initiate ICR 169 and ICR 489 transcription, the factor for transcribing methylated DNA is virus-induced.

Having a virus-induced, rather than a virion-associated, factor for transcribing methylated DNA led to another puzzle--how were the FV3 immediate-early genes transcribed? Were they unmethylated, or was the methylation in an area that was not critical for transcription? For ICR 169 at least, the explanation appears to be the latter one.

The problem was approached in two ways. First, the promoter of ICR 169 was sequenced for methyl cytosine via genomic sequencing (31). The results were positive for the two dCpdG dinucleotides that lay between the TATTTA region and the start site of transcription; the most distal dCpdG could not be identified by this technique as it was too close to the restriction site at which sequencing began (32).

However, by site-directed mutagenesis, we were able to convert each of the CG doublets into either a CCGG site, which could be methylated with HpaII, or a CGCG site, which could be methylated with HhaI (32). As with the wild-type promoter, the mutated plasmid was transcribed only when the transfected cells were subsequently infected with live or UV-inactivated virus, showing that the mutations did not alter the ability of the virion-associated transcriptional activator to promote transcription from the ICR 169 promoter. Methylation of the mutated promoters with the bacterial methylases before transfection did not affect the ability of these genes to be transcribed by UV-inactivated FV3 or by active FV3 in the absence of protein synthesis (32). Therefore, the dCpdG sequences are not in critical positions in the ICR 169 promoter, and thus there is no need for the virus-induced trans-acting protein that assists in the transcription of methylated DNA. The response of the promoter to the virion-associated trans-acting factor for immediate-early transcription, although sequence-specific (20) is independent of its methylation status.

One further point should be emphasized. A DNA methyltransferase-deficient mutant of FV3, which does not possess methylated DNA, undergoes a normal temporal transcriptional program (33), although the growth cycle of the mutant is prolonged several-fold, and the final yield is less than that obtained with the parent virus. It thus seems unlikely that the role of the FV3 factor that facilitates transcription from methylated promoters is to enable the virus to switch from one class of mRNA synthesis to another. Instead, this factor seems to facilitate transcription from methylated templates either by direct interaction with the DNA or by altering the host RNA polymerase II so that it is no longer inhibited by methylation of the template.

CONCLUSIONS

Transcriptional regulation of eukaryotic promoters is now thought to be mediated by the interaction of specific trans-acting factors with cis-responsive DNA sequences and RNA polymerase II (34). Several large DNA viruses--adenovirus (35, 25); herpesvirus (24), and SV40 (26)--have been shown to possess promoters or enhancers that bind cellular transcription factors as well as viral gene products. FV3, which has both a sequence-specific regulatory cascade and an ability to override the inhibitory effect of DNA methylation on transcription, offers an exceptional opportunity to examine eukaryotic transcriptional regulatory mechanisms from a novel point of view.

ACKNOWLEDGEMENTS

This work was supported by research grant CA 07055 and Cancer Center Support (CORE) grant CA 21765 from the National Cancer Institute and by the American Lebanese Syrian Associated Charities (ALSAC).

REFERENCES

1. Willis, D.B., Goorha, R., Miles, M.F. and Granoff, A. J. Virol. 24:326-342, 1977.
2. Goorha, R. and Granoff, A. Virology 60:237-250, 1974.

3. Willis, D. and Granoff, A. *Virology* 73:543-547, 1976.
4. Granoff, A., Came, P.E. and Breeze, D.C. *Virology* 29:133-148, 1966.
5. Willis, D.B., Goorha, R. and Chinchar, V.G. In: *Current Topics in Microbiology and Immunology* (Ed. D. B. Willis), Springer-Verlag, Heidelberg, 1985, pp. 77-103.
6. Willis, D.B., Goorha, R. and Granoff, A. *Virology* 98:476-479, 1979b.
7. Goorha, R. *J. Virol.* 43:519-528, 1982.
8. Goorha, R. *J. Virol.* 37:496-499, 1981.
9. Goorha, R., Willis, D.B. and Granoff, A. *J. Virol.* 32:442-448, 1979.
10. Willis, D. and Granoff, A. *Virology* 107:250-257, 1980.
11. Razin, A. and Riggs, A.D. *Science* 210:604-610, 1980.
12. Thompson, J.P., Granoff, A. and Willis, D.B. *Proc. Natl. Acad. Sci. USA* 83:7688-7692, 1986.
13. Willis, D. and Granoff, A. *Virology* 86:443-453, 1978.
14. Lopez, C., Aubertin, A.M., Tondre, L. and Kirn, A. *Virology* 152:365-374, 1986.
15. Tham, T.N., Mesnard, J.M., Tondre, L. and Aubertin, A.M. *J. Gen. Virol.* 67:301-308, 1986.
16. Mesnard, J.M., Tham, T.N., Tondre, L., Aubertin, A.M. and Kirn, A. *Virology* 165:122-133, 1988.
17. Beckman, W., Tham, T.N., Aubertin, A.M. and Willis, D.B. *J. Virol.* 62:1271-1277, 1988.
18. Willis, D.B., Foglesong, D. and Granoff, A. *J. Virol.* 53:905-912, 1984b.
19. Willis, D. and Granoff, A. *J. Virol.* 56:495-501, 1985.
20. Willis, D.B. *Virology* 161:1-7, 1987.
21. Willis, D.B. Abstracts of 7th Poxvirus-Iridovirus Workshop, Heidelberg, 1988.
22. Aubertin, A.M. Abstracts of 7th Poxvirus-Iridovirus Workshop, Heidelberg, 1988.
23. Baldwin, A.S. and Sharp, P.A. *Proc. Natl. Acad. Sci. USA* 85:723-727, 1986.
24. Kristie, T.M. and Roizman, B. *Proc. Natl. Acad. Sci. USA* 84:71-75, 1987.
25. Kovesdi, I., Reichel, R. and Nevins, J.R. *Cell* 45:219-228, 1986.
26. Dynan and Tjian, *Cell* 35:79-87, 1983.
27. Raymondjean, M., Cereghini, S. and Yaniv, M. *Proc. Natl. Acad. Sci. USA* 85:757-761, 1988.
28. Willis, D.B., Goorha, R. and Granoff, A. *Virology* 98:328-335, 1979.
29. Willis, D.B., Goorha, R. and Granoff, A. *J. Virol.* 49:68-91, 1984.
30. Kruczek, I. and Doerfler, W. *Proc. Natl. Acad. Sci. USA* 80:7586-7590, 1983.
31. Church, G.M. and Gilbert, W. *Proc. Natl. Acad. Sci. USA* 81:1991-1995, 1984.
32. Thompson, J.P., Granoff, A. and Willis, D.B. *J. Virol.* 62:4680-4685, 1988.
33. Goorha, R. and Antol, K. *Virology* (in press)

34. Kingston, R.E., Baldwin, A.S. and Sharp, P.A. Cell 41:3-5, 1985.
35. Carthew, R.W., Chodosh, L.A. and Sharp, P.A. Cell 43:439-448, 1985.

9

REGULATION OF PROTEIN SYNTHESIS IN FROG VIRUS 3-INFECTED CELLS

A.M. AUBERTIN, T.N. THAM and L. TONDRE

Groupe de Recherches de L'INSERM U74 et Laboratoire de Virologie de la Faculté de Médecine de l'Université Louis Pasteur, 3 rue Koeberlé, 67000 STRASBOURG, France.

ABSTRACT

One of the first consequences of frog virus 3 (FV3) interaction with the host cell is a marked inhibition of cellular protein synthesis. One or several proteins present in the virus particles are responsible for the observed inhibition, which results in the initiation step of cellular message translation being impaired. Viral proteins are sequentially synthesized and coordinately regulated. They are classified into three major groups on the basis of their temporal synthesis. The first group comprising mRNAs is translated in the presence of residual host protein synthesis. Production of the second group of viral proteins is accompanied by a complete shut off of cellular translation. The last group of proteins is synthesized as a result of selective translation of late gene transcripts since several transcription products of immediate early or early genes, although present, are not translated late in infection. Two observations may be related to the translational discrimination between the transcripts of early and late genes. Virus-induced or modified factors are produced and are required for efficient translation of late viral mRNA. The 5' leader of some late transcripts of immediate early genes shows additional sequences when compared to the corresponding immediate early transcripts, suggesting that these sequences could impair translation. Thus both

transcriptional and translational regulation are combined to control FV3 gene expression.

INTRODUCTION

Many viral infections alter the host cell and shut off synthesis of cellular macromolecules. Although it is an attractive idea that modification of host cell metabolism is important for a productive infection in order to facilitate the expression of the viral genome, it certainly cannot be proposed as a general rule. Inhibition of translation of cellular mRNAs after viral infection is, in many cases, a highly discriminatory event. However despite extensive knowledge of the molecular biology of viral replication, little is known of the mechanisms underlying the translational selectivity, except in the case of picornaviruses (1).

Frog virus 3 (FV3) that belongs to the family Iridoviridae and was isolated by Granoff et al (2), has been shown to be very toxic for cells in culture (3) and for animals (4). The virus rapidly inhibits host DNA, RNA and protein syntheses (5-8). The aim of this chapter is to summarize our current understanding of FV3 interaction with host cells, focusing on the aspects of translational regulation.

EFFECTS OF FV3 ON HOST CELL PROTEIN SYNTHESIS

Conditions for expression of the inhibitory activity

Infection of eukaryotic cells with FV3 is accompanied by a dramatic inhibition of cellular protein synthesis which is dependent on the multiplicity of infection. It has been observed even in the case of a non-productive infection, for example in infected cells incubated at supraoptimal temperatures for virus multiplication or in cells infected with virus particles inactivated either by heat or by gamma or ultraviolet irradiation (8, 10-13). Thus host protein synthesis is greatly diminished in the absence of virus gene expression, sug-

gesting that a structural component of the virion is responsible for this shut off.

Role of structural proteins

Virus particles can be dissociated by combined treatment with nonionic detergent and high salt concentration. Several viral proteins remain in solution after elimination of the detergent and salt, this is shown by comparison of the polypeptide composition of the solution to that of the virus suspension (Fig. 1A). Mammalian cells treated with the soluble viral proteins (SVP) display reduced syntheses of both nucleic acids and proteins (13-15).

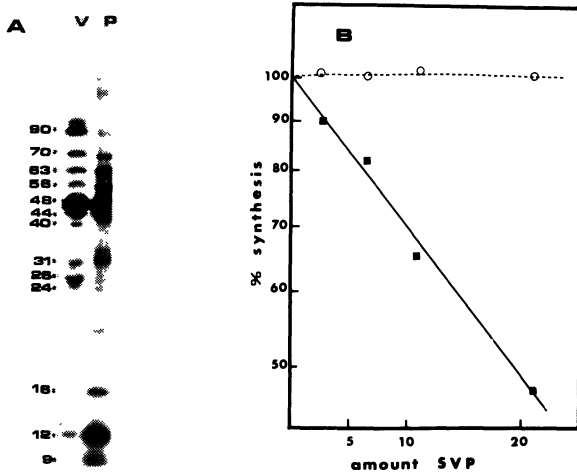


Fig. 1. A) Polypeptide composition of FV3 virus particles (V) and solubilized viral proteins (P). Fluorogram of ^{35}S -methionine-labeled polypeptides analyzed by SDS-12% polyacrylamide gel electrophoresis. Polypeptides are indentified by their molecular weights ($\times 10^{-3}$). B) Inhibition of protein synthesis in CHO cells as a function of the amount of soluble viral proteins added (SVP, expressed in μg incubated with 5×10^4 cells), native SVP ■, heat inactivated SVP (1 hr, 80°C)○.

The extent of inhibition is a function of the amount of SVP added to the cell culture as illustrated for protein synthesis in Fig. 1B. The inhibitory activity can be neutralized by antibodies directed against the virion structural proteins (13) but not by monospecific antibodies against the major capsid protein of 48 kD or the polypeptide of 44 kD (unpublished data). This demonstrates unambiguously that structural proteins of the virions play a major role in the establishment of inhibition.

Mechanisms of the shut off.

Attempts have been made to determine the mechanism by which this inhibition takes place. As concomitant inhibition of RNA synthesis occurs, the first point was to rule out that inhibition of protein synthesis was a consequence of a diminution of the RNA pool. Experiments have shown that incubation of cells in the presence of actinomycin D which completely blocks transcription, reduced protein synthesis but infection of actinomycin D-treated cells with FV3 enhanced the inhibition (8). Furthermore, degradation of preexisting cellular mRNA, checked by velocity sedimentation in sucrose gradients, was not detected (11, 12) and host mRNA could still be translated in vitro (12). This shows that there is no extensive deterioration of host mRNA and it indicates that the virus may exert an independent effect on translation.

Several works reported the rapid disaggregation of polysomes following FV3 infection (8, 11, 12). One of them also demonstrated that protein chain elongation was unaffected (12). These data led to the conclusion that inhibition of host cell protein synthesis by FV3 is the result of a selective effect on a step essential for the initiation of translation. That FV3 is capable of specific inhibition is further sustained as it selectively inhibits equine herpes virus type 1 translation in a temporal class-dependent manner (16).

It is known that initiation of translation is influenced by the intracellular concentrations of monovalent ions, particularly sodium ions. An optimal translation of host messages in FV3-infected cells could not be restored by varying the sodium concentration in the culture medium, although a modification of the sodium influx after infection could be demonstrated (unpublished data).

To gain further information, a cell-free protein-synthesizing system was established from mammalian cells in which the endogenous mRNAs are translated. Protein synthesis was very low in translation systems prepared from CHO cells infected at 37°C with heat-inactivated FV3 or treated with the soluble viral proteins. The inhibition could not be reversed by modifying the ionic concentration in the lysate. Analysis of subfractions of the lysate showed that the ribosomal fraction activity was impaired by infection (13). An analogous observation has been made for the ribosomal fraction prepared from livers of mice inoculated with FV3 (17).

Furthermore, addition of soluble viral proteins to an active in vitro translation system inhibited protein synthesis. This suggests that direct interaction of a viral protein with an element of the translation machinery may be responsible for the effect (13).

SEQUENTIAL SYNTHESIS OF VIRAL PROTEINS

Kinetics

The viral genome is expressed in a cascade manner. The precise kinetics of viral protein synthesis varies, depending on the multiplicity of infection, the incubation temperature and the cell line. In fathead minnow (FHM) cells infected with an input multiplicity of 50 plaqueforming units per cell, most of the viral polypeptide species were already detected after an hour of infection (10, 18, 19). In these experiments, to facilitate the detection of viral polypeptides at an early time, cells were pretreated with heat-inactivated FV3 to

inhibit host mRNA translation. The 35 polypeptides identified by SDS-polyacrylamide gel electrophoresis were classified in three groups according to the time during the growth cycle at which their maximal rate of synthesis occurred (18).

In mammalian cells, baby hamster kidney cells (BHK) or Chinese hamster ovary cells (CHO), classification of polypeptides was based on the time of appearance as a sequential induction was clearly observed after infection with the virus alone (20, 21). In CHO cells incubated at 29°C, immediate early polypeptides were detectable as soon as 30 min after infection, followed after 1 hr by delayed early proteins and the late species after 3-4 hr (Fig. 2). Once early proteins are produced, there is a complete shut off of host translation which is not observed at higher temperatures (35^o-37^oC).

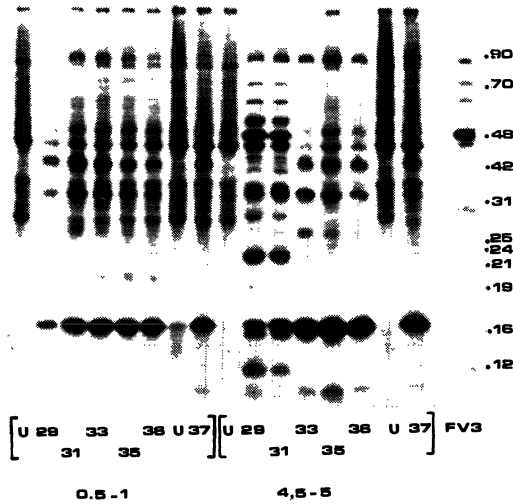


Fig. 2: Fluorogram of FV3-infected CHO cell polypeptides synthesized at different temperatures as indicated in brackets. Infected cells were collected at 1 or 5 hr postinfection at the end of a 30 min labeling period with ³⁵S-methionine as noted on the last line. Identical amounts of radioactive polypeptides were loaded on a SDS-12% polyacrylamide gel and subjected to electrophoresis.

In BHK cells as many as 90 infected cell-specific polypeptides were visualized by two-dimensional gel electrophoresis (22). However it is not known whether they are all the products of distinct genes or for some of them are proteins at different stages of post-translational modification. Several polypeptides were shown to be phosphorylated (22, 23) and depending on the degree of phosphorylation, their electrophoretic mobilities may vary.

Limited expression of the viral genome

Role of viral proteins. In infected cells incubated at supraoptimal temperatures for virus multiplication (above 32 C) the expression of the viral genome is restricted (Fig. 2). Depending on the temperature, early or only immediate early polypeptides are synthesized (20, 21).

The replacement of some amino acids, arginine or phenylalanine, by their analogs, canavanine or fluoro-phenylalanine, in the culture medium also limits the number of viral polypeptides synthesized (18, 20, 21, 24). This indicates that some of these early proteins must be functional to allow the expression of late genes. The transition from delayed early phase to late phase most likely involves more than one protein as the presence of different analogs generates different polypeptide profiles (Fig. 3).

The restricted expression of the FV3 genome early in infection is mainly caused by transcriptional regulation. It has been shown that the transcription of immediate early genes takes place in the absence of protein synthesis (25) but functional immediate early proteins are necessary for the transcription of the second group of genes (20, 26, 27). In addition, early polypeptides (immediate early and/or delayed early proteins) are involved in the transcription of late genes (19, 20).

Influence of DNA replication. The role of viral DNA

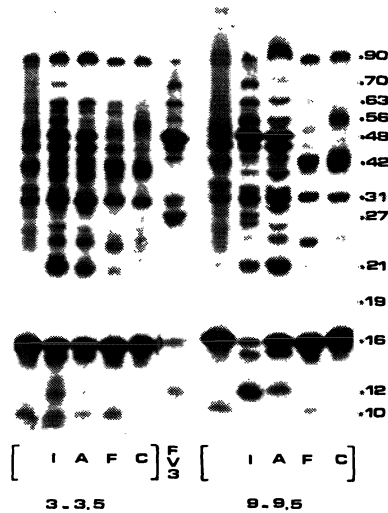


Fig. 3: Fluorogram of FV3-infected CHO cell polypeptides synthesized under different restrictive conditions, analyzed by SDS-polyacrylamide gel electrophoresis. Proteins were labeled with ^{35}S -methionine 30 min before collection at 3.5 hr or 9.5 hr postinfection. Infected cells were incubated at 29°C in normal medium (I), or in medium containing 10^{-3} M AraC (A), fluorophenylalanine (F) or canavanine (C). The unlabeled tracks correspond to cells infected at 37°C and incubated in normal medium. FV3 refers to virus structural polypeptides used as molecular mass markers.

replication in the expression of the different classes of genes is not well defined as the observations reported do not lead to the same conclusions. In several experiments, the inhibition of DNA replication was followed by a great diminution of the amount of late proteins produced, but most if not all late species were detectable as in Fig. 3 (10, 23, 28).

In other experiments, DNA replication was strictly required to allow late gene expression (20, 29). It has been proposed that in this case, a template modified by ongoing DNA replication may be needed for full expression of late genes (29). Thus both the structure of the

template and/or the number of template molecules available may contribute to limiting late gene expression below the detectable level, a restriction which most likely takes place at the transcriptional level.

TRANSLATIONAL CONTROL OF VIRAL MESSAGES

Different observations have led to the idea that a control mechanism may also be present at the translational level.

Role of proteins

The first report indicated that while immediate early and delayed early genes were still transcribed concomitently with late genes, these transcripts were no longer translated (18). Modification of the biological activities of early proteins by incorporation of amino acid analogs in the polypeptides has produced indirect evidence for participation of some viral proteins in this regulation (19).

In addition, in vitro translation of different messages showed that transcripts of late genes are poorly translated; the efficiency varies with the RNA species and can be greatly increased by addition of factors extracted from infected cells (30): Nevertheless, no in vitro translation products could be detected for RNA originating from several regions of the genome and transcribed only at late time (31). Further analyses are needed to establish whether they are strictly dependent upon specific factors to be translated or whether they have no message activity at all. For the moment, there is no genetic evidence for the existence of a virus-coded factor involved in the translation of late RNA species. Among the ts mutants analyzed, none of them presented at nonpermissive temperature, a wild type pattern of late mRNAs without late proteins, but these mutants belong to only 19 complementation groups (32).

Structure of mRNAs

In cases where selective translation of some

messages is observed, discrimination takes place at the level of initiation. Several observations made during studies on the organization of the FV3 genome and transcriptional mapping showed them to be related to translational regulation.

The gene p42 is one of the genes transcribed at the very beginning of infection and 6 hours later its message is still present but synthesis of the protein is not detectable. At late times, two RNA species complementary to the 5' region of the immediate early mRNA are produced and they are much more abundant than the mRNA (33). It has not been established whether the complementary RNAs code for proteins or not, nor whether they can form, *in vivo*, a hybrid with the message. This last possibility cannot be excluded for the present time and an engagement of the message in a hybrid could be a way of limiting the expression of that gene.

The 5' leader. The characterization of the transcription products of two other immediate early genes has revealed that the RNA sizes, estimated by Northern blot analysis, were different at the beginning and at late times of infection.

The gene p46, situated on the genome within the fragment Sall-F, is transcribed at the very beginning of infection into a message 1.3 kb in size. Later a family of transcripts, ranging from 1.7 kb to 0.59 kb, is produced. S1 mapping experiments have shown that these molecules have the same 3' end but their start sites are different (33).

For a second immediate early gene (p42b) located in fragment HindIII F, the size of the early mRNA is 1.3 kb and the late RNA, 1.35 kb; the 5' end of the late transcript is at about 50 nucleotides upstream to the 5' end of the immediate early site (unpublished data). *In vitro* translation of hybrid-selected RNA, transcribed from genes p46 and p42b, has revealed that the immediate

early RNAs are efficiently translated but no message activity was detected for the late RNAs (31). Although these experiments were not designed to compare strictly the message activity of the RNAs but to draw a map of FV3 genes, these observations suggest that the additional leader regions in the late transcripts may impair the message activity of the RNAs.

Raghow and Granoff (34) have shown that internal methylation of late RNA species remained undetected, but all classes of messages presented the methylated cap structure. A control mechanism occurring via a modification of this structure of the RNAs is therefore unlikely.

The initiator codon. The mechanism of initiation implies the recognition of the 5' end of the message and the cap structure by several factors. It is followed by the binding of the 40s ribosomal subunit which then scans the mRNA sequence until an AUG codon is reached. While for most mRNAs translation starts at the first AUG encountered, some mRNAs (less than 10% of the molecules analyzed) have one or more AUG upstream to the start site for protein synthesis (1). In such mRNAs these AUG triplets are placed in a context which differs from the optimal context for initiation defined by the consensus sequence A/GCCAUGG (35).

The open reading frames of the four immediate early mRNAs for which the sequences are known, start with the first AUG and two if not three of the flanking nucleotides, particularly the A in position 3, a nucleotide which has been shown to be important. These open reading frames are identical to those of the consensus sequence. Their sequences are given below and the position of the sequence relative to the major start site of the message, determined by nuclease mapping, is indicated:

ICR 169 (from ref. 36)	+ 16	ACAAUGC	+ 22
ICR 489 or p42 (from ref. 37)	+ 29	AACAUGG	+ 35
p46 (unpublished data)	+ 143	AUCAUGG	+ 149

p42b (unpublished data) + 39 ACA AUGA + 45

The length of the 5' nontranslated domains are not different from those of the two late gene messages sequenced.

p70 (unpublished data) + 13 GACAUGU + 19

p48 (unpublished data) + 170 AAGAUGU + 176

For these late messages (p70, p48) the homology with the consensus sequence is lower than for the immediate early messages. Furthermore for the p48 message, the RNA encoding the major capsid protein, the open reading frame starts with the fourth AUG codon, none of the four codons having more than one nucleotide besides AUG, common to the consensus sequence.

Secondary structure. Secondary structure in the messages, specially in the leader region, may theoretically have various effects. Although it is conceivable that a structure may serve to determine which AUG will initiate translation, the most documented effect of an intramolecular structure in the leader is a decrease in the translational efficiency. One or several inverted repeats were found in the 5' region of late transcripts from immediate early or late genes, but the hairpins never exceeded 25 Kcal/mol, a structure susceptible to melting by the 40S ribosomal subunit once bound to the RNA. Nevertheless elements such as ions or factors present in the intracellular environment of the RNAs may stabilize the structure.

The 3' termini of FV3 messages lack poly A (38). The untranslated region is never long (40-100 nucleotides). A hyphenated dyad symmetry preceding the 3' end is consistently found for the messages sequenced.

The function of this domain is hypothetical: this structure may be a signal recognized for generating the message's 3' end, and/or the inverted repeat may favor an intramolecular pairing thereby protecting the RNAs from exonucleases.

The free energy of the hairpin is different for each

RNA (-10.6 to -28.6 Kcal/mol). Whether the variations in the stability of the hairpins may be correlated to the half life of the messages or not remains a matter of speculation, as is an eventual regulation of the expression via an alteration of mRNA stability.

CONCLUSIONS AND PERSPECTIVES

The specific inhibition of host protein synthesis after FV3 infection is characteristic of the ability of viruses to direct the cellular macromolecular synthesis machinery to their advantage. In a first step, several or one structural protein(s) of the virion generate(s) a defect in the translational machinery. Immediate early viral messages are translated and a complete shut off of host translation occurs only when the second group of genes is expressed. Additional investigations are required whether it is due to the synthesis of a new factor or to the fact that the intracellular concentration of some structural proteins is now higher as they accumulate in the cytoplasm, or even to competition between host and viral messages.

As regards the mechanism of translational regulation of early and late viral mRNAs, a first temporal switch is effected at the level of transcription as the mRNAs that encode the different classes of proteins are synthesized sequentially. Nevertheless early RNAs persist at late times but are not translated.

The necessity of specific factors for an efficient translation of late mRNAs species has been established but some questions are still open. Are there late messages that are completely dependent on factors for their translation? Are these factors sufficient to favor the translation of late species in the presence of early ones?

A fine analysis of the influence of the 5' non-translated sequences in late transcripts of immediate early genes on their translation is needed. The study of

late transcripts of other early genes should indicate if a difference at the 5' end is generally observed and if the modifications in the transcripts play a role in the regulation of gene expression.

REFERENCES

1. Kozak, M. In: *Advances in Virus Research* (Eds. K. Maramorosch, F.A. Murphy and A.J. Shatkin), Academic Press, inc., 31: 229-292, 1986.
2. Granoff, A., Came, P.E. and Breeze, D.C. *Virology* 29: 133-148, 1966.
3. Drillien, R., Spehner, D. and Kirn, A. *Biochem. Biophys. Res. Commun.* 79: 105-111, 1977.
4. Kirn, A. *C R Acad Sci (Serie D)*, Paris 272: 2504-2506, 1971.
5. Maes, R. and Granoff, A. *Virology* 33: 491-502, 1967.
6. Mc Auslan, B.R. and Smith, W.R. *J. Virol.* 2: 1006-1015, 1968.
7. Aubertin, A.M., Decker, C. and Kirn, A. *Radiat. Res.* 44: 178-186, 1970.
8. Guir, J., Braunwald, J. and Kirn, A. *C R Acad Sci (Serie D)*, Paris 270: 2605-2608, 1970.
9. Aubertin, A.M., Hirth, C., Travo, C., Nonnenmacher, H. and Kirn, A. *J. Virol.* 11: 694-701, 1973.
10. Goorha, R. and Granoff, A. *Virology* 60: 237-250, 1974.
11. Zylber-Katz, E. and Weisman, P. *Arch. Virol.* 47: 181-185, 1975.
12. Raghov, R. and Granoff, A. *Virology* 98: 319-327, 1979.
13. Cordier, O., Aubertin, A.M., Lopez, C. and Tondre, L. *Ann. Virol. Inst. Pasteur* 132E: 25-39, 1981.
14. Aubertin, A.M., Travo, C. and Kirn, A. *J. Virol.* 18: 34-41, 1976.
15. Drillien, R., Spehner, D. and Kirn, A. *FEMS Lett.* 7: 87-90, 1980.
16. Chinchar, V.G. and Caughman, G.B. *Virology* 152: 466-471, 1986.
17. Elharrar, M. and Kirn, A. *FEMS Lett.* 1: 13-16, 1977.
18. Willis, D.B., Goorha, R., Miles, M. and Granoff, A. *J. Virol.* 24: 326-242, 1977.
19. Goorha, R., Willis, D.B. and Granoff, A. *J. Virol.* 32: 442-448, 1979.
20. Elliott, R.M. and Kelly, D.C. *J. Virol.* 33: 28-51, 1980.
21. Cordier, O., Tondre, L., Aubertin, A.M. and Kirn, A. *Virology* 152: 355-364, 1986.
22. Elliott, R.M., Bravo, R. and Kelly, D.C. *J. Virol.* 33: 18-27, 1980.
23. Martin, J.P., Aubertin, A.M., Lecerf, F. and Kirn, A. *Virology* 110: 349-365, 1981.

24. Martin, J.P., Aubertin, A.M., Tondre, L. and Kirn, A. J. Gen. Virol. 65: 721-732, 1984.
25. Willis, D. and Granoff, A. Virology 86: 443-453, 1978.
26. Willis, D.B., Goorha, R. and Chinchar, V.G. Curr. Top. Microbiol. Immunol. 116: 77-106, 1985.
27. Lopez, C., Aubertin, A.M., Tondre, L. and Kirn, A. Virology 152: 365-374, 1986.
28. Goorha, R., Willis, D.B., Granoff, A. and Naegele, R.F. Virology 112: 40-48, 1981.
29. Chinchar, V.G. and Granoff, A. Virology 138: 357-361, 1984.
30. Raghov, R. and Granoff, A. J. Biol. Chem. 258: 511-578, 1983.
31. Tondre, L., Tham, T.N., Mutin, P.H. and Aubertin, A.M. Virology 162: 108-117, 1988.
32. Chinchar, V.G. and Granoff, A. J. Virol. 58: 192-202, 1986.
33. Mesnard, J.M., Tham, T.N., Tondre, L., Aubertin, A.M. and Kirn, A. Virology 165: 122-133, 1988.
34. Raghov, R. and Granoff, A. Virology 107: 283-294, 1980.
35. Kozak, M. Nucleic Acid. Res. 9: 5233-5252, 1981.
36. Willis, D.B., Foglesong, D. and Granoff, A. J. Virol. 53: 905-912, 1984.
37. Beckman, W., Tham, T.N., Aubertin, A.M. and Willis, D.B. J. Virol. 62: 1271-1277, 1988.
38. Willis, D. and Granoff, A. Virology 73: 543-547, 1976.

10

MOLECULAR BIOLOGY OF FISH LYMPHOCYSTIS DISEASE VIRUS

P. SCHNITZLER, A. RÖSEN-WOLFF and G. DARAI

Institut für Medizinische Virologie der Universität
Heidelberg, Im Neuenheimer Feld 324, 6900 Heidelberg
Federal Republic of Germany.

ABSTRACT

The fish lymphocystis disease virus (FLDV) can be classified genetically into two different strains: FLDV strain 1 (FLDV-f) occurs in flounders and plaice, whereas strain 2 (FLDV-d) is usually found in lesions of dabs. The genome structure of FLDV was found to be circularly permuted and terminally redundant combined with a high degree of methylation at CpG sequences. A defined and complete gene library of the FLDV genomes was established. The physical maps of the viral genomes were constructed for the restriction endonucleases BamHI, BstEII, EcoRI, and PstI. Two repetitive DNA elements were identified at the genome coordinates 0.034 to 0.052 (1413 bp) and 0.718 to 0.736 (1413 bp) of FLDV-f. The degree of DNA nucleotide homology between both regions was found to be 99%. The analysis of the DNA nucleotide sequence of the repetition in the genome of FLDV-d (1410 bp; EcoRI DNA fragment J) indicates that these repetitive DNA elements are highly conserved (94% homology). The DNA sequences of each strand of the individual repetitive element possess one open reading frame (150 to 339 amino acid residues). FLDV virions contain at least 33 polypeptides ranging in molecular weight from 220 to 14 Kd. A nucleoside triphosphate phosphohydrolase activity was found to be associated with FLDV. The thymidine kinase gene of FLDV-f has been identified at the genome coordinates 0.669 to 0.718 of the viral map units.

INTRODUCTION

Fish lymphocystis disease virus (FLDV) has been tentatively classified as a separate genus of the iridovirus family. Iridoviruses were previously called icosahedral cytoplasmic deoxyriboviruses (ICDV). The Iridoviridae family contains four genera including lymphocystis disease virus (proposed name Lymphocystivirus, Willis, 1989 (1)).

FLDV is a causative agent of lymphocystis disease (LD) which frequently appears in Pleuronectidae (flatfish) such as Pleuronectes platessa (plaice), Platichthys flesus (flounder), Limanda limanda (dab), and Trigla gurnardus (gurnard). Fish lymphocystis disease is characterized by papilloma-like lesions, which can be induced experimentally in Lepomis macrochirus (bluegill) (2) and by subdermal injection of plaice and flounder (3). The mechanisms of this nonmalignant tumor induction are unknown. Since the discovery of LD in 1874 by Lowe (4), attempts have been made to isolate and propagate FLDV in vitro with limited success (5-7). As a first step towards understanding of the underlying mechanisms of this infectious disease the structure and properties of the causal virus must be elucidated. These basal molecular biological studies provide new facilities for investigation of virus host interactions which is necessary for understanding the molecular mechanisms of the viral pathogenesis.

MATERIALS AND METHODS

A total of 30 fish with LD lesions caught near the Doggerbank areas were analyzed individually, including 20 flounders, six dabs, and four plaice. Virions of FLDV from LD lesions of each species of fish were isolated, purified, and examined by electron microscopy as

described previously (8). Fig. 1 shows homogenous masses of FLDV virions routinely observed in preparations of LD lesions obtained from different fish species.

The experimental approach for this study (e.g. isolation and purification of virions, analysis of viral polypeptides, determination of virion enzyme activity, DNA extraction, electron microscopy, restriction enzyme analysis, nick translation, DNA hybridization, molecular cloning, physical mapping, DNA nucleotide sequence determination, and computer-assisted analysis) was carried out as described previously (8-16).

RESULTS

STRUCTURE OF THE VIRAL GENOME

In order to identify and characterize the FLDV genomes, DNAs of different FLDV isolates were analysed using different restriction endonucleases. Representative results of this analysis are given in Figs. 2-4 and table 1. These studies revealed that FLDV DNA of flounders and of plaice are indistinguishable, but clearly different from those of dab. According to these results two different strains exist; FLDV strain 1 (FLDV-f) is found in flounders and plaice, whereas FLDV strain 2 (FLDV-d) is usually associated with dabs inflicted with LD. A few variations in the restriction patterns of individual fish were found for flounder and dab by Bgl II and AvaI and for plaice by PstI enzyme.

Methylation of the viral genome

FLDV DNAs were digested with the HpaII (C/CGG) and Msp I (C/MeCGG) enzymes; the latter cleaves DNA in the presence of a 5-methyl group at the internal cytosine residue in

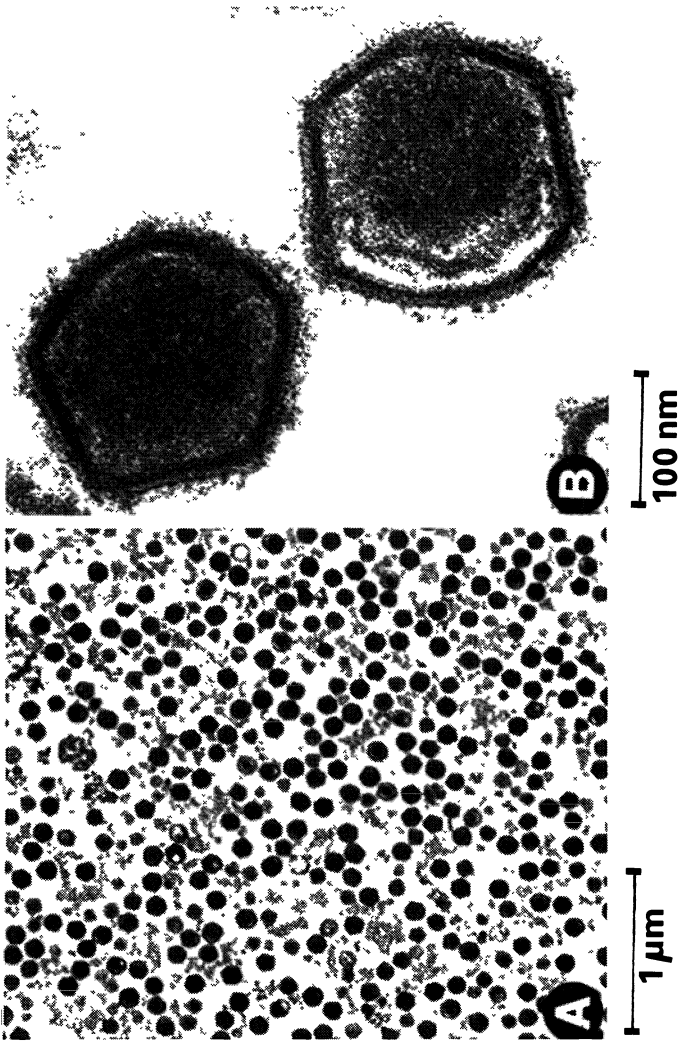
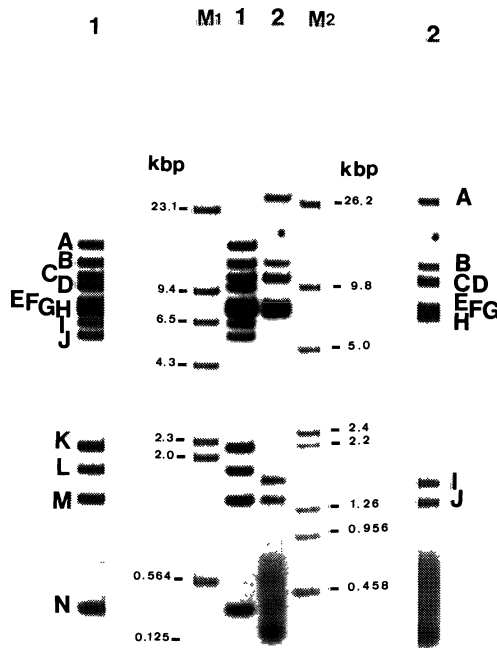


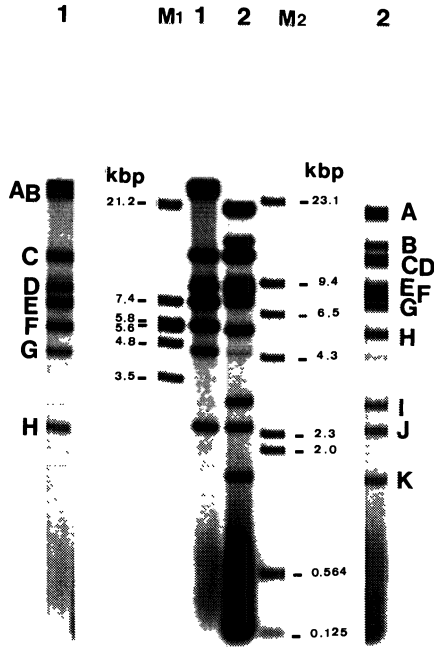
Fig. 1. Electron micrograph of fish lymphocystis disease virus; A, ultra thin section of an epidermal tumor of lymphocystis disease in *Platichthys flesus* (flounder). B, the fine structure of the intact complex virion of FLDV (for detail see 8).

the recognition sequence of the HpaII enzyme (17). As shown previously (8, 18, 19) it was found that FLDV DNAs from dab, plaice and flounder were cut many times with Msp I indicating that internal C in the recognition sequence of this enzyme is heavily methylated, since the Hpa II enzyme leaves the FLDV DNAs intact. Furthermore the content and distribution of 5-methylcytosine in DNA from FLDV was analyzed by HPLC and nearest neighbour analysis (18). It was found that 22% of all C residues, including 74% of CpG, about 1% of CpC, and 2-5% of CpA were methylated (18).



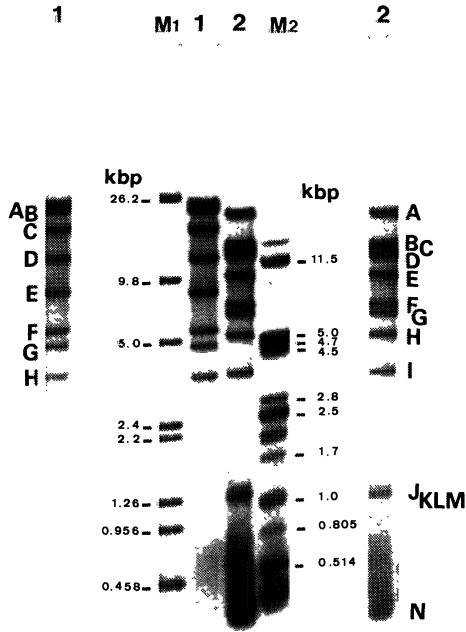
32

Fig. 2. Autoradiogram of P-DNA of FLDV isolates from flounder (lane 1) and dab (lane 2) cleaved with the endonuclease EcoRI. Phage lambda DNA digested with HindIII (M1) and MluI (M2) served as molecular weight marker. Gradient agarose slab gel (0.5 to 1%), 35x20x0.3 cm, 13 h, 95 V.



32

Fig. 3. Autoradiogram of P-DNA of FLDV isolates from flounder (lane 1) and dab (lane 2) cleaved with the endonuclease BstEII. Phage lambda DNA digested with EcoRI (M1) and HindIII (M2) served as molecular weight marker. Gradient agarose slab gel (0.5-1%), 35x20x0.3 cm, 13 h, 95 V.



32

Fig. 4. Autoradiogram of P-DNA of FLDV isolates from flounder (lane 1) and dab (lane 2) cleaved with the endonuclease PstI. Phage lambda DNA digested with MluI (M1) and PstI (M2) served as molecular weight marker. Gradient agarose slab gel (0.5 to 1%), 35x20x0.3 cm, 13 h, 95 V.

Properties of the viral genome

The molecular weight of the FLDV DNA was determined by electron microscopic measurement of the contour length of the DNA molecules of FLDV and by restriction enzyme analysis.

Purified viral DNA molecules of different FLDV isolates were examined in the electron microscope using cytochrome C spreading (20). An average length of $49 \pm 23 \mu\text{m}$ corresponding to about $93 \pm 44 \text{ Md}$ was found by measuring

Table 1: Size of DNA fragments of FLDV-f and FLDV-d genomes after digestion with restriction enzymes BamHI, BstEII, EcoRI, and PstI.

DNA fragment	Size of the DNA fragment (kbp)							
	FLDV-f				FLDV-d			
	BamHI	BstEII	EcoRI	PstI	BamHI	BstEII	EcoRI	PstI
A	48.3	29.5	14.4	24.0	65	20.5	28.5	21.0
B	17.3	26.4	12.7	21.9	28.8	14.6	12.7	14.0
C	15.1	12.5	11.2	17.1	3.1	12.6	12.2	13.5
D	13.4	8.9	9.9	12.5		12.5	11.1	12.5
E	3.1	7.4	7.9	8.3		9.0	7.9	10.3
F	0.3	5.7	7.5	5.6		8.0	7.5	7.4
G		4.4	7.4	4.7		7.4	7.4	6.8
H		2.35	7.2	3.6		5.6	7.2	5.4
I			6.6			2.8	1.6	3.7
J			5.6			2.35	1.39	1.35
K			2.25			1.5		1.3
L			1.9					1.25
M			1.39					1.2
N			0.33					0.2
Sum:	97.5	97.15	96.27	97.7	96.9	96.85	96.49	99.8

43 molecules (8). However, the determination of the molecular weight of the FLDV genome calculated from the sizes of individual DNA fragments obtained after digestion of FLDV DNAs with a variety of restriction enzymes revealed a value of 64.8 Md (8). The comparison between the molecular weight values found by restriction enzyme analysis and contour length measurement indicates that the DNA molecules are in average longer than expected from the restriction enzyme analysis, a situation known for terminal redundancy.

Circular permutation of the viral genome

In order to determine the terminal fragments of FLDV DNA, purified DNA was first treated with Lambda-5'-exonuclease or the 3'-exonuclease III of E.coli followed by digestion with different restriction enzymes. The obtained DNA cleavage patterns do not show a selective digestion of a particular fragment, instead a gradual disappearance of all viral DNA fragments. Similar results were found when another method for searching terminal fragments was employed (8). Taken together these data indicate that the FLDV DNA molecules have variable termini. Denaturation and renaturation of FLDV DNA revealed circular DNA molecules of 34.25 μ m length with two protruding single-stranded ends (Fig. 5). This contour length corresponds to a molecular weight of 65.22 Md (98 kbp), in agreement with the value obtained by restriction enzyme analysis. These circles were formed when a single strand of more than unit size circularized by a DNA molecule complementary to the sequences on both sides of the attachment point of the extra DNA tails (Fig. 5). These tails were separated by one unit length of the FLDV genome (8), indicating that the FLDV genome is circularly permuted and terminally redundant.

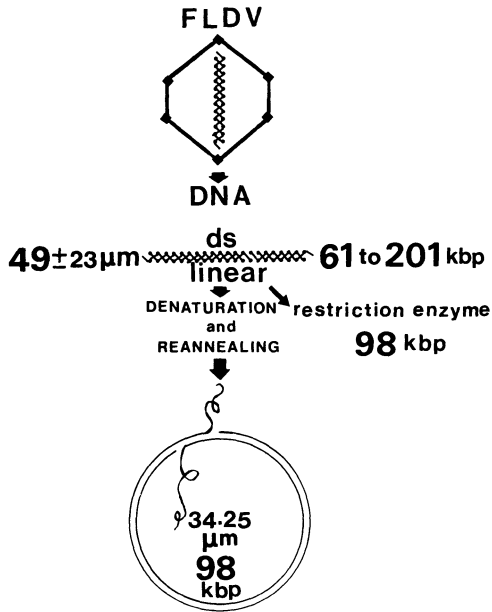


Fig. 5. Diagram demonstrating the circular permutation of the FLDV genome. The linear FLDV DNA molecule generates an open circularized doublestranded region combined with singlestranded tails on both sides of the attachment point by denaturation and renaturation (for detail see 8).

To ascertain these results it was of importance to prove whether direct molecular cloning of the complete genome of FLDV is possible and whether the physical map of the viral genome is circular.

Molecular cloning and physical mapping of the viral genome

Due to the high methylation of 22% at CpG sequences of the FLDV genome molecular cloning of the viral genome

was only successful when the competent E.coli strain GC-3 was used (10, 11). In order to molecularly clone the FLDV genome, viral DNA (FLDV-f) was cleaved with restriction enzymes EcoRI, Bam HI, EcoRI/Bam HI, EcoRI/Hind III, and the resulting DNA fragments were inserted into the EcoRI site of the plasmid vector pACYC184 and/or in the corresponding site of the plasmid vector pAT153. Bacterial colonies harboring recombinant plasmids were selected, identified and characterized (10, 11, 14). Under these conditions we succeeded in molecular cloning the complete EcoRI DNA fragments (A to N; 11, 14) of the viral genome into the corresponding site of the plasmid vector pACYC184. The successful direct insertion (without any linker or adapter) of all EcoRI DNA fragments of the FLDV-f genome in the bacterial plasmid vector indicates that each EcoRI DNA fragment of the viral genome must have two EcoRI sites at its termini. This observation supports the results of earlier analyses indicating that the FLDV-f DNA is circularly permuted and terminally redundant (8).

The physical map of the viral genome was constructed using the established gene library for the restriction enzymes BamHI, BstEII, PstI, and EcoRI as shown in Fig 6. Although the FLDV genome is linear, this analysis revealed that the restriction maps of the viral genome are circular. This finding is the final evidence for the hypothesis that the FLDV genome is circularly permuted (11, 14).

Under the same conditions the physical maps of the FLDV-d genome isolated from LD lesions of dab were constructed for the restriction endonucleases BamHI, BstEII, PstI, and EcoRI using Southern blot hybridization tests. An example of these studies is shown in Figs. 7 and 8 and the arrangement of the DNA fragments for these restriction endonucleases is shown in Fig. 9.

Fig. 7. Characterization and identification of the recombinant plasmid harbouring the EcoRI DNA fragment N (pyLV17-E-N) by Southern blot hybridization. The hybridization was carried out using labeled DNA of the recombinant plasmid pyLV17-E-N. The DNAs of FLDV isolated from flounder (lanes 1 to 6) and dab (lanes 7 and 8) were cleaved with EcoRI (lanes 2 and 7), BstEII (lane 3), and PstI (lane 6). Labeled EcoRI (lanes 1 and 8), BstEII (lane 4), and PstI (lane 5) cleaved FLDV DNA served as internal marker. Phage lambda DNA digested with MluI (M1) served as molecular weight marker. The arrows mark the position of the EcoRI, PstI, and BstEII DNA fragments which hybridize to pyLV17-E-N.

Fig. 8. Characterization and identification of the recombinant plasmid harbouring the EcoRI DNA fragment A (pyLV17-E-A) by Southern blot hybridization. The hybridization was carried out using labeled DNA of the recombinant plasmid pyLV17-E-A. The DNA of the recombinant plasmid was digested with EcoRI and separated electrophoretically on a gradient (0.6 to 1%) agarose slab gel (lane 1). The DNAs of FLDV isolated from flounder (lanes 3) and dab (lane 4) were cleaved with PstI. Labeled PstI (lanes 3 and 4) cleaved FLDV DNA served as internal marker. Phage Lambda DNA digested with MluI (M) served as molecular weight marker. The arrows mark the position of the PstI DNA fragments which hybridize to pyLV17-E-A.

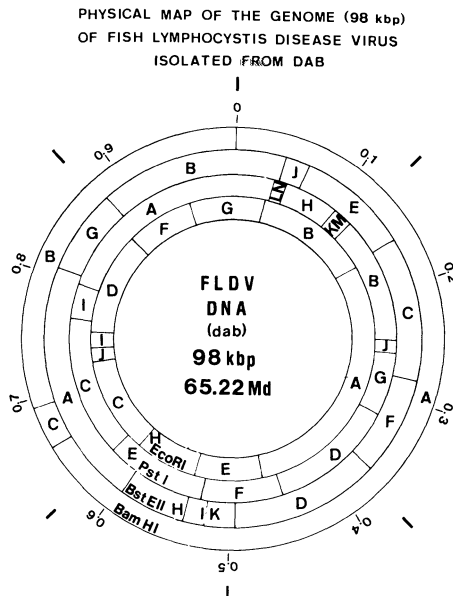


Fig. 9

Fig. 9. Physical maps of the genome of FLDV isolated from dab for the restriction endonucleases EcoRI, PstI, BstEII and BamHI. The restriction maps are circular and start at the boundary of the BamHI DNA fragments A to B.

Detection and characterization of repetitive DNA sequences in the FLDV genome

To detect possible repeat DNA sequences within the genome of FLDV-f the defined gene library of the viral genome which contains the complete EcoRI DNA fragments A to N was screened by hybridization experiments as described previously (14). A significant homology was detected between the EcoRI DNA fragments B and M of FLDV-f. This result was confirmed by electron microscopical heteroduplex analysis (14) as shown in Fig. 10.

To determine the exact position of the DNA sequence in the EcoRI DNA fragment B which is homologous to the DNA sequence of the EcoRI DNA fragment M of the viral genome, fine mapping of the EcoRI DNA fragment B was carried out. These analyses revealed that the DNA sequences (2.1 kbp) located in the left hand terminus of the EcoRI DNA fragment B between the genome coordinates 0.034 (EcoRI site) and 0.057 mu (PstI site) harbor the repetitive DNA sequences (Fig. 11).

The complete nucleotide sequence of the FLDV-f EcoRI DNA fragment M and the corresponding region of the repetition within the EcoRI DNA fragment B of the viral genome was determined (14, 15) and the results are shown in Fig. 12. The sizes of the repetitive DNA elements were found to be 1413 bp which correspond to the DNA sequences of the 5' terminus of the EcoRI DNA fragment B (0.034 to 0.052 viral map units) and to the EcoRI DNA fragment M (0.718 to 0.736 viral map units) of the FLDV-f genome. The degree of DNA nucleotide homology between both regions was found to be 99%. The base composition is 26.7% G+C

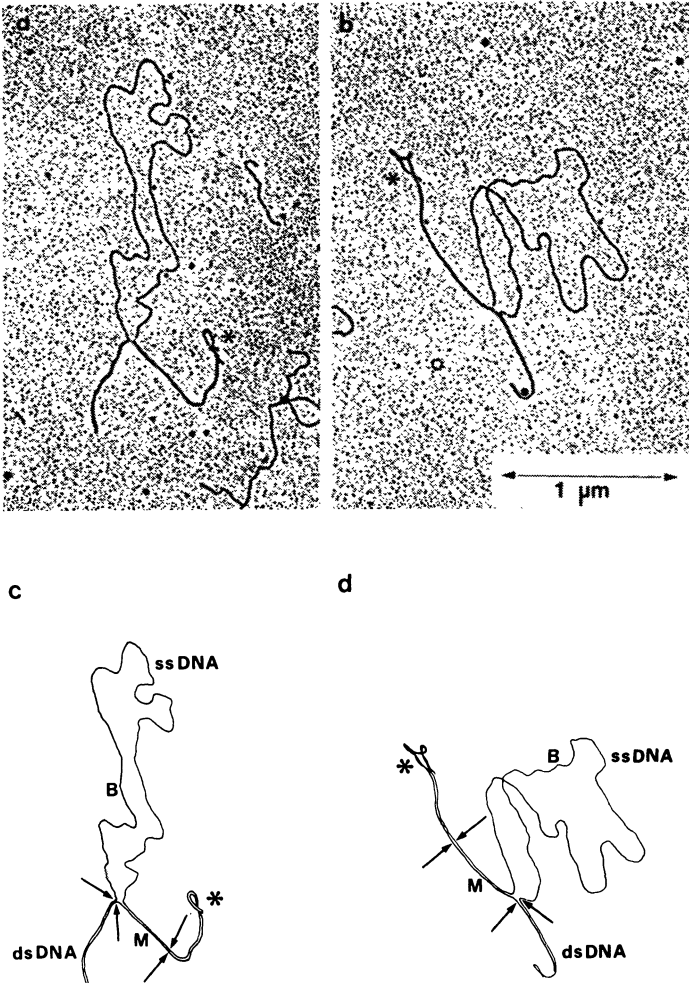


Fig. 10. Electron micrograph of heteroduplexes between the recombinant plasmids pyLV17-E-B and pyLV17-E-M (a and b) which harbour the EcoRI DNA fragments B and M of the FLDV-f genome, respectively. The samples were prepared as described previously (14). The plasmids were linearized with the BamHI which recognizes one site on the cloning vector. The asterisks point to an underwound loop structure in the vector part of the heteroduplexes. A schematic representation of the heteroduplexes is shown in (c) and (d). The arrows mark the EcoRI recognition sites of the DNA fragments B and M.

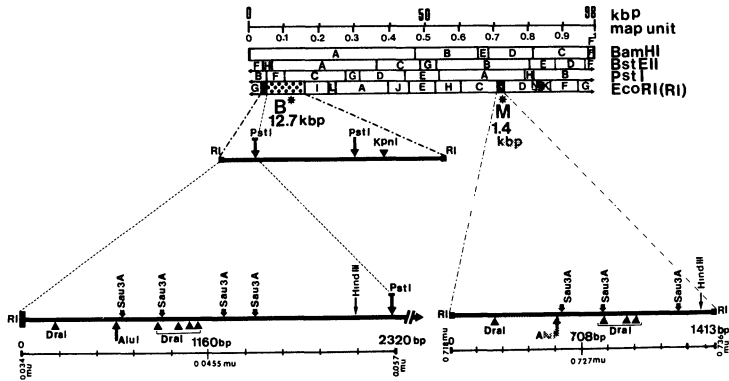


Fig. 11. Fine mapping of two repetitive DNA elements in the FLDV-f genome (black boxes). Physical maps of the viral genome are given linearized for the restriction endonuclease BamHI, BstEII, PstI, and EcoRI. The points in the part of EcoRI DNA fragment B mark the position of those DNA sequences of EcoRI DNA fragment B which are not homologous to the EcoRI DNA fragment M.

and 73.2% A+T for both repetitive DNA elements. The DNA sequence is composed of many short direct and inverted repeat sequences as described elsewhere (15).

This analysis rose substantial questions concerning the arrangement and the degree of relatedness of the repetitive DNA sequences in the genome of the second strain of FLDV isolated from dab (FLDV-d). As a first step to detect possible repeat DNA sequences within the genome of FLDV-d the viral genome was characterized by molecular cloning and physical mapping. The repetitive DNA sequences in the genome of the FLDV-d were identified by DNA-DNA hybridization tests. These analyses revealed that the genome of FLDV isolated from dab possesses repetitive DNA elements within the EcoRI DNA fragments B and J of the viral genome (see Fig. 9).

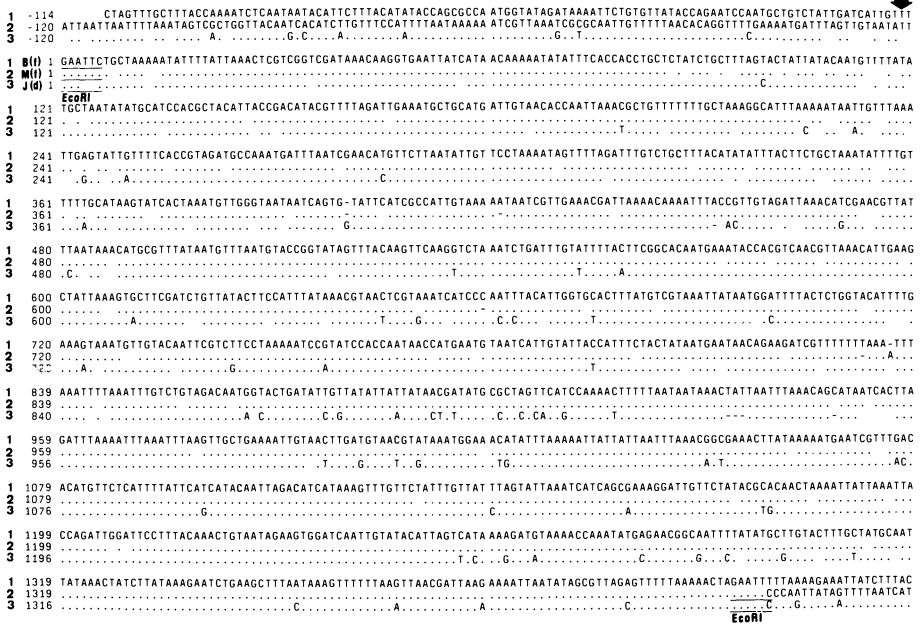


Fig. 12. Nucleotide sequence of the repetitive DNA element located in the 5' terminus of the EcoRI FLDV-f DNA fragment B including its flanking regions and the nucleotide sequence of the EcoRI FLDV-d DNA fragment J are shown in lanes 1 and 3, respectively. For comparison the DNA nucleotide sequences of the EcoRI FLDV-f DNA fragment M (15) and its flanking regions are given in lanes 2. Dots represent identical bases and dashes indicate artificial gaps introduced into the DNA sequences to achieve optimal base match. The arrow indicates the start of the DNA sequences of the repetitions.

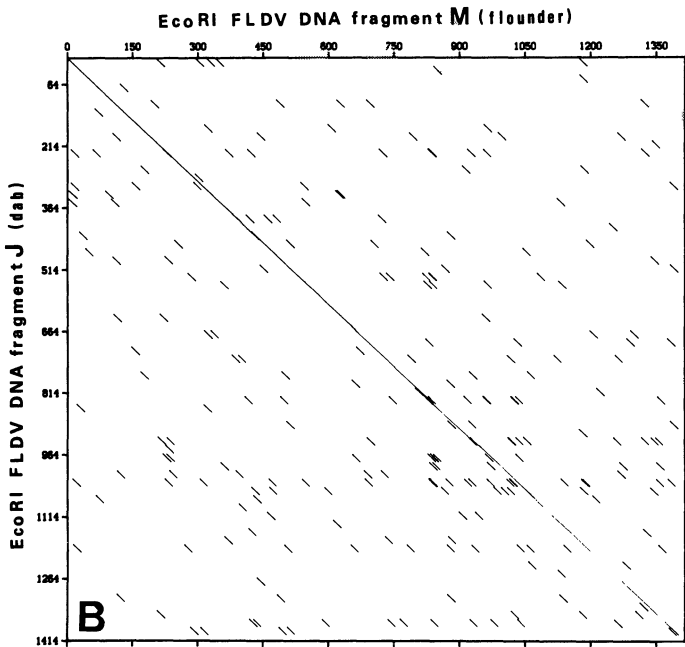
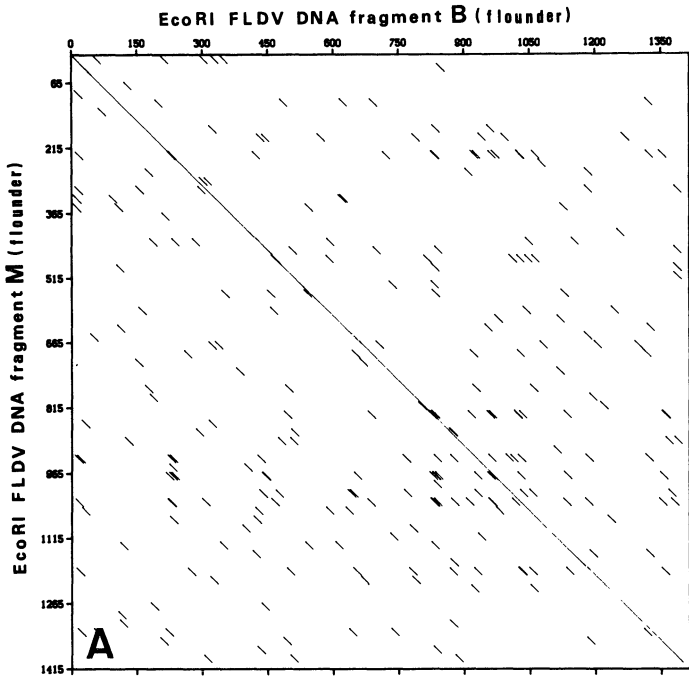
To survey the degree of relatedness between the repetitive DNA element in the genome of FLDV isolated from flounder and dab, the nucleotide sequence of the EcoRI FLDV-d DNA fragment J was determined as described elsewhere (15). The results of this study are given in the lanes 3 of Fig. 12. The size of this DNA fragment was found to be 1410 bp with a base composition of 27.44% G+C and 72.56% A+T. The DNA sequence is composed of many short direct and inverted repeat sequences (15). These studies revealed that the repetitions in the genome of FLDV isolated from flounder started exactly two

nucleotides upstream from the EcoRI sites at the 5' terminus of the EcoRI DNA fragment B (0.034 m.u.) and M (0.718 m.u.) and terminated after 1413 bp at the 3' terminus of the EcoRI FLDV-f DNA fragment M (EcoRI site; 0.736 m.u.). It is of interest that the repeat sequences within the EcoRI DNA fragment B terminated with the nucleotide motif GAATTT which is with exception of the last nucleotide identical to the EcoRI site at the 3' terminus of the EcoRI DNA fragment M.

Therefore the total DNA sequences of the EcoRI-FLDV-f DNA fragment M (1413 bp; 0.718 to 0.736 m.u.) harbor with exception of two bases one complete copy of the repeat element of the viral genome. Furthermore it was found that the DNA sequences of the EcoRI DNA fragment J of FLDV isolated from dab are nearly identical to the DNA sequences of the EcoRI DNA fragment M of the FLDV-f genome (Fig. 12). According to these data the homology between the DNA sequences of the EcoRI FLDV-f DNA fragment B and the DNA sequences of the EcoRI FLDV-f DNA fragment M and the EcoRI FLDV-d DNA fragment J was found to be 99.86% and 94.93%, respectively (Fig. 13 A to C). This indicates that the genomes of FLDV isolated from two different fish species are almost genetically identical at least at this particular region.

Coding capacity of the repetitive DNA sequences

The analysis of the coding capacity of the repetitive DNA sequences and their flanking regions was determined by computer assistance. This studies revealed that each DNA strand of the repeat elements possesses one ORF which starts within the DNA sequence of the repetition and terminates downstream of the 3' (upper strand) or upstream of the 5' (lower strand) termini of the repeat sequences as shown in Fig. 14. The corresponding ORFs of the individual repeats were termed ORF-1B, ORF-1M, and ORF-1J (upper strand) and ORF-2B, ORF-2M, and ORF-2J (lower strand). The properties of the ORFs found



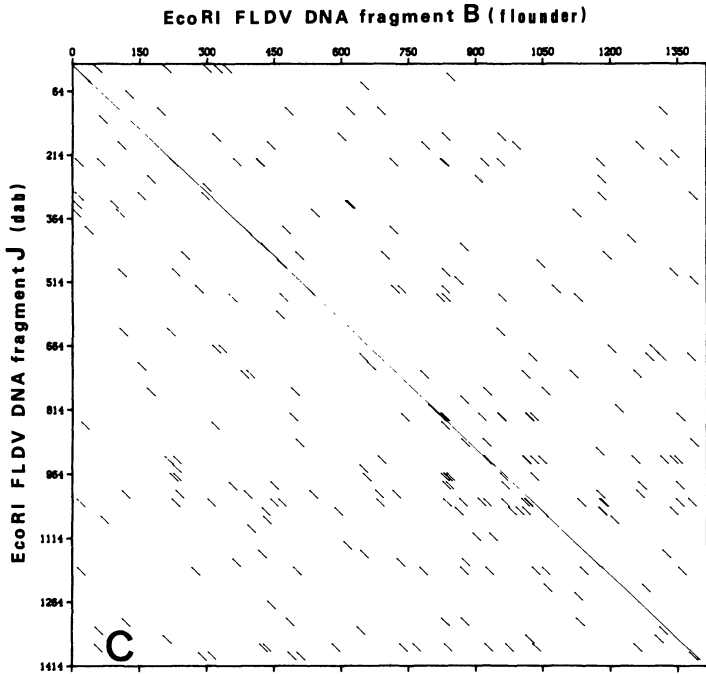


Fig. 13. Dot matrix analysis of the repetitive DNA elements within the EcoRI DNA fragments B (1413 bp, FLDV-f), M (1413 bp, FLDV-f), and J (1410 bp, FLDV-f). (A) Comparison of the repetitive DNA elements within the EcoRI DNA fragments M and B of FLDV-f; (B) comparison of the repetitive elements within the EcoRI DNA fragments M (FLDV-f) and J (FLDV-d); (C) comparison of the repetitive DNA elements within the EcoRI DNA fragments B (FLDV-f) and J (FLDV-d).

in the repetitive DNA sequences are given in Fig. 15. As shown in Fig. 15 classical or slightly modified transcriptional signals were found by all putative proteins. It is of interest that with exception of ORF-2B all other ORFs possess the eucaryotic polyadenylic acid addition signal (AATAAA) which were located 6 to 60 bp downstream of the termination signals (Fig. 15).

Comparative analysis of the amino acid sequences of each ORF was carried out as described previously (15) and

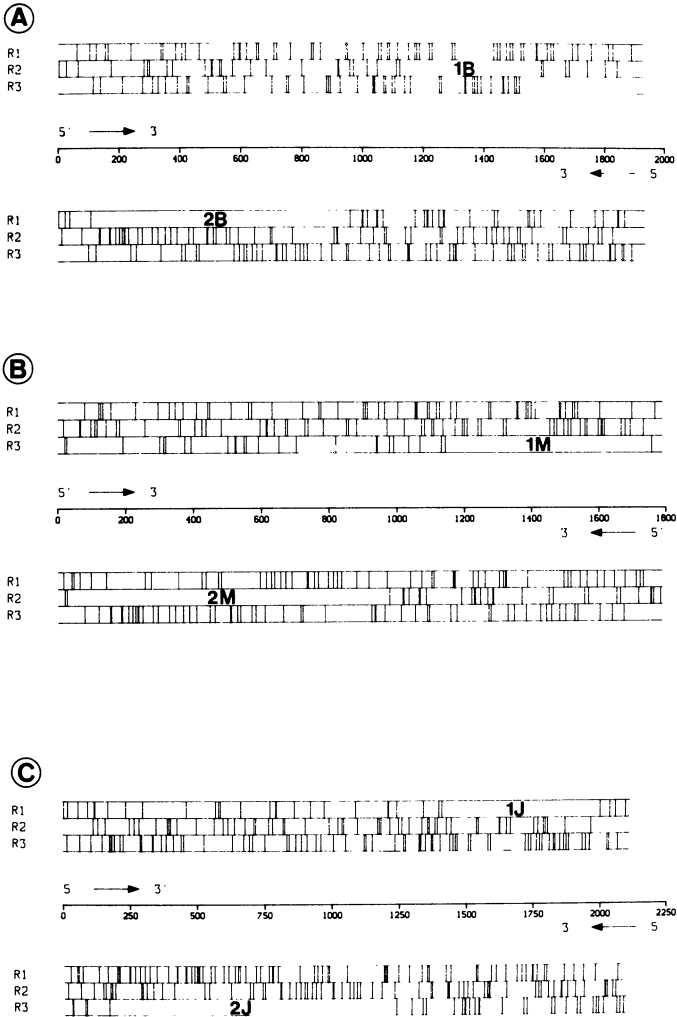


Fig. 14. Computer assisted analysis of the coding capacity of the repetitive DNA elements by the program stopcodon. Vertical lines indicate the position of stopcodons in the individual reading frames. Both DNA strands were screened in all three possible reading frames. Repetitive DNA element and flanking regions within the (A) EcoRI FLDV-f DNA fragment B, (B) EcoRI FLDV-f DNA fragment M, and (C) EcoRI FLDV-d DNA fragment J.

the results are summarized in Fig. 16 and 17. The amino acid sequences of ORF-1M (Fig. 16) and ORF-2M (Fig. 17) were used as reference for a comparison with the other ORFs of the corresponding repeats. Furthermore it was found that all putative proteins contain glycosylation signals as indicated in Fig. 16 and 17 (underlined N and marked with an asterisk).

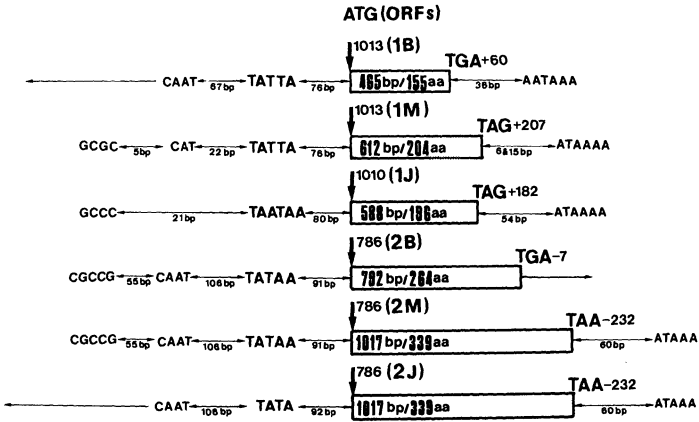


Fig. 15. The position of the classical or slightly modified promoter and termination signals found upstream and downstream of the start and termination codons of the individual ORFs, respectively.

ORF-1B	1	60
ORF-1M		METYLKIIINLNGETYKNESFDTCSHFIHHTIARHHKVCISICYLVNHRQKDCSIRTTKII	
ORF-1J		..M.....S.....T.....Q.....A.....	
ORF-1B	61V.....	120
ORF-1M		KLPDWIPLQTVIEVDQLYTLVIKDVKPMNRRTAILYACTLLCNKYLSYKESEALIKFFKLT	
ORF-1J	T.....I.....L.....	
ORF-1B	121FKRNYLYHSGFYRPINRSHG***	180
ORF-1M		IKKINIALEFLKTRIPNYSFNHTILYEPIVIELNMFNIPLDVGLYIMHYCKYKKSFKT	
ORF-1J	A.....S.N.....I.D.....Y.....Q.....	
ORF-1M	181	VWLEMTRKFTVHVTKINFCTAFH***	
ORF-1J	IYCSCY.N***	

Fig. 16. Comparative analysis of the amino acid sequence of putative proteins of the upper strand ORFs: 1B (18.5 kd), 1M (24.3 kd), and 1J (23.4 kd). The underlined asparagines (N) indicate glycosylation sites. The asterisks mark the termination codons.

```

ORF-2B 1 ..... 60
ORF-2M MITFMVIGGYGFLGRRIVQHLLSKCTRVKSIIIYDIKCTNVNWDLRVTFINGSIDRST
ORF-2J .....F.....A.....Y...E...S..I.....

ORF-2B 61 ..... 120
ORF-2M LIASMFNVDDVVFHCAEVKYKSDLDLELVNYTGTLNINACLNNVRCLYNGKFCNRFN
ORF-2J .....A.....L.N...E.....S.N.VLIVST

ORF-2B 121 ..... 180
ORF-2M DYFYNGDEYTDYYPTFSDTYAKTKYLAAVNICKADKSKTILGTILRTCSIKSGFIYGENN
ORF-2J II.TMVMNT.....

ORF-2B 181 ..... 240
ORF-2M TQFKQLFLNAFSKKTAFNWCYNHAAFQSKTYVGNVAVMHILAYKTLYNSTKADRAGGEIY
ORF-2J .....H..V.....A.....

ORF-2B 241 ..... 300
ORF-2M .....KQ***
ORF-2M FCYDNSPCLSTDEFNKIFLAEFNITTKSFSKPVLKTIARFNDFLLKWKQDVIVTSDYLKL
ORF-2J .....N..H.GL.....

ORF-2B 301
ORF-2M INTYCNFDTTKAANELDYAPLYSWSOSKYNVLSWLLTLV***
ORF-2J .....V..N.....T.....***

```

Fig. 17. Comparative analysis of the amino acid sequence of putative proteins of the lower strand ORFs: 2B (30.5 kd), 2M (39.2 kd), and 2J (38.8 kd). The underlined asparagines (N) indicate glycosylation sites. The asterisks mark the termination codons.

Promoter analysis

The promoter activity of the repetitive DNA sequence was tested using a newly constructed plasmid vector (pUC19-Cm^S-C2d) which is a derivative of pUC19 and harbors the complete polypeptide coding sequence of Tn9 chloramphenicol acetyltransferase gene (CAT). The CAT gene which contains the E.coli ribosome binding site but lacks the CAT promoter sequences was derived from pCM4 (21). The CAT gene was inserted into the HindIII site of the pUC19 in which the DNA sequences of the promoter region of the Lac-Z cassette between the restriction sites NdeI (nucleotide position 186) and Asp718 (nucleotide position 409) had been deleted. Consequently the CAT gene cannot promote and the transformants generated from this plasmid are chloramphenicol-sensitive. But it will give rise to chloramphenicol-resistant transformants when a DNA sequence with promoter function has been introduced upstream of the CAT gene.

In this study the EcoRI FLDV-f DNA fragment M harboring one copy of the repetitive DNA sequences of the viral

genome was inserted upstream of the CAT gene of pUC19-Cm^S-C2d vector, amplified using the competent E.coli K-12 C600 and screened for detecting chloramphenicol-resistant transformants. It was found that recombinant plasmids pUC19-Cm^r-LVf-EM-C4 and -C5 which harbor the FLDV-f EcoRI DNA fragment M in different orientations (Fig. 18) are able to generate chloramphenicol-resistant transformants. The transformants derived from the recombinant plasmid pUC19-Cm^r-LVf-EM-C4 which harbors the EcoRI FLDV-f DNA fragment M in the correct orientation (according to the physical map) had been found to utilize up to 2.5 mg/ml chloramphenicol substrate. This indicates that the repetitive DNA sequences of the FLDV genome possess in this orientation a strong promoter function. In contrast it was found that the transformants obtained from pUC19-Cm^r-LVf-EM-C5 which harbor the same viral insert but in the opposite orientation were only able to utilize chloramphenicol at a maximal concentration of 0.06 mg/ml. However, CAT activity was not detectable when the repetitive DNA elements were screened under the standard procedure for detecting promoter activity using mammalian cell cultures (22, 23). But this is in agreement with the results reported for the promoter function of the immediate-early FV 3 gene using CAT assay (24). A CAT activity was only found when the transfected cells were superinfected with FV 3 (24). But it is obvious that in the case of FLDV due to the insufficient virus propagation and very limited host range of the virus, analogous experiments are not feasible.

VIRAL PROTEINS

The FLDV proteins were prepared from purified virions which had been isolated directly from LD lesions of flatfish and analysed as described previously (9).

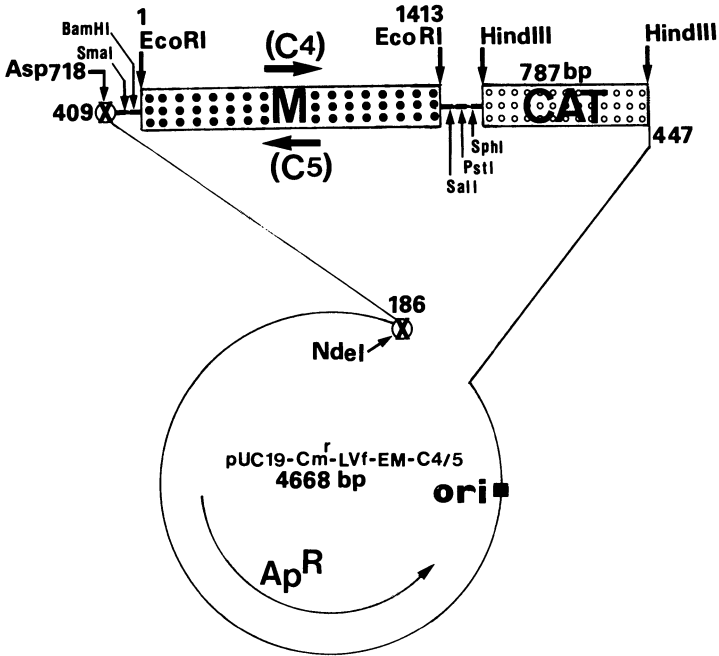


Fig. 18. Diagram of the recombinant plasmids pUC19-Cm^f-LVf-EM-C4 and C5 (4668 bp) constructed by insertion of the EcoRI FLDV-f DNA fragment M (1413 bp) upstream (18 bp) of the chloramphenicol-acetyltransferase gene of the parental vector pUC19-Cm^S-C2d. This vector contains the chloramphenicol-acetyltransferase gene which was derived from the CAT gene cartridge pCM4 (21) and inserted into the HindIII site of the pUC19 vector in which the DNA sequences between the nucleotide positions 186 (NdeI) and 409 (Asp718) had been deleted. The CAT gene consists of 787 bp including the ribosome binding region but lacks the promoter region (21). The DNA sequence of the EcoRI FLDV-f DNA fragment M (0.718 to 0.736 m.u.) which harbors one copy of the repeat element of the viral genome was inserted directionally (in both orientations) using the EcoRI/BamHI and EcoRI/SalI adapters in the BamHI and SalI sites (polylinker region) of the vector pUC19-Cm^S-C2d.

FLDV virions contain at least 33 polypeptides some of them have been shown to be glycosylated (9, 25). The molecular weights of FLDV polypeptides range from 14 to 220 kd (9). FLDV polypeptide patterns are similar when virus samples from different species (e.g. flounder and plaice) were compared. However the pattern is discernibly different from polypeptide patterns obtained from virions of dabs. In an effort to look for functional properties of the FLDV proteins, purified virions were assayed for the presence of enzymatic activities. Evidence for an FLDV-associated adenosine triphosphate phosphohydrolase has been documented (9). The ATPase seems to reside between core and envelope (13). In addition a DNase, a protein kinase, and a thymidine kinase activity were found to be associated with purified FLDV particles (13).

Thymidine kinase gene of FLDV

The thymidine kinase (TK) gene of FLDV was identified by biochemical transformation of 3T3 TK negative to 3T3 TK positive cells using specific viral DNA sequences as described previously (26). The TK locus has been mapped between the coordinates 0.669 to 0.718 (C19; 4.1 kbp, Fig. 19) of viral map units of the FLDV genome which is a part of the EcoRI DNA fragment C (11.2 kbp; 0.611 to 0.718 map units). The DNA sequence analysis of this particular region was carried out and the exact position of the initiation and termination of the TK gene (954 bp encoding 318 amino acid residues) was localized between the genome coordinates 0.678 to 0.688 of the viral map units (Fig. 19).

CONCLUSION

Fish lymphocystis disease virus is the causative virus for lymphocystis disease, a common chronic disease of pleuronectes. FLDV isolates can be classified

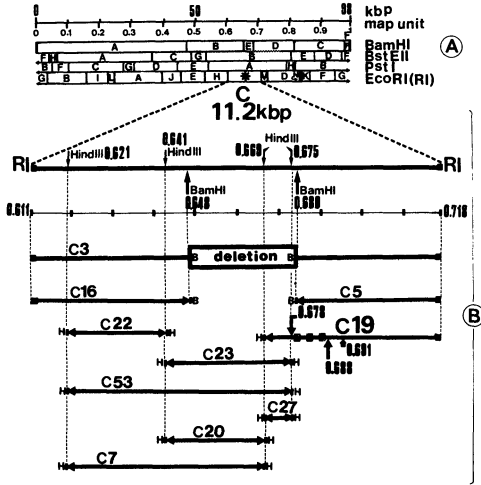


Fig. 19. Diagram of the restriction map of the EcoRI FLDV-f DNA fragment C and the map positions of the individual subclones established (panel B). Physical maps of the viral genome are given linearized (A) for the restriction endonucleases BamHI, BstEII, PstI, and EcoRI.

genetically into at least two different strains; strain 1 causes diseases in flounder and plaice, whereas the strain 2 is usually found in the lesions of lymphocystis of dabs (19). FLDV has many interesting properties e.g. the genome structure of FLDV was found to be circularly permuted and terminally redundant (8, 10) a common genomic feature to frog virus 3 (FV3) (27), insect iridescent virus type 6 (12, 14, 27), and type 9 (29) but unique among other eukaryotic viruses.

Another structural feature common to both FLDV and FV3 genome is the methylation in cytosine residues (30). However no DNA sequence homology was detectable between the DNA of FLDV and FV3 (8).

Repetitive sequences have been identified in the genome of numerous DNA and RNA viruses (31-40) which can be associated with important regulatory functions during viral replication. The search for the presence of repeti-

tive DNA sequences in FLDV DNA by DNA-DNA hybridization, electron microscopic heteroduplex mapping, and DNA nucleotide sequence analysis revealed a strong homology between the EcoRI DNA fragments B and M of FLDV-f and between the EcoRI DNA fragment B and J of FLDV-d. The coding capacity of the repetitive DNA sequences of the FLDV genome and their flanking regions was determined. This analysis revealed that each individual repeat element possesses two ORFs located at the upper and lower DNA strands. It is known that the propagation of FLDV in vitro is very limited and does not allow to use the standard molecular biological techniques necessary for the analysis of the viral RNA transcripts. From this point of view it was relevant and necessary to analyse the properties of the putative proteins in more detail. The analysis of the DNA sequences upstream and downstream of the start and termination codons of the putative proteins revealed the presence of classical or modified transcriptional signals. The detection of the eukaryotic polyadenylation signals (AATAAA) downstream (6 to 60 bp) of the termination codons of five ORFs is of great interest, because this is the first evidence for the existence of this particular signal in the family Iridoviridae (24, 41).

A search for amino acid sequence homologies between these putative proteins and the amino acid sequence of the proteins in the available data banks did not show any significant homologies (>22%) to other proteins.

Another interesting aspect for investigation of an eventual functional role of the detected repetitive elements in FLDV genome is the question whether or not the particular DNA sequences of these elements can be considered as promoters. It was found that the repetitive DNA sequences of the FLDV genome possess a strong promoter activity in prokaryotic system. In contrast CAT activity was not detectable when the repetitive DNA element was screened under the standard procedure for

detecting promoter activity using mammalian cell cultures. This is in agreement with the results reported for the promoter function of the immediate-early FV 3 gene using CAT assay (24). In this connection the following aspects should be considered: (i), it is known that the FLDV genome is naturally highly methylated (22%) in cytosine residues (17); (ii), that the molecularly cloned DNA sequences of the FLDV genome are not methylated at CpG sequences (10); (iii), that the genome of the original host (fish cells) of FLDV is also methylated (42), and (iv), that the physiological properties of the fish cell cultures are unknown and not comparable to those cell cultures routinely used for CAT assays. These facts could be essential for promoter function and gene activity of the FLDV genome in its eukaryotic target cells.

The TK gene locus of FLDV has been identified, molecularly cloned (26) and characterized. This gene is located between the genome coordinates 0.678 to 0.688 of the viral map units. This supports the previous report on the detection of a thymidine kinase gene activity in TK negative mouse cells after infection with frog virus 3 (43), another member of the family Iridoviridae.

In general it should be emphasized that with respect to the fact that the FLDV belongs to those viruses whose propagation in vitro is still very limited and insufficient the nucleotide sequence analysis of the FLDV genome is the most reliable approach for the further molecular biological characterization of this interesting virus. The determination of the nucleotide sequences of the viral genome allows to identify the translation units and the characterization of the related gene products can help to understand the transcriptional strategy of this virus.

ACKNOWLEDGEMENTS

This project was supported by the Deutsche Forschungsgemeinschaft Project II B 6-Da 142/2-1 to 2-4.

REFERENCES

1. Willis, D.B. In: Molecular Biology of Iridoviruses (Ed. G. Darai), Developments in Molecular Virology, Martinus Nijhoff Publishing, Boston, 1989, pp. 1-12.
2. Dunbar, C.E. and Wolf, K. J. Inf. Dis. 116: 466-472, 1966.
3. Russell, P.H. J. Fish Biol. 6: 771-778, 1974.
4. Lowe, K. IV. Trans. Norfolk and Norwich Nat. Soc. Fishes, 21-56, 1874.
5. Wolf, K., Gravell, M. and Malsberger, R.G. Science 151: 1004-1005, 1966.
6. Wolf, K. and Quimby, M.C. Appl. Microbiol. 25: 659-664, 1973.
7. Walker, D.P. and Hill, B.J. J. Gen. Virol. 51: 385-395, 1980.
8. Darai, G., Anders, K., Koch, H.G., Delius, H., Gelderblom, H., Samalecos, C. and Flügel, R.M. Virology 126: 466-479, 1983.
9. Flügel, R.M., Darai, G. and Gelderblom, H. Virology 122: 48-55, 1982.
10. Darai, G., Delius, H., Clarke, H., Apfel, H., Schnitzler, P. and Flügel, R.M. Virology 146: 292-301, 1985.
11. Darai, G. and Apfel, H. S. Karger, Basel, Develop. Biol. Standard. 59: 3-9, 1985.
12. Delius H., Darai, G. and Flügel, R.M. J. Virol. 49: 609-614, 1984.
13. Flügel, R.M. In: Current Topics of Microbiology and Immunology 116 (ed. D.B. Willis) Springer, Berlin/Heidelberg, 1985, pp. 130-150.
14. Schnitzler, P., Soltau, J.B., Fischer, M., Reisner, H., Scholz, J., Delius, H., and Darai, G. Virology 160: 66-74, 1987.
15. Schnitzler, P. and Darai, G. Virology (in press) 1989
16. Schnitzler, P., Delius, H., Scholz, J., Touray, M., Orth, E., Darai, G. Virology 161: 570-578, 1987.
17. Waalwijk C. and Flavell, R.A. Nucl. Acids Res. 5: 3231-3236, 1978.
18. Wagner H., Simon, D., Werner, E., Gelderblom, H., Darai, G. and Flügel, R.M. J. Virol. 53: 1005-1007, 1985.
19. Darai, G. In: Pathology of Marine Aquaculture (Pathologie en aquaculture marine) (ed. C.P. Vivares, J.-R. Bonami, and E. Jaspers) European Aquaculture Society, Special Publication No. 9. Bredene, Belgium, 1986, pp. 261-280.

20. Davis R.W., Simon, M. and Davidson, N. *Enzymol.* 21: 413-428, 1971.
21. Close, T.J. and Rodriguez, R.L. *Gene* 20: 305-316, 1982.
22. Gorman, C.M., Moffat, L.F., and Howard, B.H. *Mol. Cell. Biol.* 9: 1044-1051, 1982.
23. Crabb, D.W. and Dixon, J.E. *Anal. Biochem.* 163: 88-92 1987.
24. Beckman, W., Tham, T.N., Aubertin, A.M., and Willis, D.B. *J. Virol.* 62: 1271-1277, 1988.
25. Robin, J., Lapierre, A., and Berthiaume, L. *Arch. Virol.* 87: 297-305, 1986.
26. Scholz, J., Rösen-Wolff, A., Touray, M., Schnitzler, P., and Darai, G. *Vir. Res.* 9: 63-72, 1988.
27. Goorha R. and Murti, K.G. *Proc. Nat. Acad. Sci. USA* 79: 152-248, 1982.
28. Soltau, J.B., Fischer M., Schnitzler, P., Scholz, J., and Darai, G. *J. gen. Virol.* 68: 2717-2722, 1987.
29. Ward, V.K. and Kalmakoff, J. *Virology* 160: 507-510, 1987.
30. Willis D.B. and Granoff, A. *Virology* 107: 250-257, 1980.
31. Wittek, R. and Moss, B. *Cell* 21: 277-284, 1980.
32. Pickup, D.J., Bastia, D., Stone, H.O., and Joklik, W. K. *Proc. Natl. Acad. Sci. USA* 79: 7112-7116, 1982.
33. Bugert, J.J., Rösen-Wolff, A., and Darai, G. *Virus Genes*, 1989 (in press).
34. Fischer, M., Schnitzler, P., Scholz, J., Rösen-Wolff, A., Delius, H., and Darai, G. *Virology* 167: 497-506, 1988.
35. Fischer, M., Schnitzler, P. Delius, H., and Darai, G. *Virology* 167: 485-496, 1988.
36. Ward, V.K. and Kalmakoff, J. In: *Invertebrate Iridoviruses*, 1989 (in press).
37. Wadsworth, S., Jacob, R.J., and Roizman, B. *J. Virol.* 15: 1487-1497, 1975.
38. Åstrand, J. and Roberts, R.J. *J. Mol. Biol.* 128: 577-594, 1979.
39. Reddy, E.P., Smith, M.J., Canaani, E., Robbins, K.C., Tronick, S.R., Zain, S., and Aaronson, S.A. *Proc. Natl. Acad. Sci. USA* 77: 5234-5238, 1980.
40. Shoemaker, C., Goff, S., Gilboa, E., Paskind, M., Mitra, S.W., and Baltimore, D. *Proc. Natl. Acad. Sci.* 77: 3932-3936, 1980.
41. Willis, D., Foglesong, D., and Granoff, A. *J. Virol.* 53: 905-912, 1984.
42. Vanzushin, B.F., Mazin, A.L., Vasilyev, V.K., and Belozersky. *A.N. Biochim. et Biophys. Acta* 299: 397-403, 1973.
43. Aubertin, A. and Longchamps, M. *Virology* 58:111-118, 1974.

11

HEPATOTOXICITY OF IRIDOVIRUSES

H. LORBACHER DE RUIZ

Zentrale Versuchstieranlage der Universität Heidelberg,
Im Neuenheimer Feld 345, 6900 Heidelberg, Federal
Republic of Germany

ABSTRACT

Infection of mice or rats with Chilo Iridescent Virus, type 6 (CIV) or Frog Virus 3 (FV 3) produces an acute degenerative hepatitis leading to the death of the animals in less than 24 hr. The integrity of the viral genome is not required for pathogenic expression since solubilized viral proteins exhibit pathogenic properties similar to those of intact virus.

INTRODUCTION

Pathogenicity of viruses is commonly related to their ability to multiply within the host's cells. Synthesis of cellular RNA, DNA, and proteins of the target organs is inhibited leading finally to necrosis and cellular death.

Alternatively, cytopathic effects may be produced by direct interaction of certain viral components, such as cytotoxic proteins, with target cells (8). The acute degenerative hepatitis induced by FV 3 or CIV in mice or rats provides clear evidence for the alternate pathway (3, 11, 19, 23). Like most Iridoviruses, FV 3 and CIV are highly thermosensitive and replication is confined to poikilothermic animals (9, 10, 13).

The pathogenesis of FV 3 induced hepatitis in mice and rats is dominated by two kind of events. The early

destruction of the Kupffer cells and the endothelial cells, which are the primary targets of the virus, leads to breakages in the sinusoidal wall. Hepatocellular lysis that occurs later in the disease seems to be mediated by other factors, such as bacterial endotoxins (15) and/or leucotrienes (16, 17).

DEGENERATIVE HEPATITIS IN MICE AND RATS

Parenteral inoculation of purified or crude preparations of FV 3 or CIV into mice or rats produces a rapidly fatal hepatitis (11, 14, 19, 23). Death rate is closely related to the quantity of particles injected. There is also a directly proportional relation between the time of death and the dose of virus administered. In mice death occurs within 24 hr after injection of one LD 100 preparation of FV 3 or CIV (Table 1). The average death time in rats was found to range between 19 and 30 hours after injection of one to five LD 100 of FV 3. There exists considerable difference in sensitivity to the lethal effect of FV 3 between the two animal species and different animal strains studied (14, 19, 23).

Clinical symptoms are hardly noticeable throughout the major part of the illness except during the early and ultimate phases. The first signs of illness appear 5 to 8 hr after infection. The animals no longer take food or water and remain huddled together without moving. In this state their fur stands on end, they tremble, and mice develop severe vasodilatation of the eyes. In rats cutaneous vasodilatation of ears and feet can be seen. Shortly before death the animals display total prostration with respiratory disorders, stiffing of the limbs, and spasmodic crises (14, 23).

Acute hepatitis can also be produced with inactivated virus (4, 23) or with structural proteins solubilized from the virion (3). Intravenous administration of solubilized extracts from FV 3 kills mice within

Table 1. Induction of acute toxic hepatitis in mice, strain Balb/c, using Insect Iridescent Virus (CIV) and Frog Virus 3 (FV 3).

Inoculum	Dose/ animal	No. of animals inoculated/dead	Time of death post infection (hr)	Rate of mortality (%)
CIV, untreated	1.0 x 10 ^{11a}	18/4	23 to 25	22.5
CIV, untreated	9.2 x 10 ^{11a}	4/4	20 to 26	100
CIV, 80° C, 30 min		6/0	-	0
CIV, 0.25% SDS at 37° C, 30 min		6/0	-	0
	9.2 x 10 ^{11a}			
CIV, proteinase K, 37° C, 15 min		6/1	40	16.7
CIV, DNase I and RNase A, 37° C, 60 min		5/6	21 to 72	83.3
FV 3, untreated	1.0 x 10 ^{10b}	35/26	8 to 24	74.3

a, TCID₅₀ ; b, PFU

24 hr. Illness is not seen after heating the viral preparation for 30 min at 80⁰ C or submitting it to digestion (3, 23). These findings and the all-or-nothing response to intact virus give evidence for the toxic origin of the hepatitis.

Additionally, joint administration of FV 3 and phenol-extracted lipopolysaccharides (LPS) from *Enterobacteriae* leads to an aggravation of hepatocellular lesions and shortens the interval between infection and death (15).

DISSEMINATION OF VIRUS IN THE ORGANISM

Radioactive FV 3 has been used in mice and rats to determine its distribution in the various organs of the host. After intravenous administration of one LD 100 blood radioactivity rapidly decreased and leveled off after 20 min. At that time the virus titer has fallen by 97 %. The stability of the residual value observed during the next 6 hr of infection proved that the organic distribution of the virus was definite (14).

Dissemination of the virus seems to be determined only by two factors: the blood flow in the organs and their richness in virus-phagocytosing cells (26). Accordingly, maximal radioactivity is found in the liver, followed by the lungs, intestine, spleen, and kidneys. The liver contains more than 70 % of the virus particles. There exists a time correlation between the outbreak of hepatitis and the presence of virus in the liver. When mice were immunized prior to challenge with radioactive virus, penetration of the virus into the liver was inhibited, parenchymal damage did not occur and the animals survived (20).

MORPHOLOGICAL LESIONS

Diseased animals, infected with FV 3 or CIV, show major pathological changes in the liver, the spleen, the

kidneys, and occasionally in the upper part of the intestine and the heart. No lesions are seen in the lungs. All affected organs display a various degree of congestion. The liver, however, is heavily congested and small necrotic lesions are found in the entire organ. Histopathological studies reveal two types of lesions: massive parenchymal cell necrosis and acute capillary and portal stasis (Fig. 1). The hepatocytes show various forms of necrotic injuries, such as fatty degeneration of the cytoplasm, acidophilic necrosis, and nuclear alterations (Fig. 2).

Ultrastructural examinations of the liver from mice sacrificed 1 hr after challenge with FV 3 reveal similar signs of heavy cell damage (6, 11). Whereas the cytoplasm of the parenchymal cells remain free of lesions, display the nuclei of the hepatocytes a variety of alterations: modification in shape and chromatin condensation, margination of the perinuclear chromatin, considerable disappearance of the nucleoplasmic fibrillar material where numerous interchromatin granules are clustered, and increase of the fibrillar material of the nucleolus (Fig. 3).

The nuclear lesions, once under way, reach their maximal intensity from the onset, and it is only in the number of nuclei damaged that there is a variation according to the lapse of time. Thus, in rats infected with FV 3, 30 % of the nuclei are damaged 1 hr after infection and 60 to 70 % 3 hr later (14). Sinusoidal cells, initially Kupffer cells and then endothelial cells, are the primary target for the viral toxin (25). Shortly after infection the cytoplasm of the Kupffer cells contains numerous dense bodies, multiple small vesicles, vacuoles, and some damaged mitochondria. Generalized destruction of the Kupffer cells is completed 2 to 3 hr later and then first interruptions in the endothelial lining appear (12). Subsequently, hepatocytes

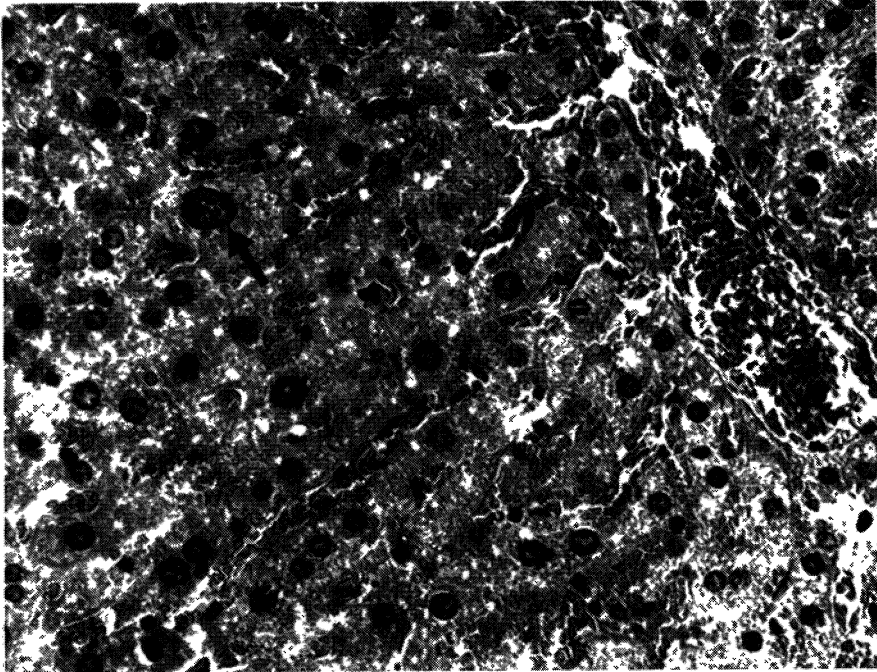


Fig. 1. Microphotograph of a liver section from a mouse, strain Balb/c, inoculated with Chilo Iridescent Virus. The animal died 18 hr p. i. (HE x 250). Hepatocytes with pycnotic nuclei and diffuse necrosis. Arrow indicates giant nuclei (Lorbacher de Ruiz, H. et al., *Med. Microbiol. Immunol.* 175, 43, 1986).

come into direct contact with the content of the sinusoid. Once deprived of the protection by the sinusoidal cells, hepatocytes take up material that they normally exclude, such as carbon, latex particles, Vaccinia virus, and become sensitive to endotoxins (12, 16, 18, 21, 22, 24, 25, 27).

Although the nuclei of the hepatocytes present already in the early stage of infection characteristic alterations, remains the cytoplasm initially free of lesions (5). It is only 4 to 14 hr later that cytoplasmatic damage can be seen: degranulation of the granular

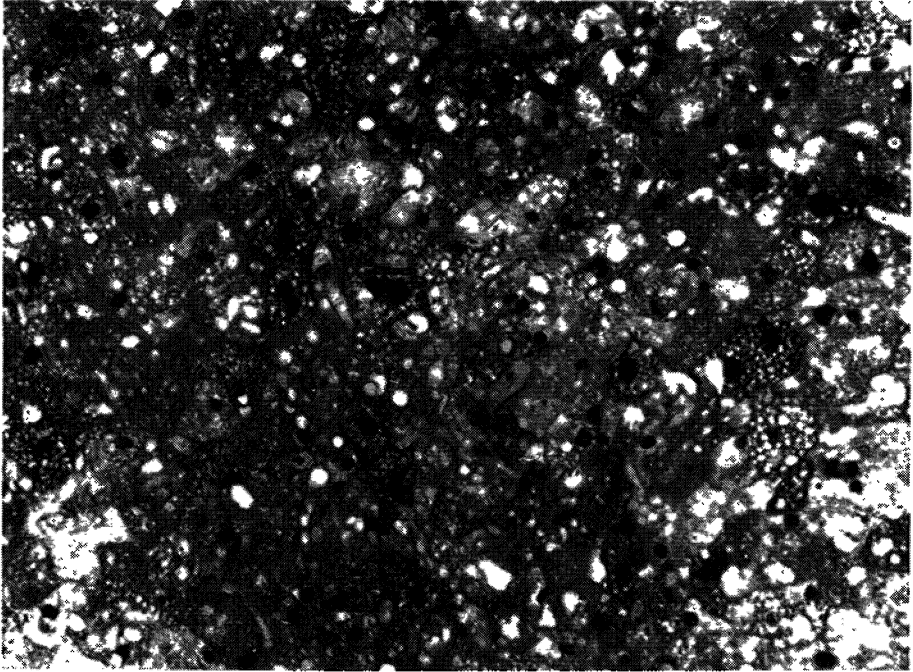


Fig. 2. Microphotograph of a liver section from a mouse, strain Balb/c, inoculated with Chilo Iridescent Virus. The animal died 29 hr p.i. (HE x 250). Microvesicular fatty changes of the cytoplasm, pycnotic nuclei and diffuse necrosis (Lorbacher de Ruiz, H. et al., *Med. Microbiol. Immunol.* 175, 43, 1986).

endoplasmatic reticulum, hypertrophy of the smooth endoplasmatic reticulum, and finally lysis of the mitochondria.

BIOCHEMICAL CHANGES IN MACROMOLECULES OF THE LIVER

Morphological damage of hepatocytes produced by FV 3 infection in mice and rats seem to coincide with perturbations in the metabolism of the liver macromolecules. Only a few hours after infection considerable inhibition in DNA, RNA, and to a lesser extent, protein synthesis can be seen. Synthesis of hepatocellular RNA decreases within 1 hr after infection and reaches a maximal value of 58 % after 3 to 4 hr (11, 14). Synthesis

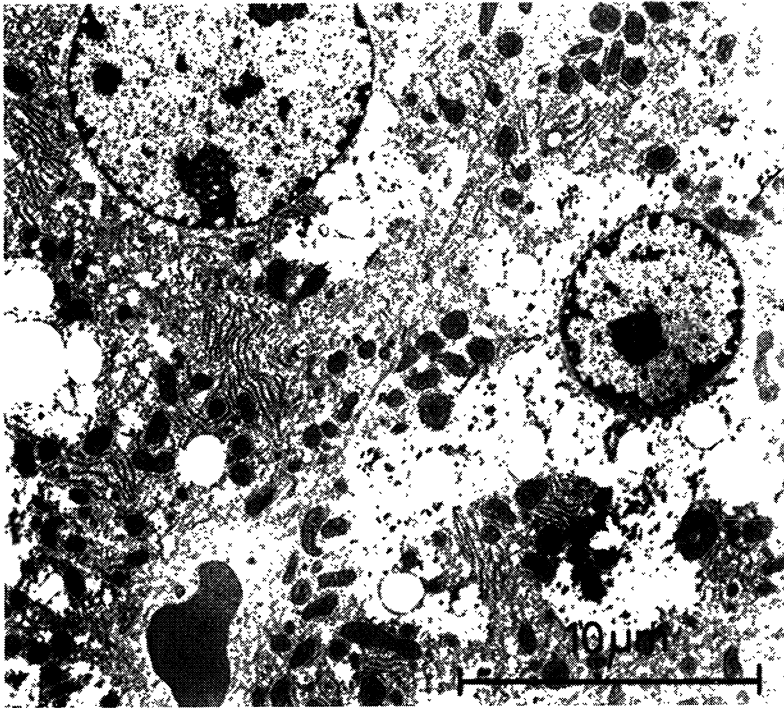


Fig. 3. Electron microphotograph of ultrathin section of a liver of a mouse, strain Balb/c, inoculated with Chilo Iridescent Virus and sacrificed when moribund 23 hr p.i. The parenchymal cells show similar signs of heavy cell damage. Formation of numerous lipid droplets, loss of mitochondrial cristae, and small cytoplasmic vacuolation reflect toxic and hypoxic disorder and a metabolic brake-down. Glycogen deposits are emptied. Golgi zones and polysomes are broken down, while the stacks of the granular reticulum are still intact (Lorbacher de Ruiz, H. et al., *Med. Microbiol. Immunol.* 175, 43, 1986).

activity is then maintained at a constant level at a mean residual rate of 45 %, at least for 8 hr. There's no preferential inhibition of the ribosomal or messenger RNA synthesis.

In hepatocyte nuclei from FV 3 infected mice inhibition of RNA polymerase activity reaches 50 to 60 % 4 hr after challenge. Isolated hepatocyte nuclei of these

animals demonstrate also a smaller amount of active DNA polymerase.

Metabolic alterations in the cytoplasmatic fraction of hepatocytes, however, are seen only at the late stage of infection. Activity of certain cytoplasmatic enzymes, such as DNA polymerase and thymidine kinase remain unaffected until 8 hr post-infection. Evidence is given that certain morphological alterations of the hepatocytes can be linked with metabolic changes. Furthermore, temporal as well as quantitative correlation between metabolic inhibition and the occurrence of morphological lesions seems to exist.

Studies in vivo and in vitro with soluble viral extracts (SVE) prepared from FV 3 reveal similar effects on nucleic acid synthesis of the host cell (1, 2, 11). Comparable observations are made after infection with CIV (23). Shut-off of macromolecular metabolism occurs within 17 hr after infection of non-permissive cell lines (8). Synthesis of DNA, RNA, and proteins can be inhibited also by viral extracts alone.

CONCLUSIONS

Similarities of action in the hepatotoxic mechanism of FV 3 and CIV infection in experimental animals suggest that this activity is associated with one or several structural proteins of these Iridoviruses. Lesions occur under permissive and non-permissive conditions for virus replication and are seen in the absence of intact viral DNA. Rapid manifestation of biochemical and morphological changes in the host cells, preferentially the nuclei, and correlation between inoculum size and the lapse of time before death, are strong evidence for the toxic nature of these proteins.

FV 3 infection provides a new experimental model for studies of the pathogenesis of hepatic diseases. On account to its particular structure the virus is taken

over by phagocytic cells; it is thus concentrated in the Kupffer cells and becomes uncoated. The subsequent release of toxic proteins leads to the lysis of the Kupffer cells, which are particularly sensitive to any metabolic inhibition (7). A deficiency in the clearance of endogenous endotoxins occurs and is exacerbated by damage to the endothelial lining. The endothelial cells seem to suffer only indirect damage since they contain either viral particles or viral proteins.

The following hepatocellular degeneration is initiated by viral proteins. The presence of these proteins is responsible for the inhibition of cellular macromolecular synthesis and for the nuclear damage of the hepatocytes. Hepatocytolysis, however, has to be attributed to either potentially harmful mediators, e.g. leucotrienes, released from impaired Kupffer cells (16, 17), or to the interaction of endogenous endotoxins that are not properly cleared (15).

Determination of the nature of these viral proteins could provide a better understanding of their action and role in hepatic disease.

REFERENCES

1. Aubertin, A. M., Hirth, C., Travo, C., Nonnenmacher, H., and Kirn, A. J. *Virology* 11: 694-701, 1973.
2. Aubertin, A.M., Travo, C., and Kirn, A. J. *Virology* 18: 34-41, 1976.
3. Aubertin, A.M., Anton, M., Bingen, A., Elharrar, M., and Kirn, A. *Nature* 265: 456-457, 1977.
4. Bingen-Brendel, A., Bätzenschlager, A., Gut, J. P., Hirth, C., Vetter, J.M., and Kirn, A. *Ann. Inst. Pasteur* 122: 125-142, 1972.
5. Bingen, A., and Kirn, A. J. *Ultrastructure Res.* 45: 343-355, 1975.
6. Bingen, A., and Kirn, A. J. *Ultrastructure Res.* 50: 167-173, 1975.
7. Brinton, M.A., and Plagemann, P.G.W. *Intervirology* 12: 349-356, 1979.
8. Cerutti, M., and Devauchelle, G. *Arch. Virology* 63: 297-303, 1980.

9. Cerutti, M., Guerillon, J., Arella, M., and Devauchelle, G. *CR Acad. Sci. Paris* 292: 797-802, 1981.
10. Devauchelle, G., Attias, J., Monnier, C., Barray, S., Cerutti, M., Guerillon, J., and Orange-Balange, N. *Current Topics in Microbiology and Immunology* 116: 37-48, 1985.
11. Elharrar, M., Bingen, A., Gendrault, J.L., and Kirn, A. In: *Pathogenesis and Mechanisms of Liver Cell Necrosis*. MTP Press Ltd, Lancaster, 1975, pp 75-86.
12. Gendrault, J. L., Steffan, A. M., Bingen, A., and Kirn, A. In: *Kupffer Cells and Other Liver Sinusoidal Cells*. Elsevier North Holland Biomed. Press, Amsterdam, 1977, pp 223-232.
13. Granoff, A., Came, P. F., and Breeze, D.C. *Virology* 29: 133-148, 1966.
14. Gut, J. P., Anton, M., Bingen, A., Vetter, J. M., and Kirn, A. *Lab. Invest.* 45: 218-228, 1981.
15. Gut, J. P., Schmitt, S., Bingen, A., Anton, M., and Kirn, A. *J. Infect. Dis.* 149: 621-629, 1984.
16. Hagman, W., Steffan, A. M., Kirn, A., and Keppler, D. *Hepatology* 7: 732-736, 1987.
17. Hagman, W., and Keppler, D. In: *The Liver: Biology and Pathobiology*. Raven Press Ltd., New York, 1988, pp 793-806.
18. Kief, H., Baehr, H., Deutschlaender, N., and Engelbart, K. In: *Activation of Macrophages*. Excerpta Medica, Amsterdam, 1974, pp 31-39.
19. Kirn, A., Gut, J. P., Bingen, A., and Hirth, C. *Arch. ges. Virusforsch.* 36: 394-397, 1972.
20. Kirn, A., Gut, J. P., Steffan, A. M., and Gendrault, J. L. *Interviol.* 2: 244-252, 1973/74.
21. Kirn, A., Gut, J. P., Bingen, A., Steffan, A.M. *Hepatology* 3: 105-111, 1983.
22. Knook, D. L., and Sleyster, E. C. *Biochem. Biophys. Res. Comm.* 96: 250-275, 1980.
23. Lorbacher de Ruiz, H., Gelderblom, H., Hofmann, W., and Darai, G. *Med. Microbiol. Immunol.* 175: 43-53, 1986.
24. Mori, M., and Novikoff, A. B. *J. Cell Biol.* 72: 695-706, 1977.
25. Popper, H. In: *The Liver: Biology and Pathobiology*. Raven Press Ltd., New York, 1988, pp 1087-1103.
26. Sljivic, V.S. *Experientia* 25: 1004-1006, 1969.
27. Steffan, A.M., and Kirn, A. *J. Reticuloendothel. Soc.* 26: 531-537, 1979.

12

AFRICAN SWINE FEVER VIRUS

JOÃO V. COSTA

Gulbenkian Institute of Science, Apartado 14, P-2781
Oeiras Codex, Lisboa, Portugal.

ABSTRACT

African swine fever is a devastating disease of swine caused by an icosahedral enveloped DNA virus which grows in the cytoplasm of infected cells. The virus infects domestic pigs and African or European wild boars, and can be transmitted by soft ticks. A peculiar feature of the infection is the lack of induction of neutralizing antibodies, which has prevented the production of a conventional vaccine. The viral particle contains about 50 proteins, including cell proteins like actin and tubulins that are specifically encapsidated. In contrast to most enveloped viruses, there is no glycoprotein in the virus particle. The viral genome is a double-stranded DNA molecule of about 180 kbp. The extremes of the viral DNA are cross-linked by short imperfectly paired hairpin loops which are complementary to each other. At the ends of the genome there are also terminal inverted repeats composed of tandems of short direct repeats. The virus grows in swine macrophages but can easily be adapted to grow in monkey cells. Penetration is done by receptor-mediated endocytosis. Although the presence of the nucleus is required, viral replication occurs only in the cytoplasm. The virus particle thus has all the enzymes needed for early transcription and processing of mRNA. More than one hundred virus-induced proteins can be identified. The kinetics of synthesis are complex. Inhibitors

of DNA replication can distinguish between early proteins, synthesized before DNA replication, and late proteins, that depend on the synthesis of viral DNA. Replication of the viral DNA is catalyzed by a phosphonoacetic acid-sensitive virus-induced DNA polymerase. The mechanism of DNA replication is not well known. Large concatemers seem to be an intermediate in replication.

THE DISEASE

African swine fever is the most devastating disease of swine. Its agent is a DNA virus, with an icosahedral capsid and an envelope, that grows in the cytoplasm of infected cells and which was classified until recently as an iridovirus. Three main reasons make African swine fever the most important threat to swine populations all over the world: i) the virus does not induce the production of neutralizing antibodies and so the production of a conventional vaccine has not been possible; ii) wild boars and ticks that enable the replication of the virus are reservoirs difficult to control; iii) healthy carriers or animals showing mild forms of the disease that are difficult to diagnose are appearing with increasing frequency. Thus, control of the spread of the disease still relies exclusively on rapid diagnosis, drastic slaughter and sanitary barriers to the trade of pig or pork products.

Extensive descriptions and detailed reviews have been published on the history and characteristics of the disease, its dissemination and control (1-9). Hence, the description presented here will be brief.

The virus probably existed undetected in African wild boars but the disease was only recognized after the introduction into Africa of European domestic pigs. In 1921 Montgomery (1) described some cases of the disease in Kenya dating from 1910, established its viral origin, described many of the characteristics of the virus and

proposed the transmission of the disease from wild swine. He also reported the impossibility of protecting against African swine fever virus (ASFV) by passive immunization.

Until 1957, the disease was detected only in Africa but in that year an outbreak was diagnosed in Portugal, near the airport of Lisbon (10). It is presumed that it was due to feeding pigs with infected spills from a meal served during a flight from Angola. This first outbreak out of Africa was apparently eradicated at the cost of about 17,000 dead pigs, either from the illness or slaughtered because they had been in contact with sick animals.

In 1960 the disease reappeared in Portugal (11) and spread to Spain (12). At that time the disease could not be completely eradicated and became endozootically established in the Iberian peninsula. The inoculation of about half-a-million pigs in Portugal with an attenuated vaccine (13) probably contributed to further spread of the disease in Portugal, in a milder or even unrecognized clinical form.

After the disease became established in Portugal and Spain, it also appeared in the 60s and early 70s in France (14), Italy (15) and Cuba (16). Later, coinciding with a period of very frequent outbreaks in Portugal and Spain, in 1977-78, the disease was detected in Malta (17), Sardinia (18), Brazil, Haiti and the Dominican Republic (19). In most of these cases the disease was eradicated, with very important losses, but it still exists in Haiti and Sardinia. The latest appearances of the disease out of the areas where it is endemic occurred in Belgium in 1985 and in The Netherlands in 1986.

Initially, African swine fever always occurred as a fulminating hyperacute disease with practically 100% lethality. After an incubation period of 4 to 10 days, sick animals show high fever, dyspnea, erythema, pro-

stration, and die within one to three days (1, 20). After the disease became established in the Iberian Peninsula, acute and subacute forms of the disease became more frequent and are the most commonly observed clinical forms of the disease (21, 22). The clinical picture is not pathognomonic and is easily confused with other diseases, namely classical hog cholera. The first symptom is high fever, followed soon after by constitutional symptoms like inappetence, adynamia and somnolence. Infection of the reticuloendothelial system and of circulating macrophages causes circulatory and vascular damage, leading to hemorrhages in the skin, kidney, lymph nodes and large intestine. Spleen enlargement due to hyperplasia and pulmonary consolidation or edema are also observed. Death usually supervenes within 4-8 days after the appearance of the symptoms. Subacute forms are essentially similar to acute forms but the symptoms are generally less accentuated, the course of the disease is slower, and the mortality is lower.

Pigs that survive the subacute disease may develop a chronic form (20-22). This form of the disease was also observed in pigs that received attenuated live vaccines in Portugal and Spain (13). Pneumonia is a common feature, together with arthritis and skin ulcerations. The mortality rate is highly variable.

In all the forms of the disease virus replication occurs mainly in mononuclear phagocytting cells. In lymphatic tissues macrophages and reticular cells are the main target cells while monocytes and occasionally polymorphonuclear leukocytes and megakaryocytes are the main cells infected in the blood or bone marrow (23).

The lack of a pathognomonic clinical picture emphasizes the need of final laboratory diagnosis (for a review, see ref. 24). In acute or subacute cases, and some chronic infections, diagnosis is done by isolation of the virus. A variety of methods is available for

identification of viral antigens in infected tissues or blood. The most used test for some years was hemadsorption but it is laborious, time-consuming and leaves some nonhemadsorbing isolates undetected. The method has been replaced most frequently by immunofluorescence using serum from animals immunized with virus of low virulence. As an alternative to the immunological detection of the virus, DNA probes are being produced and their diagnostic value is under evaluation (25; G. Ribeiro, personal communication). Molecular probes will also be very useful for the sanitary control of pork products. In chronic infections or in healthy carriers it is difficult or impossible to detect the virus in infected tissues and the diagnosis is usually done by detecting antibodies against ASFV. Immunofluorescence of ELISA are the most commonly used methods of serological diagnosis.

THE VIRUS IN THE NATURE

The only mammals that are infected by ASFV are the domestic pig and other members of the family Suidae. In Africa the virus is carried by healthy wart hogs (Phacochoerus aethiopicus) and bush pigs (Potamochoerus porcus) (1). The giant forest hog (Hylochoerus meinertzhageni) is also sensitive to the virus (26). In the western hemisphere feral pigs could also be experimentally infected (27). After the infection became established in the Iberian Peninsula and in Sardinia, European wild boars (Sus scrofa ferus) have also played the role of African wild swine as reservoirs in the nature (12). In Africa, only young wild boars have viremia and propagate the virus. A more efficient way of transmission than contact is probably needed for maintaining the virus in its natural reservoirs.

The first demonstration of vector transmission was due to Sánchez Botija who isolated the virus from Iberian soft ticks (Ornithodoros erraticus) found in piggeries

affected by outbreaks of African swine fever (28). Following this report, the interest on parasites of African wild boars was renewed, in spite of the many unsuccessful previous attempts to find a vector. The virus could then be isolated from soft ticks (Ornithodoros porcinus porcinus, formerly O. moubata) inhabiting warthog burrows (29). Plowright and his collaborators demonstrated that the virus replicates in the insect's gut after ingestion, spreads to other organs including the sexual organs and the salivary glands, and that ticks transmit the virus to swine during engorgement (30). The virus is transmitted between ticks by transovarial, transtadial and sexual routes (31, 32). It seems that most or all Ornithodoros species can replicate and transmit the virus. Another African species, O. savignyi, and three American species, O. coriaceus, O. turicata, and O. puertoricensis, have been experimentally infected (referred to by Hess, 33). There may be other vectors in areas where the soft ticks do not exist. However, none of the other parasites of swine that have been tested was found to be susceptible to the virus (30).

IMMUNOLOGY

The most striking aspect of the immune response against ASFV is the lack of production of neutralizing antibodies both by pigs recovering from the disease and by laboratory animals inoculated with the virus (34). This is not due to a generalized impairment of antibody production as the animals synthesize virus-specific antibodies that fix complement (34), inhibit hemadsorption by infected cells (35), or immunoprecipitate viral antigens (36, 37). In spite of the absence of neutralization, an immune protection seems to be elicited as surviving animals or animals inoculated with attenuated virus are resistant to reinfection with homologous virulent

virus (38). Antibodies detected by antibody-dependent cell cytotoxicity (ADCC) or by complement-dependent antibody lysis were shown to reduce virus production in vitro (39, 40) and may be responsible for the protection observed in vivo. Alternatively, cellular immunity may be the mechanism responsible for protection. After inbred swine with defined swine lymphocyte antigen haplotypes were available, MHC-I-restricted cell-mediated cytotoxicity against infected macrophages could be demonstrated (41). As experiments on passive immunization with transferred cytotoxic T lymphocytes have not been reported yet, it is uncertain whether cytotoxicity is responsible for the protection against reinfection.

THE VIRUS PARTICLE

Purification

The starting material for virus purification can be extracellular virus or cell-associated virus. Extracellular virus is much cleaner but is still contaminated with membrane vesicles that are difficult to separate from the virus (42). Contamination with vesicles is particularly confusing for the study of virion proteins because the vesicles are rich in virus-induced but nonstructural proteins (43). The other difficulties in virus purification result from its considerable sensitivity to high ionic strength and to high osmotic pressure and its great tendency to form aggregates (44). Former methods included centrifugation in sucrose (44-46), Ficoll (46), sucrose-cesium chloride (47), and potassium tartrate gradients (48), after treatment such as polyethylene glycol precipitation (46, 49) or treatment with hydroxyapatite (48). Aggregation of the virus particles could be partially avoided by treating the viral materials with Tween 80 and centrifuging always at high salt concentrations. All these methods result in heavy contamination with vesicles and in very low

recovery of infectivity, less than 1% of the starting material. In 1985, Carrascosa et al. (50) introduced a new method that improved significantly the purification of the virus and will most probably become the standard method for virus purification. Extracellular virus is easily separated from the vesicles by two centrifugations in isotonic Percoll gradients and then Percoll is separated from the pelleted virus by chromatography on Sephacryl S-1000. Purified virus preparations with 15-20% of the initial infectivity can be obtained (50, 51). The degree of elimination of vesicles can be easily monitored by the absence of a 220 kilodalton virus-induced protein that is very abundant in the vesicles (43, 51) and which was previously considered as being one of the major structural proteins. Purified viral particles have a sedimentation coefficient of 3500 ± 300 S and band in Percoll at a density of 1.095 g/ml. Purified virus is stable at -70°C for some months.

Morphology

Early electron microscopy studies of ASFV demonstrated its icosahedral structure, its release by budding from the infected cells with the acquisition of an external envelope, and its morphological similarity to iridoviruses (52, 53). These initial studies were followed by a number of other observations that contributed to a model of the virus structure (for references see ref. 8). More recently, freeze-drying and computerized image processing of electron micrographs confirmed the basic features of that structure and enabled a better knowledge of the virus morphology (54). The virus particle has an average diameter of about 200 nm. Its inner component is a dense nucleoid of 70-100 nm diameter, containing the viral DNA. The nucleoid is separated from the capsid by an internal membrane with the characteristics of an unit membrane. The capsid is

icosahedral, with an estimated triangulation number between 189 and 217, which corresponds to 1892 to 2172 capsomeres. The capsomeres are seen as hexagonal prisms, 13 nm long and 5-6 nm wide, with a central hole. The intercapsomere distance is between 7.4 and 8.1 nm.

The viral genome

The effect of inhibitors of DNA synthesis on virus replication (55, 56) and the autoradiographic detection of thymidine incorporation into the cytoplasmic inclusion bodies (57) gave a first indication that ASFV is a DNA virus. The study of DNA from purified virus showed that viral DNA is a double-stranded linear molecule of about 170 kbp, with a sedimentation coefficient of 60S, a length of about 58 nm and a $Cot_{1/2}$ of 0.6 g/mol/s (58). The viral DNA bands in CsCl gradients at 1.7 g/cm³ corresponding to G+C content of 41% and a T_m of 86⁰C.

In alkaline sucrose gradient centrifugation viral DNA shows two fractions with sedimentation coefficients of 85S and 95S, respectively (59). These coefficients are considerably larger than the 73S sedimentation coefficient of the slightly larger T4 phage DNA. Those values are consistent with a linear or circular single-stranded DNA with a length twice that observed for viral double-stranded DNA. So, like poxvirus DNA, the genome of ASFV is cross-linked at the extremes. This can be confirmed by the rapid reassociation of terminal fragments of ASFV DNA (60, 61). Sequencing of isolated terminal fragments of ASFV DNA demonstrated that the genome is cross-linked by two 37 nucleotide-long hairpin loops with imperfect matching and rich in A+T (62). The loops are present in two equimolar forms which are inverted and complementary, like the "flip-flop" termini of poxvirus DNA.

When heteroduplexes formed by reannealing denatured terminal fragments of ASFV DNA are observed by electron microscopy, Y-shaped molecules are observed. The

double-stranded stem is 2.4 kbp long and corresponds to inverted terminal repeats (63). Again, this is a similarity with poxvirus DNA and a distinction from iridovirus DNAs, which are circularly permuted and terminally redundant (64). The inverted terminal repeats are composed of unique sequences that are scattered among 42 tandem direct repeats of 34 nucleotides, five repeats of 24 nucleotides, and three repeats of 33 nucleotides (65).

Restriction site maps were constructed using the Badajoz-71 strain DNA cleaved with restriction endonucleases SalI, EcoRI, KpnI, PvuI, and SmaI (66) or the Lisbon-60 strain DNA cleaved with EcoRI, SalI, and BamHI (61). The comparison of these maps shows only a moderate variability, for instance seven differences in the 31 EcoRI sites. When the restriction site maps of DNA from field isolates from Africa, Europe and Central America are compared, a central region of highly conserved homology is found (67). In contrast, the regions close to the ends of the genome are variable, this variability being due mainly to deletions and additions. Two multi-gene families are located at those regions and this can provide a basis for recombinations leading to that variability.

The genome of Vero cell-adapted ASFV, both Badajoz-71 strain (60) and Lisbon-60 strain (G. Ribeiro, personal communication) have been cloned in bacteriophage lambda and in plasmids. Recently, the DNA of an African field isolate was also cloned in lambda (68). A collection of recombinants of ASFV DNA partially cleaved with NcoI and inserted in an expression vector, pKK-233, was also prepared (G. Ribeiro, personal communication).

Structural proteins

There are considerable discrepancies between published reports on ASFV structural proteins, both in their number and in their molecular weights. This is probably due to differences in purification procedures and methods

of protein analysis rather than to gross differences in the viral strains that were studied. Virus purified by sucrose gradient centrifugation and analysed by SDS-PAGE was seen to be composed by 28 to 33 polypeptides ranging from 11 kilodaltons (kD) to 230 kD or 243 kD (68, 46). However, the larger polypeptide from virus purified by Percoll gradient centrifugation is a 150 kD polypeptide (43, 50). Comparative studies using the same virus purified by the two methods indicate that the larger species previously found are due to contamination with membrane vesicles rich in nonstructural virus-specific proteins (51). SDS-PAGE of virus purified by Percoll gradient centrifugation separates 26 to 34 polypeptides ranging in molecular weight from 10 to 150 kD (43, 50). Two-dimensional electrophoresis enhanced the analysis of viral proteins (43). Fifty four proteins were resolved, 30 in conventional isoelectric focusing gels and 24 in NEPHGE gels. The most abundant structural proteins are a neutral 150 kD protein and a basic 72 kD protein. Some SDS-PAGE bands, including some major proteins, correspond to multiple proteins of the same molecular weight that can only be separated by two-dimensional electrophoresis.

Some bands observed in SDS-PAGE gels of purified virus are more intense when the virus is extracted from cells labeled before infection. This fact, together with the precipitation of the virus by serum against uninfected cells, led to the suggestion that cellular proteins were encapsidated into the virus particle (50). Two-dimensional analysis also enables the confirmation of this hypothesis, 14 of the 54 structural polypeptides having been identified as cellular in origin. Three of them were identified by Western immunoblotting as actin, α -tubulin, and β -tubulin. The cellular proteins in the virion are not external contaminants adsorbed to the virus surface (43). The role of those cellular proteins and the mechanism of their encapsidation are not known.

Six of the structural proteins are phosphorylated. All these phosphoproteins are of viral origin and one of them, a basic protein of 17 kD, is a major component of the viral particle (51). The search for glycoproteins in the virus particle has given contradictory results. The finding of three structural glycoproteins with molecular weights of 89, 56, and 51 kD (68) was not confirmed (69) and again is probably due to limitations of the purification method that was used. However, the virus is precipitated by lectins. This can be explained by the presence in the virion of several species of glycolipids (69). The absence of glycoproteins at the surface of ASFV particles may be related to the lack of neutralizing antibodies against the virus. It is also possible that no viral protein is exposed at the surface of the viral particle and thus no neutralizing antibody response is elicited. Detergent or chloroform treatment of purified virus resulted in the disappearance of cellular proteins only (41).

VIRUS-CELL INTERACTION

The most efficient system for in vitro replication of ASFV are pig macrophages, prepared from bone marrow or buffy coat (70) or from pulmonary washings (71). Field isolates grow well in these cultures and yields of 1000 - 2000 HAU₅₀ (hemadsorption units) per cell or titers of $1.5 - 2.5 \times 10^8$ HAU₅₀/ml can be obtained. The virus can also be adapted to grow in pig kidney cells (72) or in Vero cells or other monkey kidney cells (73) and most of the studies on the biochemistry and molecular biology of the virus have been done using monkey cell-adapted virus. The yield and titer of the virus produced in monkey cells are about one log lower than in porcine macrophages but this difference is largely compensated by the facility in obtaining much larger numbers of monkey cells and the possibility of plaque titration.

ASFV infectivity is inhibited by chloroquine, the virus being retained uncoated in large vacuoles with lysosomal appearance (74). This suggests that penetration occurs by a mechanism of adsorptive endocytosis and this was confirmed by an electron microscopy study of the early phases of infection (75). After adsorption the viral particles are seen associated mainly with microvilli but also with coated pits. The particles are internalized inside endosomes and can also be seen in large vacuoles with the morphology of multivesicular bodies. Later they are present in secondary lysosomes, where they start to be uncoated.

The growth cycle has a duration of about 18 to 24 hours, depending on the virus isolate and the cell system. DNA replication has a maximum by 8 hours post infection and the first cell-associated virus begins to be detected one or two hours later, followed soon by the appearance of infective virus in the culture medium. Extracellular virus can represent as much as 50% of the virus yield. The cytopathic effect of ASFV consists of vacuolization and rounding-up of cells, with clumping of the chromatin and the appearance of nuclear fibrillar structures. The cells detach from the culture surface and finally are lysed. The virus morphogenesis occurs in perinuclear areas, rich in fibrillar and membranous material and often surrounded by enlarged Golgi apparatus and by ribosomes (76). The migration of the virus particles to the cell membrane is inhibited by treatment with colchicine and cytoskeleton elements are reorganized around the assembly sites (77). This association between virus growth and maturation and the cytoskeleton may explain the inclusion of cytoskeleton proteins in the virus particle (43).

Replication of the virus occurs in the cytoplasm. However, the presence of the nucleus is required (78). No viral growth can be detected in cells enucleated by

cytochalasin treatment. The block in virus replication seems to be at the level of viral DNA replication, which differs from the role of the nucleus in late translation and maturation of poxviruses. A second level of block may also occur in ASFV-infected enucleated cells because virus replication is still inhibited when enucleation is done only late after infection.

Virus-specific enzymes

ASFV genome encodes for several enzymes, which are listed in Table 1. Some of the enzymes are present in the virus particle, whereas other enzyme activities are induced in infected cells but are not present in the virions. A DNA virus that grows only in the cytoplasm of infected cells, like ASFV, has to bypass the limitation coming from the fact that cells are prepared to transcribe and replicate DNA only in the nucleus. So the enzymes required for at least the early transcription and processing of mRNA must be carried into the cytoplasm by the virus particle itself.

Table 1. ASFV-specific enzymes

Enzyme	Reference
VIRION ENZYMES:	
RNA polymerase	48
Poly-A polymerase	79
RNA guanylyltransferase	79
Guanine-7-methyltransferase	79
Nucleoside-2'-methyltransferase	79
Protein kinase	47
Nucleoside triphosphatase	80
Topoisomerase	81
Single-stranded DNA nuclease	82
INDUCED ENZYMES:	
DNA polymerase	83
Thymidine kinase	84
Ribonucleotide reductase	

The RNA polymerase of ASFV is a DNA-dependent RNA polymerase which is present in the virions and is active on viral DNA still partially encapsidated (48). The enzyme requires higher concentrations of ATP than the other ribonucleotide triphosphates. The enzyme activity is sensitive to actinomycin D but, differently from cellular RNA polymerase II, it is resistant to α -amanitin. Rifamycin derivatives inhibit ASFV-specific RNA polymerase activity, with a pattern of inhibition which is close to that of vaccinia virus RNA polymerase (81). RNAs transcribed in vitro by the viral RNA polymerase from partially solubilized virions are capped, methylated and polyadenylated (79). This indicates that the virus particles also carry the enzymes needed for post transcription modification of viral mRNAs. Two nucleoside triphosphate phosphohydrolase activities, with a different K_m for ATP, are also detectable in purified virions (80). These triphosphatase activities are possibly coupled to transcription, as the in vitro transcription system from disrupted virus is strongly dependent on ATP. Indirect evidence for the presence in the virions of a topoisomerase whose activity would be required for transcription comes from the observation that coumermycin A1 inhibits in vitro transcription (81).

Two other enzymes apparently unrelated to transcription are also present in purified virions: a protein kinase (47) and a single-stranded DNA nuclease (82). Their presence in the virions suggests that they are needed for very early stages in infection. The nuclease is possibly required for the removal of the cross-links of viral DNA and the protein kinase may be necessary to phosphorylate and consequently activate one or more of the enzymes required for early transcription. The protein kinase activity of ASFV is not dependent on cyclic AMP and virion proteins themselves are substrates for the phosphorylation (47). The virion substrates were not identified. The viral DNase is a late protein which is

active only on single-stranded DNA. Its activity is inhibited by antiserum against ASFV and the enzyme was found to be an endonuclease with a maximum of activity at neutral pH (82).

ASFV also induces the synthesis of other virus-specific enzymes that are not encapsidated in the virions. These enzymes are a DNA polymerase (83), a thymidine kinase (84), and a ribonucleotide reductase (C.V. Cunha and J.V. Costa, unpublished results). The three enzymes are synthesized early after infection and can be distinguished from the cellular equivalent enzymes by different effects of changes in reaction conditions or by different kinetics of action. The most distinctive feature of ASFV-specific DNA polymerase is its sensitivity to phosphonoacetic acid (85). A stronger indication that these enzymes are encoded for by the virus genome rather than being overproduced cell enzymes is given by the isolation of viral mutants resistant to phosphonoacetic acid, to bromodeoxyuridine, and to hydroxyurea which are mutant in DNA polymerase, thymidine kinase, and ribonucleotide reductase genes, respectively (M.I. Marques and J.V. Costa, unpublished results). The gene for DNA polymerase was cloned in a plasmid expression vector and the gene was mapped at a position about 110 kbp from the left end of the genome (G. Ribeiro, personal communication).

Transcription and translation

ASFV gene expression is regulated by DNA replication, which divides transcription and translation into an early and a late phase. The shift from the early to the late phase of gene expression is dependent on viral DNA synthesis as it is abolished by inhibitors of DNA replication. In these conditions, the early transcription and translation are maintained for long times while in untreated cells many early genes are no longer expressed at late times after infection (36, 43). As discussed below, a distinct immediate phase of transcription and

translation preceding the early phase may also exist.

Early and late transcripts were mapped by hybridization to restriction digestion fragments of viral DNA (86). Early mRNAs hybridize to four distinct regions of the genome, two of them coinciding with both terminal regions of variability. Late mRNA hybridizes to those four early regions and to the remaining regions of the genome. It is not known whether the hybridization of late mRNA to the early regions of the genome is due to early transcription at late times or to stability of RNAs transcribed early after infection.

The study of ASFV transcription can be greatly facilitated by the availability of in vitro systems. As described above, in vitro transcription can be catalyzed by the RNA polymerase present in partially disrupted virus (48). Those in vitro transcripts are indistinguishable from in vivo early transcripts (86). One of the limitations of this system is that it only uses virion DNA as template. F. Caeiro in my laboratory prepared an in vitro system from cytoplasmic extracts from cells permeabilized with lysolecithin. These extracts catalyze the transcription of either early or late mRNAs, can couple transcription to in vitro translation, and can be made dependent on exogenous DNA templates after treatment with micrococcal nuclease.

Virus-specific proteins synthesized by infected cells have been studied by SDS-PAGE (36, 87) and by two-dimensional electrophoresis (43, 88). SDS-PAGE revealed only about 40 virus-specific proteins corresponding to about one fifth of the genome capacity. Two-dimensional analysis increased considerably the resolution of virus-induced proteins. One hundred and six virus-specific proteins could be detected, 35 of them being early proteins resistant to the inhibition of DNA synthesis and the remaining 71 being late proteins (43). The resolution between proteins with the same molecular weight but

different pI is important because they can have different biological or biochemical properties. For instance, they can differ in being structural or not, in phosphorylation, or in their affinity to DNA. Eight early proteins and 11 late proteins are phosphoproteins (51) and 19 virus-specific proteins are glycosylated (89), one of them being the 220 kD protein described above as one of the main components of the membrane vesicles that contaminate extracellular virus. Chromatography on DNA-cellulose followed by two-dimensional electrophoresis enabled the characterization of 20 DNA-binding virus-specific proteins (90). DNA binding proteins may be processive enzymes acting on DNA, or regulatory proteins, or components of the nucleoprotein in the core of the virus particle. A considerable enrichment in DNA polymerase and RNA polymerase activities was found in the DNA-binding fraction of virus-induced proteins.

Two-dimensional analysis may also be required for unambiguous gene mapping of ASFV. A translation map was constructed by in vitro translation of infected cell RNAs selected by hybridization to restriction fragments of viral DNA (86). Many proteins with the same molecular weight are assigned to different fragments. In some cases this can be due to an artifact as the sum of the molecular weights of the proteins mapped in a given fragment is significantly higher than the coding capacity of the fragment. Alternatively, the ambiguities can be due to the inability of SDS-PAGE to identify different proteins with the same molecular weight.

The study of the kinetics of synthesis of virus-specific proteins showed a complex pattern, with new proteins starting to be synthesized at almost every hour after infection (43). It also demonstrated the existence of a third group of constitutive virus-specific proteins that are synthesized from the beginning to the end of the infections cycle and are not regulated by viral DNA

replication.

It is not clear whether there is an immediate phase of expression of proteins that is needed for the expression of the other early proteins. No difference could be found in proteins synthesized in vitro from RNAs from cells treated with cycloheximide or with cytosine arabinoside (86). If the transcription and translation of early genes was dependent on previous expression of immediate early genes, then different effects of the two inhibitors would be expected. This was observed in vivo as cells treated with cycloheximide from some time before infection and labeled for short times with ^{35}S -methionine in the presence of actinomycin D, after the release of the cycloheximide block, synthesize only a limited number of early proteins (51, 87). Ten of the proteins characterized previously as early proteins could be identified by two-dimensional electrophoresis in this experiment and can be presumed to be immediate early proteins.

DNA replication

Viral DNA replication seems to occur in the cytoplasm of infected cells (51, 91), although it was reported once that DNA replication takes place in the nucleus (92). This contradictory result is probably due to problems in cell fractionation. I have noticed several times that the cytoplasmic perinuclear cell factories tend to fractionate with the nucleus instead of remaining with the cytoplasmic fraction.

Almost nothing is known about the mechanism of ASFV DNA replication. Preliminary results from my laboratory indicate that replication is continuous, without the synthesis of Okazaki fragments (M. Meireles and J.V. Costa, unpublished results). Replicative intermediates band in alkaline sucrose gradients like parental molecules with one or two nicks and a growing chain linked to the parental chain. This is compatible with the self-priming models proposed to explain poxvirus DNA repli-

cation (93, 94), which is not surprising if we consider the structural similarity of the DNA of poxvirus and ASFV. The ASFV-specific endonuclease (82) may be the enzyme responsible for the specific nicks postulated by those models. The models also admit the formation of concatemers with head-to-head and tail-to-tail configurations. By sucrose gradient centrifugation of replicative DNA we could not get clear evidence for such concatemers, but the corresponding double-size terminal fragments can be detected by hybridization with Southern blots of replicative DNA (52). However, these double-size terminal fragments appear in very low abundance indicating that concatemers are an exceptional conformation of replicative DNA or that they are resolved very quickly into mature DNA monomers. It is not known whether these concatemers are true intermediates of replication or they result from recombination associated with or following replication.

The cytoplasmic extracts from infected cells described above for transcription and translation were adapted for the study of viral DNA replication. In vitro replicative DNA seems to be indistinguishable from DNA replicating in vivo. These extracts can be made dependent on exogenous templates after treatment with micrococcal nuclease and may also allow further understanding of the mechanism of viral DNA replication.

TAXONOMY

For many years, ASFV has been classified as an iridovirus, mainly on the basis of its morphology. However, as stressed often in this review, the structure of ASFV DNA, the overall pattern of gene expression of the virus, its enzymatic equipment, and all that is known about its molecular biology make it closer to poxviruses than to iridoviruses. This hybrid set of properties forms a bridge between the two families, Iridoviridae and Pox-

viridae and leads to the definition of a new unnamed family, with ASFV as the only representative (95).

REFERENCES

1. Montgomery, R.E. *J. comp. Path.* 34: 159-191, 243-262, 1921.
2. Detray, O.E. *Adv. vet. Sci.* 8: 299-333, 1963.
3. Hess, W.R. *Virology Monographs*, Springer Verlag, Wien-New York, 9: 1-33, 1971.
4. Coggins, L. *Progr. med. Virol.* 18: 48-63, 1974.
5. Hess, W.R. *Adv. vet. Sci. comp. Med.* 25: 39-69, 1981.
6. Hess, W.R. *In: Comparative Diagnosis* (Eds. E. Kurstak and C. Kurstak), Academic Press, New York, 1981, vol. 3 part A, pp. 169-202.
7. Wilkinson, P.J. *In: Virus Diseases of Food Animals. A World Geography of Epidemiology and Control* (Ed. E.P.J. Gibbs), Academic Press, New York, 1981, vol. II, pp. 767-786.
8. Wardley, R.C., Andrade, C.M., Black, D.N., Castro Portugal, F.L., Enjuanes, L., Hess, W.R., Mebus, C., Ordas, A., Rutili, D., Sanchez Vizcaino, J., Vigario, J.D., Wilkinson, P.J., Moura Nunes, J.F. and Thomson, G. *Arch. Virol.* 76: 73-90, 1983.
9. Viñuela, E. *Curr. Topics Microbiol. Immunol.* 116: 151-170, 1985.
10. Manso Ribeiro, J., Rosa Azevedo, J.A., Teixeira, M.J.O., Braco Forte, M.C., Rodrigues Ribeiro, A.M., Oliveira, E., Noronha, F., Grave Pereira, C. and Dias Vigário, J. *Bull. Off. int. Epizoot.* 50: 516-534, 1958.
11. Manso Ribeiro, J. and Rosa Azevedo, J.A. *Bull. Off. int. Epizoot.* 55: 88-106, 1961.
12. Polo Jover, F. and Sanchez Botija, C. *Bull. Off. int. Epizoot.* 55: 107-147, 1961.
13. Manso Ribeiro, J., Nunes Petisca, J.L., Lopes Frazão, F. and Sobral, M. *Bull. Off. int. Epizoot.* 60: 921-937, 1963.
14. Larenaudie, B., Haag, J. and Lacaze, B. *Bull. Acad. Vet. Fr.* 37: 257-259, 1964.
15. Mazzaracchio, V. *Ann. Inst. Sup. San.* 4: 650-673, 1968.
16. Oropesa, P.R. *Reporte Preliminar de Brote de Fiebre Porcina Africana en Cuba*. Instituto de Medicina Veterenaria, La Habana, Cuba, 1971.
17. Wilkinson, P.J., Lawman, N.J.P. and Johnston, R.S. *Vet. Rec.* 106: 94-97, 1980.
18. Contini, A., Cossu, P., Rutili, D. and Firinu, A. *In: African Swine Fever*, CEC/FAO EUR/8466 EN, Brussels, 1982, pp. 1-6.
19. Mebus, C.A., Dardini, A.H., Hamdy, F.M., Ferris, D.H., Hess, W.R. and Callis, J.J. *Proc. U.S. Anim. Hlth. Assoc.* 82: 232-236, 1978.

20. Ordas Alvarez, A. and Marcotegui, M.A. In: African Swine Fever (Ed. Y. Becker), Martinus Nijhoff Publishing, Boston, 1987, pp. 11-20.
21. Sánchez Botija, C., Ordas, A., and Gonzalez, G. Bull. Off. int. Epizoot. 72: 841-847, 1969.
22. Henriques, R.P., Nunes Petisca, J.L. and Costa-Durão, J. Bull. Off. int. Epizoot. 85: 461-466, 1976.
23. Colgrove, G., Haelterman, E.O. and Coggins, L. Amer. J. vet. Res. 30: 1343-1359, 1969.
24. Sánchez-Vizcaíno, J.M. In: African Swine Fever (Ed. Y. Becker), Martinus Nijhoff Publishing, Boston, 1987, pp. 63-72.
25. Tabarés, E. Arch. Virol. 92: 233-242, 1987.
26. Heuschele, V.P. and Coggins, L. Bull. epizoot. Dis. Afr. 13: 255-256, 1965.
27. McVicar, J.W., Mebus, C.A., Becker, H.N., Belden, R.C. and Gibbs, E.P.J. J. am. vet. Med. Assoc. 179: 441-446, 1981.
28. Sánchez Botija, C. Bull. Off. int. Epizoot. 60: 895-899, 1963.
29. Plowright, W., Parker, J. and Pierce, M.A. Nature 221: 1071-1073, 1969.
30. Plowright, W. Vector transmission of African swine fever virus. Commission of the European Communities, EUR 5904 EN, Brussels, 1977.
31. Plowright, W., Percy, C.T. and Pierce, M.A. Res. Vet. Sci. 11: 582-584, 1970.
32. Plowright, W., Perry, C.T. and Greig, A. Res. Vet. Sci. 17: 106-113, 1974.
33. Hess, W.R. In: African Swine Fever (Ed. Y. Becker), Martinus Nijhoff Publishing, Boston, 1987, pp. 5-9.
34. De Boer, C.J. Arch. ges. Virusforsch. 20: 164-179, 1967.
35. Malmquist, W.A. Am. J. vet. Res. 24: 450-459, 1963.
36. Tabarés, E., Martinez, J., Ruiz Gonzalvo, F. and Sánchez Botija, C. Arch. Virol. 66: 119-132, 1980.
37. Letchworth, G.J. and Whyard, T.C. Arch. Virol. 80: 265-274, 1984.
38. Detray, D.E. Am. J. vet. Res. 18: 811-816, 1957.
39. Norley, S.G. and Wardley, R.C. Res. vet. Sci. 35: 75-79, 1983.
40. Norley, S.G. and Wardley, R.C. Immunology 46: 75-82, 1982.
41. Martins, C., Mebus, C., Scholl, T., Lawman, M. and Lunney, J. Ann. N.Y. Acad. Sci. 532: 462-464, 1988.
42. Trautman, R., Pan, I.C. and Hess, W.R. Am. J. vet. Res. 41: 1874-1878, 1980.
43. Esteves, A., Marques, M.I. and Costa, J.V. Virology 152: 192-206, 1986.
44. Sánchez Botija, C., McAuslan, B.R., Tabarés, E., Wilkinson, P., Ordás, A., Friedmann, A., Solana, A., Ferreira, C., Ruiz-Gonzalvo, F., Dalsgaard, C., Marcotegui, M.A., Becker, Y. and Schlomai, J. Studies on African swine fever virus: purification and

- analysis of virions. Commission of the European Communities, Brussels, EUR 5626e, 1977.
45. Black, D.N. and Brown, F. J. gen. Virol. 32: 509-518, 1976.
 46. Schloer, G.M. Virus Res. 3: 295-310, 1985.
 47. Polatnick, J., Pan, I.C. and Gravell, M. Arch. ges. Virusforsch. 44: 156-159, 1974.
 48. Kuznar, J., Salas, M.L. and Viñuela, E. Virology 101: 169-175, 1980.
 49. Enjunes, L., Carrascosa, A.L. and Viñuela, E. J. gen. Virol. 32: 479-492, 1976.
 50. Carrascosa, A.L., del Val, M., Santarén, J.F. and Viñuela, E. J. Virol. 54: 337-344, 1985.
 51. Esteves, A. PhD Thesis, Lisbon, 1986.
 52. Breese, S.S. and DeBoer, C.J. Virology 28: 420-428, 1966.
 53. Almeida, J.D., Waterson, A.P. and Plowright, W. Arch. ges. Virusforsch. 20: 392-396, 1967.
 54. Carrascosa, J.L., Carazo, J.M., Carrascosa, A.L., Garcia, N., Santisteban, A. and Viñuela, E. Virology 132: 160-172, 1984.
 55. Haag, J., Lucas, A., Larenaudie, B., Ruiz Gonzalvo, F.R. and Carnero, R. Rec. med. Vet. 142: 801-808, 1966.
 56. Plowright, W., Brown, F. and Parker, J. Arch. ges. Virusforsch. 19: 289-304, 1966.
 57. Vigário, J.D., Relvas, M.E., Ferraz, F.P., Ribeiro, J.M. and Pereira, C.G. Virology 33: 173-175, 1967.
 58. Enjuanes, L., Carrascosa, A.L. and Viñuela, E. J. gen. Virol. 32: 479-492, 1976.
 59. Ortin, J., Enjuanes, L. and Viñuela, E. J. Virol. 31: 579-583, 1979.
 60. Ley, V., Almendral, J.M., Carbonero, P., Beloso, A., Viñuela, E. and Talavera, A. Virology 133: 249-257, 1984.
 61. Correia, M.C. PhD Thesis, Lisbon, 1987.
 62. González, A., Talavera, A., Almendral, J.M. and Viñuela, E. Nucl. Acid. Res. 14: 6835-6844, 1986.
 63. Sogo, J.M., Almendral, J.M., Talavera, A. and Viñuela, E. Virology 133: 271-275, 1984.
 64. Goorha, R. and Murti, K.G. Proc. Natl. Acad. Sci. USA 79: 248-252, 1982.
 65. Viñuela, E. In: African Swine Fever (Ed. Y. Becker), Martinus Nijhoff Publishing, Boston, 1987, pp. 31-49.
 66. Almendral, J.M., Blasco, R., Ley, V., Beloso, A., Talavera, A. and Viñuela, E. Virology 133: 258-270, 1984.
 67. Viñuela, E. In: Concepts of Viral Pathogenesis (Eds. A.L. Notkins and M.B.A. Oldstone), Springer-Verlag, Wien, 1987, pp. 243-247.
 68. Tabarés, E., Marcotegui, M.A., Fernández, M. and Sánchez-Botija, C. Arch. Virol. 66: 107-117, 1980.
 69. del Val, M., Carrascosa, J.L. and Viñuela, E. Virology 152: 39-49, 1986.

70. Malmquist, W.A. and Hay, D. *Am. J. vet. Res.* 21: 104-108, 1960.
71. Carrascosa, A.L., Santarén, J.F. and Viñuela, E. *J. Virol. Meth.* 3: 303-310, 1982.
72. Malmquist, W.A. *Am. J. vet. Res.* 23: 241-247, 1962.
73. Enjuanes, L., Carrascosa, A.L., Moreno, M.A. and Viñuela, E. *J. gen. Virol.* 32: 471-477, 1976.
74. Geraldès, A. and Valdeira, M.L. *J. gen. Virol.* 66: 1145-1148, 1985.
75. Valdeira, M.L. and Geraldès, A. *Biol. Cell.* 55: 35-40, 1985.
76. Moura Nunes, J.F., Vigário, J.D. and Terrinha, A.M. *Arch. Virol.* 49: 59-66, 1975.
77. Carvalho, Z.G., Alves de Matos, A.P. and Rodrigues-Pousada, C. *Virus Res.* 11: 175-192, 1988.
78. Ortin, J. and Viñuela, E. *J. Virol.* 21: 902-905, 1977.
79. Salas, M.L., Kuznar, J. and Viñuela, E. *Virology* 113: 484-491, 1981.
80. Kuznar, J., Salas, M.L. and Viñuela, E. *Arch. Virol.* 69: 307-310, 1981.
81. Salas, M.L., Kuznar, J. and Viñuela, E. *Arch. Virol.* 77: 77-80, 1983.
82. Barros, M.F., Cunha, C.V. and Costa, J.V. *Virology* 155: 183-191, 1986.
83. Polatnick, J. and Hess, W.R. *Arch. ges. Virusforsch.* 38: 383-385, 1972.
84. Polatnick, J. and Hess, W.R. *Am. J. vet. Res.* 31: 1609-1613, 1970.
85. Moreno, M.A., Carrascosa, A.L., Ortin, J. and Viñuela, E. *J. gen. Virol.* 39: 253-258, 1978.
86. Salas, M.L., Rey-Campos, J., Almendral, J.M., Talavera, A. and Viñuela, E. *Virology* 152: 228-240, 1986.
87. Escribano, J.M. and Tabarés, E. *Arch. Virol.* 92: 221-232, 1987.
88. Urzainqui, A., Tabarés, E. and Carrasco, L. *Virology* 160: 286-291, 1987.
89. del Val, M. and Viñuela, E. *Virus Res.* 7: 297-308, 1987.
90. Esteves, A., Ribeiro, G. and Costa, J.V. *Virology* 161: 403-409, 1987.
91. Pan, I.C., Shimizu, M. and Hess, W.R. *Am. J. Vet. Res.* 41: 1357-1367, 1980.
92. Tabarés, E. and Sanchez Botija, C. *Arch. Virol.* 61: 49-59, 1979.
93. Moyer, R.W. and Graves, R.L. *Cell* 27: 391-401, 1981.
94. Baroudy, B.M., Venkatesan, S. and Moss, B. *Cold Spring Harbor Symp. quant. Biol.* 47: 723-729, 1983.
95. Brown, F. *Intervirology* 25: 141-143, 1986.

13

DIVERSITY OF THE AFRICAN SWINE FEVER VIRUS GENOME

L.K. DIXON, P.J. WILKINSON, K.J. SUMPTION and F. EKUE

AFRC Institute for Animal Health, Pirbright Laboratory, Ash Road,
Pirbright, Woking, Surrey GU24 0NF, U.K.

ABSTRACT

African swine fever is caused by a cytoplasmically located virus particle that, although structurally similar to the Iridoviridae, has a number of similarities with Poxviridae. The genomes of African swine fever virus (ASFV) isolates from ticks inhabiting warthog burrows in different areas of Zambia were genetically very diverse. Differences between genomes of isolates from ticks inhabiting neighbouring warthog burrows were also detected and probably resulted from point mutations that had occurred at various positions along the virus genome. The genomes of isolates from domestic pig outbreaks in two regions where disease is endemic (Europe/W. Africa and E. Zambia/Malawi) were also compared. Genomes of viruses within each of these areas were closely related to each other and usually varied as a result of additions or deletions of sequences at positions close to both termini. Restriction enzyme mapping defined seven regions of the genome where length variations occurred. In most of these regions length variations were quite small (<2kb) but in a region between 7 and 20kb from the left hand terminus large variations (up to 9kb) were found. Two other variable length regions contained tandemly repeated sequences. The results are discussed in terms of the selective constraints imposed by virus replication in ticks and warthogs compared to domestic pig populations.

INTRODUCTION

Virus characteristics

African swine fever (ASF) is caused by a cytoplasmically located virus particle that is structurally related to the

Iridoviridae. The nucleoprotein core has a diameter of about 80nm and is surrounded by a lipoprotein envelope and the capsid. Extracellular virus has an external envelope derived by budding through the plasma membrane (1, 2). African swine fever virus (ASFV) was originally classified in the family Iridoviridae (3, 4), but recent molecular evidence has shown that ASFV is similar to the Poxviridae and differs from the Iridoviridae in several important respects (see 5 for review). Recently ASFV has been removed from the Iridovirus group and is the only known member of a separate virus group which has not yet been named (6).

ASFV contains a linear double-stranded DNA genome about 170 to 180 kb (kilobase pairs) long. The ends of the genome are covalently crosslinked (7,8) by a partially basepaired hairpin loop 37 nucleotides long. This hairpin loop is present in two equimolar forms that are inverted and complementary with respect to each other (9). Adjacent to the terminal crosslinks are inverted terminal repeats which are 2.4 kb long and consist of sets of tandem repeats (10,11). Thus the structure of the ends of the ASFV genome is similar to that of Poxviridae (12, 13) indicating that the ASFV genome replicates by a similar mechanism (13, 14). In contrast the genomes of several Iridoviridae have been shown to be circularly permuted and terminally redundant (15, 16, 17).

ASFV transcription is not dependent on host cell RNA polymerase II and virions contain an RNA polymerase (18), mRNA capping and polyadenylation enzymes (19) and a DNA topoisomerase (20). Similar enzymes are present in Poxvirus particles (21, 22, 23, 24, 25) but have not been demonstrated in Iridovirus particles (see 26 and other chapters in this volume). Other enzyme activities detected in ASF virions include protein kinase (27), nucleoside triphosphate hydrolases (28) and deoxyribonucleases including one enzyme with specificity for single-stranded DNA (29).

Over 100 virus induced proteins are synthesised during ASFV infection. These fall into three temporally regulated classes including those expressed early during infection only, those expressed both early and late during infection and those expressed late in infection after DNA replication (30, 31, 32).

More than 30 virus structural proteins have been characterised (30, 33, 34, 35).

Geographical distribution of ASF

ASF was first described in Kenya in 1921 (36) and since then the disease has been reported from most African countries south of the Sahara (see 37, 38 for reviews). Elsewhere in Africa, disease was introduced to the Cameroon in 1982 and it is now endemic there (39) and outbreaks have occurred in Algeria, Senegal and Benin. In 1957 ASF spread to Portugal and although that outbreak was eradicated (40), disease reappeared in 1960, possibly caused by a new introduction of virus (41). Since then disease has been endemic in the Iberian peninsula, although a large part of the north and east of Spain has recently been declared free of ASF (42). Sporadic outbreaks of ASF have occurred elsewhere in Europe (most recently in Belgium 1985 (43), Holland 1986), the Caribbean, Dominican Republic and South America (Brazil). These outbreaks have been successfully eradicated, but ASF remained endemic in Sardinia after its introduction in 1978 (see 37, 38).

Host range and mechanisms of transmission of ASFV

ASFV infects both domestic and European wild suidae (Sus scrofa) in addition to warthogs (Phacochoerus aethiopicus) and bush pigs (Potamochoerus porcus) (36, 44, 45). Apart from these vertebrate hosts, ASFV can also infect a number of species of soft ticks belonging to the genus Ornithodoros. Ornithodoros moubata acts as a virus vector in southern Africa (46, 47) and Ornithodoros erraticus in south-west Spain and Portugal (48).

In Africa south of the Sahara ASFV is widely distributed in populations of both warthogs and O.moubata which inhabit warthog burrows. The proportion of ticks infected with virus shows considerable variation between different regions (37, 47, 49, 50, 51). Bushpigs are less frequently infected than warthogs (45).

ASFV can be transmitted between O.moubata transovarially, transtadially and transexually, usually from male to female (52, 53). Ticks may be persistently infected for periods of at least three years, during which time they remain capable of transmitting virus to pigs on which they feed (49). The remarkable adaptation of ASFV to its tick vector have led to

suggestions that ASFV was originally a tick virus (49). Ticks may be infected by feeding on viraemic blood, although the titre of virus required to infect ticks, the titre to which virus replicates in ticks and the proportion of ticks that become infected varies depending on both the virus isolate and the tick population (37, 54, 55). Neither direct vertical nor direct horizontal transmission of ASFV between warthogs has been demonstrated (36, 44, 47, 56) and the tick vector plays an essential role in the transmission cycle between warthogs and ticks.

Warthogs become infected by bites from infected ticks. Adult warthogs show no signs of disease although virus is present in their tissues (37). However, viraemia has been demonstrated in young warthogs, despite no obvious signs of disease and it is likely that young warthogs, rather than adult warthogs, act as the source of virus which infects clean ticks that feed on them (57). An analysis in two areas of east Africa (Serengeti and W. Uganda) of the proportion of warthogs of different age groups from which ASFV could be isolated, indicated that most of the warthogs became infected in the first six months of life (37).

The most likely mechanism of ASFV transmission from infected tick/warthog populations to domestic pigs is by bites from infected ticks or by ingestion of infected warthog tissues (37, 58). In contrast to the situation in warthogs, once ASFV is introduced into domestic pig populations it can be readily transmitted between pigs in the absence of a tick vector. During acute disease sufficient virus is present in excretions and secretions (particularly those containing blood) to transmit disease by contact (59) and airborne transmission over short distances can also occur (60). Nevertheless, in some areas, such as Malawi where ASFV infected ticks have been found in pig pens, ticks may play a role in transmission of disease within domestic pig populations (61).

The original descriptions of ASF in Africa were of a peracute haemorrhagic fever with mortality rates of up to 100% in domestic pigs (36). Whilst many African isolates of ASFV cause disease of this peracute form, more recent isolates of ASFV from regions where disease is endemic in domestic pig populations,

such as Europe, have reduced virulence (62, 63, 64). A greater proportion of pigs infected with these less virulent isolates may have a sub-acute or chronic form of the disease. Apparently healthy recovered animals may intermittently develop viraemia and act as sources of infection for healthy animals (55). Disease outbreaks in which the mortality rate is 100% are more likely to be self-limiting than outbreaks in which infected animals undergo inapparent disease. The emergence of ASFV isolates of reduced virulence for domestic pigs has undoubtedly contributed to the dissemination of ASFV in domestic pig populations.

Diversity of African swine fever virus

Methods used to study diversity The difficulty because pigs die too quickly of obtaining antisera to ASFV antigens from pigs infected with virulent ASFV isolates hampered early attempts to study antigenic variation. The availability of several ASFV strains attenuated by growth in tissue culture meant that sera could be obtained from pigs inoculated with these attenuated viruses and challenged with homologous virulent virus (65, 66, 67, 68, 69). The absence of neutralizing antibodies in these sera meant that virus isolates could not be differentiated using in vitro neutralization assays. However pigs inoculated with attenuated virus were protected, when challenged with homologous virulent virus and protection tests were used to identify immunologically related viruses. The ability of sera to inhibit haemadsorption of pig erythrocytes to pig monocytes infected with homologous, but not heterologous, virus isolates has also been used to subgroup virus isolates. This approach could not be used for isolates that did not cause haemadsorption (70, 71). More recently panels of monoclonal antibodies which recognize a number of ASFV structural proteins have been used to study the antigenic variation of virus isolates and restriction enzyme fragment analysis and mapping have been used to study variability of the ASFV genome (54,72,73,74,75,76,77,78,79).

Variation of African swine fever virus following serial passage in tissue culture and in isolates from pigs It has been suggested that the failure of ASFV to induce neutralizing antibodies may be due to variation of 'critical' antigens (72). A panel of monoclonal antibodies which recognize 10 ASFV structural

proteins has been used to investigate whether antigenic variants were present within an ASFV population isolated from infected pigs. Seven virus clones, isolated by culture at limiting dilution in pig monocytes, were obtained from a pig infected with a Spanish virus isolate (Ba71). Binding of monoclonal antibodies to these virus clones showed that one clone had changes in proteins p150, p37 and p14, a second clone had slight changes in protein p220/150, a third had changes in protein p27 and four clones were identical (72). In a separate experiment the stability of virus clones during passage in pig monocytes was investigated. Clones from three different virus isolates obtained by limiting dilution in pig monocytes, were passaged 20 times in pig monocytes at a low multiplicity of infection. The three viruses did not show changes in binding to monoclonal antibodies up to passage 10, but virus from passage 11 to 20 was different from the original virus. These differences were mainly in proteins p27, p24 and p17 (72). The antigenic variants detected by cloning virus isolates from an infected pig were therefore probably viruses which were present in the original virus population and did not result from changes in the virus during the cloning procedure. Since the pig from which these variant clones were isolated had not been inoculated with a cloned virus the frequency with which such variants arise during virus passage in pigs is not clear.

Virus clones differing in properties including virulence for domestic pigs, haemadsorption and binding to a panel of monoclonal antibodies which recognize virus protein p14 have been isolated from an infected pig. These characteristics were stable for at least three passages in tissue culture in Vero cells (73).

Virus genome heterogeneity has been observed in plaque-purified tissue culture adapted virus (E70) isolates after serial passage in tissue culture. This heterogeneity was detected by the appearance of submolar bands in restriction enzyme digests of virus DNA after more than 30 passages in monkey kidney cells or 5 passages in pig monocyte cultures (74). These submolar bands were resolved into discreet molar bands following plaque-purification of virus. Mapping the genomes of 4 variant viruses showed that restriction enzyme fragments located at both termini, one

fragment about 25kb from the right hand terminus (SmaI H) and one fragment in the centre of the genome varied in length when virus variants were compared to the parent viruses (74). In a separate study no changes were observed in the SalI restriction pattern with respect to the predominant virus in the original population after 100 passages in pig monocytes of isolate Ba71H (75).

In summary, evidence indicates that virus variants differing antigenically, in genome structure and in biological properties are present as subpopulations in ASFV isolates from infected pigs. Variants also emerge during sequential passage in tissue culture and have been detected after fewer passages in pig monocytes than in non-porcine cell lines. It is not clear how frequently such variants arise during infection of pigs or other hosts and the significance, if any, of such virus variants in explaining the failure of ASFV to induce neutralizing antibodies remains unclear. However, amplification of variants differing in biological properties within virus populations could obviously occur as a response to selective pressure.

Several reports describe major genome rearrangements that occur during adaptation of ASFV to tissue culture cell-lines (75, 76, 77). Comparison of the genome maps of tissue culture adapted virus isolates with those of unadapted virus showed that most changes resulted from deletions or additions of sequences from regions close to both termini. In two separate studies large deletions, of 7kb and 15kb of sequences between about 7 and 23kb from the left hand terminus, were observed during adaptation to tissue culture (MS and Vero monkey cell lines)(75, 77). In addition, small increases in the size of both terminal fragments and of a fragment about 25kb from the right hand terminus occurred (77). This latter fragment also varied in length in virus variants isolated following sequential passage in MS tissue culture cells.

Diversity of African swine fever virus isolates from disease outbreaks and wildlife sources Binding to a panel of monoclonal antibodies and genome analysis have also been used to compare ASFV isolates from disease outbreaks in Europe, the Caribbean and Africa as well as from wildlife sources in Africa. To avoid genome rearrangements that may occur during virus adaptation in

tissue culture, genome comparisons were carried out using DNA prepared from virus grown in pig monocytes or from the red blood cell fraction of infected pig blood. Evidence from restriction enzyme analysis indicated that virus isolates from domestic pig outbreaks in Europe, the Caribbean, Brazil and West Africa (Angola and Cameroon) were all closely related to each other (75, 78). However, some differences were detected between these isolates both by restriction enzyme analysis and by binding to a panel of monoclonal antibodies (72, 75). Mapping the genomes of 18 isolates from domestic pig outbreaks in Europe, the Caribbean, Brazil and Angola showed that SallI restriction enzyme sites were conserved in the central region of the genome and that the length of this region of 125kb was constant. Variation between the genomes of these isolates resulted from DNA additions or deletions in regions up to about 40 kb from the left hand terminus and 15 kb from the right hand terminus of the genome. Sequences of up to 16 kb were deleted from the left terminal region of the genome (75). Nucleotide sequence analysis showed that two multigene families are encoded within this left terminal region. One family, which is adjacent to the terminal inverted repeats, has copies at both ends of the genome. The second family is located in the region between 10 and 20 kb from the left hand terminus and deletion or addition of genes within this multigene family accounts for the length variation in this region of the genome observed between virus isolates (11).

In contrast, genome analysis of a limited number of African isolates from countries other than Cameroon and Angola showed that isolates collected from domestic pigs or warthogs in widely dispersed geographical locations over a long timespan were genetically very diverse (54, 75, 78).

In recent studies, we have analysed the genomes of ASFV isolates collected from wildlife sources at similar times within defined areas of different regions of Zambia (79) and of domestic pig isolates from an area in Malawi and eastern Zambia where disease is endemic. In addition we have analysed genomes of European domestic pig isolates.

MATERIALS AND METHODS

Viruses

Virus isolates were obtained either from blood/serum samples collected from pigs or from ticks collected from warthog burrows or pig pens (51, 61). Initially samples were screened by culture in pig bone marrow cells and assayed for presence of virus by haemadsorption of pig erythrocytes to infected cells (60, 61). Positive samples were then inoculated intravenously into pigs to provide a virus stock and material for extraction of virus DNA.

Isolation of virus DNA

In order to avoid possible genome rearrangements that might occur during adaptation of virus to growth in tissue culture, DNA was prepared from virus isolated from the red blood cell fraction of infected pig blood. The method used was essentially as described by Wesley and Tuthill (78). Blood samples were collected on the first day of fever. Clarified red blood cell lysates were treated with DNAase (50 μ g/ml) and 1% Tween 80 to remove contaminating cellular DNA and were then loaded on step gradients containing 15% and 50% sucrose in TNE buffer (0.1M NaCl, 10mM EDTA, 10mM Tris pH8.0). Following centrifugation at 25000rpm in the Beckman SW28 rotor for one hour at 4°C, virus was harvested from the interface between the sucrose layers. DNA was prepared from isolated virus by lysis of virus with 1% Sodium dodecyl sulphate and pronase (500 μ g/ml) followed by phenol extraction and ethanol precipitation of virus DNA. Best results were obtained when fresh blood was used to prepare DNA.

Restriction enzyme analysis and mapping of virus genomes

Virus DNA was digested with restriction enzymes according to the manufacturers recommendations. Fragments were separated by electrophoresis on 0.6%, 1% or 2% agarose gels in 40mM Tris-acetate buffer, pH8.0. Bands were visualised either by staining with ethidium bromide or by autoradiography of dried gels containing restriction enzyme fragments, end labelled with ³²P-dATP using the Klenow fragment of DNA polymerase (80). In order to map the order of restriction enzyme fragments separated DNA fragments were transferred from gels (81) onto Hybond-N filters (Amersham) and attached to filters by baking at 80°C for 2 hours. These filters were then sequentially hybridised with

either bacteriophage lambda or plasmid clones containing overlapping DNA inserts spanning the complete genomes of either the Malawi (Lil20/1) isolate (82) or a Vero cell adapted Spanish isolate (Ba71V) (83). Cloned DNA was labelled with ^{32}P -dATP using the random oligonucleotide primer method (84, 85). Hybridization of filters to denatured probes was carried out at 65°C in $5 \times \text{SSC}$ ($1 \times \text{SSC}$ is 150mM -NaCl and 15mM trisodium citrate), $10 \times$ Denhardt's solution, $50\mu\text{g/ml}$ denatured salmon sperm DNA, 0.3% SDS. Filters were washed at 65°C in $0.1 \times \text{SSC}$, 0.1% SDS and exposed to X-ray film. Radioactive probes were eluted from filters by washing for 30 minutes at 42°C in 0.4M NaOH and for 30 minutes at 42°C in 0.1M Tris HCl pH7.5, $0.2 \times \text{SSC}$, 0.2% SDS.

RESULTS

Comparison of the genomes of ASFV isolates from ticks inhabiting warthog burrows in different areas of Zambia

ASF in domestic pigs has only been reported in Eastern Zambia, although ASFV has been isolated from ticks inhabiting warthog burrows in four National Parks or adjoining Game Management Areas in North, South, East and Central Zambia (51). Restriction enzyme analysis showed that genomes of virus isolates from ticks inhabiting warthog burrows in each of these four areas were very different. Mapping restriction enzyme fragments showed that the regions which varied between isolates were distributed throughout the virus genome although some restriction enzyme sites, particularly in the the right hand third of the genome, were conserved in all these isolates (79). Table 1 indicates the number of restriction enzyme fragments conserved when different pairs of these virus isolates were compared.

The genomes of seven isolates from ticks inhabiting the same or neighbouring warthog burrows within one small area in Southern Zambia (Livingstone Game Park) were compared and found to be more closely related to each other than were the genomes of isolates from ticks inhabiting warthog burrows in different areas of Zambia. However, variation between the genomes of the isolates from Livingstone Game Park was observed and usually resulted from point mutations or small deletions resulting in gain or loss of restriction enzyme sites which had occurred at various positions

along the virus genome (79)(see Fig.1). Four distinct virus genotypes were distinguished amongst these seven isolates.

Table 1 Comparison of the number of Bam HI restriction enzyme fragments conserved in ASFV isolates.

	Sum 14	Kab 6	Mfue 6	Liv 13	Lil 20/1	Malta 78
Sum 14	21	11	13	8	12	ND
Kab 6		24	22	5	11	ND
Mfue 6			22	8	13	ND
Liv 13				23	9	ND
Lil 20/1					23	9
Malta 78						25

The number of Bam HI restriction enzyme fragments containing homologous sequences that are identical or very similar in length between different pairs of virus isolates are indicated. Isolates were from ticks inhabiting warthog burrows in different regions of Zambia (Sum 14, Kab 6, Mfue 6, Liv 13) or from domestic pig outbreaks in Malawi (Lil 20/1) or Malta 1978 (79, 82). ND indicates results were not determined.

Restriction enzyme site mapping indicated that one virus isolate (Liv 5a) may have originated by earlier recombination between two distinguishable viruses. The region between 0 and 23kb from the left hand terminus of this isolate was the same as that of the Liv 13 virus isolate whereas in all other regions of the genome where differences in restriction enzyme sites were observed (between 50 kb from the left hand terminus to the right hand terminus) the Liv5a genome was the same as that of the Liv10 virus genome (79). The Liv5a virus isolate may therefore have been derived by recombination, between virus isolates with genomes similar to the Liv13 and Liv10 isolates at a position between 23 and 50 kb from the left hand terminus.

Small variations in the length of terminal restriction enzyme fragments were observed but no large deletions or additions of sequences at positions close to the left hand terminus of the genome were observed when virus isolates from ticks inhabiting warthog burrows were compared. In addition, the left terminal region of the genome was consistently long in these isolates from ticks in comparison to some domestic pig isolates.

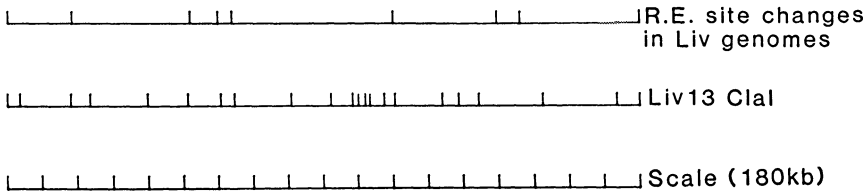


Fig.1 The ClaI restriction enzyme site map of the Liv13 virus genome is shown. Positions on the genome where restriction enzyme site gains or losses were observed when seven isolates from Livingstone Game Park were compared are indicated above.

Comparison of the genomes of ASFV isolates from domestic pig sources in Eastern Zambia and Malawi

Virus isolates were obtained either from O.moubata inhabiting pig pens in villages or from blood samples collected from pigs. In Malawi O.moubata is widely distributed in villages (61). In contrast O.moubata has a limited distribution in villages in Zambia (Wilkinson, P.J., Sumption, K.J. and Mwanaumo, B. unpublished results) and most Zambian isolates were from blood or serum samples collected from pigs. Comparison of the genomes of 26 virus isolates, collected between 1982 and 1988 from the adjoining areas of Eastern Zambia and Central Malawi, (Fig.2) showed that these virus isolates were all closely related to each other. Variation between the genomes of these isolates resulted from differences in the length of restriction enzyme fragments within 40 kb from the left hand terminus and 25 kb from the right hand terminus and in one fragment in the centre of the genome. Variable and constant length fragments were identified within these terminal regions by mapping with additional restriction enzymes which cut more frequently (Fig.3)(Sumption, K.J., Dixon, L.K., Wilkinson, P.J. and Lade, R. unpublished results). A total of seven distinct regions of the virus genome which varied in length were identified in these virus isolates from domestic pig sources in Eastern Zambia and Malawi (Fig.3).

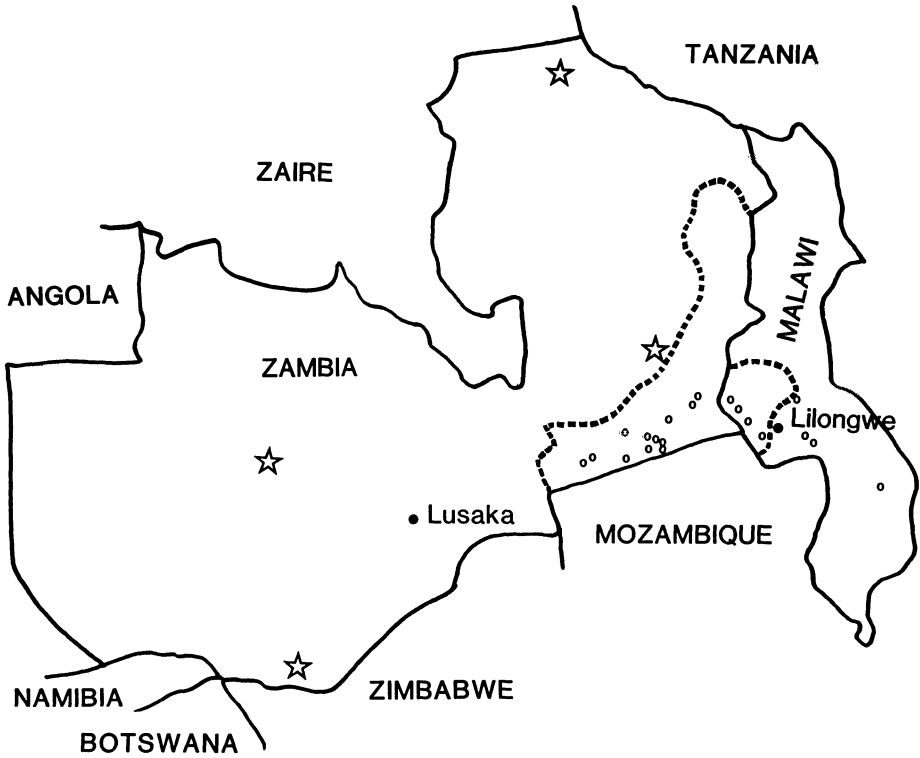


Fig.2 National boundaries are marked in solid lines. The areas of E.Zambia and Malawi where ASF is endemic are indicated by a dashed-line. Villages from which ASFV isolates were collected between 1982 and 1988 for genome analysis are marked with open circles. National Parks from which isolates were obtained from ticks inhabiting warthog burrows are marked with open stars.

The variations in length of each of these variable regions were usually less than 1 kb, but in the region between 7 and 20 kb from the left hand terminus (VR2), deletion or additions of sequences up to 8 kb were observed (Fig.3)(Sumption, K.J., Dixon, L.K. Lade, R. and Wilkinson, P.J. unpublished results). This region probably encodes the multigene family identified by Vinuela and colleagues (11).

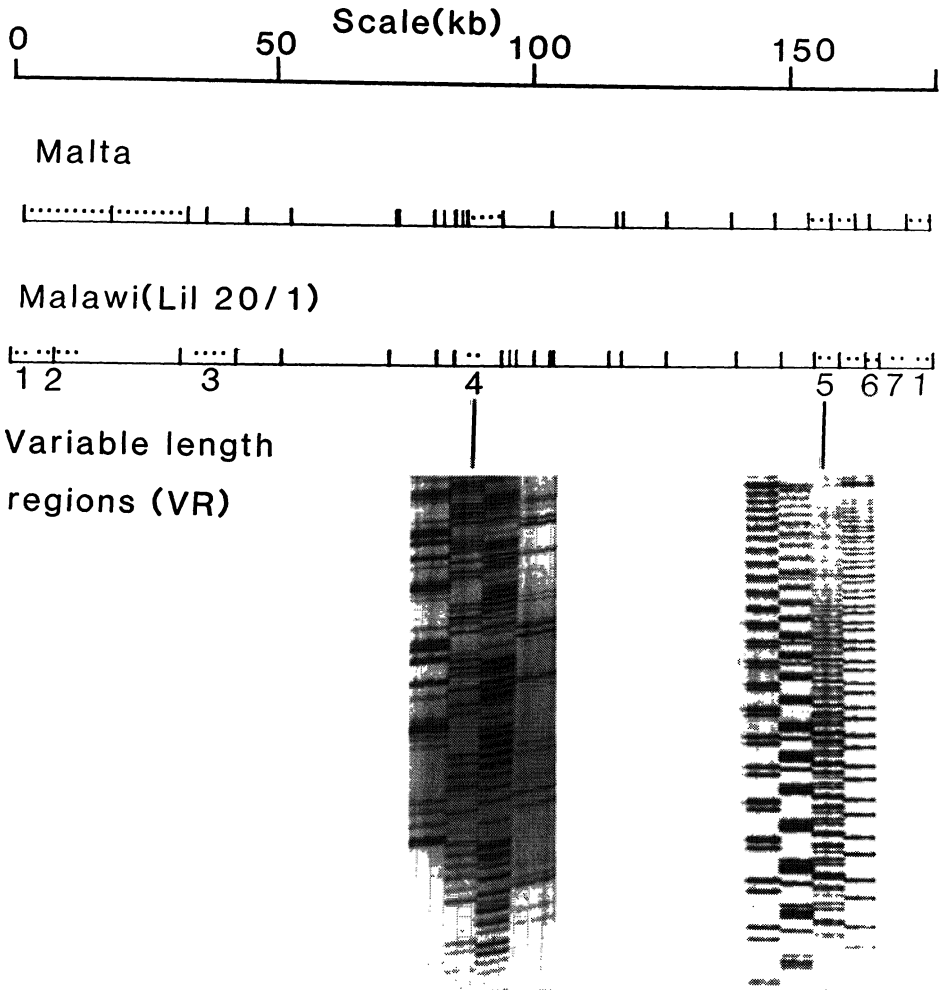


Fig.3 BamHI restriction enzyme site maps for the Malta 1978 and Malawi (Lil 20/1) virus genomes are shown. Regions of the genome which varied in length when different virus isolates from either Malawi/E.Zambia or Europe/W.Africa were compared are shown. The variable length BamHI fragments were determined in isolates from Europe/W.Africa. In Malawi/E.Zambia additional restriction enzyme sites were mapped allowing the variable length regions to be more accurately determined. Sequencing gels showing tandemly repeated sequences within variable length regions 4 and 5 are shown.

Two of the other variable length regions (VR4 and VR5) have been analysed by nucleotide sequencing (Fig.3). One of these is located about 25 kb from the right hand terminus and the other is in the centre of the genome. Both these regions contain sets of tandemly repeated sequences (Dixon, L.K., Bristow, C. and Sumption, K.J. unpublished results) and the variations in length of these regions of the genome in different virus isolates could be explained by variation in the number of tandem repeats present within these sequences.

The similarity between the genomes of these isolates from domestic pigs in Malawi and Eastern Zambia, in contrast to the genetic diversity observed between isolates from wildlife sources, indicates that all these domestic pig isolates may have been derived from a single introduction of virus from a wildlife source into the domestic pig population. Disease may therefore be persisting in the endemic area by circulation within the domestic pig population rather than by continual reintroductions of virus from wildlife sources. This is supported by additional epidemiological studies (Sumption, K.J., Wilkinson, P.J., Hutchings, G.H. and Mwananmo, B. unpublished results).

Comparison of the genomes of virus isolates from domestic pig outbreaks in Europe and W. Africa

Mapping the genomes of recent and earlier European isolates of ASFV with BamHI restriction enzyme showed that the Lisbon 1960 isolate differed from some recent European virus isolates (Malta 1978, Sardinia 1978 & 1982, Belgium 1985, Holland 1986) by the mobility of only one restriction enzyme fragment located in the centre of the genome. Seven 1986 Portuguese isolates from different regions of the country were identical and differed from the other European isolates in the mobility of both terminal fragments, the fragment adjacent to the left terminal fragment (between 16 and 30 kb from the left hand terminus) and the variable fragment in the centre of the genome (Fig.3). The Lisbon 1957 isolate had an additional 6 kb sequence in the region 10 kb from the left hand terminus of the genome and varied in the mobility of two additional restriction enzyme fragments close to the right hand terminus (Wilkinson, P.J., Ekue, F., Lade, R. and

Dixon, L.K. unpublished results). The results of this analysis are consistent with either a single introduction of ASFV into Europe in 1957 or more than one introduction of closely related viruses. The similarity between European and West African virus isolates suggests that West Africa may have been the region from which virus was first introduced into Europe.

The genomes of the European virus isolates were very different from those of domestic pig isolates in Malawi & Zambia. Comparison of the number of restriction enzyme fragments conserved in length indicates that domestic pig isolates circulating in Europe are as genetically different from those circulating in Malawi & Zambia as are those from ticks inhabiting warthog burrows in different regions of Zambia (Table 1). Our results are mostly in agreement with previous results (75). We used BamHI to map the genomes of virus isolates. This enzyme cuts the virus genome more frequently than Sali, which was used by Blasco *et al.* (75) and we have therefore been able to identify some additional restriction enzyme fragments where small length variations occur; for example one fragment in the centre of the genome and two fragments between 25 and 15 kb from the right hand terminus.

DISCUSSION

The analysis of the diversity of the ASFV genome has raised some interesting questions but before considering these it is worth reflecting on some of the evolutionary pressures which may be involved in the selection of particular virus genomes. Firstly, ASFV has undoubtedly been present for a very long time in wildlife sources. ASFV has reached an equilibrium with its hosts in the transmission cycle between soft ticks and warthogs, whereby infection in both hosts is inapparent and the virus can persist for very long periods. Virus replication in ticks is essential for the persistence of virus in this transmission cycle since neither direct vertical nor horizontal transmission of virus between warthogs occurs (36, 44, 47, 56). Movement of virus between widely dispersed geographical locations is likely to be quite restricted in this situation. There is evidence, discussed in the introduction, that the combination of virus strain and

tick population, may be important in determining how efficiently virus replicates in ticks and is transmitted from ticks to warthogs. When new virus strains are introduced into a tick/warthog populations there may be selection of viruses which are more efficiently transmitted and maintained within this population. Pressures on virus in the tick/warthog population include selection of viruses which can replicate in both the arthropod and mammalian host, viruses which may be efficiently transmitted within tick populations and from ticks to warthogs and viruses which can persist in both the tick and warthog host without either killing the host(s) or being eliminated by the host's defence mechanisms. It is worth considering that there may have also been selection for hosts which can survive ASFV infection.

Once introduced into domestic pig populations ASFV can be readily transmitted between pigs by a variety of mechanisms and replication in the tick vector is therefore not essential for virus transmission within pig populations. However, the relative importance of the various mechanisms for maintaining virus in pig populations may vary depending on local circumstances. Thus in areas such as Malawi, soft ticks are present in pig pens and may form a virus reservoir for infection of healthy animals (61). Virus isolates which cause mortality rates approaching 100% in pigs are only likely to persist if there is frequent contact with uninfected domestic pigs, movement of infected pig meat or the presence of ticks in pig pens to act as a virus reservoir. The emergence of virus isolates with reduced virulence for domestic pigs means that pigs in which infection is inapparent or recovered pigs that are reinfected may be important reservoirs of infection for healthy pigs. Movement of either infected pigs or infected meat provides a mechanism for widespread dissemination of virus in domestic pig populations (55).

Continuous transmission of ASFV within domestic pig populations over many years may have resulted in the selection of isolates with reduced virulence for domestic pigs, such that infected pigs may survive infection. Pigs that survive infection may retain virus in tissues for six months at least (55) and be intermittently viraemic over long time periods which might be

important for virus dissemination within pig populations. There may thus be selection for viruses which are able to avoid the immune system of the pig and persist in the host. Such viruses may also be selected during replication in warthogs. Since replication in ticks is not essential for virus transmission in pig populations the disease is endemic in many areas where ticks are not present. The removal of the constraints imposed by virus replication in ticks may be an important factor in the evolution of viruses within domestic pig populations. In addition to imposing constraints on the structure of virus proteins which are involved in interactions with host proteins, replication in the tick vector may require additional genes that are not required for virus replication in mammalian hosts. Specific genes required for virus transmission by insect vectors have been characterised in plant viruses such as wound tumour virus and cauliflower mosaic virus (86,87). Mutant Sindbis viruses that display different abilities to replicate in vertebrate and mosquito cell lines have also been described (88, 89). Differences in protein glycosylation between vertebrate and insect cells probably explain the ability of one Sindbis virus mutant to replicate in insect but not vertebrate cell lines (90, 91).

The genomes of virus isolates from tick/warthog sources in Zambia were very diverse. This diversity was distributed throughout the virus genome and resulted from both point mutations and small variations in length of restriction enzyme fragments. Thus the reservoir of ASFV present in wildlife sources throughout sub-Saharan Africa constitutes a virus pool of enormous genetic diversity which undoubtedly reflects the independent evolution of geographically separate virus isolates over extremely long periods. It may also indicate a rapid divergence of virus genomes as the possible result of selection pressure from genetically diverse hosts since we have found that genomes of virus isolates collected at the same time from ticks inhabiting the same or neighbouring warthog burrows differed from each other (Fig.1). Differences between these virus genomes resulted from gain or loss of restriction enzyme sites at various positions along the virus genome, probably as a result of point mutations or small deletions.

Two "families" of closely related viruses have been identified circulating in domestic pig populations; one is currently circulating in West Africa and Europe but has previously caused outbreaks in the Caribbean and South America and the other is in Malawi and Eastern Zambia. It is possible that each of these virus families was derived from a single introduction of virus from wildlife sources into domestic pig populations.

Genome analysis of isolates from each of the two families of domestic pig viruses showed remarkable conservation of restriction enzyme sites between virus genomes within each family. No differences were detected between the genomes of some isolates which were obtained thirty years apart. Variation between isolates usually resulted from differences in the length of restriction enzyme fragments located within 40 kb from the left hand terminus, 25 kb from the right hand terminus or in one fragment in the centre of the genome. The variable length regions of the genome have been mapped using additional restriction enzymes and can be subdivided into several distinct regions. The molecular basis for the length variation has been determined by nucleotide sequencing of some variable regions. Small variations in the length of fragments located within 2.4 kb from both termini (Sumption, K., Dixon, L.K., Wilkinson, P.J. unpublished results) probably resulted from variation in the number of tandem repeats within the terminal inverted repeats (11), as has been observed in Poxvirus genomes (92). In addition we have located tandemly repeated sequences at two other variable length regions on the ASFV genome (VR4 & 5) and variation in the length of these fragments probably also results from variation in the number of tandem repeats within these repeated sequences. Tandem repeats in non-coding regions have not been described in Poxvirus genomes at positions other than within the terminal inverted repeats, although they have been described in the genomes of other viruses including Iridoviridae (93, 94, 95) and Herpesviridae(96). The function of these internal tandemly repeated sequences is unknown, but they may provide targets for recombination either between different virus genomes or between different regions of the same virus genome. Genetic recombination between genomes of

poxviruses in both animals and cell culture is well documented (97, 98, 99, 100, 101, 102, 103). Recombination between poxvirus sequences inserted into plasmids and homologous sequences on virus genomes also occurs when plasmids are transfected into virus infected cells (104, 105, 106). Although recombination can take place between homologous genes on different virus genomes, regions containing tandemly repeated sequences in non-coding regions of the genome may act as hot spots for recombination. Our analysis indicated that one ASFV isolate, from a tick inhabiting a warthog burrow, may have been derived by recombination between two distinct virus isolates. The putative recombination site in this virus genome has not been defined by nucleotide sequencing but is not located within the two regions containing tandemly repeated sequences that we have characterised. In Poxvirus genomes DNA rearrangements involving deletion of sequences from one end of the genome and transposition of sequences from one end of the genome to the other have been described and analysed by nucleotide sequencing (107, 108, 109, 110, 111). No obvious repeated sequence was involved in these DNA rearrangements (110, 111). Although genomes in which similar transpositions occurred have not been described for ASFV, the presence of repeated sequences in non-coding regions at different positions on the ASFV genome might facilitate such rearrangements.

Large variations in length of up to 16 kb were observed in a region of the ASFV genome located between about 7 and 20 kb from the left hand terminus. The genomes of some domestic pig isolates and of tissue culture adapted viruses have short sequences in this region of the genome, whereas other domestic pig isolates and the isolates from ticks which we analysed have long sequences. Sequence analysis showed that this region of the genome encodes a multigene family whose function is not yet known (11). Viruses with different length left terminal regions can replicate equally well in tissue culture and cause disease of similar pathogenicity in domestic pigs (Wilkinson, P.J, Sumption, K.J, Hutchings, G unpublished results). This region of the genome therefore does not encode genes required for virus replication in tissue culture or pigs or genes important for virus virulence.

Gene duplication and sequence divergence of duplicated gene copies provides a mechanism for evolution of proteins which differ in sequence but have similar functions. It has been suggested that antigenic variation of 'critical' antigens may provide a mechanism by which ASFV can evade the immune system. Evolution of multigene families encoded on the ASFV genome might provide a mechanism for generating such antigenic variants (11). Alternatively this multigene family might encode proteins which interact with variable proteins in the tick host. Possession of an array of divergent but related proteins may confer a selective advantage by allowing virus replication to take place in a broad spectrum of genetically diverse ticks. The observation that tick isolates consistently have long sequences in this region of the genome suggests that these sequences are selected during virus replication in the tick/warthog cycle. The removal of this selective pressure may result in the progressive loss of sequences from this region of the genome and may account for the variable length of the left terminal region observed in domestic pig isolates. Viruses in which the length of this region remain short and unchanged over a period of thirty years may have a sequence in this region whose length is stable during passage in pigs.

Analysis of orthopoxvirus genomes showed that, within this genus, there was considerable conservation in the centre of the genome and that species-, strain- and variant specific differences were due mainly to variation in sequence and length of terminal regions (112, 113). This led to suggestions, which are now being verified by more detailed molecular analysis, that the centre of the genome encodes genes essential for virus replication and that the termini encode genes important for host specificity and virus pathogenesis. The genetic diversity of ASF virus isolates from ticks is greater than that observed within an individual species or genus of the Poxviridae. However, viruses within two areas where disease is endemic in domestic pigs were closely related to each other. Variation between these closely related isolates usually resulted from differences in the length of regions close to both termini. Thus it is also possible that in ASFV the centre of the genome encodes genes required for virus

replication whereas regions close to the termini encode host specific genes and genes involved in virus pathogenesis.

REFERENCES

1. Breese, S.S.Jr. and DeBoer, C.J. *Viol.* 28: 420-428, 1966.
2. Carrascosa, J.L., Carazo, J.M., Carroscosa, A.L., Garcia, N., Santisteban, A. and Vinuela, E. *Viol.* 132: 160-172, 1984.
3. Matthews, R.E.F. *Intervirology* 17: 1-199, 1982.
4. Goorha, R. and Granoff, A. *Comp. Virol.* 14: 347-399, 1979.
5. Vinuela, E. *Curr. Top. Microbiol. Immunol.* 116: 151-170, 1985.
6. Brown, F. *Intervirology* 25: 141-143, 1986.
7. Ortin, J., Enjuanes, L. and Vinuela, E. *J. Virol.* 31: 579-583, 1979.
8. Almendral, J.M., Blasco, R., Ley, V., Beloso, A., Talavera, A. and Vinuela, E. *Viol.* 133: 258-270, 1984.
9. Gonzalez, A., Talavera, A., Almendral, J.M. and Vinuela, E. *Nucl. Acids Res.* 14: 6835-6844, 1986.
10. Sogo, J.M., Almendral, J.M., Talavera, A. and Vinuela, E. *Viol.* 133: 271-275, 1984.
11. Vinuela, E. In: *Developments in Veterinary Virology. African swine fever virus* (Ed. Y. Becker), Martinus Nijhoff Publishers, 1987, pp31-49.
12. Geshelin, P. and Berns, K.I. *J. Mol. Biol.* 88: 785-796, 1974.
13. Baroudy, B.M., Venkatesan, S. and Moss, B. *Cell* 28: 315-324, 1982.
14. Moyer, R.W. and Graves, R.L. *Cell* 27: 391-401, 1981.
15. Goorha, R. and Murti, K.G. *Proc. Natl. Acad. Sci. USA* 79: 248-252, 1982.
16. Darai, G., Anders, K., Koch, H.G., Delius, H., Gelderblom, H., Samelec, G. and Flugel, R.M. *Viol.* 125: 466-479, 1983.
17. Delius, H., Darai, G. and Flugel, R.M. *J. Virol.* 49: 609-614, 1984.
18. Kuznar, J., Salas, M.L. and Vinuela, E. *Viol.* 101: 169-175, 1980.
19. Salas, M.L., Kuznar, J. and Vinuela, E. *Viol.* 113: 484-491, 1981.
20. Salas, M.L., Kuznar, J. and Vinuela, E. *Arch. Virol.* 77: 77-80, 1983.
21. Moss, B., Rosenblum, E.N. and Gershowitz, A. *J. Biol. Chem.* 250: 4722-4729, 1975.
22. Kates, J., McAuslan, B.R. *Proc. Natl. Acad. Sci. USA* 58: 134-141, 1967.
23. Barbosa, E. and Moss, B. *J. Biol. Chem.* 253: 7692-7697, 1978.
24. Martin, S.A., Paoletti, E. and Moss, B. *J. Biol. Chem.* 250: 9322-9329, 1975.
25. Bauer, W.R., Ressner, E.C., Kates, J. and Patzke, J.V. *Proc. Natl. Acad. Sci. USA* 74: 1841-1845, 1977.
26. Willis, D.B., Goorha, R. and Chinchar, V.R. *Curr. Top. Microbiol. Immunol.* 116: 77-106, 1985.
27. Polatnick, J., Pan, T.C. and Gravell, M. *Arch. ges. Virusforsch.* 44: 156-159, 1974.

28. Kuznar, J., Salas, M.L. and Vinuela, E. Arch. Virol. 96: 307-320, 1981.
29. Barros, M.F., Cunha, C.V. and Costa, J.V. Virol. 155: 183-191, 1986.
30. Esteves, A., Marques, M.I. and Costa, J.V. Virol. 152: 192-206, 1986.
31. Santaren, J.F. and Vinuela, E. Virus Res. 5: 391-405, 1986.
32. Urzainqui, A., Tabares, E. and Carrascosa, L. Virol. 160: 286-291, 1987.
33. Carrascosa, A.L., Del Val, M., Santaren, J.F. and Vinuela, E. J. Virol. 54: 337-344, 1985.
34. Schloer, G.M. Virus Res. 3: 295-310, 1985.
35. Tabares, E., Marcotegui, M.A., Fernandez, M. and Sanchez-Botija, C. Arch. Virol. 66: 107-117,
36. Montgomery, R.E. J. Comp. Path. 34: 159-191 and 243-262, 1921.
37. Plowright, W. In: Infectious Diseases of Wild Mammals 2nd edition (Eds. J.W. Davis, L.H. Karstad and D.O. Trainer) Ames: Iowa State University Press, pp178-190, 1981.
38. Wilkinson, P.J. In: Virus Diseases of Food Animals. A world geography of epidemiology and control Vol II (Ed. E.P.J. Gibbs) Academic Press pp767-786, 1981.
39. Ekue, N.F. and Tanya, V.N. Science and Technology Review Cameroon 1: 65-69, 1986.
40. Manso Ribeiro, J., Rosa Azevedo, J.A., Teixeira, M.J.O., Braco Forte, M.C., Rodrigues Ribero, A.M., Oliveira, E., Noronha, F., Grave Pereira, C. and Dias Vigarario, J. Bull. Off. Int. Epiz. 50: 516-534, 1958.
41. Manso Ribiero, J. and Rosa Azevedo, J.A. Bull. Off. Int. Epiz. 55: 88-106, 1961.
42. Council Decision of 14 December 1988. Number 89/21/EEC Official Journal of the European Communities L9/24-27, 1989.
43. Biront, P., Castryck, F. and Leunen, J. Vet. Rec. 120: 432-434, 1987.
44. De Tray, D.E. J. Am. Vet. Med. Ass. 138: 78-90, 1961.
45. Thomas, A.D. and Kolbe, F.F. J. S. Afr. Vet. Med. Ass. 13: 1-11, 1942.
46. Plowright, W., Parker, J. and Peirce, M.A. Nature 221: 1071-1073, 1969.
47. Plowright, W., Parker, J. and Peirce, M.A. Vet. Rec. 85: 668-674, 1969.
48. Botija, C.S. Bull. Off. Int. Epiz. 60: 895-899, 1963.
49. Plowright, W. In: Hog cholera/Classical swine fever and African swine fever (Ed. B. Liess) EEC Publication Eur 5904 EN pp575-587, 1977.
50. Pini, A. and Hurter, L.R. J. S. Afr. Vet. Ass. 46: 227-232, 1975.
51. Wilkinson, P.J., Pegram, R.G., Perry, B.D., Lemche, J. and Schels, H.F. Epid. Inf. 101: 547-564, 1988.
52. Plowright, W., Perry, C.T. and Peirce, M.A. Res. Vet. Sci. 11: 582-584, 1970.
53. Plowright, W., Perry, C.T. and Greig, A. Res. Vet. Sci. 17: 106-113, 1974.
54. Thomson, G.R. Onderstepoort J. Vet. Res. 52: 201-209, 1985.
55. Wilkinson, P.J. Prev. Vet. Med. 2: 71-82, 1984.
56. Heuschele, W.P. and Coggins, L. Bull. Epiz. Dis. Afr. 17: 179-183, 1969.

57. Thomson, G.R., Gainaru, M., Lewis, A., Biggs, H., Nevill, E., Van Der Pypekamp, M., Gerber, L., Esterhysen, J., Bengis, R., Bezuidenhout, D. and Condy, J. In: African swine fever (Ed. P.J. Wilkinson) EEC Publication Eur 8466 EN pp85-100, 1983.
58. Thomson, G.R., Gainaru, M.D. and Van Dellen, A.F. Onderstepoort J. Vet. Res. 47: 19-22, 1980.
59. Greig, A. and Plowright, W. J. Hyg. 68: 673-682, 1970.
60. Wilkinson, P.J., Donaldson, A.I., Greig, A. and Bruce, W. J. Comp. Pathol. 87: 487-495, 1977.
61. Haresnape, J.M., Wilkinson, P.J. and Mellor, P.S. Epid. Inf. 101: 173-185, 1988.
62. Mebus, C.A. and Dardiri, A.H. Am. J. Vet. Res. 41: 1867-1869, 1980.
63. Wilkinson, P.J., Wardley, R.C. and Williams, S.M. In: African swine fever (Ed. P.J. Wilkinson) EEC Publication Eur 8466 EN pp74-84, 1981.
64. McVicar, J.W. Am. J. Vet. Res. 45: 1535-1541, 1984.
65. Botija, C.S. Bull. Off. Int. Epiz. 60: 901-919, 1963.
66. Coggins, L., Moulton, J. and Colgrove, G. Cornell Vet. 58: 525-540, 1968.
67. Hess, W.R., Heuschele, W.P. and Stone, S.S. Am. J. Vet. Res. 26: 141-146, 1965.
68. Malmquist, W.A. Amer. J. Vet. Res. 24: 450-459, 1963.
69. Pan, E.C. and Hess, W.R. Am. J. Vet. Res. 46: 314-320, 1985.
70. Coggins, L. Bull. epiz. Dis. Afr. 16: 61-64, 1968.
71. Vigario, J.D., Terrinha, A.M. and Moura Nunes, J.F. Archiv. ges. Virusforsch. 45: 272-277, 1974.
72. Garcia-Barreno, G., Sanz, A., Nogal, M.L., Vinuela, E. and Enjuanes, L. J. Virol. 58: 385-392, 1986.
73. Pan, I.C., Whyard, T.C., Hess, W.R., Yuasa, N. and Shimizu, M. Virus. Res. 9: 93-106, 1988.
74. Santurde, G., Tuiz Gonzalvo, F., Carnero, M.E. and Tabares, E. Arch. Virol. 98: 117-122, 1988.
75. Blasco, R., Aguero, M., Almendral, J.M. and Vinuela, E. Virol. 168: 330-338, 1989.
76. Wesley, R.D. and Pan, I.C. J. Gen. Virol. 63: 383-391, 1982.
77. Tabares, E., Olivares, I., Santurde, G., Garcia, M.J., Martin E. and Carnero, M.E. Arch. Virol. 97: 333-346, 1987.
78. Wesley, R.D. and Tuthill, A.E. Prev. Vet. Med. 2: 53-62, 1984.
79. Dixon, L.K. and Wilkinson, P.J. J. Gen. Virol. 69: 2981-2993, 1988.
80. Maniatis, T., Fritsch, E.G. and Sambrook, J. In: Molecular Cloning: A Laboratory Manual New York, Cold Spring Harbor Laboratory 1982.
81. Southern E.M. J. Mol. Biol. 98: 503-518, 1975.
82. Dixon, L.K. J. Gen. Virol. 69: 1683-1694, 1988.
83. Ley, V., Almendral, J.M., Carbonero, P., Beloso, A., Vinuela, E. and Talavera, A. Virol. 133: 249-257, 1984.
84. Feinberg, A.P. and Vogelstein, B. Analytical Biochemistry 132: 6-13, 1983.
85. Feinberg, A.P. and Vogelstein, B. Analytical Biochemistry 137: 266-267, 1984.
86. Nuss. D.L. Advances in Virus Research 29: 57-93, 1984.

87. Lung, M.C.J. and Pirone, T.P. *Viol.* 60: 260-264, 1974.
88. Kowal, K.J. and Stollar, V. *Viol.* 114: 140-148, 1981.
89. Durbin, R.K. and Stollar, V. *Viol.* 135: 331-344, 1984.
90. Durbin, R.K. and Stollar, V. *Viol.* 154: 135-143, 1986.
91. Hsieh, P., Rosner, M.R. and Robbins, F.W. *J. Biol. Chem.* 258: 2548-2554, 1983.
92. Moss, B., Winters, E. and Cooper, N. *Proc. Natl. Acad. Sci. USA* 78: 1614-1618, 1981.
93. Schnitzler, P., Delius, H., Scholz, J., Touray, M., Orth, E. and Darai, G. *Viol.* 161: 570-578, 1987.
94. Fischer, M., Schnitzler, P., Delius, H. and Darai, G. *Viol.* 167: 485-496, 1988.
95. Fischer, M., Schnitzler, P., Scholz, J., Rosen-Wolff, A., Delius, H. and Darai, G. *Viol.* 167: 497-506, 1988.
96. Wadsworth, S., Jacob, R.J. and Roizman, B. *J. Virol.* 15: 1487-1497, 1975.
97. Fenner, F. and Comben, B.M. *Viol.* 5: 530-548, 1958.
98. Bedson, H.S. and Dumbell, K.R. *J. Hyg.* 62: 141-146, 1964.
99. Bedson, H.S. and Dumbell, K.R. *J. Hyg.* 62: 147-158, 1964.
100. Strayer, D.S., Cabirac, G., Sell, S. and Leibowitz, J.L. *J. Natl. Cancer Inst.* 71: 91-104, 1983.
101. Chernos, V.I., Antonova, T.P. and Senkevich, T.G. *J. Gen. Virol.* 66: 621-626, 1985.
102. Chernos, V.I., Senkevich, T.G., Chelyapov, N.V., Antonova, T.P., Vovk, T.S. and Mitina, I.V. *Acta virologica* 31: 193-202, 1987.
103. Gershon, P.D., Kitching, R.P., Hammond, J.M. and Black, D.N. *J. Gen. Virol.* 70: 485-489, 1989.
104. Sam, C.K. and Dumbell, K.R. *Annales de Virologie de l'Institut Pasteur* 132E: 135-150, 1981.
105. Panicali, D. and Paoletti, E. *Proc. Natl. Acad. Sci. USA* 79: 4927-4931, 1982.
106. Mackett, M., Smith, G.L. and Moss, B. *Proc. Natl. Acad. Sci. USA* 79: 7415-7419, 1982.
107. Moyer, R.W., Graves, R.L. and Rothe, C.T. *Cell* 22: 545-553, 1980.
108. Esposito, J.J., Cabradilla, C.D., Nakano, J.H. and Obijeski, J.F. *Viol.* 109: 231-243, 1981.
109. Archard, L.C., Mackett, M., Barnes, D.E. and Dumbell, K.R. *J. Gen. Virol.* 65: 875-886, 1984.
110. Pickup, D.J., Ink, B.S., Parsons, B.L., Hu, W. and Joklik, W.K. *Proc. Natl. Acad. Sci. USA* 81: 6817-6821, 1984.
111. Kotwal, G.J. and Moss, B. *Viol.* 167: 524-537, 1988.
112. Mackett, M. and Archard, L.C. *J. Gen. Virol.* 45: 683-701, 1979.
113. Esposito, J.J. and Knight, J.C. *Viol.* 143: 230-251, 1985.

I N D E X

- Actin, 138, 145-146, 151-152, 154-155, 157, 247, 257
- Actinomycin D, 190, 261
- Adenosine triphosphate phosphohydrolase, 229
- Adenosylmethionine, 167
- Adenovirus, 18, 131, 178, 182, 184
- Adenovirus type 2, 21
- Adenovirus type 3, 94
- ADP, 105
- Aedes albopictus, 24, 26, 32, 35
- Aedes albopictus cell, 20-21, 23
- Africa, 248-249, 251, 256, 271, 273-274, 277-278, 284-285, 288-289
- African green monkey kidney cell, 21
- African swine fever (ASF), 4, 248, 252, 271-272, 283
- African swine fever virus (ASFV), 2, 5, 10, 14, 16, 24, 247, 249, 251-252, 254-256, 258-259, 261-263, 265-266, 274-277, 280, 285-291
- Agriculture, 48-49
- Agrotis ipsilon, 116
- Algae, 14
- Algae virus, 4
- Algeria, 273
- Amanitin, 261
- Amino acid sequence, 48, 66, 75-76, 123-124, 223, 225-226, 231
- Amphibian, 6, 138
- Amphibian virus, 4-5, 7, 10
- AMV reverse transcriptase, 35
- Angola, 249, 278
- Animal, 235-237, 241, 249, 251
- Animal virus, 4
- Antibody, 18, 20, 28, 119, 121, 124-127, 139, 143, 147, 247-248, 251-253, 258, 275, 277
- Antigenic variant, 276, 291
- Anti-sense RNA, 179
- Aquatic Blackfly larvae (Diptera), 29
- Ara C, 166, 194
- Arginine, 38, 40, 74, 193
- Asparagine, 74
- Aspartic acid, 74
- Arthropod, 287
- ATPase, 8, 81, 229
- Australia, 115
- Autophosphorylation, 87, 98
- Azacytidine, 169
- Baby hamster kidney cell (BHK), 142-143, 145-150, 152-153, 155, 192, 193
- Bacteriophage, 8, 9, 22, 55-56, 106-107, 169, 256
- Baculovirus, 135
- Belgium, 249, 273, 285
- Benin, 273
- Biological insecticide, 49
- Black beetle virus, 125-126
- Bombyx mori, 116
- Bragg reflection, 15
- Brazil, 249, 273-278
- Bromodeoxyuridine, 262
- Budding, 272
- Bush pig, 251, 273
- c-AMP, 105
- Cameroon, 273-278
- Camponotus pennsylvanicus virus, 23
- Canavanine, 193-194
- Caribbean, 273, 278
- Carp gill necrosis virus, 7
- Cauliflower mosaic virus, 288
- Chilo iridescent virus (CIV), 3, 5-6, 8, 10, 14-16, 22, 42, 47-49, 51-52, 54, 60-62, 64-65, 69, 74-79, 81-82, 84-85, 87-93, 95-103, 105-109, 115, 118, 121, 123, 126, 128, 130, 235-238, 242
- Chilo suppressalis (Lepidoptera), 3, 48, 83

- Chinese hamster ovary cell (CHO), 189, 192, 194
 Chironomus pulmosa, 3
 Chironomus pulmosus virus, 3, 6
 Chloramphenicol, 227
 Chloramphenicol acetyltransferase (CAT), 15, 176-177, 179, 181-182, 226-228, 231-232
 Chlorella-like, 14
 Chloriridovirus, 5-6, 14
 Chloroquine, 259
 Choristoneura fumiferana, 83
 Chromatin, 20
 Chromatin-like structure, 16
 Chromatography, 168, 254, 264
 Chymotrypsin, 16
 Cilia, 138
 Circular permutation, 1, 8-9, 22, 29, 42, 47, 49-50, 52, 78, 83, 130, 203, 211-213, 230, 256, 272
 Classification, 1, 5
 Cod ulcus syndrome virus, 7
 Colchicine, 143, 148, 259
 Coleoptera, 14-15, 115-116
 Coleopterous scareb, 3
 Colladonus montanus (Homoptera:Cicadellidae), 49
 Complementary, 61-62, 196, 211, 247
 Computer-assisted analysis, 49, 63, 68, 205, 221, 224, 254
 Concatemer, 8-9, 22, 174, 266
 Consensus sequence, 48, 65-66, 75
 Contour length measurement, 209, 211
 Costelytra zealandica (CzIV), 113-119, 121-134, 121-125, 128-134
 Coumermycin, 261
 CpA, 207
 CpG, 9, 31, 207, 232
 Cross-link, 9, 247, 255, 261, 272
 Cryptogram, 2
 Ctenopseutis obliquana, 116
 Cuba, 249
 Cyanogen bromide, 124, 135
 Cyclic AMP, 8, 261
 Cyclic AMP-independent protein kinase, 141
 Cycloheximide, 175, 178-181, 265
 Cysteine, 74
 Cytochalasin B and D, 155-157, 260
 Cytochrome C, 209
 Cytosine, 9, 29, 31, 163, 165-166, 181, 230
 Cytoskeleton, 20, 137-138, 140-141, 157, 259
 Dab, 7, 203-205, 208-209, 216, 220, 222-223, 229-230
 dATP, 105
 Dense matrix, 20
 Deoxycytosine, 165
 Deoxyribonuclease, 84, 105, 272
 Diglyceride, 83
 Diptera, 14-15, 29
 Direct repeat, 48, 60, 63, 68, 71, 219-22
 Disease, 236, 243, 247-250
 Disulfide bond, 88, 95, 97, 106-108
 Disulfide-linked protein, 81, 89, 105
 DNA-binding protein, 82, 86, 98-99, 103, 264
 DNA-dependent RNA polymerase, 15, 174
 DNA methylase, 165-166, 168
 DNA methyltransferase, 9
 DNA polymerase, 248, 262, 264, 279
 DNA sequence, 229
 DNase, 229, 261
 DNA sequence homology, 55-56, 60, 62, 68, 71, 217
 DNA topoisomerase, 272
 Dominican Republic, 249, 273
 Dot matrix analysis, 60, 63, 68, 223

- Dot-blot assay, 114
Dye-ligand chromatography, 167
- Edmonton, 5
E1A promoter 5', 182
Endemic, 249, 271, 273-274, 278, 283, 285, 291
Endonuclease, 79, 164, 169
Endotoxin, 236
England, 3
Enhancer, 178, 184
Epidermal tumor, 19, 206
Epiphyas postvittana, 116
Equine herpesvirus type 1, 20
Escherichia coli (E.c.), 26-27
E.c. strain DH5a, 26
E.c. strain DH5aF', 26
E.c. strain HB101, 26, 130
E.c. strain JM83, 130
E.c. strain JM101, 26-27
E.c. strain JM103, 26
E.c. strain JM109, 26
E.c. strain K-12 C600, 227
E.c. lambda 5'-exonuclease, 211
E.c. 3'-exonuclease III, 211
E.c. exonuclease III, 50
Estigmene acrea (Caterpillar), 20-21, 23-26, 32, 37-39
Eukaryotic chlorella-like, 14
Eukaryotic RNA polymerase II, 174
Eukaryotic virus, 1, 8, 9, 22, 50, 52, 181, 230
Europe, 256, 271, 273, 275, 278, 284, 286, 289
Evolutionary, 1, 13, 22, 32
Exocytosis, 138
Exonuclease, 198
- Fathead minnow (FHM) cell, 176-177, 179, 181, 191
Fish cell culture, 232
Fish lymphocystis disease virus (FLDV), 5, 7, 14, 16, 22, 24, 31, 42, 49-50, 78, 128, 130, 203-205, 210, 212-214, 217, 219-224, 226-231
Flagella, 138
Flounder, 5, 7, 203-209, 214, 216, 220, 222-223, 229-230
Fluorophenylalanine (FPA), 180, 193
Freeze-etching, 16
Freshwater fish, 14
Frog, 7, 10
Frog erythrocytic virus, 16
Frog virus 3 (FV3), 5-9, 14, 16-17, 19-22, 24, 29, 31, 50, 128, 130, 137, 141-146, 148-157, 163-170, 173-184, 187-188, 190-194, 196, 198, 227, 230, 232, 235-239, 241-243
Galleria mellonella, 24-26, 29, 32, 40-42, 83-84, 116
Gene expression, 21, 25, 29, 139, 173, 188, 193, 196, 200
Gene library, 52, 75, 203, 217
Genetic diversity, 291
Giant forest hog, 251
Glutamic acid, 74
Glutamine, 74
Glycine, 74
Glycogen, 19
Glycosylation, 17, 84, 225-226, 229, 247, 258, 264, 288
Goldfish, 6
Goldfish virus, 6-7, 9
Grace's insect medium, 25, 78
Grass grub, 114
Green rice leafhopper (Nephtotettix cincticeps), 49
GTP, 105
Guanine-7-methyltransferase, 260
- Haemorrhagic fever, 274
Hairpin, 198, 247, 255, 272
Haiti, 249
Heliothis armigera, 116

- Hepatitis, 235-238
Hepatocyte, 238-239, 241, 243
Hepatocytolysis, 244
Hepatotoxic, 242
Herpesviridae, 289
Herpesvirus, 18, 23, 131, 143, 184
Heteroduplex mapping, 47, 58, 217-218, 231, 255
Histidine, 38, 74, 90
Histogram, 58
Hitchhiking, 15
Hog cholera, 250
Holland (see Netherlands)
Homology, 115, 132-134, 198, 221, 231
Horse-radishperoxidase (HRPO), 119
Host range, 14-15, 22, 115, 119, 130, 273
Hybridization, 15, 20-21, 24-25, 27-28, 32, 35-36, 49, 54, 113, 132-135, 175, 205, 213, 219, 231, 263, 266
Hylochoerus meinertzhageni, 251

Iberian peninsula, 249-251, 273
Icosahedral cytoplasmic deoxyribovirus (ICDV), 4, 13-14, 17, 41, 48, 204
Immediate-early gene, 22, 83, 104, 180, 196, 227, 232
Immediate-early ICR 169 gene, 79, 176-177, 181, 183
Immediate-early ICR 489 gene, 79, 178-180, 183
Immediate-early ICR 534 gene, 179, 181
Immediate-early promotor, 169, 175, 177, 179, 181
Immediate-early protein, 176, 180
Immediate-early mRNA, 178, 196
Imperfect repetition, 63, 69, 71
Insect iridescent virus type 1 (IV1), 3, 6, 15, 115-116, 130-131
Insect iridescent virus type 2, 3, 6, 15, 106-107, 115-116
Insect iridescent virus type 3, 3, 6
Insect iridescent virus type 4, 3, 6
Insect iridescent virus type 5, 3, 6
Insect iridescent virus type 6 (see CIV)
Insect iridescent virus type 7, 6
Insect iridescent virus type 8, 6
Insect iridescent virus type 9, 6, 29, 107, 113-116, 130-131
Insect iridescent virus type 11-15, 6
Insect iridescent virus type 16, 113-115, 128, 130
Insect iridescent virus type 18, 6
Insect iridescent virus type 22, 29, 116, 130
Insect iridescent virus type 24, 105
Insect iridescent virus type 25, 116
Insect iridescent virus type 29, 16
Insect iridescent virus type 35, 3
Insect pest, 114
Intermediate filament (IF), 137-139, 141, 144-145, 147-149, 151, 157
International Committee on Taxonomy of Viruses (ICTV), 2, 4-5
Inverted repeat, 58, 60, 63, 66, 68, 72, 219-220, 247
Iodosulfanilic acid, 85, 90, 92
Ireland, 13, 42
Iridescent virus from mosquitoes (RMIV), 23
Iridescent virus of octopus, 19
Iridovirus-like agent, 7

- Irish TIV (Ir-TIV), 25-26, 32, 34
 Isoleucine, 74
 Isometric virus, 16
 Italy, 249
 Japan, 3, 48
 Kenya, 4, 248, 273
 Kupffer cell, 236, 239, 244
 Lac-Z cassette, 226
 Lactoperoxidase, 115, 122-123, 127
 Lampbrush chromosomes, 138
 Large iridescent insect virus, 5, 14
 Larvae, 3, 9, 13, 15, 18-19, 25-26, 83-84, 113-116
 Lasperyasia pomonella, 116
 Leopard frog, 4
 Lepidoptera, 14, 115-116
 Lepidopteran pest, 113
 Lepidopterous rice stem borer, 3
 Lepomis macrochirus, 204
 Leucine, 74
 Limanda limanda, 204
 Lipophilic polypeptide, 102
 Lipopolysaccharide, 40
 Lisbon, 249
 Livingston Game Park, 280, 282
 Lucke renal adenocarcinoma, 6
 Lymphocystis disease (LD), 4, 204, 213, 227, 229
 Lymphocystis disease virus (LDV), 5, 7, 24, 204
 Lymphocystivirus (see LDV)
 Lysine, 38, 74
 Lysolecithin, 263
 Macromolecular synthesis, 20, 81-82, 84, 102, 108-109, 140, 173, 199
 Malawi, 271, 274, 278, 281-287, 289
 Malta, 249, 281, 285
 Matrix proteinaceous, 16
 Measles virus, 155, 157
 Mercaptoethanol, 88
 Mesosome-like structure, 105
 Methionine, 38-40, 74, 189, 192, 194
 Methyl cytosine, 29, 183
 Methylation, 9, 29, 31, 163-164, 175, 180, 182-183, 203, 205, 230, 232, 261
 Methyltransferase, 181, 184
 Microfilament, 137-138, 151-152, 155, 157
 Microinjection, 148, 151
 Microtubule, 137-138, 141-143, 148-150
 Microvillus-like projection, 152-154, 156
 Mithimna separata, 116
 Mitochondria, 239, 241
 Molecular cloning, 49-50, 52, 131, 205, 212, 219, 232
 Monkey cell, 247
 Monkey kidney cell, 258, 276
 Mosquito, 3, 6
 Mosquito iridescent virus, 5, 16-17
 Mouse, 235-238, 241-242
 Mouse cell, 232,
 mRNA, 79, 173-180, 182, 184, 187-188, 190, 192, 195, 199, 242, 247, 261, 263, 272
 Mycoplasma agent of stone fruits, 49
 Nearest neighbour analysis, 207
 Netherlands, 249, 273, 285
 Neutron scattering, 16
 New South Wales (Australia), 3, 115
 New Zealand, 113-114
 Newt virus, 9
 Newts, 4, 6
 Nillahootie redfin perch virus, 7
 Northern blot hybridization, 175, 196
 Nuclear polyhedrosis virus, 16, 131
 Nucleoside triphosphate phosphohydrolase, 203,

- 260-261, 272
 Nucleoside-2-methyltransferase, 260
 Nucleotide sequence, 176, 178, 203, 205, 217, 220
 Nucleotide phosphohydrolase, 84
 Octopus vulgaris disease virus, 7
 Octylglucoside, 82, 87, 95, 100-101, 104, 108
 Odontria striata, 115
 Odontria suppressalis, 116
 Okazaki fragments, 265
 Onionskin model, 24
 Opagonia, 114
 Open reading frame (ORF), 48, 60, 65-66, 69, 71-75-78-79, 203, 221, 223, 225-226, 231
 Origin of DNA replication, 48
 Ornithodoros, 252, 273
 Ornithodoros coriaceus, 252
 Ornithodoros erraticus, 251, 273
 Ornithodoros moubata, 252, 273, 282
 Ornithodoros porcinus porcinus, 252
 Ornithodoros puertoricensis, 252
 Ornithodoros savignyi, 252
 Ornithodoros turicata, 252
 Orphan virus, 10
 Orthopoxvirus, 291
 Outbreak, 249, 252, 271, 273, 275, 277-278, 281, 285, 289
 Oxford, 113
 Packaging, 9, 22-23, 174
 Palmitic acid, 102
 Papilloma-like lesion, 204
 Parasite, 19
 Peptide repetition, 79
 Phacochoerus aethiopicus, 251, 273
 Phagocytosis, 138
 Phalloidin, 151
 Phenylalanine, 74, 180
 Phosphatidylcholine, 102
 Phosphatidylinositol, 83, 102
 Phosphohydrolase, 15, 105
 Phospholipids, 100, 102
 Phosphonoacetic acid, 262
 Phosphoproteins, 258, 264
 Phosphorylation, 17, 82, 84, 87, 100, 109, 137, 146-148, 154, 193, 258, 264
 Phosphorylase B, 117
 Phylogenetic relationships, 1, 4
 Physical mapping, 47, 49-50, 52, 54, 57, 113, 123, 130, 132, 135, 203, 205, 212-214, 216-217, 219, 230, 271, 276, 278-279, 280, 282
 Picornavirus, 188
 Pig, 14, 247-251, 258, 271, 274-282, 285-291
 Piscine erythrocytic necrosis virus (PENV), 7
 Piscine virus, 4, 10
 Plaice, 7, 203-205, 207, 229-230
 Planotortrix excessana, 116
 Plant virus, 4, 288
 Plasmid vector, 226, 262
 Plasmid vector pACYC184, 52, 60, 213
 Plasmid vector pAT153, 52, 213
 Plasmid vector pBR322, 33
 Plasmid vector pBR328, 130
 Plasmid vector pCM4, 226, 228
 Plasmid vector pKK233, 256
 Plasmid vector pKm2, 52
 Plasmid vector M13, 26-27, 36
 Plasmid vector pUC8, 130
 Plasmid vector pUC19, 130, 226
 Plasmid rescue, 76
 Platichthys flesus, 204, 206
 Pleuronectes, 229
 Pleuronectidae, 204
 Poliovirus, 125-126
 Polyadenylation, 22, 42, 69, 74, 79, 139, 231,

- 261, 272
 Polyadenylic acid, 223
 Polydnavirus, 23
 Polyethylene glycol, 253
 Polyhedrin gene, 33
 Polymerase, 83, 173-174, 180, 242-243, 248
 Polyvinylpyrrolidone, 86
 Pork, 248
 Portugal, 249-250, 273, 285
 Post-translational modification, 17, 193
 Potamochoerus porcus, 251, 273
 Poxviridae, 10, 24, 266, 271, 291
 Poxvirus, 2, 10, 21, 105, 131, 174, 255-256, 260, 265-266, 272, 289-290
 Proline, 74
 Promoter, 10, 22, 69, 174-184, 225-227, 231-232
 Protein kinase, 15, 81-82, 84, 87, 229, 260, 261, 272
 Protein phosphatase, 141
 Pulse-chase experiments, 22, 147
 Putative gene, 48, 75-76
 Putative proteins, 78, 223, 225-226, 231
 Rabbit, 120-121, 123-126
 Rana pipiens, 4
 Ranavirus, 5-7, 24
 Rat kidney cell, 140
 Rat, 235-236
 Reassociation kinetic, 14
 Recombinant, 15, 26, 33, 55-56, 58, 60, 76, 216, 228, 256
 Recombination, 256, 266, 289-290
 Repetitive DNA sequences, 47-48, 54, 57, 61-64, 66, 68, 70, 130-131, 133, 203, 217, 219-221, 223-224, 226-227, 230-231, 256, 285, 289
 Replication, 1, 3-4, 8-9, 13-14, 19-22, 24-25, 32, 76, 83, 84, 108, 141, 157, 174, 181, 188, 193-194, 230, 235, 242, 247-248, 250, 255, 258-260, 262, 265
 Ribonuclease, 141
 Ribonucleotide reductase, 260, 262
 Ribonucleotide reductase gene, 262
 Ribonucleotide Triphosphate, 261
 Ribosome binding, 228
 Rice stem borer, 48, 83
 Rifamycin, 261
 RNA polymerase, 8-10, 108, 260-261, 263-264
 RNA polymerase II, 8, 22, 175, 177, 181, 184, 261, 272
 S1 mapping, 24, 176-177
 Sahara, 273
 Salmon sperm DNA, 28
 Sardinia, 249, 251, 273, 285
 Scarabaeid, 115
 Scarabaeid larvae, 114
 Sendai virus, 138
 Senegal, 273
 Sequencing, 22, 175, 178, 183, 255, 284
 Serengeti, 274
 Sericesthis iridescent virus (SIV), 15, 18, 106, 114, 118
 Sericesthis paludosa, 3
 Sericesthis pruinosa, 115
 Serine, 74
 Serine-threonine protein kinase, 8
 Shropshire, 3
 Silkworm Bombyx mori, 19
 Simulium, 29
 Site directed mutagenesis, 181, 183
 Small iridescent insect virus, 5, 14-15, 83
 South America, 273
 South Canterbury, NZ, 114
 South Island, NZ, 114
 Southern blot hybridization, 52, 55-56, 113, 130, 132, 213, 216
 Southern Mole cricket iridescent virus, 130

- SP6 RNA polymerase, 176
 Spain, 249-250, 273, 276, 280
 Spectroscopy, 109
 Stem-loop structure, 47, 58, 60, 68, 72
 Stoichiometry, 97
 Sub-Saharan, 288
 Suidae, 251, 273
 Sulfhydryl residues, 82, 85, 90-91, 95, 106
Sus scrofa, 273
Sus scrofa ferus, 251
 SV40, 178, 184
 Swine, 248, 251-252
- Tadpole edema virus (TEV), 6,9
 Tandem repeats, 58, 68, 78,247, 284-285, 289-290
 Taxol, 149-151
 Terminal cross-links, 272
 Terminal inverted repeats, 289
 Terminal redundancy, 1, 8-9, 22, 29, 42, 47, 49-50, 78, 83, 130, 203, 211-213, 230, 272, 256
 Termination codons, 69, 72, 74, 76, 79, 225, 231
 Threonine, 74,105
 Thymidine, 21, 102-103, 255
 Thymidine kinase, 180, 203, 229, 232, 260, 262
 Thymine, 165
 Tick, 248, 252, 271, 273, 274, 279-281, 286, 287, 288, 291
 Tipula iridescent virus, 3, 5, 13-14, 16-29, 31-42, 78, 114, 118, 126
 Tipulid larvae, 26
 Tipula oleracea, 19
 Tipula paludosa, 3, 13
 Toads, 4
 Topoisomerase, 260-261
 Transacting protein, 173, 176-181
 Transcription, 13, 23-24, 32, 38, 42, 75, 102, 104, 173-177, 181-184, 187-188, 190, 193, 195, 232, 261-263, 265-266, 272
- Transcription mapping, 175, 178, 196
 Transcription signals, 22, 74-76, 176, 180, 184, 231
 Transfection,183
 Translation, 20-21, 187-188, 190-193, 195-199, 232, 262-266
 Transmission, 6, 19, 249, 251-252, 273-274, 286-288
Trigla gurnardus, 204
 Triphosphatase, 261
 Trypsin, 96
 Tryptic peptide, 82, 95, 97
 Tryptophan, 74
 ts-mutants, 148, 175, 180, 195
 Tubulin, 137, 142-143, 154, 247, 257
 Tumore, 4,7,19
 Tyrosine, 74, 90, 122
- Uganda, 274
 United States, 48
 Uridine, 165
- Vaccine, 247-250
 Vaccinia virus, 10, 15, 19, 22, 240, 261
 Valine, 74
 Vero cell, 277
 Vesicular stomatitis virus, 138
 Vimentin, 137-138, 145-149
 Viroplasmic centers, 20
- Warthogs, 251, 273-274, 278, 286, 288
 Warthog burrows, 252, 271, 279-281, 283, 286, 290
 Western blot, 104, 119-121, 123, 125, 257
 Wild boars, 247-248, 251-252
Wiseana iridescent virus (WIV), 113-115, 117, 121, 134
Wiseana cervinata, 29
Wiseana suppressalis, 116
Wiseana cervinata, 29

Wiseana species, 9
Wound tumor virus, 288

Zambia, 271, 278, 280,
282-286, 288-289